© THE QUEEN'S PRINTER FOR
ONTARIO
2000

REPRODUCED WITH PERMISSION

L'IMPRIMEUR DE LA REINE POUR
L'ONTARIO

REPRODUIT AVEC PERMISSION

micromedia
division of IHS Canada

20 Victoria Street
Toronto, Ontario M5C 2N8
Tel.: (416) 362-5211
Toll Free: 1-800-387-2689
Fax: (416) 362-6161
Email: info@micromedia.on.ca

Ontario

Archean Metallogeny of the Mine Centre–Fort Frances Area

Ontario Geological Survey
Report 266

K. H. Poulsen

2000

©Queen's Printer for Ontario, 2000

ISSN 0704-2582
ISBN 0-7729-9507-9

All publications of the Ontario Geological Survey and the Ministry of Northern Development and Mines are available for viewing and purchase at the following locations:

Mines and Minerals Information Centre
900 Bay Street, Room M2-17
Toronto, Ontario M7A 1C3
Telephone: 1-800-665-4480 (within Ontario)
(416) 314-3800
Fax: (416) 314-3797

Mines Library
933 Ramsey Lake Road, Level A3
Sudbury, Ontario P3E 6B5
Telephone: (705) 670-5615

Purchases may be made only through:

Publication Sales
933 Ramsey Lake Road, Level A3
Sudbury, Ontario P3E 6B5
Telephone: (705) 670-5691
Fax: (705) 670-5770
1-888-415-9845(toll-free)
E-mail: pubsales@ndm.gov.on.ca

Use of Visa or Mastercard ensures the fastest possible service. Cheques or money orders should be made payable to the *Minister of Finance*.

Canadian Cataloguing in Publication Data

Poulsen, Knud Howard.
Archean metallogeny of the Mine Centre, Fort Frances area

(Ontario Geological Survey report, ISSN 0704-2582 ; 266)
ISBN 0-7729-9507-9

1. Geology–Ontario–Mine Centre Region. 2. Metallogeny–Ontario–Mine Centre Region. 3. Geology, Stratigraphic, Archean. I. Ontario. Ministry of Northern Development and Mines. II. Ontario Geological Survey. III. Title. IV. Series.

QE191.P68 2000 557.13'117 C92-092530-8

Every possible effort has been made to ensure the accuracy of the information contained in this report; however, the Ontario Ministry of Northern Development and Mines does not assume any liability for errors that may occur. Source references are included in the report and users may wish to verify critical information.

If you wish to reproduce any of the text, tables or illustrations in this report, please write for permission to the Team Leader, Publication Services, Ministry of Northern Development and Mines, 933 Ramsey Lake Road, Level B4, Sudbury, Ontario P3E 6B5.

Cette publication est disponible en anglais seulement.

Parts of this report may be quoted if credit is given. It is recommended that reference be made in the following form:

Poulsen, K.H. 2000. Archean metallogeny of the Mine Centre–Fort Frances area; Ontario Geological Survey, Report 266, 121p.

Critical Reader: B.O. Dressler
Scientific Editors: S.R. Elliott-Meadows, A. Weatherston and G.H. Brown

Contents

Foreword ix

Abstract xi

Introduction 1
  Acknowledgments 1

General Geology 3
  Introduction 3
  Wabigoon Subprovince 3
  Quetico Subprovince 6
  Subprovince Boundary 6

Stratigraphy 11
  Lithologic Units 11
    Mafic Metavolcanic Rocks 11
    Intermediate Metavolcanic Rocks 11
    Felsic Metavolcanic Rocks 11
    Ultramafic Metavolcanic Rocks 11
    Metamorphosed Chemical Sediments and Intercalated Clastic Rocks 11
    Metamorphosed Wackes and Mudstones 13
    Metamorphosed Gabbroic Rocks 15
    Metamorphosed Granitoid Rocks and Related Rocks 16
    Metamorphosed Conglomerate and Sandstone 18
    Unmetamorphosed Granitoid Rocks and Related Rocks 19
    Dike Rocks 20
    Fault Rocks 20
  Stratigraphic Succession: The Classical Approach 20
    The Core of the Rice Bay Dome 21
    Mantling Rocks of the Rice Bay Dome Near Pocket Pond 21
    Volcanic-Sedimentary Contact at Bear Passage 21
    Volcanic-Sedimentary Contact at Morton Island 24
    Eastern Margin of the Ottertail Lake Intrusion 24
    Unconformity at the Base of the Seine Metasediments 24
  A New Approach to Rainy Lake Stratigraphy 24
  Stratigraphic Summary 27

Structural Geology 29
  Introduction 29
  Structural Trends 29
  Faults and Shear Zones 29
    Boundary Faults 29
    Internal Faults 31
    Ductile Shear Zones 33
  Folds, Cleavages and Lineations 33
  Orientation of Fabric Elements 35
  Structural Cross Sections 35
  Structural Summary and Interpretation 35

Metamorphic Petrology 45
  Metamorphic Facies 45
  Metamorphic Conditions 45

Mineralization 54
  Classification and Distribution 54

Type 1: Metavolcanic-Hosted Mineralization 54
Type 2: Gabbro-Hosted Mineralization 55
Type 3: Vein Mineralization 57
Type 4: Ultramafic-Hosted Mineralization 57
Distribution Patterns of Mineralization, and Summary 57
Base Metal Mineralization Associated with Felsic Volcanic Sequences 58
Setting 58
Composition 58
Alteration 58
Origin 65
Base Metal Mineralization Associated with Iron Formation in Mafic Volcanic Rocks 68
Setting 68
Composition 68
Alteration 70
Origin 70
Gabbro-Associated Mineralization 73
Setting 73
Sulphide Mineralization 73
Oxide Mineralization 78
Origin 78
Gold-Bearing Quartz Veins 78
Morphology 78
Composition 80
Alteration 80
Isotopic Composition of Lead in Galena 81
Origin 86
Tectonics and Metallogeny 89
Tectonic and Metallogenic Summary for the Rainy Lake Area 89
Implications for Tectonics and Metallogeny of the Wabigoon Subprovince and its Margins 90
Conclusions 96
Appendix 1. Sources of Information and Nomenclature 97
Appendix 2. Petrographic Data for Metamorphic Rocks 99
Appendix 3. Electron Microprobe Analyses of Silicate and Oxide Minerals 101
Appendix 4. Sulphide Mineral Analyses 104
Appendix 5. Whole Rock Analyses 105
Appendix 6. Petrographic Data for Rainy Lake Mineralization 107
Appendix 7. Assay Data for Typical Mineralized Rainy Lake Ore Specimens 109
Appendix 8. Lead Isotopic Data and Sample Location Descriptions 114
References 116
Metric Conversion Table 121

FIGURES

1. General geological map of the western Wabigoon Subprovince and its margins 4
2. Stratigraphic columns, western Wabigoon Subprovince 5
3. Regional geology along the Wabigoon–Quetico subprovince margin 7
4. Distribution of mineralization along the Wabigoon–Quetico subprovince margin 9
5. Generalized lithologic map of the Mine Centre–Fort Frances area 12

6. Plot of whole rock geochemical data for volcanic and plutonic rocks 15

7. Modal Q-A-P plot for Rainy Lake granitoid rocks 17

8. Histograms showing modal proportions of clasts of different composition in the Seine conglomerate 18

9. Sketch maps showing field relationships at the Rice Bay Dome, Morton Island, Ottertail Lake intrusion and the Golden Star Mine 23

10. Summary map showing the location and boundaries of lithostratigraphic domains 25

11. Stratigraphic columns for individual lithostratigraphic domains 27

12. Structural and geophysical trends at the subprovince boundary at Rainy Lake 30

13. Schematic diagram showing the attitudes, facing directions and extent of individual stratigraphic markers in the Rainy Lake area 31

14. Morphological features, orientations and shear sense of Rainy Lake shear zones 35

15. Structural geology of the Nickel Lake synform, Swell Bay syncline and Shoal Lake synclinorium 39

16. Equal-area stereographic projections of D_3, S_2, F_2 and L_2 structural elements 40

17. Contoured equal-area projection of S_2 and L_2 data, and interpretation 41

18. Summary of fabric element orientation relative to the boundaries of lithostratigraphic domains 42

19. Selected structural cross sections for the Rainy Lake area 43

20. Wrench fault models 43

21. Block diagram summarizing the geology near the Rice Bay Dome, and interpretation 44

22. Metamorphic map of the Mine Centre–Fort Frances area 46

23. P-T diagram showing the estimated range of metamorphic conditions in the Rainy Lake area, and AFM diagrams for the ideal pelitic system showing the compositions of coexisting minerals in biotite schists in the Redgut Bay area 51

24. Histogram of analyses of FeS in sphalerite from Nickel Lake, ACF diagram for calc-silicate assemblages in skarn-like rocks from Pocket Pond and T-X_{CO_2} diagram for the assemblage calcite + clinozoisite + grossularite 53

25. Summary map showing the distribution of mineral deposits in the study area 56

26. Cross sections through the main showings at Gagne Lake and Wind Bay prospects, and assay plan of the Port Arthur Copper Co. Mine 59

27. Pb versus Cu+Zn content of volcanic-associated base metal sulphide mineralization, and whole rock chemical Riverin–Hodgson plots of "fresh" and chemically "altered" samples from the Gagne Lake and Wind Bay prospects 66

28. Schematic diagram illustrating the stratigraphic position and relative spacing of base metal deposits associated with felsic rocks in the Rainy Lake area 67

29. Cross section showing the position of mineralized zones at the Pocket Pond prospect, and stratigraphic columns showing the immediate host rocks for sulphide mineralization associated with mafic volcanic rocks 69

30. Summary geological map and schematic cross section of the Grassy Portage intrusion 74

31. Summary geological maps of the North Rock Mine and Mironsky prospect 76

32. Schematic plan showing the geometry of veins associated with shear zones at Rainy Lake, and detailed geological maps of the vein systems at Foley and Manhattan mines 81

33. Whole rock chemical Riverin–Hodgson plots for "fresh" and "altered" specimens associated with gold-bearing quartz veins, and Au versus Cu+Zn in specimens of sulphide mineralization at Rainy Lake 86

34. Graph of $^{207}Pb/^{204}Pb$ versus $^{206}Pb/^{204}Pb$ lead isotopic ratios in galena from Rainy Lake gold-bearing quartz veins and base metal deposits 87

35. Schematic diagrams illustrating growth curves and isochrons in lead isotope systems, "secondary" isochrons for lead isotope data, binary mixing of lead isotopes and complex mixing of lead isotopes 88

36. Schematic diagrams illustrating the volcano-sedimentary and tectonic phases of mineralization 90
37. Schematic diagrams illustrating the relationship of "pull-apart" basins to transcurrent faults, a comparison between fault systems along the southern Wabigoon margins and younger examples, potential displacement magnitudes in the Atikokan–Fort Frances area and probable orientations and shear sense of faults and shear zones in the Wabigoon Subprovince 92
38. Geological compilation map, Wabigoon Subprovince and its margins 94
A1.1 Summary map of the study area showing the sources of information used for compilation of Map 2525 98

PHOTOS

1. Pillowed metabasalt, Pocket Pond 14
2. Flow-banded, spherulitic rhyolite, Barber Lake area 14
3. Ultramafic clastic rock, Grassy Portage Bay area 15
4. Bundle of graded beds, Bear Passage 16
5. Scour at the base of a thick graded bed, Morton Island 16
6. Coarse-grained anorthosite, Bald Island, Seine Bay 17
7. Equigranular tonalite, Bad Vermilion–Shoal lakes area 18
8. Polymictic Seine conglomerate, Shoal Lake area 19
9. Cross-bedding in arenites, north of Shoal Lake 19
10. Agmatitic breccia, western margin of the Ottertail Lake pluton 20
11. Mylonite, Northeast Bay, Rainy Lake 32
12. Asymmetrical folds in mylonite, Northeast Bay, Rainy Lake 32
13. Protomylonite, Crowrock Inlet 32
14. Ductile shear zone in metagabbro, Bad Vermilion Lake 34
15. Ductile shear zone displacing igneous layering in gabbro, Redgut Bay, Rainy Lake 34
16. Planar fabric in deformed Seine conglomerate near Mine Centre 36
17. Elongate clasts in plane of foliation, in Seine conglomerate near Mine Centre 36
18. Elongate basaltic pillows near Nickel Lake 37
19. Axial planar cleavage in folded Coutchiching wackes, Morton Island shoal 37
20. Kink bands developed on flattened clasts in Seine conglomerate near Glenorchy Road 38
21. Superposition of cleavages in folded Coutchiching wackes northeast of Swell Bay 38
22. Chloritoid schist showing postkinematic texture, Shoal Lake area .. 47
23. Staurolite-garnet-biotite schist, Redgut Bay area 48
24. Weak retrograde alteration of staurolite in biotite schist, Redgut Bay area 48
25. Retrograde alteration of staurolite and garnet in biotite schist, Redgut Bay area 49
26. Helicitic inclusion trails in synkinematic garnet from biotite schist near Nickel Lake 50
27. Coexisting andalusite and fibrous sillimanite, Redgut Bay area 50
28. Siltstone that forms the hanging-wall unit, Gagne Lake prospect ... 60
29. Breccia at Gagne Lake composed of siltstone clasts in an altered spotted matrix of "dalmatianite" 60
30. Massive sulphide clast in polymictic breccia, Gagne Lake prospect . 61
31. Amygdaloidal volcanic rocks, Port Arthur Copper Co. Mine 61
32. Pyritic cherty "exhalite" that overlies the ore zone, Port Arthur Copper Co. Mine 62
33. Coarse felsic-clast breccia with chloritic and pyritic matrix in footwall mineralization at Wind Bay ... 62

34. Sphalerite-galena laminae in siltstone beds, Gagne Lake 63
35. Polymetallic sulphide ore, Gagne Lake prospect 63
36. Sphalerite and chalcopyrite seams in chloritic phyllite, Wind Bay prospect 64
37. Sulphide-silicate intergrowths, Wind Bay prospect 64
38. Sulphide "stringers" in relatively competent quartz-chlorite unit, main pit, Wind Bay 65
39. Dalmatianite in diamond-drill core, Gagne Lake prospect 67
40. Metamorphosed chert-magnetite iron formation, No.9 zone, Pocket Pond prospect 68
41. Types of mineralization associated with iron formation in mafic volcanic rocks 70
42. Garnet-epidote intergrowth, calc-silicate rock, Pocket Pond 71
43. Triple junction termination of sphalerite-pyrite-pyrrhotite 71
44. Arsenopyrite euhedra in pyrrhotite 72
45. Metamorphosed sphalerite-pyrrhotite ore, main showing, Pocket Pond 72
46. Modal layering of plagioclase and hornblende in metagabbro, Redgut Bay 75
47. Net textures, disseminations and stringers in chalcopyrite ore, North Rock Mine 75
48. Photomicrograph of cubanite lamellae in chalcopyrite, North Rock Mine 77
49. Pentlandite in pyrrhotite, North Rock Mine 77
50. Magnetite-apatite intergrowths, Traverse Inlet prospect 79
51. Rutile masses, Traverse Inlet prospect 79
52. Principal laminated vein in shear zone, Cone prospect 82
53. Principal laminated vein in shear zone with foliation-parallel third-order veins, Stellar Mine 82
54. Cleavage-parallel quartz vein, Olive Mine 83
55. Deformational textures in vein quartz 83
56. Ankerite "fibers" in quartz, South Vermilion Mine 84
57. Native gold intergrown with galena, Cone prospect 84
58. Undeformed equigranular tonalite, Cone prospect 85
59. Deformed equivalent of Photo 58 tonalite adjacent to a gold-bearing quartz vein 85

TABLES

1. Summary of geochronological data from Rainy Lake and surrounding areas 8
2. Lithologic units for the Mine Centre–Fort Frances area, Rainy Lake 13
3. Comparative stratigraphic interpretations, Rainy Lake area 22
4. Characteristics of lithostratigraphic domains, Rainy Lake 26
5. Relative chronology of folds and fabric elements in the Rainy Lake area 39
6. Metamorphic mineral assemblages, Mine Centre–Fort Frances area, Rainy Lake 47
7. Pelite geothermometry and geobarometry at Redgut Bay 52
8. Mineral deposits classification, Mine Centre–Fort Frances area 55
9. Mineralogical compositions of rocks in the Grassy Portage intrusion 75
10. Lithologic controls on gold-bearing quartz veins, Rainy Lake 80
11. Lithologic, metamorphic and metallogenic characteristics of contrasting types of tectonostratigraphic domains at Rainy Lake 89
12. Summary of tectonic models for the origin of the Wabigoon Subprovince and its margins 91
A2.1 Petrographic data, metamorphic rocks, Rainy Lake 99

A3.1 Average mineral analyses for pelites, Redgut Bay 101
A3.2 Electron microprobe analysis of coexisting garnet-biotite pairs in pelites, Redgut Bay 102
A3.3 Mineral analyses and structural formulae, calc-silicate rocks, Pocket Pond 103
A3.4 Mineral analyses from ultramafic schist, Grassy Portage area 103
A3.5 Mineral analyses from hornblende gabbro, Grassy Portage intrusion 103
A4.1 Analyses of Nickel Lake sphalerites 104
A4.2 Arsenopyrite analyses 104
A5.1 Whole rock analyses of "fresh" and "altered" rocks associated with base metal mineralization 105
A5.2 Whole rock analyses of "fresh" and "altered" rocks associated with gold mineralization 106
A6.1 Modal estimates of sulphide and oxide minerals in ore specimens, volcanic-hosted mineralization 107
A6.2 Modal estimates of sulphide and oxide minerals in ore specimens, Grassy Portage intrusion 108
A7.1 Assay data for base metal mineralization of felsic volcanic association 110
A7.2 Assay data for base metal mineralization of mafic volcanic association 111
A7.3 Assay data for copper mineralization in the Grassy Portage intrusion 112
A7.4 Assay data for gold-bearing quartz veins, Shoal Lake area 113
A8.1 Lead isotope analyses of galena for Rainy Lake mineralization 115

GEOLOGICAL MAP

Map 2525 – Precambrian Geology and Mineral Occurrences, Mine Centre–Fort Frances Area, scale 1:50 000 .... back pocket

Foreword

This report was written when the author was employed by the Ontario Geological Survey to do a metallogenic investigation of the Mine Centre–Fort Frances area. The report and map were submitted in the 1980s, but editing and production were delayed by priorities related to the Geology of Ontario Special Volume project. The report is still the most comprehensive investigation of this area and we are thus proud to have it appear in final form.

Archean Metallogeny of the Mine Centre–Fort Frances Area

K. H. Poulsen

Manuscript approved for publication by B.O. Dressler, Supervising Geologist, Precambrian Geology Section, Ontario Geological Survey, June 30, 1989. Report published with the permission of the Senior Manager, Precambrian Geoscience Section, Ontario Geological Survey.

Abstract

The rocks of the Rainy Lake area are part of the Archean Superior Province and form a fault-bounded wedge between 2 subprovinces, the Wabigoon granite-greenstone terrane to the north and the Quetico metasedimentary terrane to the south. The Quetico and Rainy Lake–Seine River faults define this wedge, which is interpreted to be a dextral wrench zone and which displays distinct stratigraphic, structural and metamorphic relationships.

Historically, the interpretation of the stratigraphy within this zone has been contentious. In the east, volcanic rocks and coeval tonalitic sills are unconformably overlain by conglomerates and arenites, while to the west, volcanic rocks, as well as wackes and mudstones that conformably succeed them, are cut by granodiorite plutons. Within this zone, direct correlation between the plutonic suites and between the sedimentary facies is difficult: external correlation with rocks in either subprovince is even more difficult.

Structurally, the systematic orientations of both ductile and brittle features are consistent with progressive shortening within the boundary zone about a west-northwest–east-southeast axis. Three structural elements have been recognized in the area: a) early, possibly recumbent folds, followed by b) upright northeasterly trending folds with well-developed cleavage, which are in turn followed by c) northwesterly striking kink bands and crenulation cleavage. Shear zones and faults also conform to the strain pattern of the wrench zone.

Metamorphic assemblages in the study area indicate temperatures of 400 to 600°C at pressures of approximately 3 kilobars. Regional metamorphism accompanied ductile deformation, and a northward increase in metamorphic grade within the zone contrasts with a similar southward increase in the Quetico Subprovince.

The stratigraphic, structural and metamorphic discordances at Rainy Lake result from tectonic activity localized along the subprovince boundary. Evidence of progressive horizontal tectonic transport within this zone suggests juxtaposition of the 2 subprovinces.

The fault-bounded wedge is characterized by an anomalous concentration of economic minerals. Stratiform volcanic-hosted mineralization consists of ironstones, base metal sulphides and intercalations of the two. Four subtypes are recognized:

1. Narrow lenses of zinc-lead sulphide mineralization (Gagne Lake type) are overlain by chert and underlain by sulphide-bearing, altered lapilli tuff, which locally consists of the assemblage chlorite + cordierite + anthophyllite.
2. Wide zones of low-grade zinc-copper sulphide mineralization (Port Arthur Copper type) consist of 1 to 20 cm wide seams of massive sphalerite-chalcopyrite-pyrite that are intercalated with similar widths of barren chlorite schist. The host rock is commonly a brecciated amygdaloidal mafic metavolcanic rock, but felsic metavolcanic rocks occur both above and below the mineralized horizon.
3. Zinc-copper mineralization (Pocket Pond type) is found in black pyritic shale and in massive pyrite-pyrrhotite lenses that are conformable to chert-magnetite ironstones.
4. Ironstones composed of chert-magnetite, massive sulphide mineralization, and minor skarn commonly contain only traces of chalcopyrite.

Layered gabbro-anorthosite sills contain both sulphide and oxide mineralization. Chalcopyrite-pyrrhotite lenses containing minor cubanite, pentlandite, molybdenite, apatite and ilmenite are distributed along the base of the Grassy Portage intrusion, the most economic concentrations composing the North Rock deposit of 300 000 t grading 1.89% copper. This type of mineralization displays magmatic net and droplet textures, as well as local zones of remobilized sulphide minerals and hydrothermal alteration. At a higher stratigraphic level in the intrusion, lower grade copper mineralization is found within a siliceous host, which may represent assimilated country rock. Iron-titanium oxide mineralization also occurs as massive magnetite-ilmenite and as irregular masses of nelsonite, a rutile-bearing rock. Oxide mineralization is also well developed in the Seine Bay anorthositic sill.

Quartz vein mineralization is of 2 types. Molybdenite, along with pyrite and local chalcopyrite, occurs in quartz stockworks and extensional veins within granodioritic intrusions near contacts with the metasedimentary country rocks. In contrast, gold, along with carbonates and base metal sulphide minerals, occurs in lenticular quartz veins associated with shear zones and regional cleavage. Gold-bearing veins occur in a variety of rock types and are restricted to zones of greenschist facies metamorphism.

A distinctive clastic ultramafic unit, which is exposed within the mafic portion of the volcanic succession, is likely of epiclastic origin, and is compositionally magnesian (21% MgO). Local zones of foliated ultramafic rock within this unit contain disseminated nickel-copper sulphide mineralization, which may result from metamorphic remobilization.

The various types of mineralization at Rainy Lake can be related to the geological evolution of the rocks of the region. Early volcanism and related hydrothermal activity generated stratiform iron and base metal mineralization. Coeval subvolcanic sills, which possibly drove convective systems, differentiated to yield magmatic sulphide and oxide concentrations. Granodiorite intruded the supracrustal sequence after initial folding, and local stockworks developed near pluton contacts. Continued folding and metamorphism, and juxtaposition of contrasting deposit types took place within a tectonic wrench zone, generating gold-bearing veins in dilational structures, and remobilizing existing mineralization. Copper is the only commodity common to all environments of mineralization, which may reflect the importance of rifts in the early history of the region.

Poulsen, K. H. 2000. Archean metallogeny of the Mine Centre–Fort Frances area; Ontario Geological Survey, Report 266, 121p.

Introduction

Situated at the boundary between the Wabigoon and Quetico structural subprovinces of the Superior Province, the Rainy Lake area has played a significant role in the evolution of ideas about the Archean geology of the Canadian Shield. It was here that Lawson (1913) proposed a stratigraphic "type" section for Archean greenstone belts, which was hotly debated because it implied widespread sedimentation prior to volcanism and the presence of a pre-existing Archean crust. Although the notion of a single Archean "type" section has become obsolete, the debate about the significance of the earliest Archean crust is still much in vogue (Baragar and McGlynn 1978; Glikson 1978). Furthermore, the Rainy Lake area remains notable in that: a) examples of all of the major rock types that are common to Archean terranes, in general, occur here within a relatively small area; and b) an anomalous concentration of mineral deposits of diverse character is localized along the subprovince boundary at Rainy Lake. While little production has been realized from them, many of these deposits are of sufficient quality to have attracted substantial exploration activity, on a nearly continuous basis, since 1893.

The present study examines the setting of mineralization in relation to the tectonic history of an area approximately 1000 km^2 in extent, between 2 major faults at the subprovince boundary. The results of the study are based primarily on field observations coupled with petrographic studies and a limited number of chemical analyses. The study emphasizes stratigraphy, structure and metamorphism, and their relationship to the mineral deposits. Field work was carried out during the summers of 1980 and 1981.

The study area had been mapped previously by a number of geologists at various scales, most recently by Harris (1974) and Wood et al. (1980a, 1980b) at a scale of 1 inch to 1/4 mile (1:15 840). While there has been general agreement on the distribution of rock types, complex structures have locally obscured primary stratigraphic relationships. These relationships were re-examined at several key localities, and new mapping by the author is integrated with the previous mapping, with the results interpreted on a 1:50 000 scale compilation map (Map 2525, back pocket). As only limited structural information was found on existing maps, mesoscopic-scale structural data were collected at representative localities across the entire study area. In addition, recently published aeromagnetic and electromagnetic data (Ontario Geological Survey 1980), which cover most of the study area, have been analyzed to identify geophysical marker units, which along with the analysis of minor structures and lithologic data, have assisted in establishing a structural interpretation for the area.

Field and petrographic data have been collected from pelites, metabasites, impure carbonates and "altered" felsic metavolcanic rocks to establish the metamorphic grade and the distribution of metamorphic assemblages throughout the area. The petrographic studies were supplemented by a study of the mineral chemistry of a suite of selected fresh specimens with the objective of interpreting the conditions and timing of metamorphism.

Approximately 85 mineral prospects were examined during the course of the field work. The quality of information that was obtained for an individual occurrence varied considerably. In some cases, extensive surface development and diamond drilling provided relatively detailed sampling, while other occurrences were merely overgrown pits and shafts which were developed in the 1890s. As an investigation of the mineralization is the major objective of the report, the following levels of documentation have been established:

1. a description of the individual occurrences, with emphasis on host rock type, deposit morphology, structures and mineralogy, thus forming a database for subsequent work (*see* Poulsen 2000)
2. a classification of the mineralization based on descriptive criteria
3. establishment of a descriptive model for each deposit class, and investigation of common characteristics and deviations from the norm. Emphasis has been placed on stratigraphic, structural and metamorphic features as well as on wall-rock alteration and isotopic composition of galena where applicable, of occurrences that are economically most significant and are best exposed

The studies of tectonics and mineralization serve as a database for an interpretation of the metallogeny of the Rainy Lake area. Aspects of metallogeny that have been treated include:

1. genetic models for each deposit class by comparison with similar, previously documented examples
2. the place of mineralization in the geological history of the area
3. the comparison of the metallogeny of the area with that of other Archean and post-Archean terranes
4. constraints on tectonic models imposed by metallogenic patterns

ACKNOWLEDGMENTS

H. Helmstaedt and J. Hodgson of Queen's University, Kingston supervised the field and laboratory work leading to this report. Field work was supported by the Mineral Deposits Section, Ontario Geological Survey. A.C. Colvine, C.E. Blackburn and J. Wood of the Ontario Geological Survey were generous in their advice and comments throughout the study, and the report has benefited from numerous discussions with them.

R. Thorpe and J. Franklin, Geological Survey of Canada, provided the lead isotope analyses along with much needed advice on their interpretation. S. Spivak, Lakehead University, Thunder Bay, drafted most of the figures that accompany the report. W. Clendinning and G. Laws provided able field assistance. Finally, the study benefited greatly from the co-operation of numerous exploration groups, prospectors and residents in the Mine Centre–Fort Frances area.

General Geology

INTRODUCTION

The study area is located at the transition between the Wabigoon granite-greenstone terrane to the north and the Quetico metasedimentary-gneissic terrane to the south. The lack of consensus on the position and nature of the subprovince boundary (Kehlenbeck 1976; Blackburn and Mackasey 1977) requires that general characteristics of each subprovince be considered, as well as the geology of the study area, including relevant aspects of immediately adjacent parts of both subprovinces.

WABIGOON SUBPROVINCE

The Wabigoon granite-greenstone terrane is exposed for a length of 900 km and a width of 150 km. The western half of the subprovince (Figure 1) consists essentially of synclinal cusps of metavolcanic and metasedimentary supracrustal rocks occurring marginal to oval batholithic complexes composed of quartzofeldspathic gneisses and granitoid rocks. The supracrustal rocks face away from the batholithic complexes to form the steeply dipping limbs of the synclines. Amphibolite facies metamorphic assemblages are common near the batholithic margins, and metamorphic grade decreases toward the axial surface traces of the synclines (Ayres 1978). Each limb contains one or more lithostratigraphic groups with apparent stratigraphic thicknesses that greatly exceed indicated depth extent (Dusanowskyi and West 1976), but lack of marker horizons and lateral continuity makes classical stratigraphic correlation among groups very difficult. In some areas, provisional stratigraphic order has been established (Figure 2), and broad evolutionary trends have been noted (Trowell, Blackburn and Edwards 1980).

Most of the volcanic sequences in the Wabigoon Subprovince have thick extensive mafic units at the base, which are succeeded by central volcanic edifices composed mainly of felsic fragmental rocks. In some areas, cyclical repetition of this sequence is indicated (Franklin et al. 1977). The lowermost sequences are exemplified by the Jutten group, Botham Bay volcanics, Eagle Lake volcanics, Wapageisi group, Snake Bay group and the Katimiagamak Lake group. All are apparently greater than 5 km thick and are characterized by massive and pillowed mafic flows, gabbroic sills and minor tuffaceous units with interbedded chemical sediments. Plagioclase-phyric basalts are common. Chemical studies of the lowermost sequences (Trowell, Blackburn and Edwards 1980) indicate that they have the characteristics of magnesian tholeiitic basalts. Unique ultramafic rocks have been identified. A submarine platformal environment of deposition is indicated.

At higher stratigraphic levels, units such as the Handy Lake, South Sturgeon, Upper Manitou, Kakagi, and parts of the Manitou and Stormy Lake groups are characterized by thick local accumulations of intercalated mafic flows and fragmental felsic volcanic rocks. Cyclical volcanism is common and deposition of the felsic components has been variously attributed to air falls, lahars, debris and ash flows, and epiclastic sedimentation. Intercalated shallow-water to subaerial sedimentary rocks (Teal and Walker 1977) indicate that these sequences were locally emergent. Felsic intrusions that have been interpreted to be subvolcanic commonly cut the volcanic sequences, which are chemically variable and appear to be composed of intercalated tholeiitic and calc-alkalic suites (Trowell, Blackburn and Edwards 1980).

In at least 4 areas of the Wabigoon Subprovince, thick mafic flow sequences apparently overlie the intercalated mafic and felsic units. These are rather monotonous sequences that are relatively iron rich compared to the lowermost mafic volcanic rocks. They have been identified as iron tholeiites based on their major element chemistry (Trowell, Blackburn and Edwards 1980).

Sedimentary rocks form substantial parts of the stratigraphic sequences and are particularly common stratigraphically above the intercalated mafic and felsic groups. Bedded graded wackes and siltstones with load casts, flame structures, convolute laminations and scours have been interpreted to be turbidites that are coeval with the Handy Lake volcanics in the Savant Lake area (Shegelski 1978). Similar turbidites are associated with graded resedimented granitic-clast conglomerates in the Minnitaki group near Sioux Lookout (Walker and Pettijohn 1971). In the same area, the Ament Bay formation of the Abram group contains nongraded cross-stratified sandstones with nongraded conglomerates. These are interpreted to constitute a subaerial alluvial fan (Turner and Walker 1973). Similar facies are recorded in the Stormy Lake group with an additional laminated siltstone-argillite unit that is interpreted to be lacustrine (Teal and Walker 1977).

The batholithic complexes are greater than 50 km in diameter and are commonly composed of smaller bodies such as gneissic domes up to 10 km wide, central batholiths, and marginal crescent-shaped granitoid intrusions. The Aulneau batholithic complex has been shown to contain up to 19 crosscutting granitoid phases (Ziehlke 1974). The larger batholithic complexes and the smaller internal gneissic domes have been interpreted as first-order and second-order gneiss diapirs, respectively. They are thought to be the products of gravitational, solid-state remobilization of tabular batholiths that were initially emplaced beneath the supracrustal sequences (Sutcliffe 1978; Schwerdtner et al. 1979; Schwerdtner and Lumbers 1980). Small felsic plutons locally cut the batholiths as well as the supracrustal sequences (Birk 1978; Birk and McNutt 1981).

Recent advances in zircon U-Pb techniques (Davis and Edwards 1982; Davis and Trowell 1982; Davis, Blackburn and Krogh 1982) have provided high-precision age determinations (*see* Figure 2) that clarify the time span of development of volcanic and sedimentary sequences and

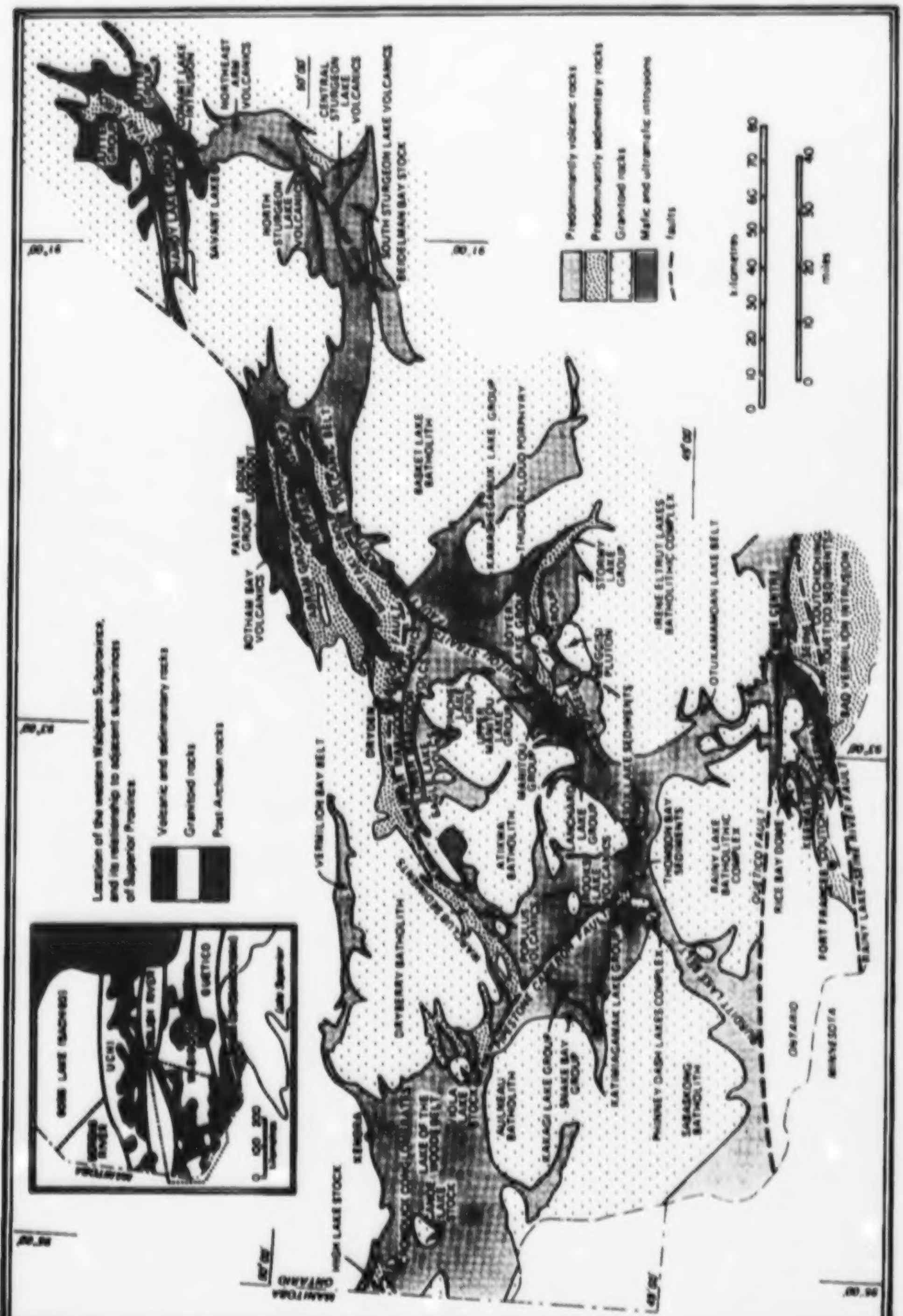
Location of the western Wabigoon Subprovince, and its relationship to adjacent subprovinces of Superior Province
Volcanic and sedimentary rocks
Granitoid rocks
Post Archean rocks
Predominantly volcanic rocks
Predominantly sedimentary rocks
Granitoid rocks
Mafic and ultramafic intrusions
faults
kilometres
0 10 20 30 40 50 60 70 80
miles
0 10 20 30 40
MANITOBA
ONTARIO
MINNESOTA

Figure 1. General geological map of the western Wabigoon Subprovince and its margins.

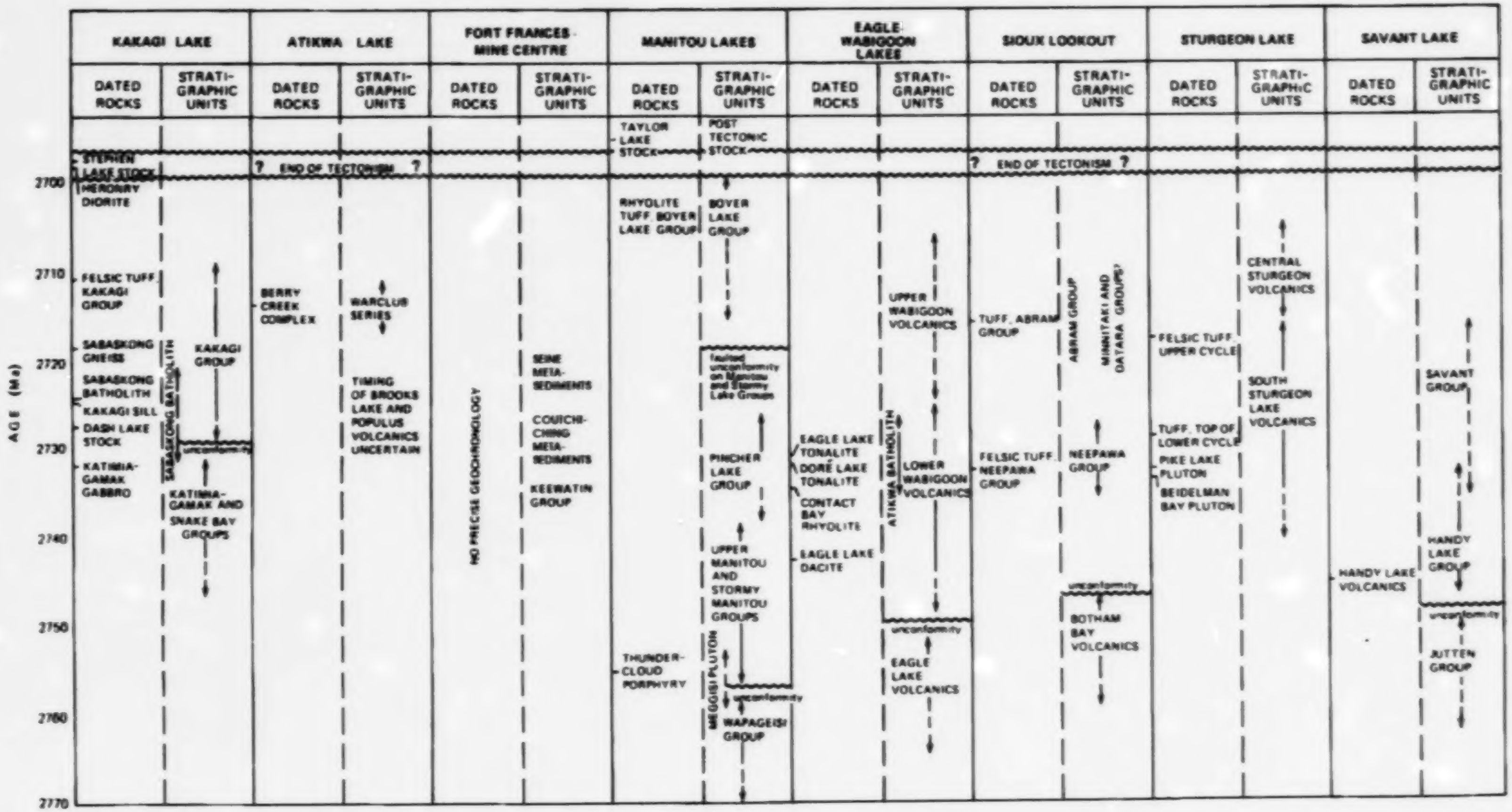
KAKAGI LAKE
ATIKWA LAKE
FORT FRANCES - MINE CENTRE
MANITOU LAKES
EAGLE-WABIGOON LAKES
SIOUX LOOKOUT
STURGEON LAKE
SAVANT LAKE
DATED ROCKS
STRATI-GRAPHIC UNITS
AGE (Ma)
2700
2710
2720
2730
2740
2750
2760
2770
STEPHEN LAKE STOCK
HERONRY DIORITE
FELSIC TUFF KAKAGI GROUP
SABASKONG GNEISS
SABASKONG BATHOLITH
KAKAGI SILL
DASH LAKE STOCK
KATIMIA-GAMAK GABBRO
SABASKONG BATHOLITH
KAKAGI GROUP
unconformity
KATIMIA-GAMAK AND SNAKE BAY GROUPS
? END OF TECTONISM ?
BERRY CREEK COMPLEX
WARCLUB SERIES
TIMING OF BROOKS LAKE AND POPULUS VOLCANICS UNCERTAIN
NO PRECISE GEOCHRONOLOGY
SEINE META-SEDIMENTS
COUTCHI-CHING META-SEDIMENTS
KEEWATIN GROUP
TAYLOR LAKE STOCK
POST TECTONIC STOCK
RHYOLITE TUFF BOYER LAKE GROUP
BOYER LAKE GROUP
faulted unconformity on Manitou and Stormy Lake Groups
PINCHER LAKE GROUP
UPPER MANITOU AND STORMY MANITOU GROUPS
THUNDER-CLOUD PORPHYRY
MEGGISI PLUTON
unconformity
WAPAGEISI GROUP
EAGLE LAKE TONALITE
DORÉ LAKE TONALITE
CONTACT BAY RHYOLITE
EAGLE LAKE DACITE
ATIKWA BATHOLITH
UPPER WABIGOON VOLCANICS
LOWER WABIGOON VOLCANICS
unconformity
EAGLE LAKE VOLCANICS
? END OF TECTONISM ?
TUFF, ABRAM GROUP
FELSIC TUFF, NEEPAWA GROUP
ABRAM GROUP
MINNITAKI AND DATARA GROUPS?
NEEPAWA GROUP
unconformity
BOTHAM BAY VOLCANICS
FELSIC TUFF, UPPER CYCLE
TUFF, TOP OF LOWER CYCLE
PIKE LAKE PLUTON
BEIDELMAN BAY PLUTON
CENTRAL STURGEON VOLCANICS
SOUTH STURGEON LAKE VOLCANICS
HANDY LAKE VOLCANICS
SAVANT GROUP
HANDY LAKE GROUP
unconformity
JUTTEN GROUP

Figure 2. Stratigraphic columns for supracrustal sequences, western Wabigoon Subprovince.

their relationships to each other, to subjacent batholithic and subvolcanic rocks, and to rocks external to the subprovince. Several significant conclusions have emerged from this work:

1. An upper limit to supracrustal development is given by the age of 2695±3.6 Ma for the posttectonic Taylor Lake stock.
2. The oldest supracrustal rocks predate 2755 Ma, the minimum age of the Thundercloud porphyry, which cuts the Wapageisi mafic volcanic rocks.
3. Major batholiths were emplaced between 2730 and 2725 Ma. This age range is comparable to that from a subjacent rhyolite from the Lower Wabigoon volcanics (2735±4 Ma).
4. Mafic magnesian units such as the Wapageisi, Jutten and Eagle groups are all older than 2740 Ma.
5. The mixed tholeiitic and calc-alkalic sequences developed between 2755 and 2711 Ma, with greatest volcanic activity at around 2730 Ma.

QUETICO SUBPROVINCE

The supracrustal rocks of the Quetico Subprovince are dominantly metasedimentary biotite schists of turbidite origin, which strike parallel to the subprovince margin. The metasedimentary strata commonly display well-developed graded bedding indicating that younging directions, despite some reversals, are dominantly northward (Hawley 1930a; Merritt 1934; Ojakangas 1972; Harris 1974; Wood et al. 1980a, 1980b; Borradaile 1982). Toward the south of the subprovince, the metasedimentary rocks become migmatitic, and primary structures and cleavage are obscured. Schist-rich and granite-rich migmatites possess bedding-parallel foliations, which are folded into large, open, shallow-plunging structures that trend east (Southwick 1972; Southwick and Sims 1980). Massive granitoid bodies of irregular shape are commonly found at the core of the major antiforms. In the west, these granites occur within a migmatitic terrane, the Vermilion granitic complex, which occupies the central part of the Quetico Subprovince.

Mineral assemblages of the metasedimentary biotite schists are indicative of a southward increase in metamorphic grade (Pirie and Mackasey 1978): pelitic rocks with greenschist facies assemblages (chlorite + sericite, chlorite + biotite) are found just to the south of the subprovince boundary, whereas amphibolite facies assemblages (biotite + cordierite + staurolite + garnet + sillimanite) have been observed in the central part of the subprovince (Southwick 1976; Pirie and Mackasey 1978). The observed sequence of assemblages is consistent with moderate metamorphic pressures of 2 to 4 kilobars and temperatures ranging as high as 600°C. Geochronological data from this part of the Quetico Subprovince show that most igneous and metamorphic events were broadly contemporaneous with those in the Wabigoon Subprovince.

SUBPROVINCE BOUNDARY

In the vicinity of Atikokan, the boundary between the Wabigoon and Quetico subprovinces is abrupt (Figure 3) and is generally thought to correspond to a single structure, the Quetico Fault (Hawley 1930b). Farther west, at Rainy Lake, a wedge of crust bounded by 2 faults forms the subprovince boundary. The northernmost Quetico Fault (Parkinson 1962) and the southernmost Rainy Lake–Seine River fault converge eastward toward the single Quetico Fault of Hawley (1930b), a fact that has caused some confusion in nomenclature (Fumerton 1982). The fault-bounded crustal wedge contains, for the most part, lithologic units similar to those in the Wabigoon Subprovince, but shows structural and metamorphic similarities to both subprovinces.

Several aspects of the geology of this crustal wedge have been described previously. Hsu (1971) and Jackson (1982) carried out strain studies on conglomerates within the eastern part of the wedge, where pebble shapes indicate a flattening type of strain. Poulsen (1980a) recognized inverted stratigraphic panels in the vicinity of the Rice Bay Dome (*see* Figure 3) and showed that the structure is much more complicated than was previously assumed. Kennedy (1984) carried out a detailed study of mylonites associated with the Quetico Fault: minor folds and brittle faults, strain patterns and magnetic fabric all suggest dextral displacements along this fault. Pseudotachylite has also been observed (Borradaile and Kennedy 1982).

The metamorphic petrology of the rocks in this area has not been studied in great detail, but since the earliest mapping, diagnostic minerals in pelitic rocks have been noted. Cordierite (Lawson 1913), staurolite and garnet (Bruce 1925a), and andalusite and sillimanite (Poulsen 1980a) have been reported in the Rice Bay–Bear Passage area (*see* Figure 3). Peterman (1959) and Poulsen (1980a) contrasted the amphibolite facies assemblages of this area with assemblages of a lower grade of metamorphism in an area to the southeast of Rice Bay. Wood et al. (1980a, 1980b) reported the presence of chloritoid in metavolcanic rocks, indicative of greenschist facies, farther to the east near Mine Centre.

Geochronological data from the area (Hart and Davis 1969; Peterman et al. 1972; Davis et al. 1980; Birk and McNutt 1981) are summarized in Table 1. A wide range of ages (2752 to 2380 Ma) has been determined. The oldest zircon ages are thought to represent a period of igneous activity equivalent to that recorded in the interior of the Wabigoon Subprovince. The 2670 Ma zircon ages for metavolcanic rocks within the boundary zone (Goldich and Peterman 1980) are somewhat younger than those from other Wabigoon metavolcanic rocks (Davis et al. 1980). Isotopic data, along with rare earth element geochemistry (Shirey and Hanson 1982, 1983), have also been used for petrogenetic interpretation. Low values for oxygen isotope compositions and initial strontium ratios for the Ottertail Lake, Rest Island, and Bear Passage plutons (*see* Figure 3) indicate a lower crust or mantle source for these granitoid rocks (Longstaffe and Birk 1981). Single Sm-Nd (2.72±0.6 Ga) and Rb-Sr (2.69±0.10 Ga) isochrons (Ashwal et al.

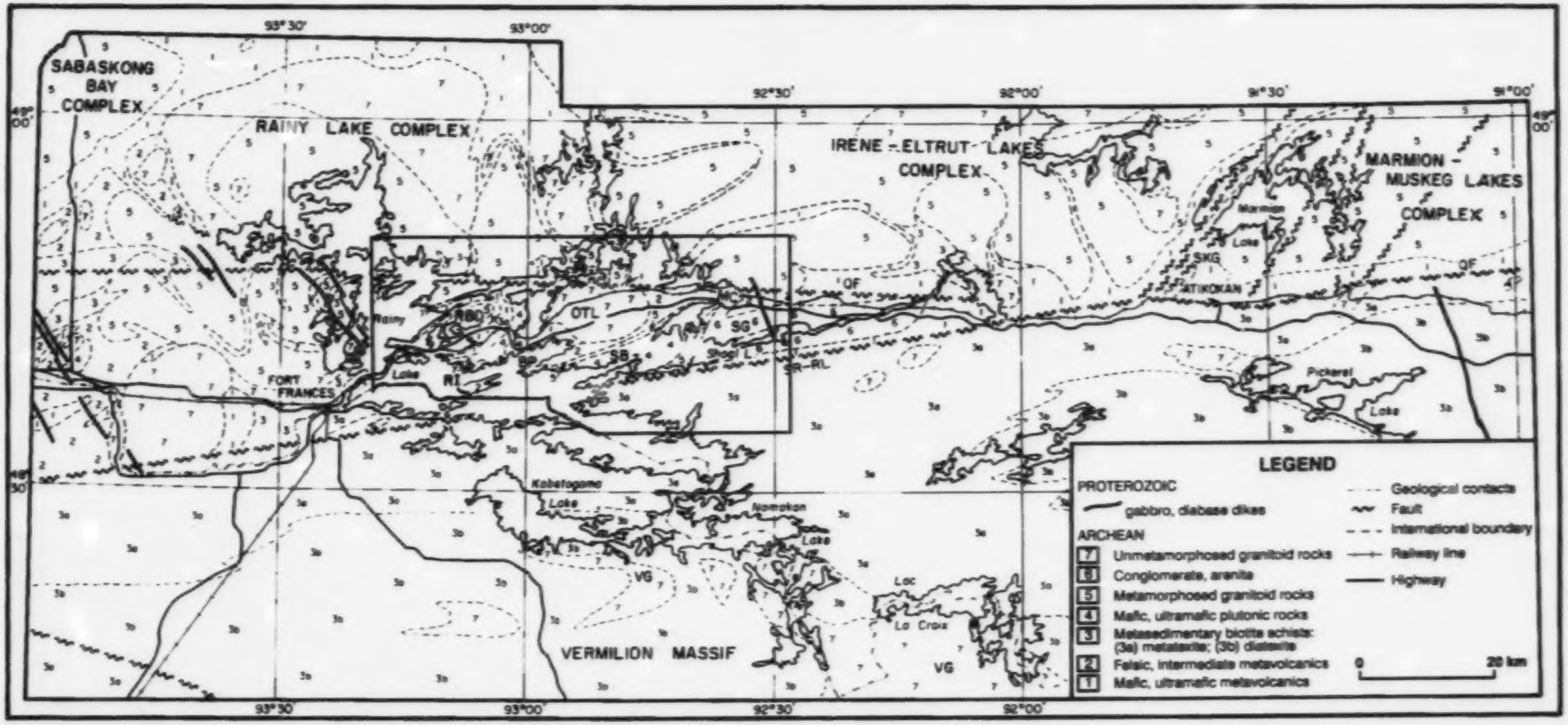
93°30'
93°00'
92°30'
92°00'
91°30'
91°00'
49° 00'
48° 30'
SABASKONG BAY COMPLEX
RAINY LAKE COMPLEX
IRENE – ELTRUT LAKES COMPLEX
MARMION – MUSKEG LAKES COMPLEX
Marmion Lake
SKG
ATIKOKAN
QF
Rainy Lake
RBD
RI
BP
OTL
SB
MC
SG
Shoal L.
SR–RL
FORT FRANCES
Pickerel Lake
Kabetogama Lake
Namakan Lake
Lac La Croix
VG
VERMILION MASSIF
LEGEND
PROTEROZOIC
gabbro, diabase dikes
ARCHEAN
7 Unmetamorphosed granitoid rocks
6 Conglomerate, arenite
5 Metamorphosed granitoid rocks
4 Mafic, ultramafic plutonic rocks
3 Metasedimentary biotite schists: (3a) metatexite; (3b) diatexite
2 Felsic, intermediate metavolcanics
1 Mafic, ultramafic metavolcanics
Geological contacts
Fault
International boundary
Railway line
Highway
0
20 km

Figure 3. Regional geology along the Wabigoon–Quetico subprovince margin, Atikokan–Fort Frances area of Ontario and adjacent parts of Minnesota. Heavy line outlines the area of the present study. Major features include the Steep Rock Group (SKG), Seine metasediments (SG), Vermilion granite (VG), Rice Bay Dome (RBD), Bear Passage (BP), Rest Island (RI), Ottertail Lake (OTL), Seine Bay (SB), Mine Centre (MC), Quetico Fault (QF) and Rainy Lake–Seine River fault (SR-RL).

Table 1. Summary of geochronological data from Rainy Lake and surrounding areas.

Lithologic Units	**Method/Age (Ma)**			**Reference**
	K–Ar	**Rb–Sr**	**U–Pb**	
Wabigoon Subprovince				
Batholith Complexes				
Sabaskong:				
granodiorite gneiss	2580 (Bi)			Peterman et al. 1972
hornblende biotite trondhjemite	2752 (Zi)			Davis et al. 1980
Rainy Lake:				
total complex (pooled)		2561±66 (9,WR)		
Stocks, small granitoid intrusions				
Phinney–Dash Lake (trondhjemite)		2732.1±2.3(Zi)		Davis et al. 1980
Burditt Lake		2543±45(9,WR)		Birk and McNutt 1981
Esox Lake		2518±42(4,WR)		Birk and McNutt 1981
Ryckman Lake		2554±63(7,WR)		Birk and McNutt 1981
Barwick (gneissic quartz monzonite)	2390 (Bi)			Peterman et al. 1972
Mine Centre–Fort Frances				
Metavolcanic Rocks	2380(WR)	2540±45(WR)	2670	Peterman et al. 1972
Metasedimentary Biotite Schists		2690(Mu)	2670	Peterman et al. 1972
Metamorphosed Granitoid Rocks				
Bad Vermilion intrusion		2467 (WR)	2670	Hart and Davis 1969
Grey gneiss, Rice Bay	2680(Mu)	2560 (WR)	2670	Peterman et al. 1972
Unmetamorphosed Granitoid Rocks				
(pooled)		2485±90(WR)	2670	Peterman et al. 1972
Rest Island		2403±104(WR)		Birk and McNutt 1981
Ottertail Lake		2461±78(WR)		Birk and McNutt 1981
Bear Pass		2654±158(WR)		Birk and McNutt 1981
	2540(Mu)			Peterman et al. 1972
Quetico Subprovince				
Quetico Metasediments				
Biotite schist (Sapawe)	2460(Bi)			Peterman et al. 1972
Migmatites, gneisses				
quartz–oligoclase–microcline–muscovite–garnet gneiss (Sapawe)	2630(Mu)	2640(Mu)		Peterman et al. 1972
Granitoid Rocks				
Vermilion granite (two samples from Rainy Lake area)		2625±95(10)		Peterman et al. 1972

Zi = zircon mineral ages
Bi = biotite mineral ages
Mu = muscovite mineral ages
WR = whole rock ages
Note: Numbers in parentheses indicate number of samples analyzed.

1981) from anorthosite at Seine Bay (*see* Figure 3) provided initial isotopic ratios indicative of a depleted mantle source for these rocks.

The area along the subprovince boundary, between Atikokan and Fort Frances and adjacent parts of Minnesota, was the site of intensive prospecting for gold in the 1890s. Gold production in the interval 1893 to 1902 came principally from 2 areas, Mine Centre and Atikokan; these were known as the Lower Seine and Upper Seine gold regions, respectively. Total production at that time and during subsequent activity was about 25 000 ounces of gold and 3000 ounces of silver. The deposits are concentrated along the subprovince boundary and are related spatially to the major faults and their splays (Figure 4).

In the early part of the twentieth century, some exploration for iron in this region resulted in limited production from the Atikokan Iron Co. mine, near Sapawe, between 1907 and 1911. The major iron ore deposits at Steep Rock Lake were developed during World War II and production began in 1945, continuing until 1979. Low-grade

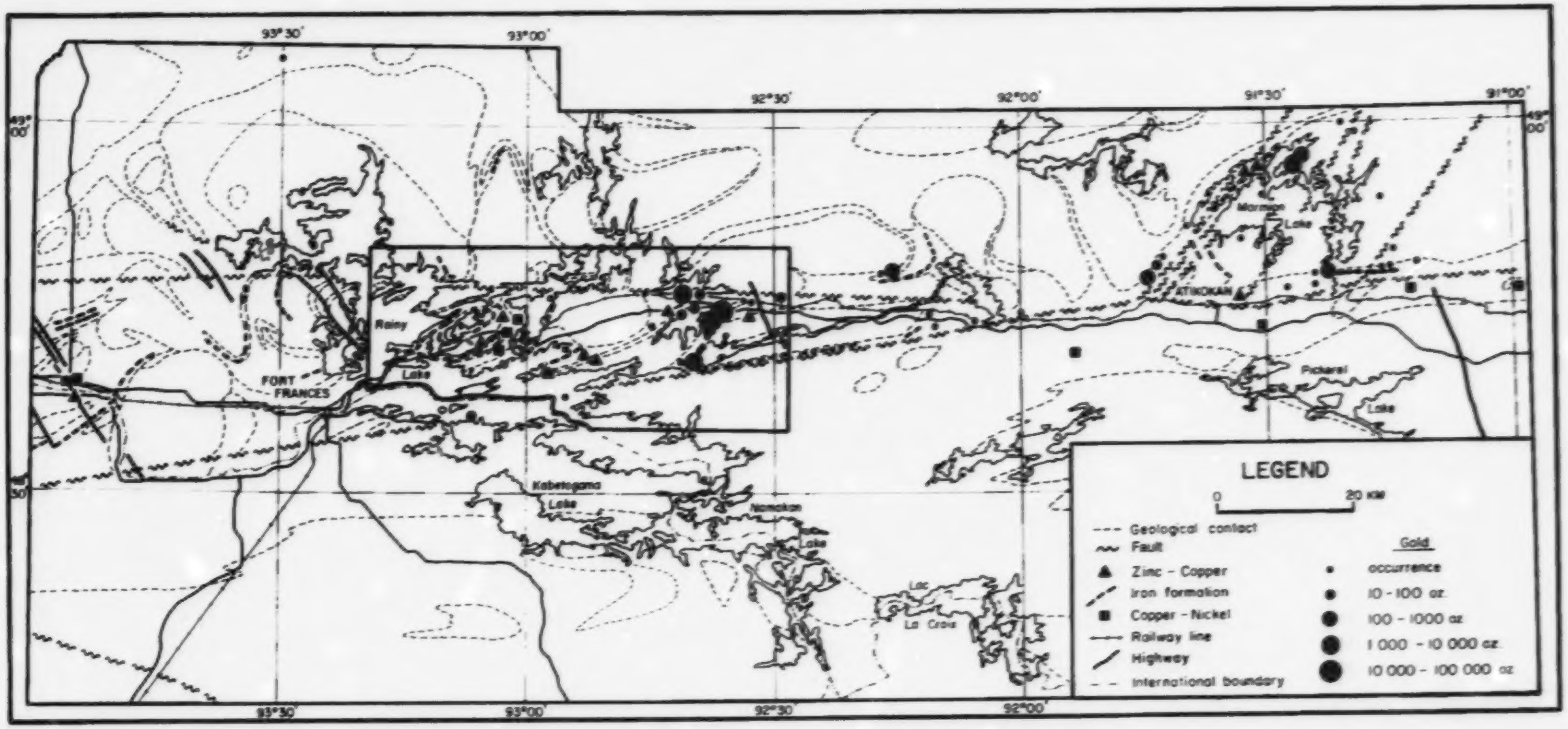
93°30'
93°00'
92°30'
92°00'
91°30'
91°00'
49°00'
48°30'
FORT FRANCES
Rainy Lake
Kabetogama Lake
Namakan Lake
Lac La Croix
ATIKOKAN
Marmion Lake
Pickerel Lake
LEGEND
0
20 km
Geological contact
Fault
Zinc - Copper
Iron formation
Copper - Nickel
Railway line
Highway
International boundary
Gold
occurrence
10 - 100 oz
100 - 1000 oz
1 000 - 10 000 oz
10 000 - 100 000 oz

Figure 4. Distribution of mineralization along the Wabigoon–Quetico subprovince margin, Atikokan–Fort Frances area of Ontario and adjacent parts of Minnesota. Heavy line outlines the area of the present study. Other symbols and lithology as in Figure 3.

iron formations are also common in the region, and tend to be concentrated near the subprovince boundary.

Several significant prospects containing base metals have also been discovered. Two broad types are present: zinc-copper mineralization occurs at specific horizons within the metavolcanic successions, and copper-nickel mineralization is associated with mafic and ultramafic rocks, particularly intrusions (*see* Figure 4). Although some of these prospects have been extensively developed, very limited base metal production has been reported from this region. Clearly there is a strong spatial correlation between known mineralization and the subprovince boundary.

Stratigraphy

LITHOLOGIC UNITS

The stratigraphy of Archean rocks at Rainy Lake has long proved to be a source of controversy. The mapping of Lawson (1889, 1913) established the first stratigraphic nomenclature, which was based upon the principles of structural superposition and crosscutting relationships. Subsequent disagreements resulted when new localities were considered or where the relationships at the original localities were reinterpreted. While Lawson's original stratigraphic interpretation largely prevailed until recently (Poulsen 1980a; Wood et al. 1980a, 1980b), there has been a proliferation of rival interpretations over the years. As a basis for stratigraphic discussion, Map 2525 (back pocket) was compiled by the author, based principally on recent mapping by the Ontario Geological Survey (Harris 1974; Poulsen 1980b, 1981; Wood et al. 1980a, 1980b). Appendix 1 contains background information to accompany the map, including sources of data, rules of nomenclature and an index to the locations of previously published maps.

The distribution of the main lithologic units is generalized in Figure 5. A revised table of lithologic units (Table 2) broadly portrays regional relationships but does not represent a strict stratigraphic column for the entire Rainy Lake region since direct stratigraphic correlation across the numerous faults in the area is not possible. Generalized descriptions of each of the major lithologic types are given below.

Mafic Metavolcanic Rocks

Metamorphic rocks of andesite to basalt composition are common, both as the dominant rock types in certain areas and as intercalations with felsic, intermediate and ultramafic rocks in others. These rocks are chlorite-bearing in the greenschist facies, and are either hornblende-bearing (iron-rich) or actinolite-bearing (magnesium-rich) basalts in the amphibolite facies. Pillowed flows are moderately common (Photo 1) and varioles, hyaloclastite and amygdules were noted locally.

Intermediate Metavolcanic Rocks

An elongate unit, in which rocks of dacite to andesite composition are common, extends northeastward from Sandpoint Island to Mine Centre (*see* Figure 5). Intercalated with these rocks of intermediate composition are minor mafic and felsic metavolcanic rocks. Chloritic clastic rocks and amygdaloidal flows are common, while pillowed flows are rare, particularly near Mine Centre. This may reflect a shallow water to subaerial depositional environment for the unit in that area. The stratigraphically highest unit within the intermediate metavolcanic rocks in the Sandpoint Island–Mine Centre area is a distinctive chloritic breccia that is directly overlain by felsic metavolcanic rocks. To the north and west of the Rice Bay Dome (at Rice Bay, *see* Figure 5), highly deformed quartz-biotite amphibolites of this unit retain relict clastic structures and are provisionally interpreted to be of similar original lithology to the units of intermediate composition at Mine Centre.

Felsic Metavolcanic Rocks

Flows and fragmental rocks of rhyolite to dacite composition are exposed in a continuous unit that extends from the Seine Bay area northeastward through Mine Centre and past the eastern margin of the map area (*see* Figure 5). Flows are common, particularly in the Mine Centre area where the thickest accumulation of felsic rocks is recorded. Volcanic structures are common and include flow lamination, autobreccias and spherulites (Photo 2). Southwestward from Mine Centre, the felsic sequence thins gradually, with tuffs and lapilli tuffs becoming more dominant. These rocks are interpreted to have been formed at a greater distance from a centre of volcanism than those at Mine Centre. Rocks of felsic composition also occur intercalated with rocks of mafic and intermediate composition at lower stratigraphic levels. Elsewhere, minor felsic metavolcanic rocks have been observed west of Rice Bay, south of Ottertail Lake, and in a narrow unit extending eastward from the northeastern corner of Shoal Lake; these units are of limited extent and none but the latter are distinguished on Map 2525.

Ultramafic Metavolcanic Rocks

A unique ultramafic unit occurs in the Redgut Bay–Grassy Portage Bay area (*see* Figure 5). Rocks from this unit have distinctive textures as well as a magnesian chemical composition; samples plot as basaltic komatiites (Figure 6a). Locally, the rock consists of angular to subrounded fine-grained clasts, up to 5 cm in diameter, set in a fine-grained chlorite-tremolite matrix (Photo 3). The rocks are moderately to strongly magnetic and, where visible fragments are not present, they are fine-grained magnetic tremolite schists. As a whole, this ultramafic unit strongly resembles the "ashrock" unit (Joliffe 1955) that overlies the iron ore horizon of the Steep Rock Group north of the Quetico Fault at Atikokan, 100 km to the east (*see* Figure 3).

Metamorphosed Chemical Sediments and Intercalated Clastic Rocks

Iron-bearing chemical metasedimentary rocks are common constituents of the volcanic sequences, particularly those dominated by mafic and ultramafic metavolcanic rocks (*see* Figure 5). The ironstones include magnetitic chert, pyritic slate, massive pyrite-pyrrhotite lenses and minor pyrrhotite-bearing marble. Chert occurs with-

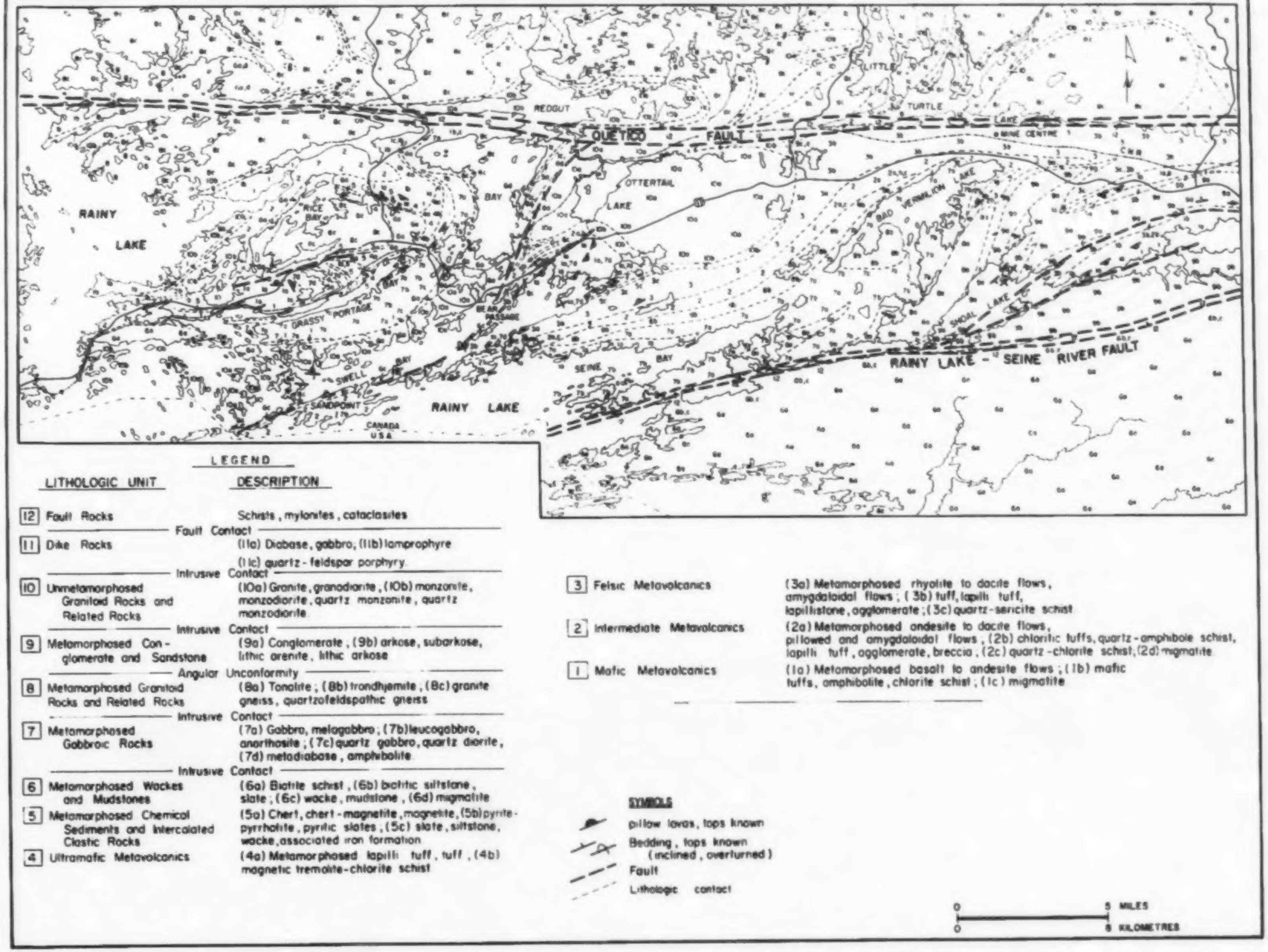
RAINY
LAKE
REDGUT
LITTLE
TURTLE
LAKE
QUETICO
FAULT
MINE CENTRE
CNR
OTTERTAIL
LAKE
BAY
RICE
BAY
GRASSY PORTAGE
BAY
SWELL
BAY
SANDPOINT
BEAR
PASSAGE
BAD
VERMILION
LAKE
SHOAL
LAKE
SEINE
BAY
RAINY LAKE - SEINE RIVER FAULT
RAINY LAKE
CANADA
USA
LEGEND
LITHOLOGIC UNIT
DESCRIPTION
12 Fault Rocks
Schists, mylonites, cataclasites
Fault Contact
11 Dike Rocks
(11a) Diabase, gabbro; (11b) lamprophyre
(11c) quartz-feldspar porphyry.
Intrusive Contact
10 Unmetamorphosed Granitoid Rocks and Related Rocks
(10a) Granite, granodiorite, (10b) monzonite, monzodiorite, quartz monzonite, quartz monzodiorite
Intrusive Contact
9 Metamorphosed Conglomerate and Sandstone
(9a) Conglomerate; (9b) arkose, subarkose, lithic arenite, lithic arkose
Angular Unconformity
8 Metamorphosed Granitoid Rocks and Related Rocks
(8a) Tonalite; (8b) trondhjemite; (8c) granite gneiss, quartzofeldspathic gneiss
Intrusive Contact
7 Metamorphosed Gabbroic Rocks
(7a) Gabbro, melagabbro; (7b) leucogabbro, anorthosite; (7c) quartz gabbro, quartz diorite, (7d) metadiabase, amphibolite
Intrusive Contact
6 Metamorphosed Wackes and Mudstones
(6a) Biotite schist, (6b) biotitic siltstone, slate; (6c) wacke, mudstone, (6d) migmatite
5 Metamorphosed Chemical Sediments and Intercalated Clastic Rocks
(5a) Chert, chert-magnetite, magnetite, (5b) pyrite-pyrrhotite, pyritic slates, (5c) slate, siltstone, wacke, associated iron formation
4 Ultramafic Metavolcanics
(4a) Metamorphosed lapilli tuff, tuff, (4b) magnetic tremolite-chlorite schist
3 Felsic Metavolcanics
(3a) Metamorphosed rhyolite to dacite flows, amygdaloidal flows; (3b) tuff, lapilli tuff, lapillistone, agglomerate; (3c) quartz-sericite schist
2 Intermediate Metavolcanics
(2a) Metamorphosed andesite to dacite flows, pillowed and amygdaloidal flows; (2b) chloritic tuffs, quartz-amphibole schist, lapilli tuff, agglomerate, breccia; (2c) quartz-chlorite schist; (2d) migmatite
1 Mafic Metavolcanics
(1a) Metamorphosed basalt to andesite flows; (1b) mafic tuffs, amphibolite, chlorite schist; (1c) migmatite
SYMBOLS
pillow lavas, tops known
Bedding, tops known (inclined, overturned)
Fault
Lithologic contact
0
5 MILES
0
8 KILOMETRES

Figure 5. Generalized lithologic map of the Mine Centre–Fort Frances area. *Based on* mapping by Blackburn (1973), Harris (1974), Poulsen (1980b, 1981) and Wood et al. (1980a, 1980b).

Table 2. Lithologic units of the Mine Centre–Fort Frances area, Rainy Lake.

PHANEROZOIC

CENOZOIC

QUATERNARY

RECENT
Lake, stream and swamp deposits

PLEISTOCENE
Till, sand, gravel and lake deposits

PRECAMBRIAN

PROTEROZOIC

Fault Rocks
Schists, mylonites, cataclasites developed in heterogeneous rock types

Dike Rocks
Diabase, gabbro, lamprophyre, quartz-feldspar porphyry

ARCHEAN

NEOARCHEAN

Unmetamorphosed Granitoid Rocks and Related Rocks
Granite, granodiorite, monzonite, monzodiorite, quartz monzonite, quartz monzodiorite

Metamorphosed Conglomerate and Sandstone
Conglomerate, arkose, subarkose, lithic arenite, lithic arkose

Metamorphosed Granitoid Rocks and Related Rocks
Tonalite, trondhjemite, granite gneiss, quartzofeldspathic gneiss[c]

Metamorphosed Gabbroic Rocks
Gabbro, melagabbro, leucogabbro, anorthosite, quartz gabbro, quartz diorite, metadiabase[b], amphibolite

Metamorphosed Wackes and Mudstones
Biotite schist, biotitic siltstone, slate, wacke, mudstone, migmatite (biotitic paleosome)

Metamorphosed Chemical Sediments and Intercalated Clastic Rocks[a]
Chert, chert-magnetite, magnetite, pyrite-pyrrhotite, pyritic slate, slate, siltstone, wacke, associated iron formation

Ultramafic Metavolcanic Rocks
Metamorphosed lapilli tuff, tuff, magnetic tremolite-chlorite schist

Felsic Metavolcanic Rocks[a]
Metamorphosed rhyolite to dacite flows, amygdaloidal flows, tuff, lapilli tuff, lapillistone, agglomerate, quartz-sericite schist

Intermediate Metavolcanic Rocks[a]
Metamorphosed andesite to dacite flows, pillowed and amygdaloidal flows, chloritic tuff, lapilli tuff, quartz-amphibole schist, agglomerate, breccia, quartz-chlorite schist, migmatite

Mafic Metavolcanic Rocks[a]
Metamorphosed basalt to andesite flows, mafic tuff, amphibolite, chlorite schist, migmatite (amphibolitic paleosome)

Notes: (a) While the table represents the broad stratigraphic order among these rock types, local intercalation of rock types is common.
(b) Sills of this type are common throughout the volcanic succession and constitute a substantial fraction of the total thickness of metavolcanic rock.
(c) This is not necessarily orthogneiss.

out ironstone as beds intercalated with siltstone at the top of the felsic metavolcanic succession along the southern shore of Swell Bay. Clastic metasedimentary rocks are associated with most occurrences of chemical metasedimentary rocks and include siltstones, slates and siliceous biotite schists.

Metamorphosed Wackes and Mudstones

The rocks of this unit have been referred to historically as the Coutchiching Group in the Rainy Lake region (Lawson

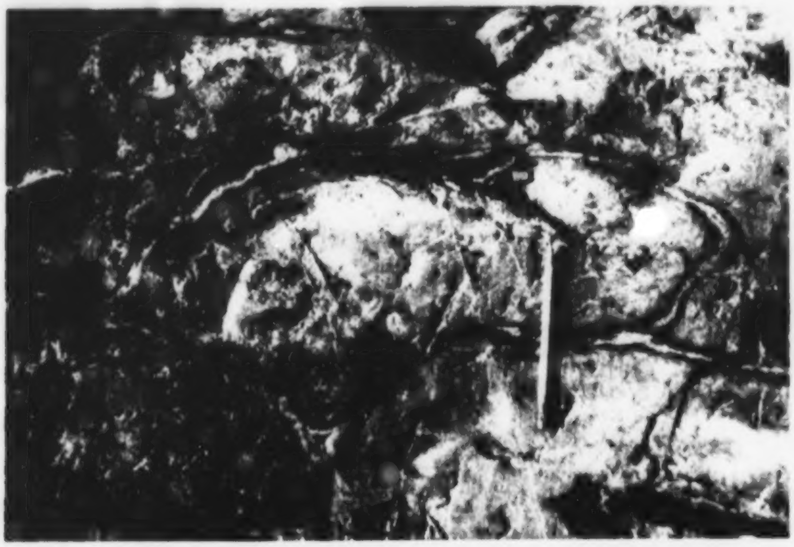

Photo 1. Pillowed metabasalt, Pocket Pond. Despite amphibolite facies metamorphism and moderate deformation, younging direction indicators are well preserved. Pencil is 15 cm long.

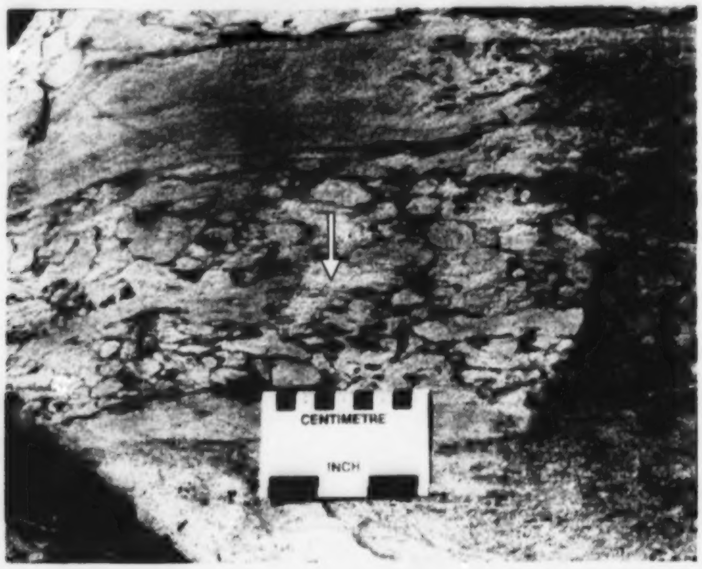

Photo 2. Flow banded, spherulitic rhyolite, Barber Lake area. Note that the spherulitic structures replace faintly laminated pumiceous rhyolite (arrow).

1913). Current appellation refers to them as Coutchiching metasediments. They form the bulk of the sedimentary component of the Quetico Subprovince to the south of the boundary zone where they are referred to informally as Quetico metasediments (Wood 1980). In addition, 2 extensive units of similar lithologic composition occur north of the Rainy Lake–Seine River fault within the boundary zone: one encircles the Rice Bay domal structure, while the other extends through the islands of Swell Bay to Bear Passage and Ottertail Lake. At the former locality, the metasedimentary rocks are metamorphosed to amphibolite facies assemblages and few primary structures are preserved; at the latter, metamorphic grades are lower and massive beds, graded "abe" Bouma sequences (Photo 4), scours (Photo 5), shale rip-ups and flame structures may be observed. Such primary features are also present in the Quetico metasediments (Ojakangas 1972; Wood 1980).

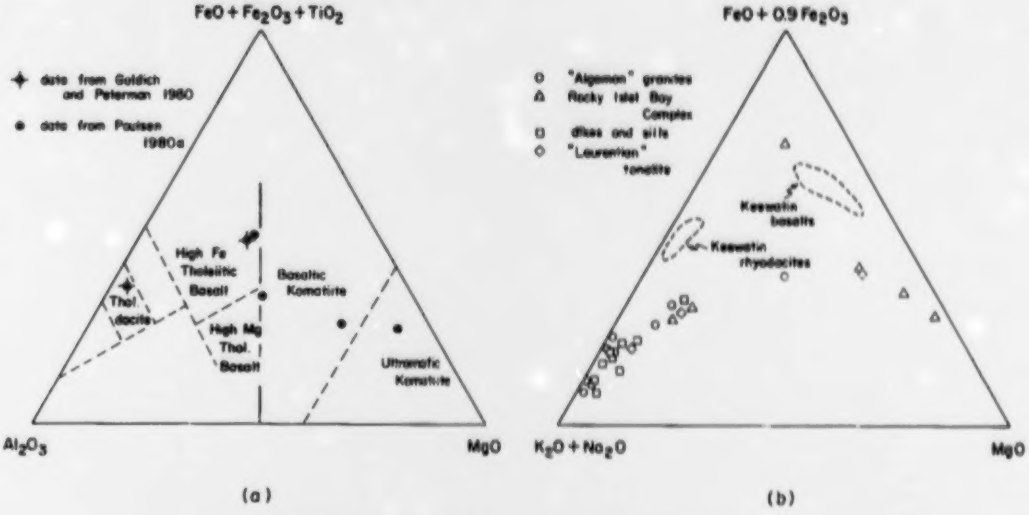

Figure 6. Plot of whole rock geochemical data for volcanic and plutonic rocks.

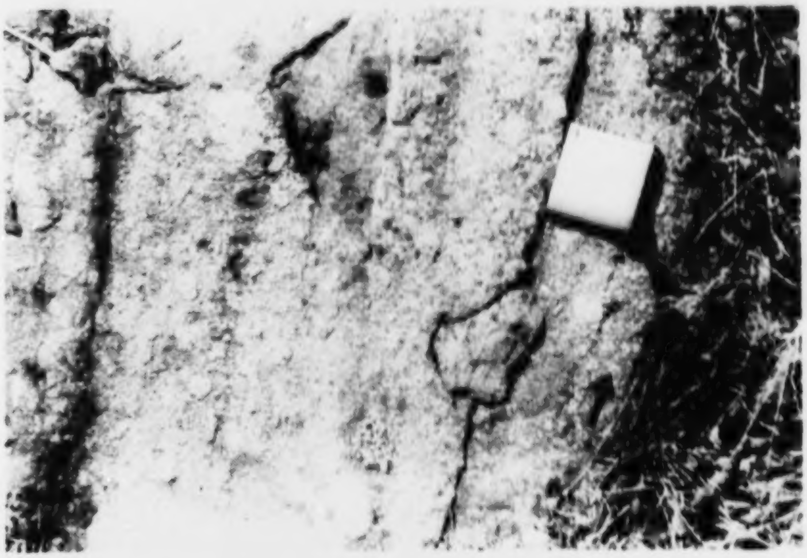

Photo 3. Ultramafic clastic rock, Grassy Portage Bay area. Most fragments are compositionally homogeneous, but some are zoned and contain darker amphibolitic cores (arrow). Compass is 7.5 cm wide.

The Coutchiching metasediments consist dominantly of feldspathic wacke and mudstone with rare feldspathic arenite and quartz arenite. Quartz clasts rarely show undulose extinction, low to intermediate anorthite compositions for plagioclase are common, and rock fragments are rare. A volcanic provenance has been suggested (Ojakangas 1972), and at several key localities within the study area stratigraphic superposition of these rocks upon volcanic rocks has been demonstrated (Poulsen, Borradaile and Kehlenbeck 1980). Wood (1980) has emphasized, however, that predepositional reworking or a quartz-rich source area are required to explain the composition of these sedimentary rocks. Further, the precise structural and stratigraphic relationships between the Quetico metasediments and rocks of similar type within the boundary zone are uncertain due to the intervening Rainy Lake–Seine River fault.

Metamorphosed Gabbroic Rocks

Two large, steeply dipping, layered gabbroic sills, the Grassy Portage and Seine Bay–Bad Vermilion intrusions, are exposed within the study area. Layering is expressed by modal variations in mineralogy, chemical variations

Photo 4. Bundle of graded beds, Bear Passage. Note that the darker pelitic tops of the beds are enhanced by staurolite porphyroblasts. The coin is 2.1 cm in diameter.

across strike and locally by rhythmic mineral layering. Rock compositions range from melagabbro to anorthosite (Photo 6), with plagioclase compositions in the range An_{45-80}. Both intrusions display systematic internal variations in composition, which, when compared to other intrusions of similar type, suggest that the Grassy Portage intrusion faces southward while the Seine Bay–Bad Vermilion sill faces northward. Much of the base of the latter intrusion is truncated by the Rainy Lake–Seine River fault, while the upper contact is with a sill of trondhjemite (unit 9, Map 2525) of unknown genetic relationship to the gabbroic rocks. In addition to the large intrusions, numerous small sills and dikes cut the metavolcanic and metasedimentary sequence. They are commonly 50 to 100 m thick and are composed of medium-grained, massive to strongly foliated amphibolite that locally resembles metadiabase. There is some compositional differentiation across the strike of many of the wider intrusions, with the development of quartz-plagioclase-magnetite accumulations toward the upper margins of the sills. Weak to moderate magnetism and irregular patches and veins of epidote-rich alteration are characteristic of these intrusions.

Metamorphosed Granitoid Rocks and Related Rocks

The medium- to coarse-grained quartzofeldspathic rocks in the Rainy Lake area have been divided historically into 2 broad groups, the Algoman and Laurentian granites of Lawson (1913). The Algoman intrusions (unit 12, Map 2525) form discrete plutons and are relatively unmetamorphosed, while the Laurentian granites (unit 9) are commonly foliated or lineated. While this criterion is satisfactory for field recognition, the metamorphosed and deformed Laurentian-type granitoid rocks possess other features that are equally diagnostic: a) they tend to be relatively poor in potassium feldspar and relatively rich in

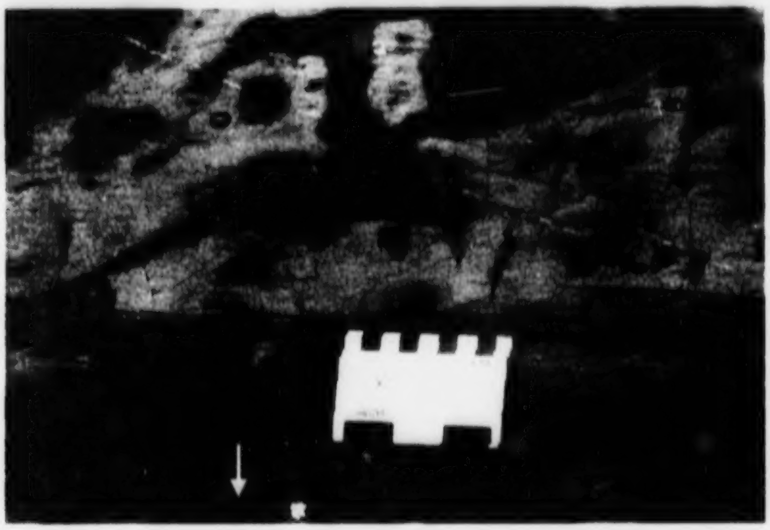

Photo 5. Scour at the base of a thick graded bed, Morton Island.

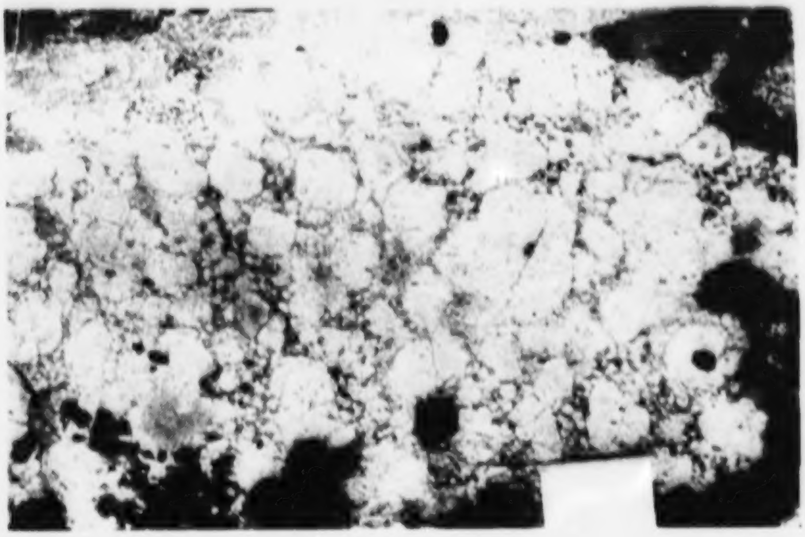

Photo 6. Coarse-grained anorthosite, Bald Island, Seine Bay. Plagioclase megacrysts (An_{80}) and the mafic matrix composed of chlorite and actinolite have a crushed and fractured appearance. Compass is 7.5 cm wide.

quartz as compared to the Algoman-type granitoid rocks (Figure 7); and b) they form bodies that are broadly conformable to layering in enclosing country rocks.

There are 3 areas within the study area in which significant volumes of this rock type are exposed: a) the Bad Vermilion Lake area, b) the Rice Bay Dome area, and c) the Black Sturgeon Bay area.

In the Bad Vermilion Lake area, 2 extensive sills, the Mud Lake trondhjemite and the Bad Vermilion tonalite, as well as several smaller bodies, intrude volcanic and gabbroic rocks. The sills are conformable to their host rocks, and only rare dikes of similar granitic composition have been observed cutting the country rocks. The trondhjemite is medium grained while the tonalite is coarse grained (Photo 7). Intensely foliated equivalents of both rock types are locally developed in shear zones.

In the Rice Bay Dome area, 3 specific rock types are present: a) quartz-plagioclase-mica schists and gneisses, b) quartz-poor mafic schists and gneisses, and c) dikes and sills of metamorphosed quartz-feldspar porphyry. The first is volumetrically dominant and has been variously interpreted as an orthogneiss (Lawson's (1913) Laurentian granite) or as a metasedimentary paragneiss (Peterman et al. 1972; Harris 1974; Goldich and Peterman 1980). Recent studies (Poulsen 1980a, 1980b; Poulsen, Borradaile and Kehlenbeck 1980) indicate that the quartz-plagioclase-mica gneiss is texturally and compositionally distinct from both the metasedimentary rocks of the region and those rocks that are clearly plutonic. Relict fragmental textures suggest a felsic volcanic origin for some of these rocks.

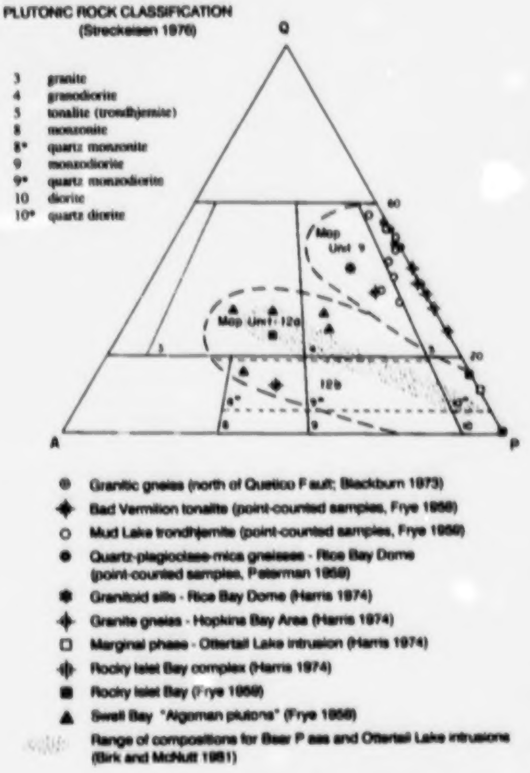

Figure 7. Modal Q-A-P plot for Rainy Lake granitoid rocks.

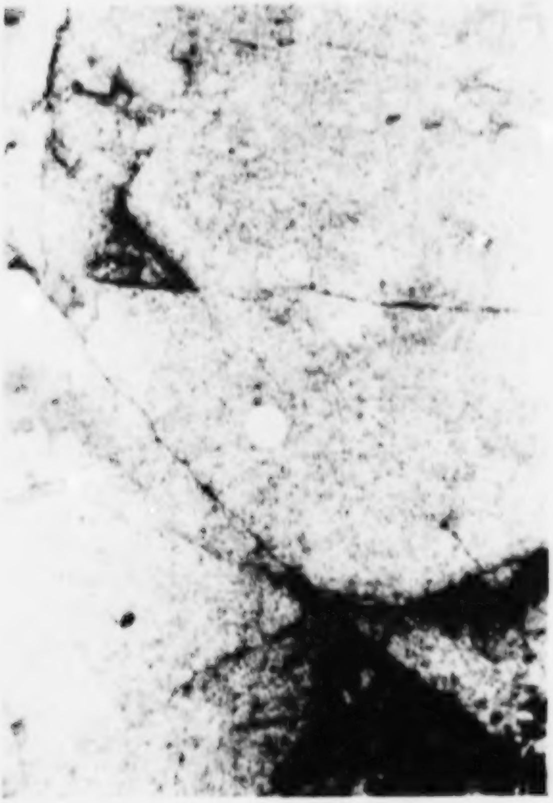

Photo 7. Equigranular tonalite, Bad Vermilion Lake intrusion, north of the Foley Mine. In foliated equivalents, the quartz grains (grey) are preserved to give a pseudo-porphyritic appearance. Coin is 2.4 cm in diameter.

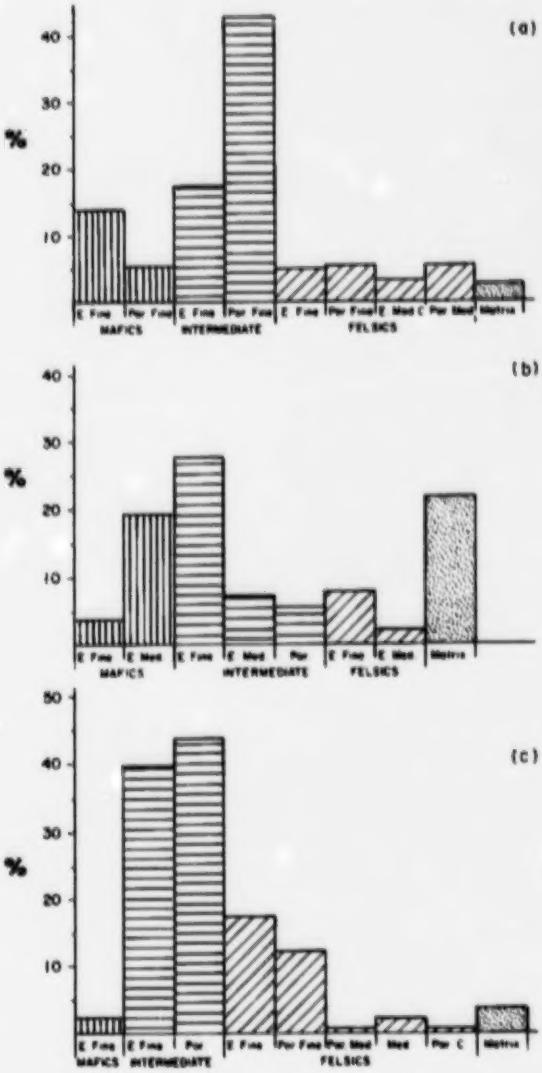

Figure 8. Histograms showing modal proportions of clasts of different composition of the Seine conglomerate, at 3 localities (*after* Wood 1980). E=equigranular, Por=porphyritic, Med=medium-grained, C=coarse-grained.

In the Black Sturgeon Bay area, a pear-shaped body of granite gneiss approximately 10 km in diameter is exposed, to the northwest of Rice Bay. The body is texturally and compositionally heterogeneous and is characterized by a strongly developed gneissic foliation, which parallels the foliation in adjacent country rocks.

Metamorphosed Conglomerate and Sandstone

Three areas underlain by conglomerate and sandstone are present: a) north and east of Shoal Lake, b) south and east of Shoal Lake, and c) in a narrow zone in the Rocky Islet Bay area. Historically, all of these rocks have been referred to as the Seine Group. Current appellation refers to them as Seine metasediments. North of Shoal Lake, conglomerate lies with angular unconformity on both coarse-grained tonalite (unit 9, Map 2525) and intermediate metavolcanic rocks (unit 2). A coarse boulder to granule conglomerate forms the base of the sequence. In general, the Seine metasediments comprise clast-supported conglomerate (Photo 8), interbedded conglomerate and arenite, arenite and minor siltstone. Relative abundance data for clasts of different compositions indicate the dominance of intermediate metavolcanic rocks (Figure 8). Framework clast sizes decrease with stratigraphic height (Wood 1980). Sandstone interbeds are relatively common, range up to 1 to 2 m in thickness, and show either parallel lamination or low-angle cross-stratification. Substantial volumes of trough-crossbedded sandstone (Photo 9) occur without conglomerate. Compositionally these are lithic arenite, lithic subarkose, and arkose (Wood 1980). Within the Seine metasediments, there is a broad-scale transition from conglomerates through to arenite. The unit has been

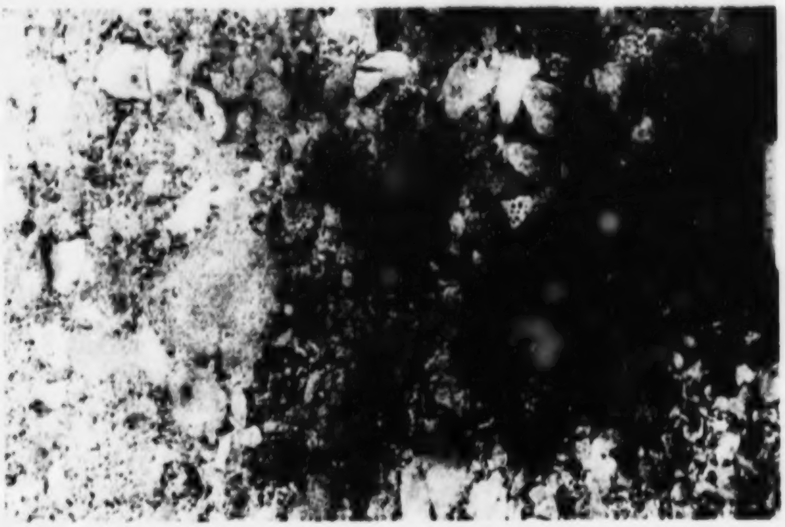

Photo 8. Polymictic Seine conglomerate, Shoal Lake area. Note the variety of volcanic clast types and their angularity. A weak anastomosed cleavage parallels the graduated edge of the compass, which is 7.5 cm wide.

Photo 9. Cross-bedding in arenites, north of Shoal Lake. Based on observations elsewhere, the cross-beds are likely troughs with axes normal to the photo. Note that the low apparent angle between the foresets and bedding is likely the result of bedding-normal shortening; note the cleavage at the bottom of the photo. Coin is 2.4 cm in diameter.

interpreted to be an alluvial fan merging into a braided fluvial system (Wood 1980).

Unmetamorphosed Granitoid Rocks and Related Rocks

The rocks of this category have been historically referred to as Algoman granites (Lawson 1913), and possess a number of features that distinguish them from the metamorphosed and deformed Laurentian-type granitoid rocks (unit 9, Map 2525):

1. They contain less quartz and are commonly richer in potassium feldspar than the Laurentian-type granitoid rocks, and typically range in composition from diorite to granite (*see* Figures 6b and 7). The 2 units are therefore compositionally distinct.
2. They are rarely foliated with the possible exception of marginal phases.

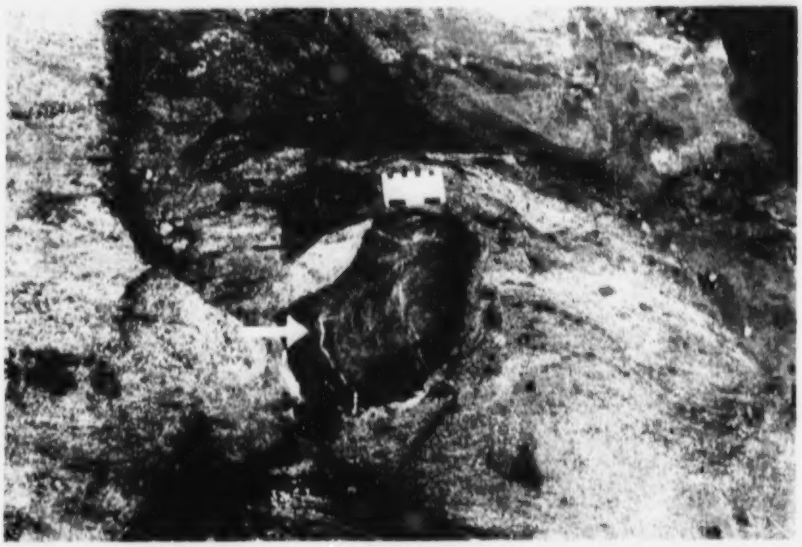

Photo 10. Agmatitic breccia, western margin of the Ottertail Lake pluton. Note the internal schistosity (arrow) in the angular xenolith, in relation to the flow (?) foliation in the coarse monzonite.

3. They form discrete discordant plutons that are elliptical to irregular in plan.
4. Agmatitic breccias are common at the pluton margins. Xenoliths commonly consist of rotated blocks of regionally foliated country rock (Photo 10).

The above criteria suggest late to posttectonic time of emplacement for these granitoid rocks.

Dike Rocks

Dikes, sills and irregular masses of plutonic rock of highly variable composition are exposed throughout the map area. Most of these appear to be late-stage intrusions in their own local context. They include northwesterly striking Proterozoic diabase dikes, biotitic lamprophyres that are commonly xenolithic, and quartz-feldspar porphyries. While all of these form bodies that are similar in morphology and in their volumetric insignificance, they likely represent a wide spectrum in absolute ages and origin.

Fault Rocks

The 2 major faults, the Quetico and Rainy Lake–Seine River faults, consist of zones of deformed equivalents of most of the other rock types in the region. The Quetico Fault zone is up to 1 km wide and contains schists, mylonites, cataclasites and pseudotachylite. The protoliths are plutonic, metavolcanic and metasedimentary rocks that are tectonically intercalated to produce a heterogeneous sequence. The rocks of the Rainy Lake–Seine River fault zone are similarly developed from different lithologies. Here, schists, phyllites and phyllonites are very chloritic, and little distinction can be made between plutonic, volcanic or sedimentary protoliths.

STRATIGRAPHIC SUCCESSION: THE CLASSICAL APPROACH

Lawson (1913) used the tools of stratigraphic superposition and crosscutting relationships to establish a stratigraphic history relating to the 5 most significant lithologic units at Rainy Lake. Lawson (1913) used the time-stratigraphic term "series", which has since been abandoned, and recognized 3 lithostratigraphic groups:

1. the Coutchiching Group, comprising biotite schists of wacke-mudstone association (unit 6, Map 2525)
2. the Keewatin Group, consisting of all metavolcanic rocks (units 1 through 5) and the gabbroic intrusions (unit 8)
3. the Seine Group, composed of conglomerate and arkose (units 10 and 11)

Lawson (1913) also divided the granitoid rocks into 2 suites:

4. Laurentian-type tonalite and trondhjemite (unit 9)
5. Algoman-type granodiorite and quartz monzonite (unit 12)

Lawson viewed the stratigraphic sequence in terms of simple vertical superposition, interpreted the Coutchiching Group as a pre-Keewatin succession, and demonstrated that the Seine Group lies with angular unconformity upon the Keewatin. The Laurentian-type granitoid rocks were considered to represent an older plutonic suite than the Algoman-type, and the erosional base of the Seine Group was thought to separate 2 orogenic cycles.

Lawson's (1913) interpretation appeared to contradict the widely held view of geologists working on similar rocks in Minnesota that the Seine and Coutchiching groups are part of a single sedimentary succession overlying the Keewatin. The issue was hotly debated and the resulting controversy became known as the "Seine–Coutchiching Problem" (Merritt 1934). Since that time, numerous new contributions on various aspects of the geology of this area have led to further revisions of earlier stratigraphic interpretations (Table 3).

The variety of interpretations shown in Table 3 reflects several factors. First, diagnostic criteria for determining a stratigraphic succession have changed with time, with the earliest interpretations relying heavily upon structural superposition. Lawson (1913) was the first to use cross-bedding, and Grout (1925) the first to use graded beds, for determining younging directions in the region. More recently, Poulsen (1980a) interpreted younging directions using newly discovered exposures of pillowed basalt. Other recent interpretations are based, in part, on the results of radiometric dating programs (*see* Table 1).

Second, most geologists have assumed that the metasedimentary biotite schists at Rice Bay and Bear Passage (Lawson's (1913) type Coutchiching) are stratigraphically equivalent to similar rocks in the Quetico Subprovince. Hawley (1930b) was the first to recognize intervening faults.

Third, the earliest stratigraphic columns were constructed on the assumption that there were no time-equivalent units of different lithologic type in the area. The possibility of such facies variations was alluded to by Bruce (1927), and Hawley (1930b, p.546) suggested the possibility that "...the conglomerate represents a near-shore phase of the finer sediments and both are of post-Keewatin age". This is the essence of many modern views of the relationship between the Seine-type conglomerates and the turbidites of the Quetico Subprovince (Mackasey, Blackburn and Trowell 1974; Wood 1980).

Finally, individual interpretations have relied heavily upon the field relationships at particular, in part widely spaced, localities. Several of these key localities were reexamined by the author and are briefly described in the following sections.

The Core of the Rice Bay Dome

The rocks exposed at the core of the Rice Bay Dome (Map 2525) were considered by Lawson (1913) to represent an "older" Laurentian granite that intruded sedimentary and volcanic rocks and was deformed with them. Other workers considered the rocks at the core of the dome to be basement gneisses beneath the Keewatin volcanic rocks, and yet others included much of the outcrop area with the Coutchiching biotite schists (*see* Table 3).

The most abundant rock type in the Rice Bay Dome is a grey, banded quartzofeldspathic schist or gneiss. These rocks locally contain abundant millimetre-sized quartz eyes, and relict volcanic clasts were identified locally. The banded rocks are intruded by leucocratic quartz-feldspar porphyry dikes and sills, which make up substantial parts of any single outcrop. Locally, enclaves of mafic schists and gneisses with abundant hornblende, biotite and epidote occur within the quartzofeldspathic schist. Relict bedding in these mafic schists suggests a tuffaceous or sedimentary origin. Collectively, these observations suggest a substantial volcanic component to the "dome" and that the term "Laurentian granite" can only apply to the small volumes of porphyritic plutonic rock that are present. Furthermore, the schists and gneisses are quite different in character from nearby biotite schists and therefore should not be correlated with the Coutchiching metasediments.

Mantling Rocks of the Rice Bay Dome Near Pocket Pond

An important observation to be considered in the stratigraphic interpretation of the Rainy Lake area is that the Coutchiching biotite schists occupy a lower structural position than the Keewatin basalts in the sequence of rocks that mantles the Rice Bay Dome. Northeast of Pocket Pond, a well-exposed section (Figure 9a) through this succession illustrates the nature of the problem. At locality A, biotite schists of Lawson's (1913) Coutchiching Group strike 300° and dip approximately 65° to the northeast. The rocks have been metamorphosed at amphibolite facies conditions and "knotty" rusty pelitic schists contain garnet and aggregates of muscovite (after staurolite) that contain fibrous sillimanite. Quartz and alkali feldspar occur in veinlets and bedding-parallel segregations in the form of intrafolial folds.

At locality B (*see* Figure 9a), a small exposure of pale green phyllite and schist, representative of unit 4 (*see* Map 2525), has been mapped for several kilometres in either direction along strike. It is a good marker unit due to its magnetic properties, which result from 5 to 10% disseminated magnetite. Its distinctive chemistry (greater than 20% MgO) and locally well-preserved clastic textures suggest an ultramafic volcanic or epiclastic origin. At this outcrop, the magnetic ultramafic unit is intruded by equigranular medium-grained metadiabase.

The pillowed metabasalts exposed at locality C (*see* Figure 9a), along with the magnetic ultramafic unit, form part of Lawson's (1913) Keewatin Group. Iron formations within this group confirm their conformability and structural position above the Coutchiching rocks, but well-preserved pillow structures (*see* Photo 1) indicate a southwestward younging. This supports the view (Poulsen 1980a) that the Rice Bay Dome is antiformal but not anticlinal. Graded bedding observed by the author in biotite schists of the Coutchiching metasediments in core from a nearby diamond-drill hole supports this contention.

Volcanic-Sedimentary Contact at Bear Passage

An important locality with respect to the historical Seine–Coutchiching controversy lies along the western shore of Bear Passage, Rainy Lake. Lawson (1913) stated categorically that here, Coutchiching biotite schists dip at a moder-

Table 3. Comparative stratigraphic interpretations, Rainy Lake area. The units interpreted to be the youngest appear at the top of each column.

Lawson (1887,1889)	**Adams et al. (1905)**	**Coleman (1898); Lawson (1913,1916); Bruce (1925a); Tanton (1927); Goldich and Peterman (1980)**[b]	**Parsons (1918); Tanton (1936); Birk and McNutt (1981)**
ALGOMAN (unnamed) – intrusive contact – LAURENTIAN – intrusive contact – KEEWATIN COUTCHICHING	COUTCHICHING Lower SEINE (unnamed) "Huronian" – unconformity – KEEWATIN – "eruptive" contact – LAURENTIAN	ALGOMAN – intrusive contact – SEINE – unconformity – LAURENTIAN – intrusive contact – KEEWATIN COUTCHICHING	LAURENTIAN "Post–Seine" ALGOMAN – intrusive contact – SEINE KEEWATIN COUTCHICHING
Grout (1925); Grout et al. (1951)	**Merritt (1934); Leith, Lund and Leith (1935); Pettijohn (1937)**	**Hart and Davis (1969); Harris (1974)**	**Mackasey, Blackburn and Trowell (1974)**
ALGOMAN – intrusive contact – COUTCHICHING "Huronian greenschist" SEINE – unconformity – LAURENTIAN – intrusive contact – KEEWATIN	ALGOMAN SEINE (including all "Coutchiching" of Quetico Subprovince) – unconformity – LAURENTIAN – intrusive contact – KEEWATIN COUTCHICHING[a] (at Rice Bay and Bear Passage)	ALGOMAN – intrusive contact – LAURENTIAN – intrusive contact – KEEWATIN – COUTCHICHING[b] (intercalated)	ALGOMAN – LAURENTIAN (undivided) – intrusive contact – SEINE – COUTCHICHING (facies equivalents) – facies boundary – KEEWATIN
Hsu (1971)	**Ojakangas (1972)**	**Wood (1980); Wood et al. (1980a, 1980b)**	**Poulsen (1980a, 1980b)**
LAURENTIAN – intrusive contact – KEEWATIN COUTCHICHING (includes Seine Group, some "greenstone")	ALGOMAN–LAURENTIAN (undivided) – intrusive contact – KEEWATIN – SEINE (intercalated) COUTCHICHING	ALGOMAN – intrusive contact – COUTCHICHING–SEINE (facies equivalents) – unconformity – LAURENTIAN – intrusive contact – KEEWATIN	ALGOMAN – intrusive contact – SEINE – unconformity – LAURENTIAN – intrusive contact – COUTCHICHING[a] KEEWATIN

---

[a] *excludes biotite schists of the Quetico Subprovince*

[b] *includes much of Lawson's Laurentian Group at Rice Bay with the Coutchiching Group*

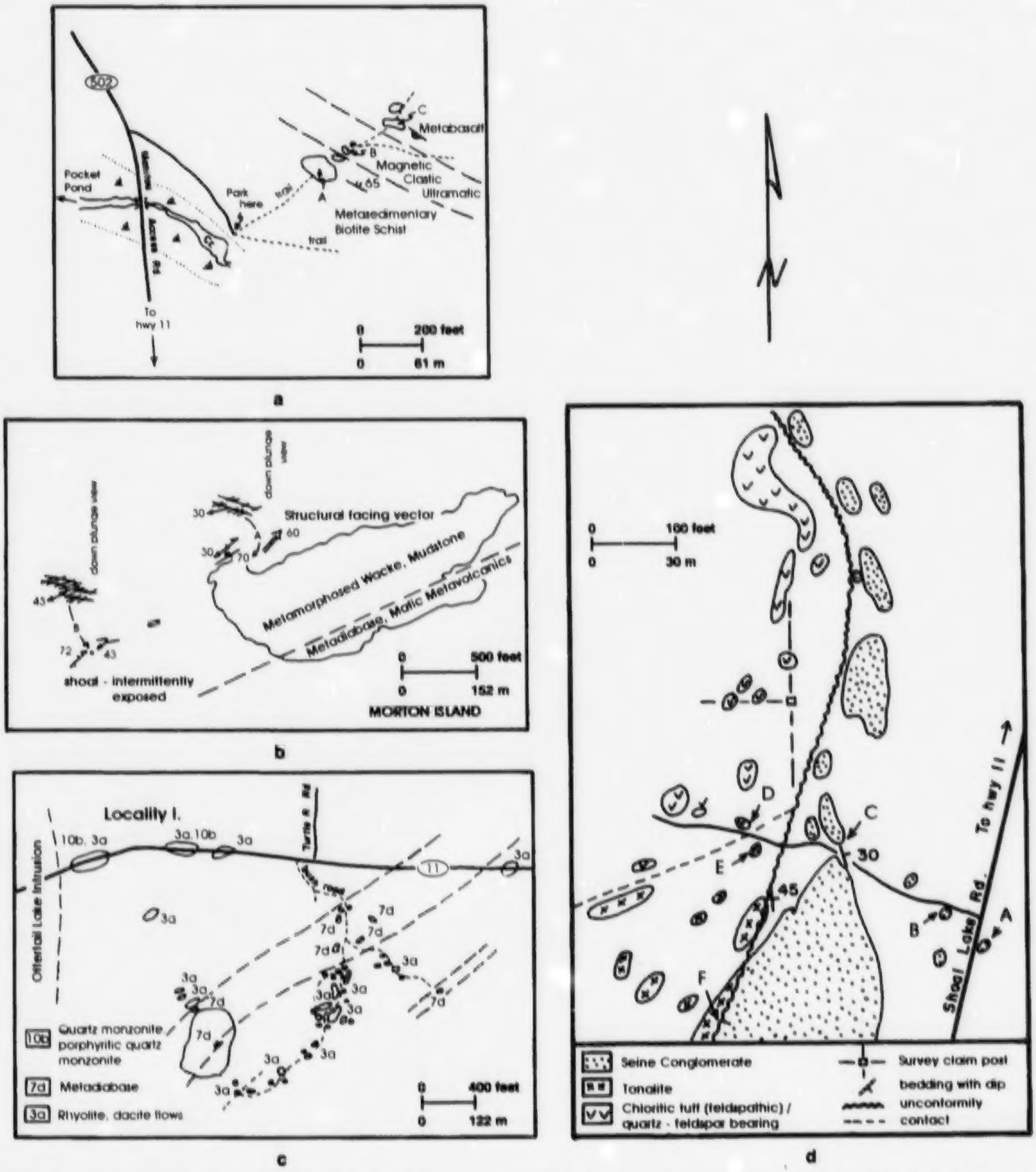
502
Pocket Pond
Park here
trail
A
B
C
Metabasalt
Magnetic
Clastic
Ultramafic
65
Metasedimentary
Biotite Schist
Access Rd
To hwy 11
0 200 feet
0 61 m
a
down plunge view
Structural facing vector
30
60
70
Metamorphosed Wacke, Mudstone
Metadiabase, Mafic Metavolcanics
43
72
shoal - intermittently exposed
0 500 feet
0 152 m
MORTON ISLAND
b
Locality I.
10b, 3a
3a,10b
3a
11
Turtle R. Rd
Ottertail Lake Intrusion
7d
10b Quartz monzonite / porphyritic quartz monzonite
7d Metadiabase
3a Rhyolite, dacite flows
0 400 feet
0 122 m
c
0 100 feet
0 30 m
D
C
E
30
45
B
A
F
To hwy 11
Shoal Lake Rd.
Seine Conglomerate
Tonalite
Chloritic tuff (feldspathic) / quartz - feldspar bearing
Survey claim post
bedding with dip
unconformity
contact
d

Figure 9. a) Sketch map of field relationships along the northeastern margin of the Rice Bay Dome, near Pocket Pond. Localities A, B, and C are described in the text. b) Sketch map showing field relationships at Morton Island. Note that the bedding-cleavage relationships are opposite to those expected to correspond with the observed northward younging direction. c) Sketch map showing the geology at the eastern margin of the Ottertail Lake intrusion. d) Sketch map showing field relationships at the base of the Seine metasediments, near the Golden Star Mine. Note the unusually shallow dip of the Seine metasediments. The metavolcanic rocks face northwesterly. Other structural symbols as in figure 18.

ate angle beneath Keewatin mafic metavolcanic rocks. The only younging direction indicator known at that time was cross-bedding, so structural order was also considered to represent stratigraphic order. Well-developed graded bedding, enhanced by the growth of staurolite and garnet in pelitic tops (*see* Photo 4) indicates that the beds are overturned at this locality, and that the biotite schists face away from the contact with the actinolitic metavolcanic rocks.

Volcanic-Sedimentary Contact at Morton Island

The metamorphic grade of the metasedimentary rocks at Morton Island is lower than that at either Pocket Pond or Bear Passage. A well-preserved graded sequence is exposed (*see* Photo 5). Grout reported this in 1925, but controversy arose because fold repetition results in local younging reversals, and no consensus could be reached on the number of fold closures present. The folds were thought to be simple first generation structures, so that younging directions were also interpreted to indicate fold geometry. Recent mapping (Poulsen 1980a) shows that this is not the case, and that sense of the intersection of bedding with axial planar cleavage is opposite to that expected from the grading in the metasedimentary rocks if the folds were right way up (Figure 9b). Therefore the relationship of the metasedimentary rocks to the metavolcanic rocks at this locality remains ambiguous.

Eastern Margin of the Ottertail Lake Intrusion

The Ottertail Lake pluton is typical of the unmetamorphosed, late tectonic "Algoman" intrusions. It is compositionally zoned with dioritic margins and a core of dominantly granodiorite. Contacts with the country rocks are discordant, and intrusive breccias are developed along its margins. A good example of such a breccia is exposed at locality 1 (Figure 9c), where a pre-existing foliation occurs in rotated blocks of epidote-rich biotite schist (*see* Photo 10). Eastward, equigranular to megacryst-bearing monzonite may be observed with blocks of country rocks containing local porphyroblasts that resemble pinitized cordierite. Rhyolitic blocks become more abundant to the east and show distinctive internal flow laminations. Ghost fragments or "fish" represent partly digested xenoliths. Pods of megacryst-rich monzonite, aplite dikes and pegmatite are well developed. Eastward, the outcrops show a transition to rhyolitic hornfels and then to granitoid-rhyolite flows.

Unconformity at the Base of the Seine Metasediments

The position of the Seine conglomerate has been interpreted in a variety of ways (*see* Table 3). The critical outcrops (Figure 9d), which expose the base of the relatively undeformed Seine conglomerate, lie between Bad Vermilion and Shoal lakes. At locality A (*see* Figure 9d), the typical Seine conglomerate (*see* Photo 8) contains abundant volcanic detritus and jaspilitic chert, and shows vague bedding and a weak cleavage. Similar clasts are present at localities B and C, where they are contained in a sandy matrix composed mainly of quartz grains up to half a centimetre in diameter. A 30° eastward dip of bedding is evident at locality C. At D, chloritic metavolcanic rocks are exposed. These form part of a volcanic sequence that faces northwestward, based on pillow shapes in outcrops several hundred metres to the west. At E, coarse-grained tonalite is exposed, and at F the contact between the "Laurentian" tonalite and the Seine conglomerate is exposed. Close examination of the contact shows a subtle transition from coarse-grained tonalite through a quartzofeldspathic sandstone *(grus)*, to a conglomerate with a sandy matrix and scattered clasts. The quartz grains maintain their size and shape across the transition, and occur locally in higher stratigraphic levels of the conglomerate (at B). These clearly established textural relationships, plus the distinctive geometry, confirm the unconformity at the base of the Seine metasediments.

A NEW APPROACH TO RAINY LAKE STRATIGRAPHY

The previous section illustrates the difficulty of establishing a unique stratigraphic column that applies to the entire study area. One of the serious problems inherent in previous interpretations is the assumption of stratigraphic continuity from place to place. Careful inspection of Map 2525, however, reveals that there are several stratigraphic discontinuities within the area bounded by the Quetico and Rainy Lake–Seine River faults, in addition to these large faults themselves. These discontinuities define lithostratigraphic domains (Figure 10) for which internal stratigraphic order can be reasonably well demonstrated. However, no recognizable stratigraphic markers can be traced contiguously from one domain to the next across their mutual boundary. In some cases, the domain boundaries are known to be faults (*see* "Structural Geology"), and in others they are marked by "back-to-back" relationships in which the sequences on opposite sides of a discontinuity face in opposite directions. It is not likely that the domain boundaries represent unconformities, as both sequences have the same attitude, nor is it likely that they are folds, because the opposing sequences are commonly lithologically dissimilar.

The structural and metamorphic aspects of the domains and their boundaries are described in greater detail in subsequent chapters. Table 4 summarizes some of their most important characteristics. Although the number of domains defined in this way is fixed for purposes of the present discussion, a more detailed study of this area in the future may result in amalgamation or subdivision of some domains.

Stratigraphic sections representative of each domain are shown in Figure 11, but in some instances, such as for the large Pocket Pond domain, the column can only be considered reliable for that part of the domain where sufficient younging direction criteria could be observed. In many parts of the study area, these criteria are scarce or obscure as a result of superimposed deformation. The thicknesses of units shown in Figure 11 are those that can be presently measured with corrections for variation in dip. They need not precisely reflect original thicknesses, since evidence for superimposed strain is common in most outcrops in the area.

Several key points concerning stratigraphic relationships are illustrated by Figure 11:

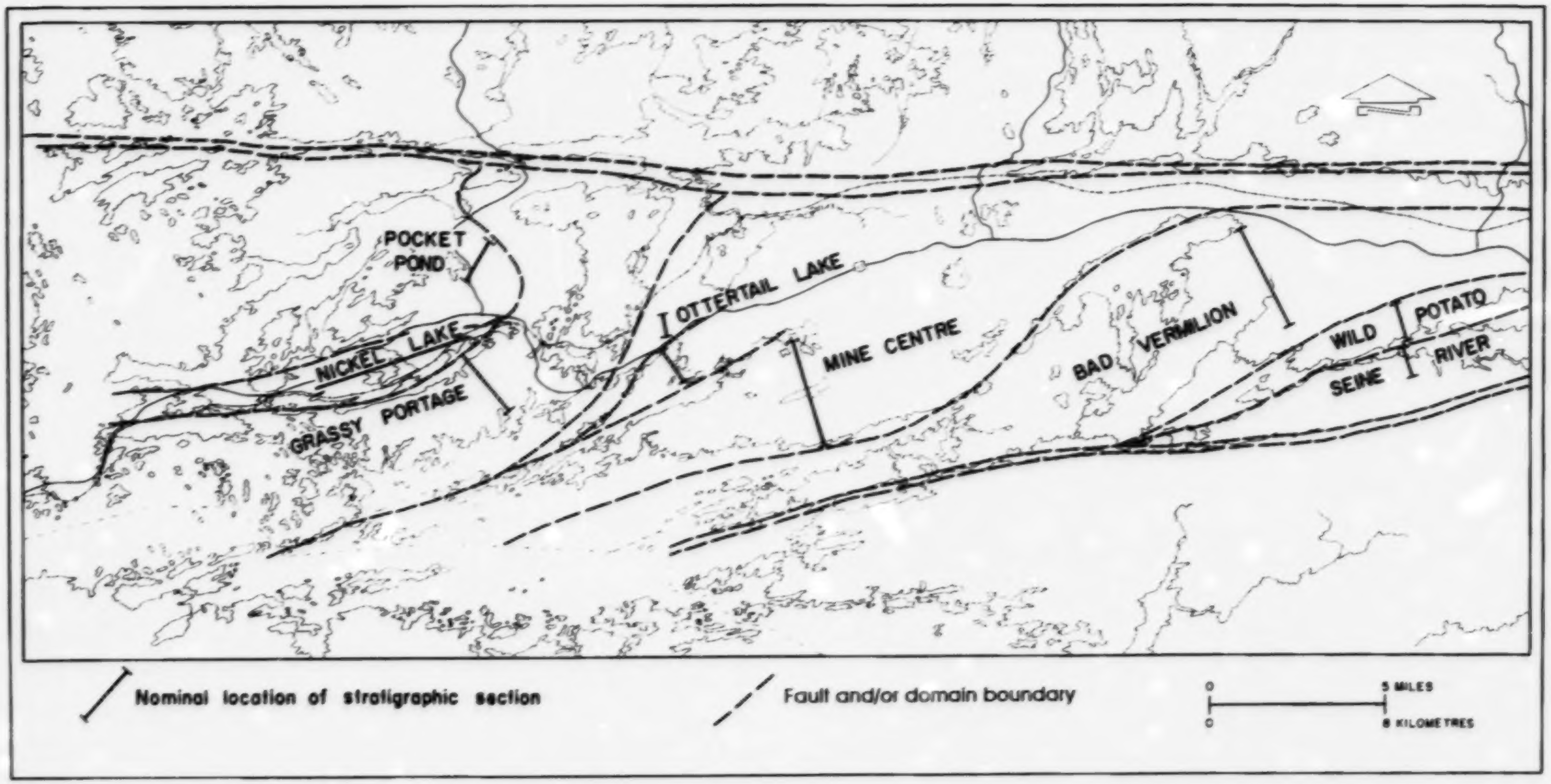
POCKET POND
NICKEL LAKE
GRASSY PORTAGE
OTTERTAIL LAKE
MINE CENTRE
BAD VERMILION
WILD POTATO
SEINE RIVER
Nominal location of stratigraphic section
Fault and/or domain boundary
0
5 MILES
0
8 KILOMETRES

Figure 10. Summary map showing the location and boundaries of lithostratigraphic domains. Locations are shown for stratigraphic columns that are representative of each domain, as illustrated in Figure 11.

Table 4. Characteristics of lithostratigraphic domains, Rainy Lake.

Name	Boundaries	Composition
	Northwestern Domains	
Pocket Pond	on the north by the Quetico Fault, on the south by an internal fault, and on the east by an apparent "back-to-back" relationship in mafic volcanic rocks; of unknown extent to the west; may be further divisible	at Pocket Pond, basalt, ultramafic volcanic rocks and biotite schists; elsewhere similar supracrustal rocks, but also large volumes of granite gneiss and quartzofeldspathic rock with an unknown relationship to the volcanic rocks
Nickel Lake	on the north by a well-defined fault which truncates the north limb of a synform; on the south by a mutual boundary with the Grassy Portage domain	an eastward- and downward-facing sequence of basalt, metadiabase, ultramafic volcanic rocks and biotite schists
Grassy Portage	on the northwest by successive truncation of mappable southward-facing units, including the Grassy Portage intrusion; on the south by the southernmost extent of wackes and mudstones; and on the east by a northeasterly striking fault	dominantly a southeastward-facing sequence of basalt, ultramafic volcanic rocks, gabbro and biotite schists; includes a chain of Algoman granodioritic plutons
Ottertail Lake	on the northwest by a common fault boundary with the Grassy Portage domain; on the southeast by a "back-to-back" relationship with the Nickekousemannicanning domain	basalt, metadiabase, minor felsic volcanic rocks, biotite schists
Nickekousemannicanning	opposing facing and different rock types from the Ottertail Lake and Mine Centre domains	basalt, metadiabase, minor felsic to intermediate volcanic rocks
	Southeastern Domains	
Name	**Boundaries**	**Composition**
Mine Centre	on the north by the Grassy Portage and Nickekousemannicanning domains and Ottertail Lake intrusion; on the south by a shear zone (verified by widely spread drill holes) that successively truncates volcanic and gabbroic units; may be further divisible	rhyolite, intermediate tuffs and breccias, minor basalt; trondhjemite and gabbros; conglomerate and arenite
Bad Vermilion	on the north by a common boundary with the Mine Centre domain; on the south by an abrupt truncation of units on the Rainy Lake–Seine River fault, and by a geophysically and photogeologically indicated lineament with "back-to-back" younging relationships; may be further divisible	anorthosite, tonalite; mixed felsic to mafic volcanic rocks; conglomerate and arenite
Wild Potato	on the north and south by geophysical and topographic lineaments; mappable units are truncated at the boundary; precise position of the southern boundary is uncertain, as the domain may or may not include biotite schists with iron formation	basalt, metadiabase and felsic to intermediate volcanic rocks
Seine River	on the north by the Wild Potato domain and on the south by the Rainy Lake–Seine River fault; may be stratigraphically coherent or possibly a group of discrete narrow domains	arenite, minor conglomerate; may include iron formation in pelitic rocks

1. While volcanic rocks are extensively distributed in the area, stratigraphic thicknesses in any one domain are not large. Furthermore, if intrusions are omitted from the columns, no volcanic section exceeds 3500 m, and most are considerably less.
2. Basalts and ultramafic rocks make up a large percentage of the volcanic rocks in the western domains, while mixed sequences dominated by felsic volcanic rocks are typical of the eastern ones.
3. There is no direct link between the Coutchiching and Seine metasediments. They are restricted to different domains, but both occur at a high stratigraphic level in their respective sequences.

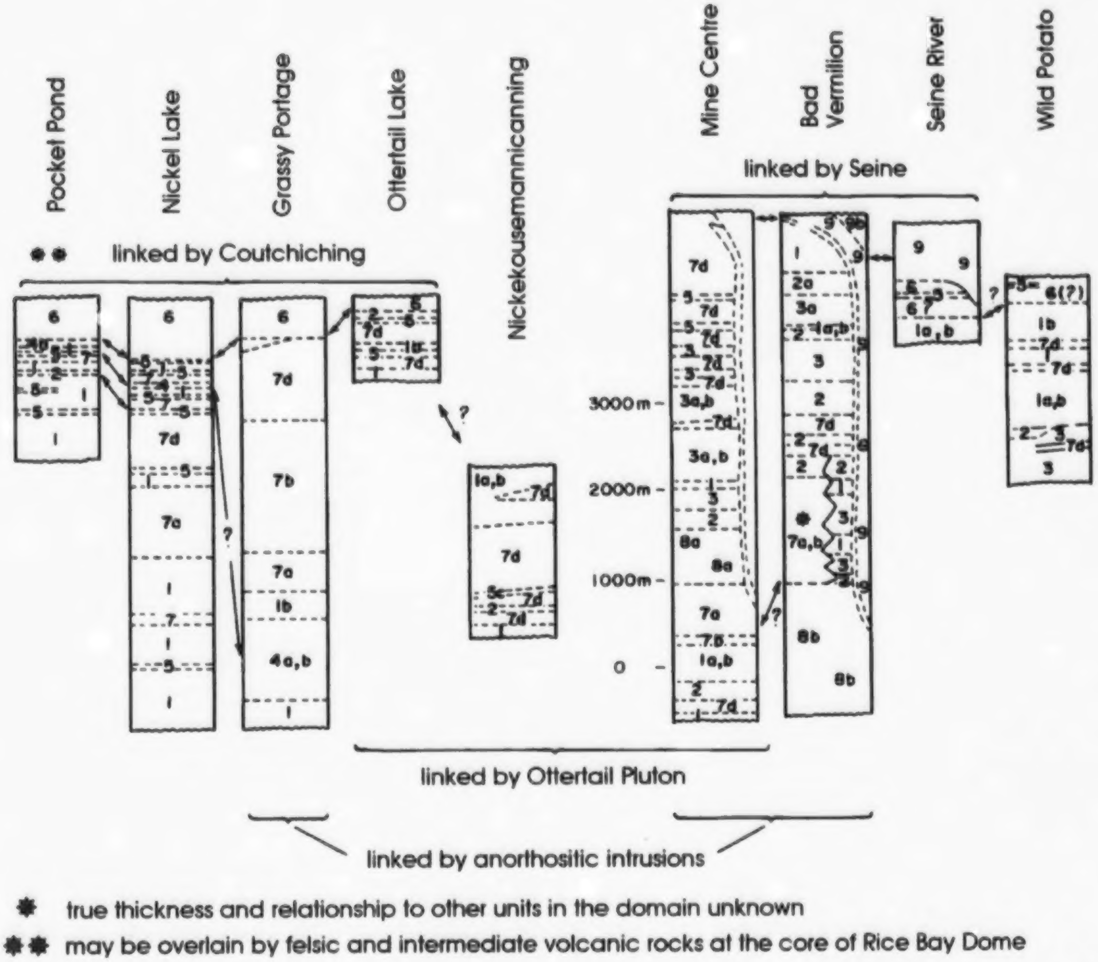
Pocket Pond
Nickel Lake
Grassy Portage
Ottertail Lake
Nickekousemannicanning
Mine Centre
Bad Vermilion
Seine River
Wild Potato
✱✱ linked by Coutchiching
linked by Seine
3000m
2000m
1000m
0
linked by Ottertail Pluton
linked by anorthositic intrusions
✱ true thickness and relationship to other units in the domain unknown
✱✱ may be overlain by felsic and intermediate volcanic rocks at the core of Rice Bay Dome

Figure 11. Stratigraphic columns for individual lithostratigraphic domains. The 4 western domains contain Coutchiching-type sedimentary rocks, while the 4 eastern ones contain Seine sedimentary rocks. The Ottertail Lake pluton cuts the 3 central domains and therefore postdates their juxtaposition. Numerical symbols for rock types correspond to Figure 5.

4. The Ottertail Lake pluton cuts the Ottertail Lake, Nickekousemannicanning and Mine Centre domains, and therefore the time of its intrusion represents a minimum age for the juxtaposition of these domains.
5. Gabbroic to anorthositic sills occur only in the Grassy Portage, Mine Centre and Bad Vermilion domains. If these intrusions are coeval, they may represent a link between the domains. Coutchiching sedimentary rocks are cut by the Grassy Portage intrusion, while Seine sedimentary rocks overlie the Bad Vermilion anorthositic intrusion.

STRATIGRAPHIC SUMMARY

In the previous sections, the main lithologic units in the Rainy Lake area are described, and both their classical interpretations and a new domainal approach are presented. This approach does not represent a solution to the historical "Seine–Coutchiching problem", but does cast it into a new perspective. It illustrates that 2 essential types of domain are present (*see* Figure 10): those in the west, which are dominated by mafic and ultramafic rocks and sedimentary rocks of wacke-mudstone association; and the 4 eastern domains, which contain substantial felsic volcanic rocks, felsic plutonic sills and sedimentary rocks comprising conglomerates and arenites, and which lie with angular unconformity on the other units. There is no demonstrable depositional link between these 2 types of domain.

It is suggested that, although some of the historical stratigraphic terms may be retained in a lithostratigraphic sense, they should be modified as follows:

1. The term Coutchiching metasediments (formerly Coutchiching Group) should refer only to the biotite schists of wacke-mudstone association that occur in

the western domains, and any contiguous extension of these. This includes Lawson's (1913) type locality to the west of the study area. Similar rocks in the Quetico Subprovince to the south of the Rainy Lake–Seine River fault are best termed Quetico metasediments (Wood 1980). There is no evidence bearing on the stratigraphic equivalence of the 2 groups.

2. The term Seine metasediments (formerly Seine Group) remains a useful term to describe the conglomerates and arenites exposed in the eastern domains, as well as any contiguous extension of these to the east or west. The important locality between Bad Vermilion Lake and Shoal Lake establishes the lower stratigraphic boundary for these rocks. Highly deformed conglomerates that occur northwest of Rice Bay may be referred to as "Seine-like", but their stratigraphic position has not been established.

3. The term Keewatin is of little value, as it is generally redundant and synonymous with "volcanic rocks", not only at Rainy Lake but in any Archean part of the Canadian Shield. It is preferable to designate the volcanic rocks in the Rainy Lake area in an informal sense by the domain in which they occur (i.e., Nickel Lake volcanics). Collectively these could be referred to as "Keewatin-type".

4. The terms Laurentian and Algoman are useful local designations for the granitoid rocks. The former is synonymous with sodic plutonic rocks, trondhjemite and tonalite suites, and the latter should be used to refer to granitoid rocks containing substantial potassium feldspar. No age relationships should be implied using these terms, although collectively the Algoman plutons are probably younger. The schists and gneisses of probable felsic volcanic origin that occupy the core of the Rice Bay Dome should neither be termed Laurentian (Lawson 1913) nor Coutchiching (Goldich and Peterman 1980).

Structural Geology

INTRODUCTION

The suggestion that the study area comprises discrete lithostratigraphic domains with discordant boundaries raises the questions of their structural significance and of the kinematic history that resulted in their formation. Mesoscopic-scale structural data were collected routinely during field mapping for later analysis of the large-scale structures. The rocks of the area show evidence of progressive deformation involving a transition from penetrative ductile features such as folds and cleavage to localized brittle structures such as faults and shear zones. The following sections review, in turn, broad structural trends, boundary faults and their related internal shear zones, and penetrative planar and linear fabrics, which are common throughout the area. Orientation data are interpreted, structural sections presented, and finally all aspects of the structure are integrated and interpreted using a kinematic model that is supported by published theory, experiment and comparative geology.

STRUCTURAL TRENDS

Large-scale structural patterns in the study area have been established, not only by lithologic mapping, but also by independent photogeological and geophysical interpretation.

The Rainy Lake area was glaciated in the Pleistocene (Zoltai 1961, 1965), but extensive deposition occurred only to the south and west of the study area, leaving a large area of very thin surficial cover in the vicinity of Mine Centre–Fort Frances. Dominant glacial advances from the northeast (Harris 1974) have produced pronounced lineaments evident on aerial photographs, which coincide mainly with known bedrock features, including lithologic contacts, faults and joints. Figure 12 is a map depicting bedrock airphoto lineaments derived from 1:75 000 scale aerial photographs.

Low-altitude aeromagnetic and electromagnetic surveys (Ontario Geological Survey 1980) resulted in 1:20 000 scale geophysical maps that are available for the entire study area. Magnetic and INPUT electromagnetic anomalies are known to correlate with distinctive stratigraphic markers (i.e., ironstones), as well as with structural dislocations. These linear geophysical anomalies have also been incorporated into Figure 12. They are of particular value in establishing continuity of structures in water or drift-covered areas.

Additional structural information can be derived from the known attitudes of compositional layering in the various igneous and sedimentary rock sequences in the area (Figure 13). These, along with primary younging direction indicators, allow estimation of the attitudes and facing directions of stratigraphic "panels" that contain marker horizons of known lateral extent.

The patterns shown in Figures 12 and 13 illustrate the essential features of the broad geological structure. The 2 boundary faults are marked by both topographic and geophysical discontinuities. The "domal" structural style to the north of the Quetico Fault contrasts with the "sigmoidal" patterns between the faults and the "straight" trends in the Quetico Subprovince to the south of the Rainy Lake–Seine River fault. Within the fault block, a somewhat discontinuous structural style is suggested (*see* Figure 13). The complex but broadly elliptical fold structure in the Rice Bay–Bear Passage area contrasts with the long curvilinear trends in the eastern part of the area. Northwesterly and northeasterly trending transverse features are evident from both topographic and geophysical data. A prominent northerly striking magnetic anomaly near the eastern margin of the map correlates directly with a known diabase dike, and the geophysical data clearly verifies that it crosses the Quetico Fault.

FAULTS AND SHEAR ZONES

Boundary Faults

The 2 most prominent structural features in the study area are the Quetico and the Rainy Lake–Seine River faults. Both truncate distinctive lithologic units which merge at a low angle with the faults in a manner that suggests a dextral sense of displacement (Map 2525).

The Quetico Fault, up to 1 km wide, strikes east and contains heterogeneous rock types possessing an intense steep foliation that parallels the fault. Mylonite (Photo 11) is common and pseudotachylite occurs locally. The mylonite itself is commonly folded into minor folds of dextral asymmetry (Photo 12). Felsic plutonic rocks are the most probable protoliths of mylonites, and protomylonites containing centimetre-sized feldspar porphyroclasts (Photo 13) are similar to porphyritic quartz monzonites that are common phases of the Algoman intrusions. This observation, plus the marked truncation of the Ottertail Lake pluton, indicate clearly that the fault postdates the emplacement of the late-stage Algoman granitoid suite.

The rocks of the Rainy Lake–Seine River fault zone contrast lithologically with those of the Quetico Fault. The sharp contact with the Quetico metasedimentary rocks is marked by a zone as little as 50 m wide, composed of chlorite schist and phyllonite. Some of these schists have been mapped historically as mafic volcanic rocks, but detailed examination reveals that they are commonly heterolithic with enclaves of conglomerate, iron formation and carbonate-rich schist. The nature of this zone is well illustrated by the changes that occur in metagabbro along the fault near the Scott Islands. Outcrops of gabbro to the north of the fault contain local chloritic shear zones that parallel the trace of the main fault. The width and abundance of these zones increase southward to the main schistose zone, which marks the fault. Small folds superimposed on the steep schistosity and sigmoidal quartz veins in the vicinity

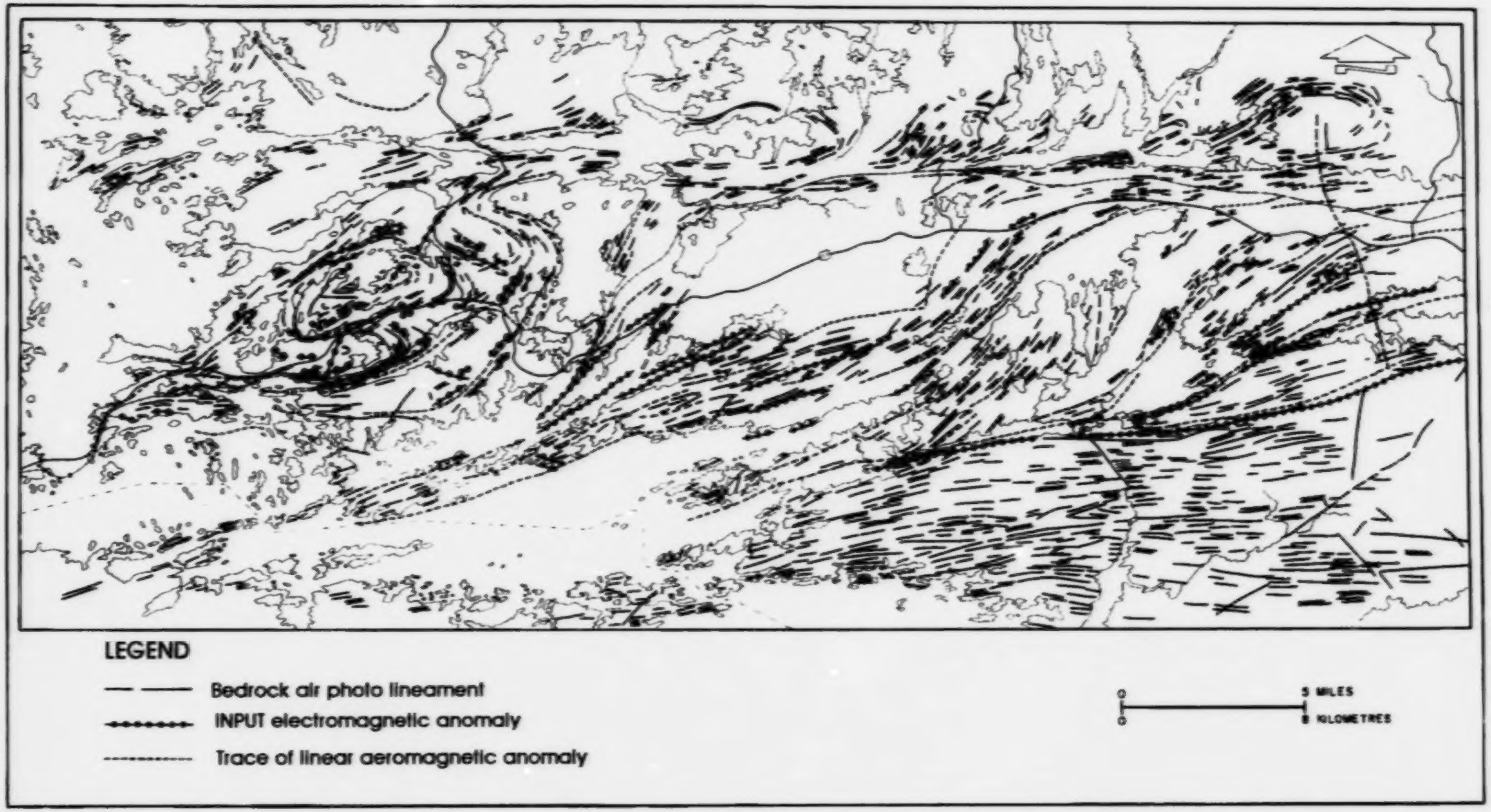
N
LEGEND
Bedrock air photo lineament
INPUT electromagnetic anomaly
Trace of linear aeromagnetic anomaly
0
5 MILES
0
8 KILOMETRES

Figure 12. Structural and geophysical trends at the subprovince boundary at Rainy Lake. Geophysical data were derived from 1:20 000 scale magnetic and electromagnetic maps (Ontario Geological Survey 1980), and air photo lineaments were interpreted from 1:75 000 scale aerial photographs.

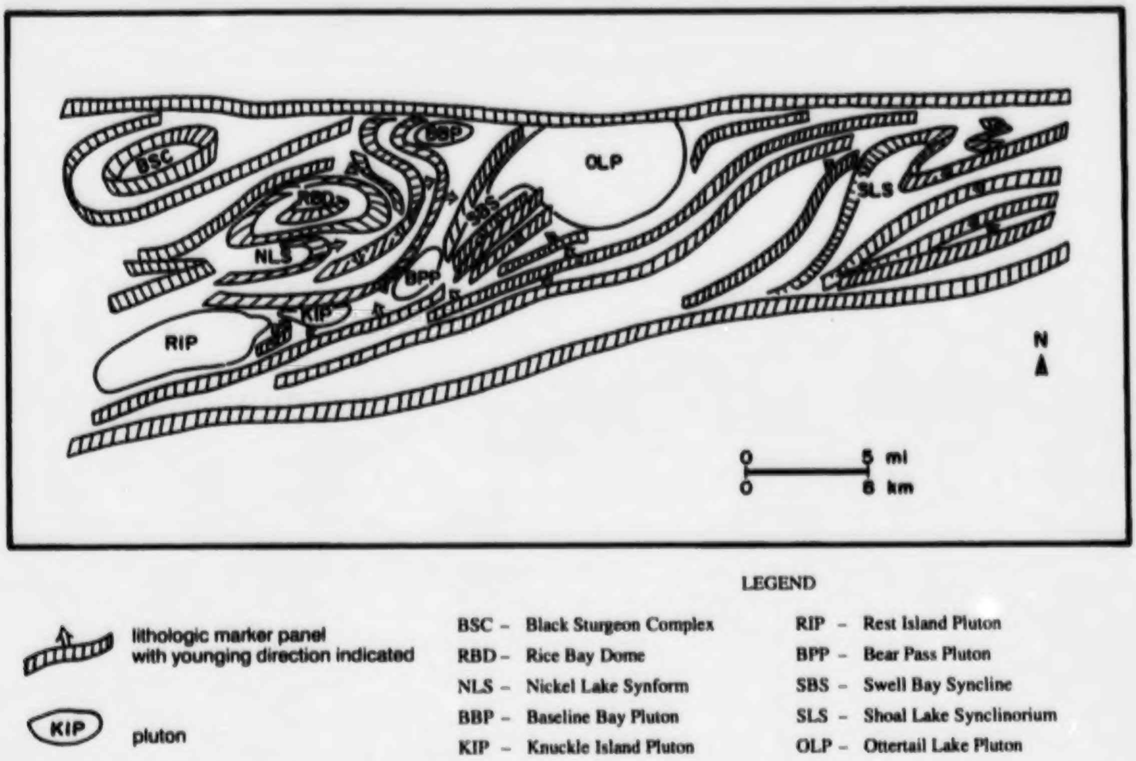
BSC
RBD
NLS
BBP
SBS
OLP
SLS
BPP
KIP
RIP
N
0 5 mi
0 8 km
LEGEND
lithologic marker panel with younging direction indicated
KIP pluton
BSC – Black Sturgeon Complex
RBD – Rice Bay Dome
NLS – Nickel Lake Synform
BBP – Baseline Bay Pluton
KIP – Knuckle Island Pluton
RIP – Rest Island Pluton
BPP – Bear Pass Pluton
SBS – Swell Bay Syncline
SLS – Shoal Lake Synclinorium
OLP – Ottertail Lake Pluton

Figure 13. Schematic diagram showing the attitudes, facing directions and extent of individual stratigraphic markers in the Rainy Lake area. Note the elongate traces in plan of plutons and domal structures and their concordance with the general structural trend.

of the fault near Neil Point, Minnesota, 3 km southwest of Red Pine Island, indicate a right-hand sense of displacement.

Internal Faults

The essential features of the boundary faults have long been recognized (Hawley 1930a; Parkinson 1962; Davies 1973; Fumerton 1982). Faults internal to the study area have a considerably more subtle expression. These faults correspond largely to the lithostratigraphic domain boundaries postulated in the previous chapter. Direct observation of these structures is rarely possible since they are located in drift-covered areas of low topographic relief. Apart from being stratigraphic discontinuities, there are other criteria that support their existence. They invariably correspond to distinctive topographic lineaments, and in many cases are coincident with airborne electromagnetic anomalies (*see* Figure 12). Diamond-drill data also indicate that the domain boundaries are faults. For example, wide zones of "talc-chlorite-carbonate schist" (Assessment Files, Resident Geologist's Office, Kenora) correspond to the boundary between the Mine Centre and Bad Vermilion domains. Locally, as along the northern boundary of the Nickel Lake domain (*see* Figure 10), abrupt changes in structural trend mark the fault. Direct outcrop-scale evidence for these faults is very weak in some cases. For example, a lithologic contact between Coutchiching sedimentary rocks and various volcanic rocks can be traced continuously from Sandpoint Island along Swell Bay through Morton Island and Wreck Point toward Ottertail Lake (Map 2525). This contact represents the southern boundary of the Grassy Portage and Ottertail Lake domains, and outcrops along it consist of biotitic and chloritic phyllites with intense cleavage and local transposed bedding. The discordant nature of the contact is only appreciated in consideration of the fact that both northward- and southward-facing volcanic sequences abut against it. Ojakangas (1972) previously proposed that the extension of this contact in Minnesota is likely a fault.

The internal faults appear to be localized by flexures in the boundary faults, as illustrated by the merging pattern south of Shoal Lake (Map 2525). The timing and sense of displacement on the internal faults is not known. The distribution of the Seine metasediments in the Shoal Lake area, however, is suggestive of imbrication due to dextral offset of a once continuous unit, a sense of displacement compatible with that of the boundary faults.

While the Quetico Fault was active after emplacement of the Ottertail Lake pluton, the 3 domains at the eastern end of Swell Bay appear to have been juxtaposed prior to its emplacement.

Photo 11. Mylonite, Northeast Bay, Rainy Lake. Compass is 7.5 cm wide.

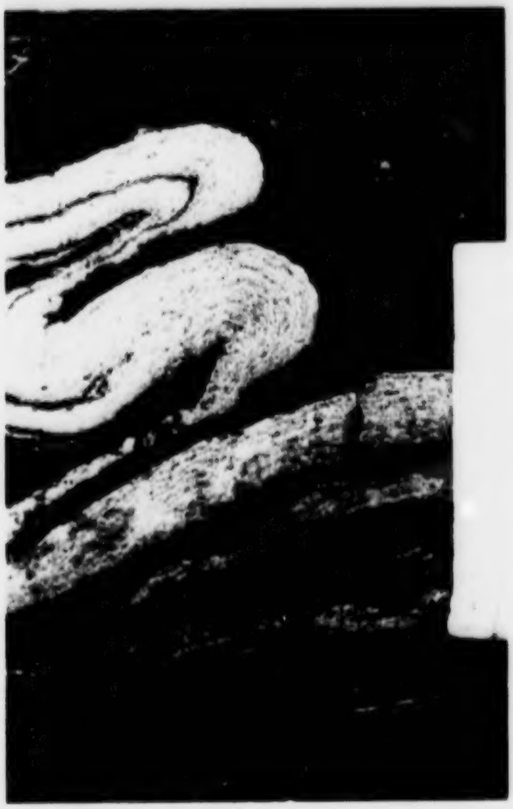

Photo 12. Asymmetrical folds in mylonite, Northeast Bay, Rainy Lake. Compass is 7.5 cm wide.

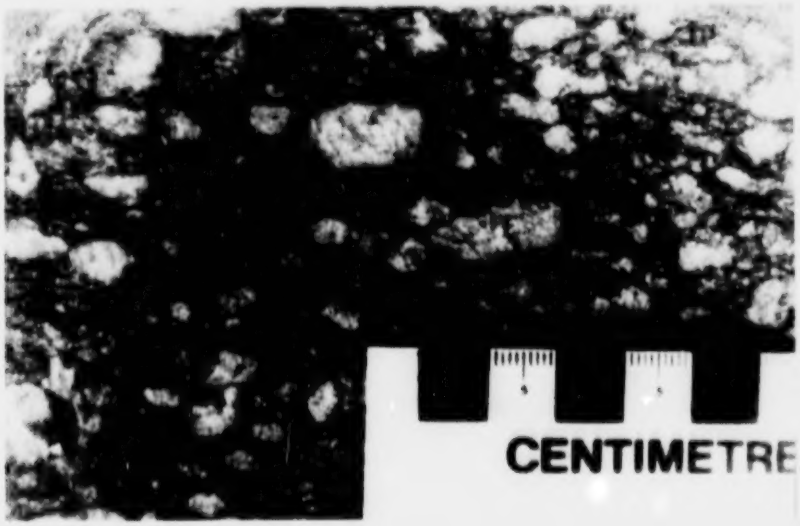

Photo 13. Protomylonite, Crowrock Inlet. The microcline porphyroclasts are typical of megacrysts that are common to many of the Algoman intrusions.

Ductile Shear Zones

Mesoscopic ductile shear zones are a common feature within individual lithostratigraphic domains. They are particularly prominent in plutonic rock masses such as the tonalites and trondhjemites near Bad Vermilion Lake, and the gabbroic rocks along Seine Bay and in the Grassy Portage Bay area. In areas of greenschist grade metamorphism, the shear zones commonly contain quartz veins, some of which are gold-bearing (*see* "Mineralization"). Shear zones are equally common in rocks of the amphibolite facies, without quartz veining and associated mineralization. The shear zones are typically centimetres to metres wide and possess an oblique internal foliation (Photo 14), which allows determination of a sense of displacement. This displacement sense can locally be confirmed where the intrusion contains displaced markers, such as the modal layering in the gabbro at Redgut Bay (Photo 15). The shear zones and their foliations are generally steep, and along with subhorizontal slickensides on central discrete faults parallel to the shear and local sigmoidal vein arrays, generally indicate subhorizontal displacements.

Figure 14a summarizes the essential morphological features associated with a typical shear zone. Attitudes and, where possible, shear senses were recorded for shear zones across the study area. These data (Figure 14b) show a clear separation into 2 groups: a northwesterly striking sinistral set, and a westerly striking dextral set that overlaps in orientation with the Quetico and Rainy Lake–Seine River faults. If these 2 sets are interpreted as conjugates (McKinstry 1953), then the shear zones are but a further reflection of dextral wrench faulting in the area (Figure 14c).

FOLDS, CLEAVAGES AND LINEATIONS

A conspicuous feature in most outcrops containing metavolcanic and metasedimentary rocks is a steeply dipping tectonic foliation. It consists variously of a continuous rock cleavage, a schistosity, or a planar fabric defined by the dimensional orientation of ellipsoidal features such as clasts in conglomerate (Photo 16), pillowed basalts, spherulites or megacrysts. Most commonly, where three-dimensional observation is possible, a linear fabric element may also be observed within the plane of the foliation. This linear fabric element is defined by the elongation of the ellipsoidal markers described above (Photos 17 and 18), by preferred dimensional orientation of mineral grains such as amphiboles, or by a linear intersection of the foliation with another feature such as bedding. Small folds are also common in the area. These are accompanied by axial plane foliations (Photo 19) of the type described above, and have fold axes that are parallel to the other types of linear structures where these are present in the same outcrop. In some outcrops, more than one set of fabric elements is present, and commonly there is evidence that one set superposed another. The clearest examples involve kink bands (Photo 20) and crenulation at a high angle. Such features are particularly abundant in the Bear Passage area (Poulsen 1980a), but are present locally throughout the study area.

The attitudes of linear and planar fabric elements of the type described above were systematically recorded with due regard for evidence of superposition. A simple deformational chronology (Table 5) was established, beginning with the youngest fabric set (D_3) comprising the northwesterly striking crenulation cleavage and kink bands (S_3) and corresponding fold axes and intersection lineations (L_3). The pre-D_3 penetrative cleavages (S_2) commonly have an easterly strike and make a relatively low angle with bedding markers (*see* Photo 16). In a few cases, two such cleavages (S_{2a} and S_{2b}) were observed in the same outcrop cutting bedding with opposite senses of asymmetry, with only rare evidence of which is older (Photo 21). These anomalous cases are fortunately rare and were only observed in outcrops in the Wind Bay, Gagne Lake and Ottertail Lake areas.

The necessity of applying the terms S_2 and L_2 to what is commonly a first (and only) tectonic foliation is illustrated by considering the relationship of these small structures to larger folds. Three examples serve to illustrate the problem: the Nickel Lake synform, the Swell Bay syncline and part of the Shoal Lake synclinorium (Figure 15). In the case of the Nickel Lake synform (Figure 15a), the minor structures are compatible with the major one, but reasonable quality exposures of pillowed basalt indicate that the fold is downward facing. Stratigraphically the synform represents an anticline that likely developed on a previously folded, probably inverted sequence.

The Swell Bay syncline (Figure 15b) can be defined by lithologic mapping and numerous younging direction measurements from graded beds. These low-grade rocks possess one strong cleavage S_{2a} and small folds (*see* Photo 21). The S_3 crenulation cleavage is ubiquitous. The intersection lineation, formed by S_{2a} and bedding, plunges 70° east, and the sense of asymmetry of cleavage on bedding is independent of the facing of beds. S_{2a} therefore transects the axial surface S_1 of a fold defined by the lithologic data.

A third similar example occurs in outcrops of Seine metasediments, northeast of Shoal Lake (Figure 15c). Here, lithologic symmetry and several younging direction determinations based on scour channels and trough-crossbeds indicate a stratigraphic syncline. An oblique foliation is present in conglomerate beds (*see* Photo 16), and is everywhere associated with a shallow eastward-plunging stretching lineation that is coaxial to the intersection of bedding and cleavage. Here, also, the asymmetry of cleavage on bedding is independent of the facing direction of the beds, and the foliation (S_2) transects the trace of the lithologically defined (F_1) syncline. Locally, however, reversals in bedding–cleavage asymmetry were also noted: this reflects the presence of small F_2 folds as well.

The above examples show that both F_1 and F_2 folds are present in the study area. Fabric development (S_2, L_2) appears to relate only to the D_2 deformation, and small-scale D_2 structures on the limbs of F_1 folds have axes that are not parallel to the axes of these larger, lithologically defined folds. F_1 folds occur in the youngest sedimentary unit, the Seine metasediments, so that an early deformation D_0 (*see*

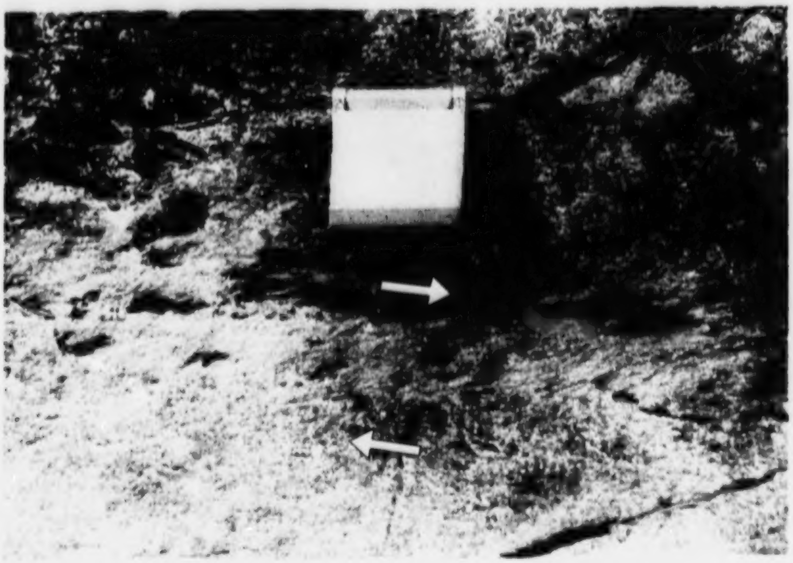

Photo 14. Ductile shear zone in metagabbro, Bad Vermilion Lake. Note that the steep asymmetrical foliation indicates a dextral sense of shear (arrows). Compass is 7.5 cm wide.

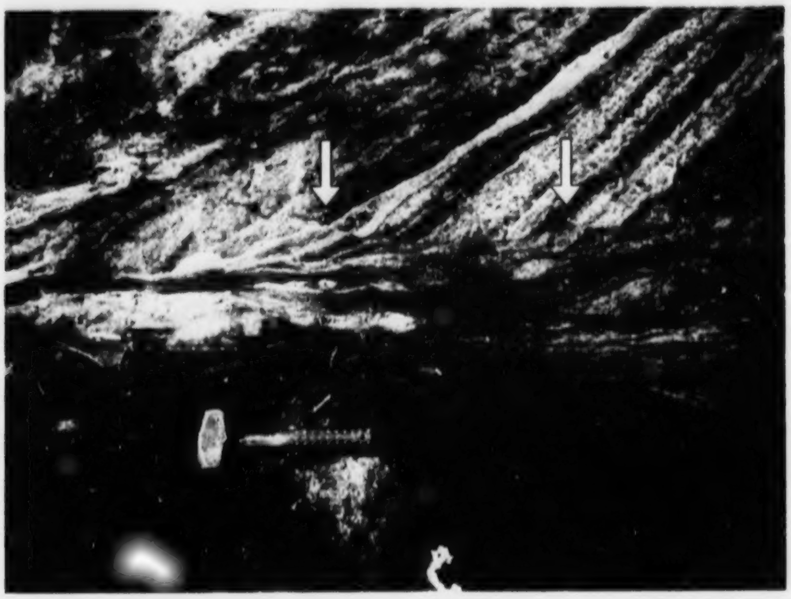

Photo 15. Ductile shear zone displacing igneous layering in gabbro, Redgut Bay, Rainy Lake. Note the sympathetic dextral offsets of brittle fractures (arrows). Hammer is 27.5 cm long.

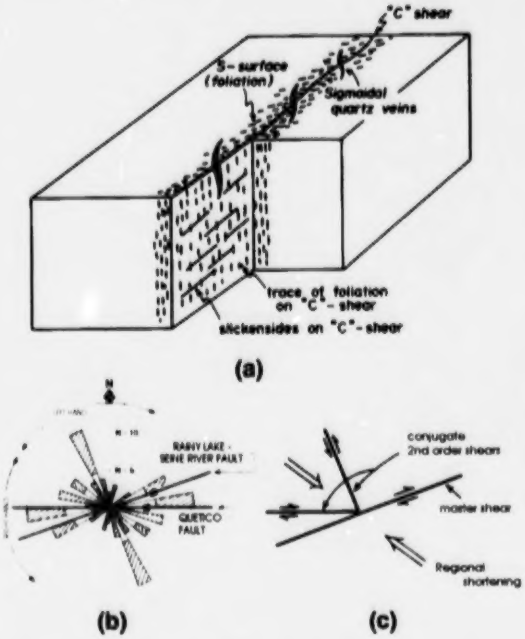
"C" shear
S-surface (foliation)
Sigmoidal quartz veins
trace of foliation on "C"-shear
slickensides on "C"-shear
(a)
N
RAINY LAKE - SEINE RIVER FAULT
QUETICO FAULT
conjugate 2nd order shears
master shear
Regional shortening
(b)
(c)

Figure 14. a) Schematic diagram illustrating the essential morphological features of Rainy Lake shear zones. Many zones contain a central shear fracture ("C" shear) on which subhorizontal slickensides are common. b) Rose diagram showing the orientations and shear sense observed for Rainy Lake shear zones. Nonstippled sectors represent zones for which shear sense is indeterminate. c) Sketch illustrating the "second-order" shear model to explain data in b). In the present case, the "master" structure is the Rainy Lake–Seine River fault.

Table 5) of unknown style is required to account for the profound angular unconformity at the base of this unit.

ORIENTATION OF FABRIC ELEMENTS

All fabric data collected by the author were plotted on conventional equal-area stereographic projections. The D_3 data (Figure 16a) reflect the restricted orientations of the crenulation cleavage and kink bands. The spread in L_3 merely reflects the variable orientation of bedding that is cut by these structures. D_2 fabric elements (Figures 16b, 16c and 16d) conform to the east-northeast structural trends within the study area. A plot of all L_2 and S_2 data, which have been contoured by the Schmidt method (Figure 17a), illustrates 2 main points:

1. All foliations strike east to east-northeast, are quite steep and show greater dispersion of strike than dip. Their orientations are, in part, controlled by their proximity to faults with steep internal foliation.
2. The lineations are broadly coplanar, but are concentrated into 2 somewhat triangular clusters, with variable trends but with consistent shallow plunges averaging 35°. There are few lineations that are extremely steep or extremely shallow.

Figure 18 schematically summarizes the orientation data with respect to the lithostratigraphic domains. In some domains (e.g., Seine River, Ottertail Lake), trends of lineations are substantially different from those in neighbouring domains; in others (Pocket Pond, Mine Centre), opposite ends of the same domain have lineations with opposing plunges. There does not appear to be any direct relationship between fold asymmetry and orientation (*see* Figure 16c), but folds of dextral asymmetry are twice as abundant as those with sinistral asymmetry.

The possible significance of the above observations will be examined in the last section of this chapter.

STRUCTURAL CROSS SECTIONS

One of the objectives of structural investigation in an area is to determine the subsurface geometry of rock masses using surface observations. Variations in the trend and plunge of lineations are commonly used to project surface geology into subsurface or above-surface profiles or cross sections (Stockwell 1950). An essential assumption of this method is that the lineations reflect variations in the orientation of large structures. In the present case, this assumption is likely valid for D_2 features such as the Rice Bay Dome and the Nickel Lake synform, but not valid for F_1 lithologic folds which are transected by D_2 structures. In the latter case, a "down-plunge" projection will yield highly erroneous results; the construction of cross sections must be accomplished using only planar data and the constraints of the surface geology, a method that yields results subject to large errors in interpretation. Three serial vertical cross sections (*see* Figure 18 for locations) were constructed using rigorous projection where warranted, and subjective interpretation elsewhere. These sections (Figure 19) further illustrate the confinement of certain rock types to particular structural domains, as well as the transition from the gneissic domes and plutons of the western domains to the steep straight structural trends to the east.

STRUCTURAL SUMMARY AND INTERPRETATION

The preceding sections describe the essential structural features in the study area. Any interpretation of the structural history must address several key points:

1. the lenticular lithostratigraphic domains and their discordant boundaries
2. the steep boundary faults
3. the regular orientation and sense of displacement of small ductile shear zones
4. the regionally developed subvertical foliation that transects large lithologic folds
5. the shallow bimodal orientations of minor folds and lineations, and the dominance of folds of dextral asymmetry
6. the downward-facing stratigraphic panels in the Rice Bay, Nickel Lake and Bear Passage areas

A structural model that considers the rocks of the study area to be part of a dextral wrench zone is proposed to ex-

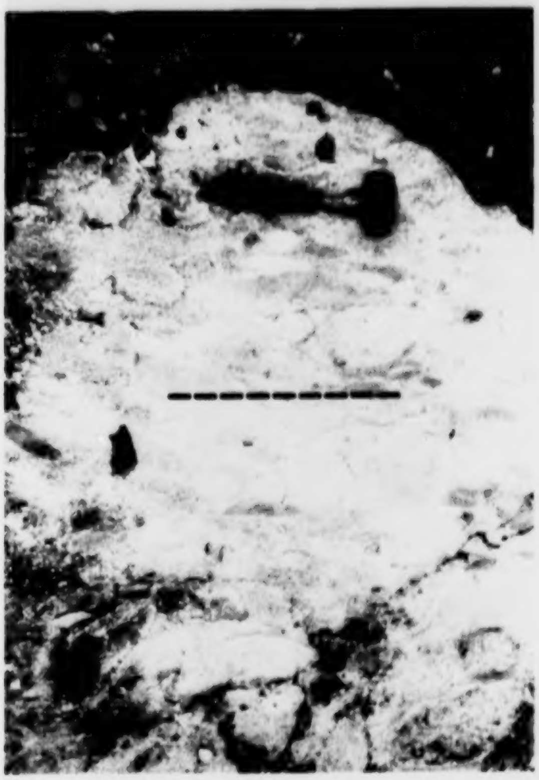

Photo 16. Planar fabric in deformed Seine conglomerate near Mine Centre. The trace of this foliation (dashed line) is seen on a subhorizontal surface. Hammer is 27.5 cm long.

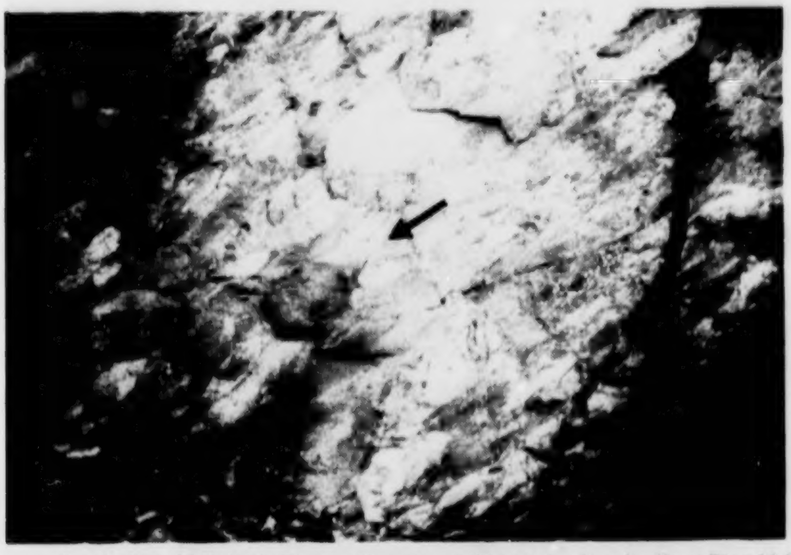

Photo 17. Elongate clasts in plane of foliation, in Seine conglomerate near Mine Centre. Same locality as Photo 16. Hammer is 27.5 cm long.

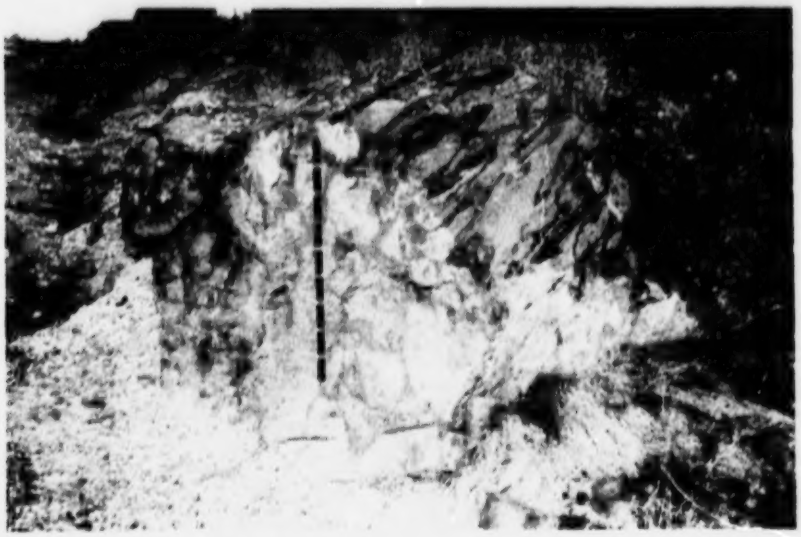

Photo 18. Elongate basaltic pillows near Nickel Lake. The pillow elongation direction is approximately parallel to the hornblende prisms in the metabasalt (arrow). A penetrative cleavage (dashed surface) is approximately normal to an "AC" joint (flat, light coloured, near-vertical surface at front of outcrop). Hammer (located near intersection of dashed lines) is 27.5 cm long.

Photo 19. Axial planar cleavage in folded Coutchiching wackes, Morton Island shoal (*see* Figure 9b). Hammer is 30 cm long.

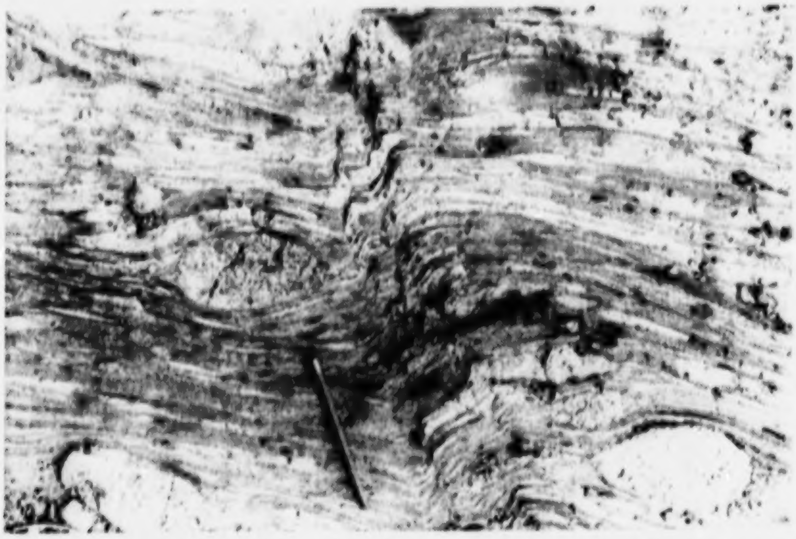

Photo 20. Kink bands developed on flattened clasts in Seine conglomerate near Glenorchy Road. Note the differential flattening of clasts of different composition, and the extreme flattening in comparison to Photos 8 and 16. Pencil is 15 cm long.

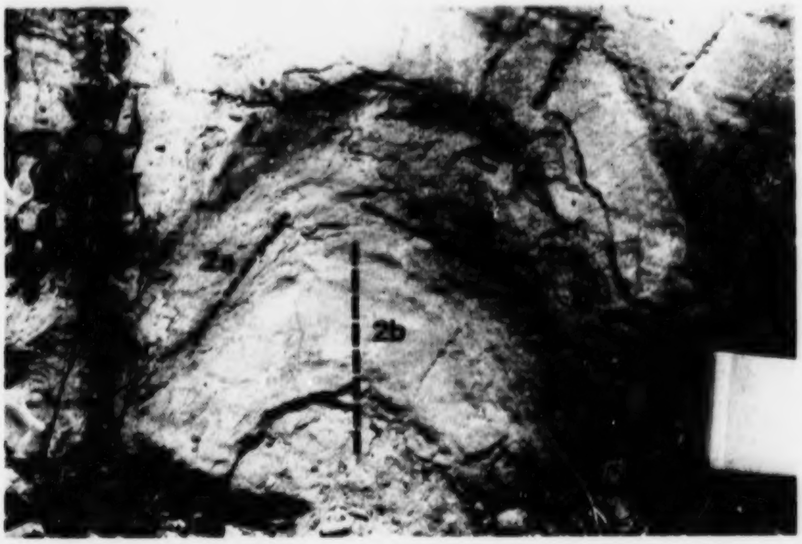

Photo 21. Superposition of 3 cleavages in folded Coutchiching wackes northeast of Swell Bay. Cleavage orientations are indicated by dashed lines and labelled according to the nomenclature of Table 5. Compass is 7.5 cm wide.

Table 5. Relative chronology of folds and fabric elements in the Rainy Lake area.

Deformation	Folds	Fabric
D_3	F_3: centimetres to tens of metres; northwest trend	S_3: crenulation cleavage, kink bands L_3: intersection lineations, fold axes
D_2	F_2: centimetres to tens of kilometres; east-northeast trend	S_2: cleavage, axial planar to small folds; locally 2 cleavages S_{2a} and S_{2b} at shallow angle to each other L_2: fold axes, stretching lineations, mineral elongation
D_1	F_1: tens of kilometres, lithologically defined; east-northeast mean trend	S_1: absent to rare; may be present in amphibolite facies rocks as foliation subparallel to layering
D_0	F_0(?) – pre-Seine deformation of unknown style; possibly faulting only	none

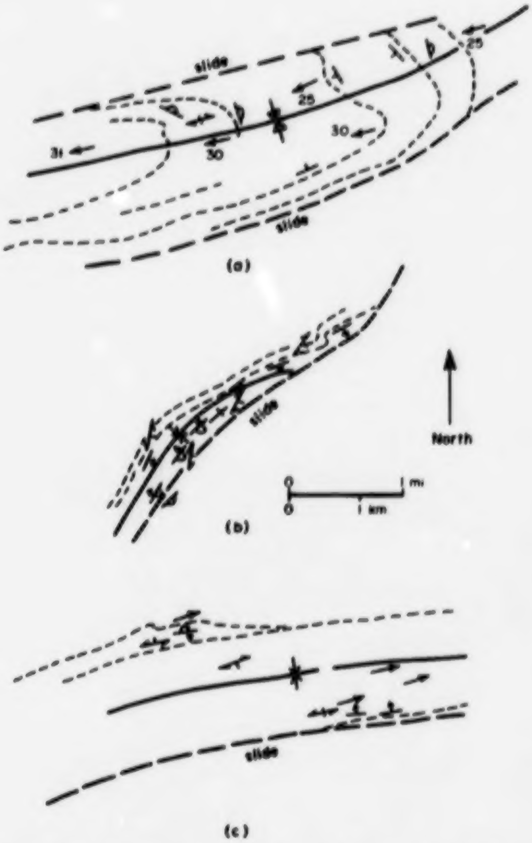

Figure 15. a) Structural geology of the Nickel Lake synform. Note that, while the fabric elements are congruent with the shape of the fold, the synform is actually an anticline. The light dashed lines reflect stratigraphic trends, and the heavy dashed lines represent postulated domain boundaries or tectonic slides. b) Structural geology of the Swell Bay syncline. The bedding–cleavage asymmetry is independent of younging directions. Symbols as in (a). c) Structural geology of part of the Shoal Lake synclinorium. Bedding–cleavage asymmetry is independent of younging directions. Symbols as in (a).

plain these features. A schematic representation of this model (Figure 20a) compares favourably with experimental data and natural examples (Freund 1970; Tchalenko 1970; Lowell 1972; Wilcox, Harding and Seely 1973; Ramsay 1980) as illustrated in Figures 20b and 20c, respectively.

The lenticular lithostratigraphic domains with their steep curved boundaries are well in accord with model experiments (*see* Figure 20b) and with the "millipede" inhomogeneous strain models of Bell (1981). In other words, much strain is localized in discrete shear zones bounding less deformed domains. In the Rainy Lake area, these boundary shears may, in part, be controlled by lithologic contacts and have many of the characteristics of tectonic slides (Hutton 1979).

The boundary faults are an integral part of this model, as they represent the most direct evidence of dextral transcurrent displacements as deduced from criteria cited earlier. It appears, however, that the prominent Quetico Fault is a late-stage expression of the wrench zone in the form of a low-angle second-order shear (*see* Figure 20b), and that the overall trend of the wrench zone is marked by the Rainy Lake–Seine River fault.

The regular orientation and shear sense of small ductile shear zones (*see* Figure 14c) is in good agreement with the wrench zone model. According to the concept of McKinstry (1953), they are predominantly second-order shears. Similar structures have been observed in model experiments (*see* Figure 20b).

The model experiments of Lowell (1972) predict the formation of folds with curved axial traces that trend at a mean angle of approximately 45° to the wrench zone (*see* Figure 20b). Note that the amount of curvature of the axial traces, and even the very presence or absence of folds in a lenticular structural domain, appear to be controlled by the displacements on the local domain boundary. Ramsay and Graham (1970) have proposed that cleavage associated with a shear zone has a predictable orientation relative to the direction of displacement—vertical and northeasterly striking in the present case—and that the cleavage reflects the orientation of the XY plane of the finite strain ellipsoid. If the cleavage, in part, postdates the formation of domains with early folds and is controlled by finite strain in the entire wrench zone, then it is predictable that early folds, which have been rotated in their local domain, will be transected by the cleavage. Furthermore, it is probable that some early folds rotated significantly in a clockwise sense prior to the formation of cleavage, thus establishing a geometry that favours formation of minor (D_2) folds of dextral asymmetry (Figure 20d).

The shallow bimodal orientation of the D_2 lineations and fold axes may be related to the wrench zone in a num-

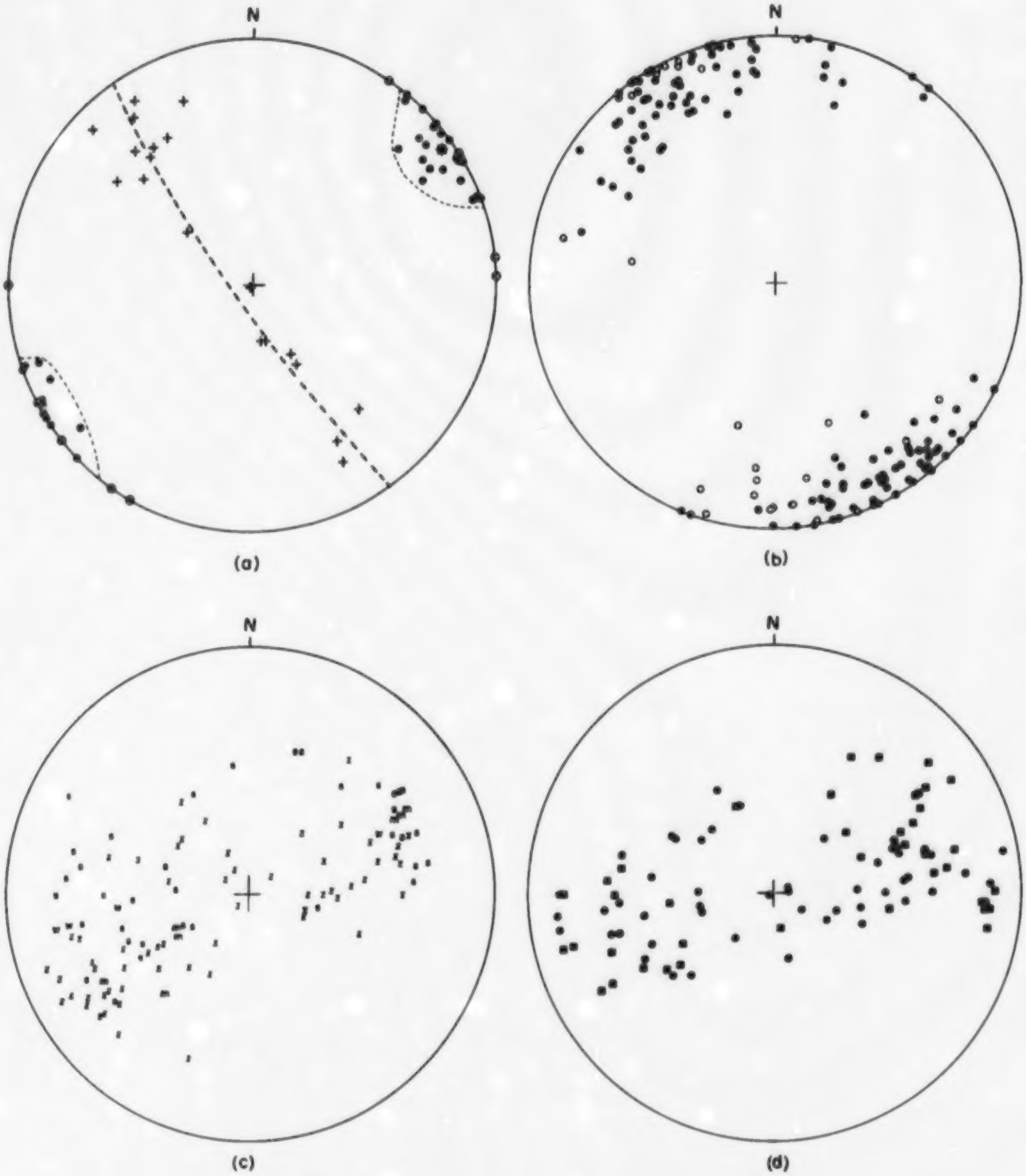

(a) (b) (c) (d)

Figure 16. Equal-area stereographic projections. a) Poles to D_3 cleavage (closed circles), kink bands (open circles) and the mean cleavage orientation (asterisk) are shown, as well as lineations (crosses). b) Poles to S_2 cleavage (closed circles) and fold axial surfaces (open circles). c) 104 minor F_2 fold axis orientations. Asymmetry of folds (s,z,m,w) is also shown. d) L_2 mineral lineations (circles) and stretching lineations (squares). The latter include mullions. 91 lineations are plotted.

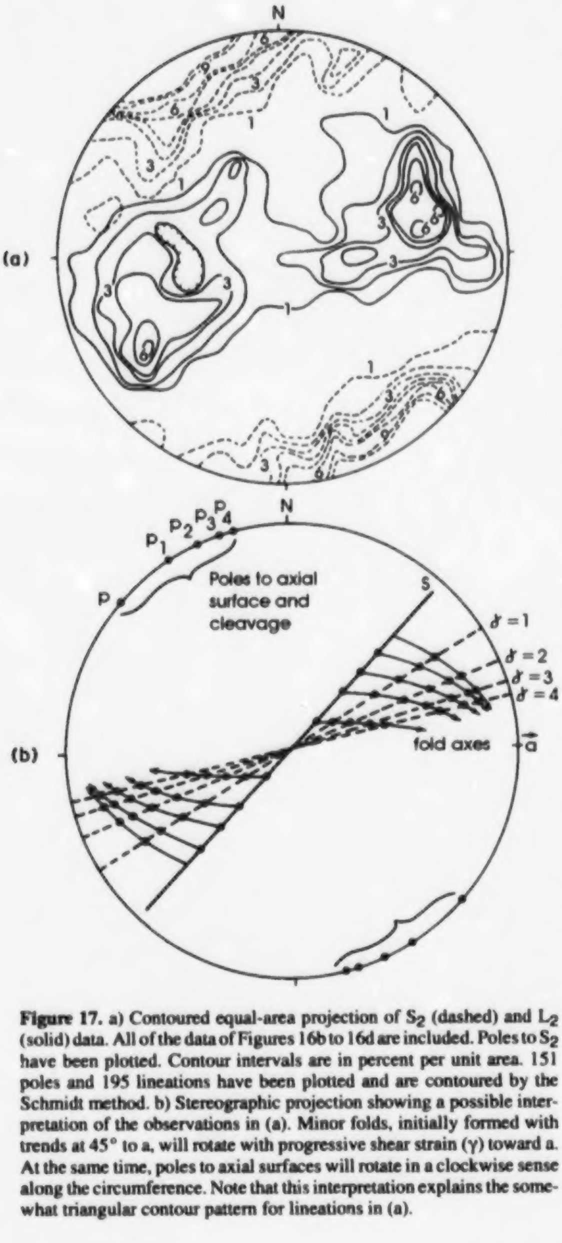

Figure 17. a) Contoured equal-area projection of S_2 (dashed) and L_2 (solid) data. All of the data of Figures 16b to 16d are included. Poles to S_2 have been plotted. Contour intervals are in percent per unit area. 151 poles and 195 lineations have been plotted and are contoured by the Schmidt method. b) Stereographic projection showing a possible interpretation of the observations in (a). Minor folds, initially formed with trends at 45° to a, will rotate with progressive shear strain (γ) toward a. At the same time, poles to axial surfaces will rotate in a clockwise sense along the circumference. Note that this interpretation explains the somewhat triangular contour pattern for lineations in (a).

ber of different ways. First, the experiment of Lowell (1972) (*see* Figure 20b) does predict periclinal structures such as the Rice Bay Dome; however the bimodal character of the lineations is also evident well away from that structure. Second, conjugate sets of fold axes of shallow plunge have been documented in transcurrent mylonite zones (Berthe and Brun 1980), where they are thought to result from the folding of layered, strongly anisotropic material. A third, more satisfactory, explanation assumes that these lineations formed parallel to the intersection of the initial D_2 cleavage and variably oriented (i.e., previously folded) beds.

The locus of such axes, for the present example, is the (initial) cleavage plane S of Figure 17b. Progressive dextral simple shear will deform these lineations, if they are assumed to behave passively, along trajectories containing the displacement direction "a". Successive positions for each point result from increasing shear strains ($\gamma=1,2,3,4$). Note that, in the same deformation, the pole to cleavage (P) is successively rotated to P_1, P_2, etc. (*see* Figure 17b). This type of deformation path has the property of forcing initially steep and shallow lineations toward a common shallow orientation. However, at moderate shear strains ($\gamma=3,4$), only the originally shallowest lineations approach the horizontal. If this type of strain is inhomogeneously developed across a wrench zone, then 2 somewhat triangular clusters of lineations will develop, since all linear elements within a single triangle will be variably rotated toward a common subhorizontal position that defines the apex of the triangle. This is, in fact, the pattern observed in the study area (Figure 17a). Note that the reference frame for Figure 17b has been rotated to correspond to a "best fit" to the data of Figure 17a. This results in an inferred displacement direction "a" which trends approximately east.

The final distinctive aspect of the structural geology in the study area is the presence of inverted stratigraphic panels (Pocket Pond, Bear Passage) and downward-facing F_2 folds (Nickel Lake). Poulsen (1980a) recognized these features, and suggested that they were a result of refolding of the previously inverted limbs of large fold nappes. This interpretation was supported by the observation of downward structural facing of small folds at Morton and Sandpoint islands (Poulsen, Borradaile and Kehlenbeck 1980). Such nappes might be of a regional nature and unrelated to the development of a wrench zone, or may be directly related to it as predicted by the models of Lowell (1972).

Figure 21 illustrates schematically the possible geometry of folds that satisfies observed bedding attitudes and younging directions near Rice Bay. However, modification of this geometry by faulting (tectonic slides) is also required to fully satisfy the present map pattern. The nappe hypothesis implies that the earliest F_1 folds were recumbent, but an equally viable alternative is that they were upright to slightly overturned. F_2 folds that presently face downward would initally face sideways and become progressively downward facing as a result of inhomogeneous simple shear as described by Cobbold and Quinquis (1980). A similar interpretation has been applied to downward-facing folds adjacent to the Great Alpine Fault of New Zealand (Lillie and Gunn 1964).

In summary, an internally consistent model of a tectonic wrench zone is proposed for the study area. The nature of pre-Seine deformation is unknown and the earliest structures are large, lithologically definable folds with a northeasterly trend. Because these folds have long axial traces, their plunges, although unknown, are probably shallow. Contemporaneously or subsequently, lenticular stratigraphic domains formed by dissection of early fold limbs along discordant domain boundaries. Movement, largely of a transcurrent nature, resulted in the rotation of early folds in a clockwise sense. Continued displacements

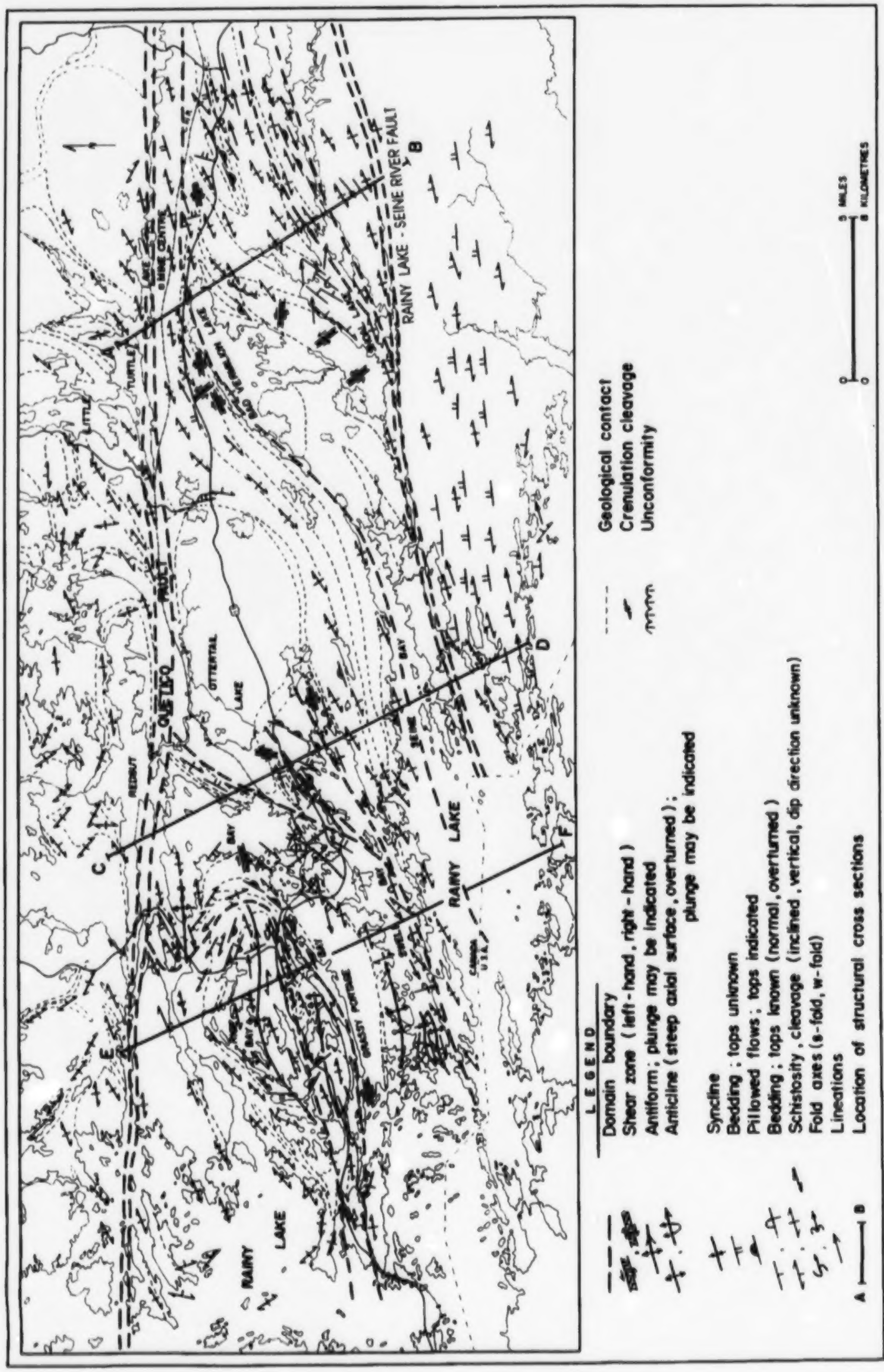
LEGEND
Domain boundary
Shear zone (left-hand, right-hand)
Antiform; plunge may be indicated
Anticline (steep axial surface, overturned); plunge may be indicated
Syncline
Bedding; tops unknown
Pillowed flows; tops indicated
Bedding; tops known (normal, overturned)
Schistosity, cleavage (inclined, vertical, dip direction unknown)
Fold axes (s-fold, w-fold)
Lineations
Location of structural cross sections
A
B
Geological contact
Crenulation cleavage
Unconformity
0
5 MILES
0
8 KILOMETRES
RAINY LAKE
QUETICO FAULT
RAINY LAKE - SEINE RIVER FAULT
OTTERTAIL LAKE
REDGUT BAY
LITTLE TURTLE LAKE
BAD VERMILION LAKE
GRASSY PORTAGE BAY
SEINE BAY
RAINY LAKE
CANADA
U.S.A.
C
D
E
F
B

Figure 18. Summary diagram showing the orientation of fabric elements relative to the boundaries of lithostratigraphic domains.

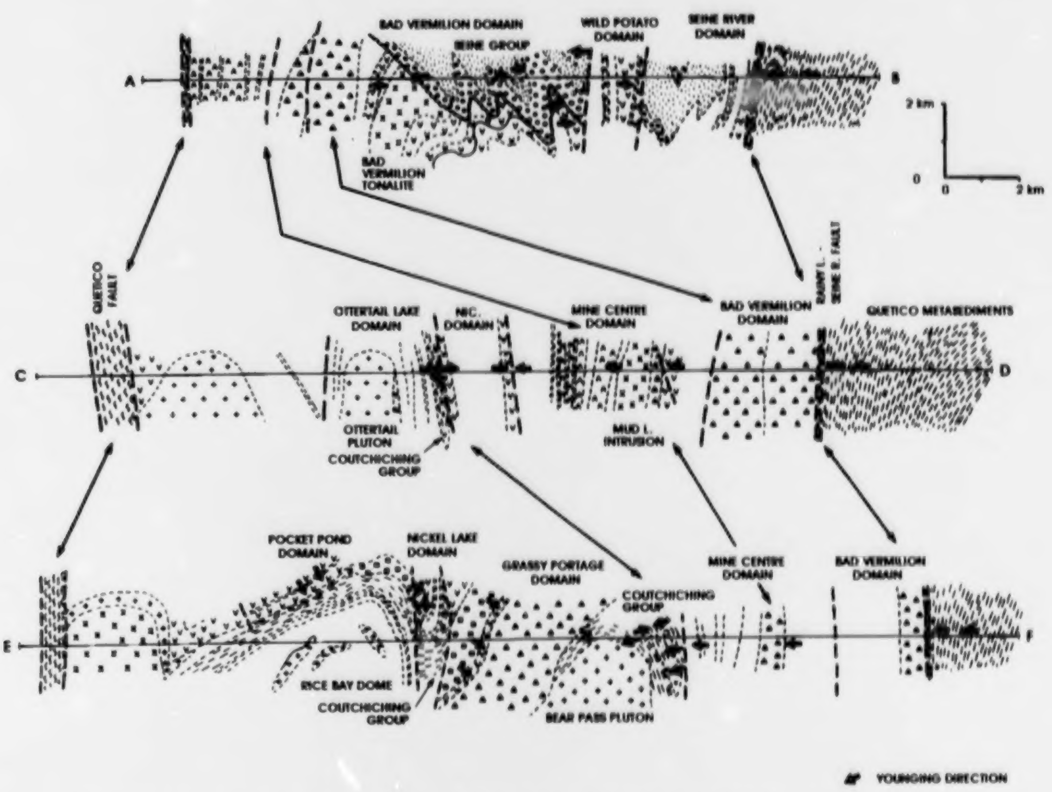
BAD VERMILION DOMAIN
SEINE GROUP
WILD POTATO DOMAIN
SEINE RIVER DOMAIN
A
B
2 km
0
0
2 km
BAD VERMILION TONALITE
QUETICO FAULT
RAINY L. - SEINE R. FAULT
OTTERTAIL LAKE DOMAIN
NIC. DOMAIN
MINE CENTRE DOMAIN
BAD VERMILION DOMAIN
QUETICO METASEDIMENTS
C
D
OTTERTAIL PLUTON
COUTCHICHING GROUP
MUD L. INTRUSION
POCKET POND DOMAIN
NICKEL LAKE DOMAIN
GRASSY PORTAGE DOMAIN
COUTCHICHING GROUP
MINE CENTRE DOMAIN
BAD VERMILION DOMAIN
E
F
RICE BAY DOME
COUTCHICHING GROUP
BEAR PASS PLUTON
YOUNGING DIRECTION

Figure 19. Selected structural cross sections for the Rainy Lake area. Locations of section lines are shown in Figure 18.

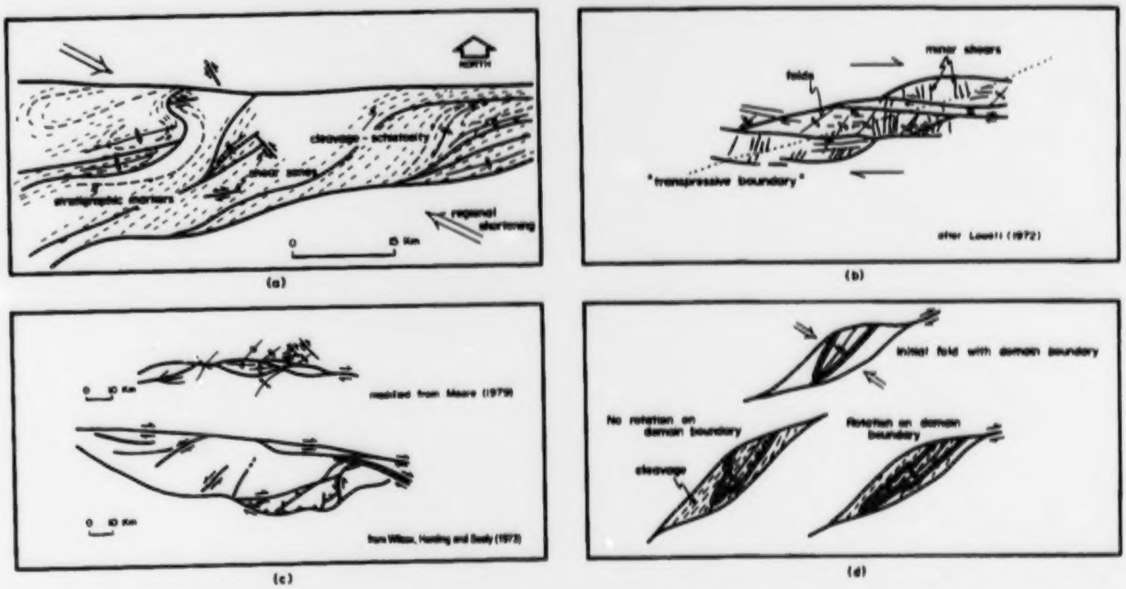
NORTH
cleavage - schistosity
shear zones
stratigraphic markers
regional shortening
0
15 Km
(a)
minor shears
folds
"transpressive boundary"
after Lowell (1972)
(b)
0
10 Km
modified from Moore (1979)
0
10 Km
from Wilcox, Harding and Seely (1973)
(c)
initial fold with domain boundary
No rotation on domain boundary
Rotation on domain boundary
cleavage
(d)

Figure 20. a) Schematic diagram showing structural observations, interpreted by a wrench fault model. b) Clay cake model experiments showing features associated with wrench faults. Adapted from Tchalenko (1970) and Lowell (1972). c) Natural examples of tectonic wrench zones and their geometry. d) Schematic diagram showing clockwise rotation of large fold limbs to form dextral asymmetry of later small folds. In the absence of rotation, the small structures mimic the major ones.

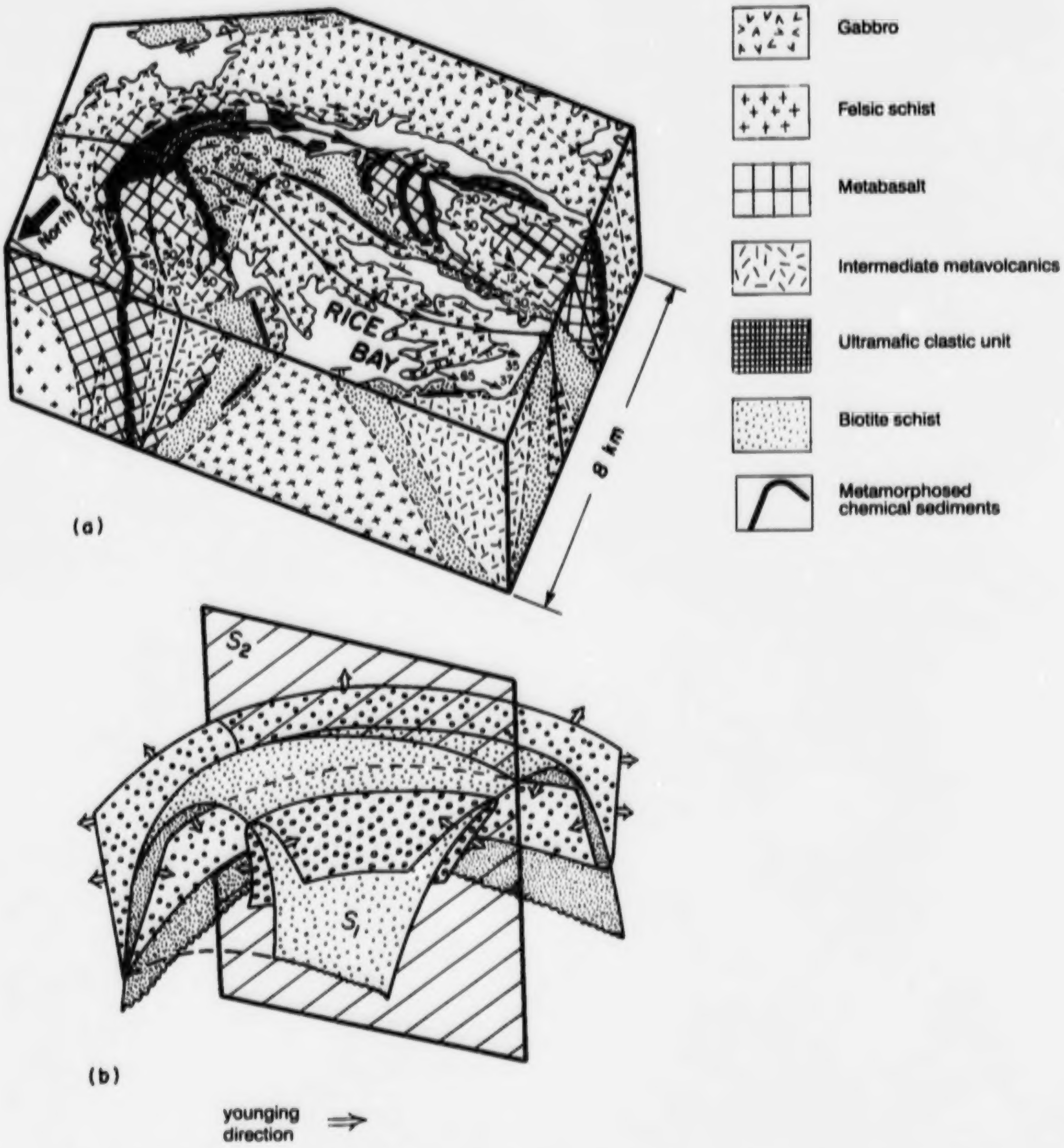
Gabbro
Felsic schist
Metabasalt
Intermediate metavolcanics
Ultramafic clastic unit
Biotite schist
Metamorphosed chemical sediments
North
RICE BAY
8 km
(a)
S2
S1
(b)
younging direction

Figure 21. a) Block diagram summarizing the geology near the Rice Bay Dome; *see* Map 2525 for standard structural symbols. b) Schematic diagram illustrating the form of folds necessary to satisfy the observations in (a). S_1 (stippling) and S_2 (diagonal lines) are indicated. This is but one possible interpretation of the data.

in the wrench zone as a whole resulted in the formation of a steep penetrative cleavage, and new large folds developed in the western part of the area. Ductile shear zones developed in competent units, and a general clockwise rotation of folds and fabric elements took place. Finally, the shear displacements localized on a few of the larger faults in which the size of asperities was reduced and on which relatively large displacements were generated. The result is the preservation of part of the original wrench zone in the study area. Corresponding parts may be present to the north and east of the Quetico Fault, and to the south and west of the Rainy Lake–Seine River fault. The broad-scale tectonic significance of such a wrench zone will be discussed further below (*see* "Tectonics and Metallogeny").

Metamorphic Petrology

METAMORPHIC FACIES

Earlier studies (Lawson 1913; Bruce 1925a; Peterman 1959; Harris 1974; Poulsen 1980a; Wood et al. 1980a, 1980b) have identified the presence of metamorphic minerals characteristic of the greenschist and amphibolite facies, but the precise spatial boundary between them has not been previously defined. Field and petrographic study of metamorphic assemblages has enabled the author to map the metamorphic facies (Figure 22). The distinction between the greenschist facies rocks and those of the amphibolite facies is based largely on the study of pelitic and mafic bulk compositions, although supporting evidence has been gained from local occurrences of calcareous and ultramafic rocks. Table 6 lists the observed assemblages that were used to construct Figure 22. Supporting petrographic data are listed in Appendix 2. For the purposes of this discussion, the term "metapelite" includes not only metasedimentary clastic rocks but also chemically altered felsic to intermediate metavolcanic rocks. The mafic rocks include metadiabases as well as metabasites.

Inspection of Table 6 reveals that most of the observed assemblages that distinguish the facies at Rainy Lake are those used elsewhere for the same purpose (Turner 1981, p.209). The relatively common occurrence of garnet, biotite, muscovite and quartz in metapelites, and hornblende and plagioclase without chlorite in metabasites, makes it easy to map the amphibolite facies rocks to which these assemblages belong. This facies is also characterized by the presence of porphyroblasts such as staurolite, andalusite and cordierite in "knotty schists" (metapelites), also useful in distinguishing this facies in the field. Anglin (1982) described grunerite in silicate-rich portions of iron formation within amphibolite facies rocks near Gagne Lake.

In general, metapelites of the greenschist facies are characterized by an absence of porphyroblasts, even though they are chemically identical to those of the amphibolite facies (Poulsen 1980a). Skarn-like assemblages in impure carbonate horizons within iron formation and in metamorphosed veins in metabasite of the greenschist facies contain calcite, grossularite, and zoisite with diopside. Anglin (1982) described stilpnomelane from the greenschist facies near Gagne Lake. Chloritoid (Photo 22) with chlorite, muscovite and calcite in altered metavolcanic rocks near Shoal Lake is diagnostic of the greenschist facies, and ubiquitous mafic rocks contain abundant chlorite.

A significant feature of most amphibolite facies metapelites is the clear evidence of selective retrograde alteration of the porphyroblasts. The nature of these retrograde effects can be demonstrated in the Bear Passage–Redgut Bay area, where fresh porphyroblasts (Photo 23) become progressively altered in a southwestward direction. In samples with the weakest alteration, andalusite and staurolite (Photo 24) are selectively replaced by fine-grained white mica and chlorite, while garnets remain fresh. Complete replacement of staurolite is accompanied by the retrograde alteration of garnet rims to iron-chlorite (Photo 25). Intense alteration is marked by the complete replacement of garnet by chlorite; staurolite and andalusite in these rocks are generally indistinguishable except where the unique habit of staurolite is evident. The intense alteration of porphyroblasts is also accompanied by the development of abundant chlorite after biotite within the matrix.

Ovoid porphyroblasts up to 4 cm long have only been observed at localities where some degree of alteration is present. While they are distinctive in outcrop, these porphyroblasts appear as indistinct aggregates of chlorite, muscovite and quartz in thin section. Poulsen (1980a) has interpreted these to be cordierite, although no fresh cordierite has been identified in these rocks. In any one outcrop, these porphyroblasts are localized in particular beds that are possibly enriched in iron and magnesium. They do not make up part of the staurolite-bearing assemblages.

The intensity of the retrograde alteration in the metapelites was mapped in a qualitative sense by considering the state of preservation of garnet: fresh, rimmed, and completely pseudomorphed garnets define the zones of increasing retrogressive alteration in Figure 22. The patterns developed are in part a function of the distribution of pelitic rocks and in part a function of the density of sampling. Nonetheless, the close spacing of samples in the Bear Passage area attests to the progressive and penetrative nature of the retrograde effects. In this area and elsewhere along Swell Bay, the retrogressive effects appear to correlate spatially with late-stage granitoid plutons. In the Rice Bay Dome area, correlation is less obvious, although granitoid dikes are quite common in the biotite schists in this area.

Extensive retrograde alteration of the amphibolite facies metapelites makes it impossible to map prograde reaction isograds in this area. Further, this area has been erroneously designated as being of greenschist facies on the metamorphic map of Canada (Geological Survey of Canada 1978). In spite of the alteration, the presence of local fresh assemblages permits both qualitative and quantitative interpretation of the conditions of prograde metamorphism.

METAMORPHIC CONDITIONS

The distribution of metamorphic mineral assemblages (*see* Figure 22) indicates that rocks in the northwestern part of the study area have been metamorphosed to medium grade. The boundary between low- and medium-grade rocks occurs within metapelites along Swell Bay and also corresponds, in part, to a postmetamorphic fault in the Redgut Bay area. Contact metamorphism is suggested by the close spatial relationship between the metamorphic boundary and Algoman intrusions, particularly the Otter-

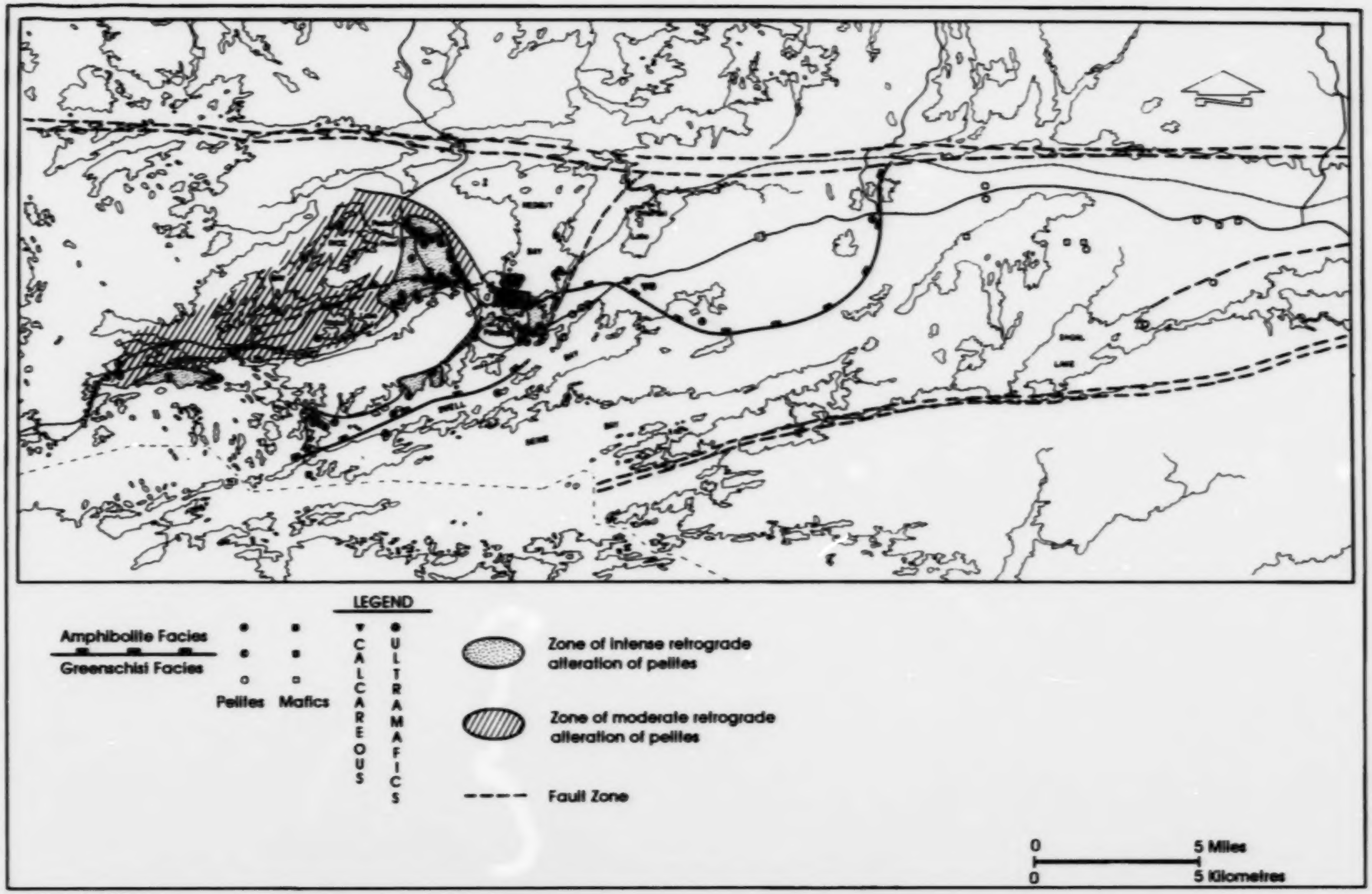
LEGEND
Amphibolite Facies
Greenschist Facies
Pelites
Mafics
CALCAREOUS
ULTRAMAFICS
Zone of intense retrograde alteration of pelites
Zone of moderate retrograde alteration of pelites
Fault Zone
0
5 Miles
0
5 Kilometres

Figure 22. Metamorphic map of the Mine Centre–Fort Frances area. Solid symbols represent thin-section verification of amphibolite facies assemblages, open symbols represent greenschist facies assemblages and other symbols indicate indeterminate assemblages.

Table 6. Metamorphic mineral assemblages, Mine Centre–Fort Frances area, Rainy Lake.

Greenschist Facies	
Metabasites	chlorite + albite + quartz + carbonate + magnetite
	chlorite + epidote + quartz + carbonate + magnetite
Altered metavolcanics	quartz + chlorite + sericite + albite
	chloritoid + chlorite + sericite + quartz + carbonate
Metapelites	quartz + albite + muscovite + chlorite
	quartz + biotite + muscovite + chlorite + albite
Amphibolite Facies	
Metabasites	hornblende + plagioclase + quartz + epidote + sphene
	actinolite + magnesium chlorite + talc + magnetite
	actinolite + magnesium chlorite + quartz
	hornblende + epidote + biotite + plagioclase + quartz
Altered metavolcanics	cordierite + anthophyllite + chlorite (retrograde assemblage)
Metapelites	garnet + staurolite + magnesium chlorite + biotite + plagioclase + quartz
	garnet + staurolite + magnesium chlorite + biotite + andalusite + quartz
	garnet + staurolite + magnesium chlorite + biotite + sillimanite + andalusite + quartz
	staurolite + andalusite + biotite + quartz
	muscovite + garnet + biotite + sillimanite
Impure marble	calcite + diopside + garnet + epidote

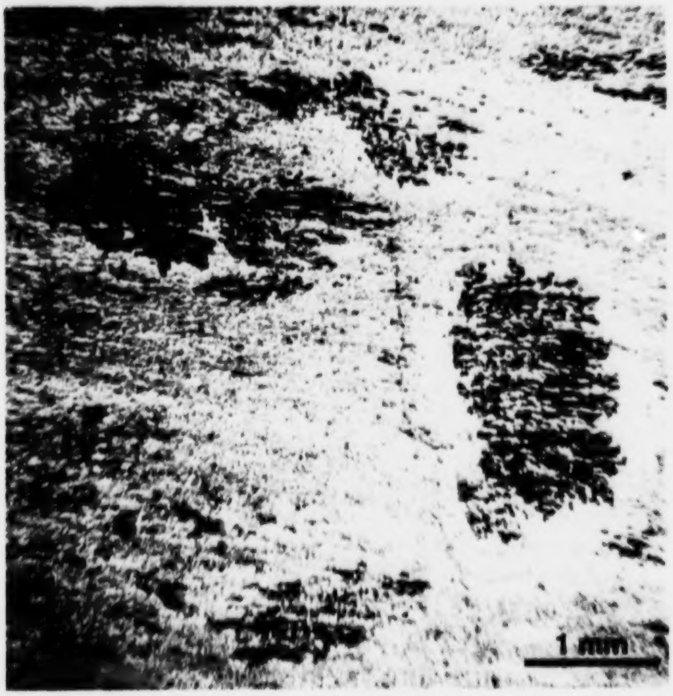

Photo 22. Photomicrograph of a chloritoid schist, Shoal Lake area. Note the continuity of internal and external foliation with respect to the chloritoid grains. These are interpreted to be postkinematic porphyroblasts.

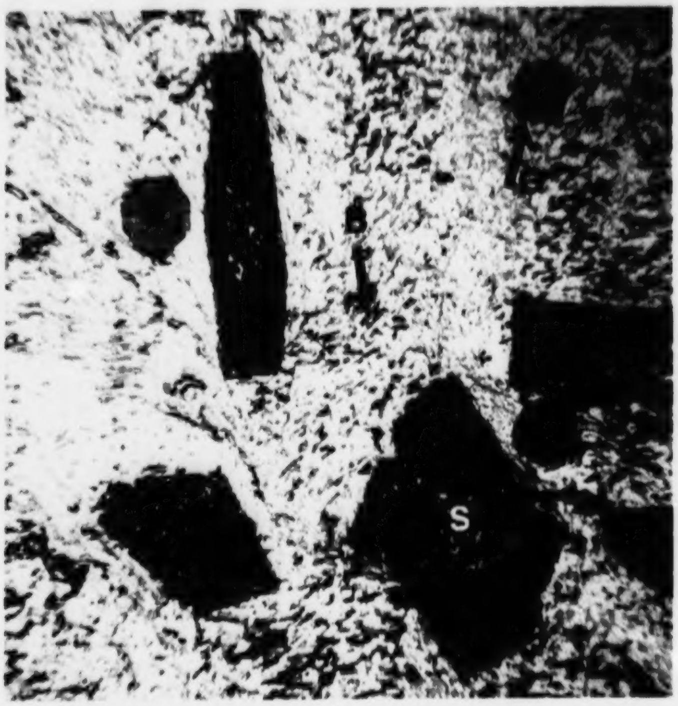

Photo 23. Photomicrograph of a staurolite (S)-garnet (G)-biotite (B) schist, Redgut Bay area. Note that the porphyroblasts are postkinematic with respect to the biotite foliations. Scale as in Photo 22.

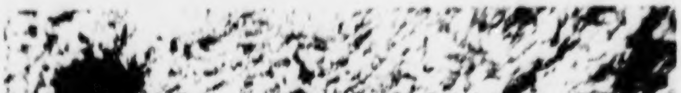

Photo 24. Photomicrograph of weak retrograde alteration of staurolite (S) in biotite schist, Redgut Bay area. Garnet (G) remains fresh. Scale as in Photo 22.

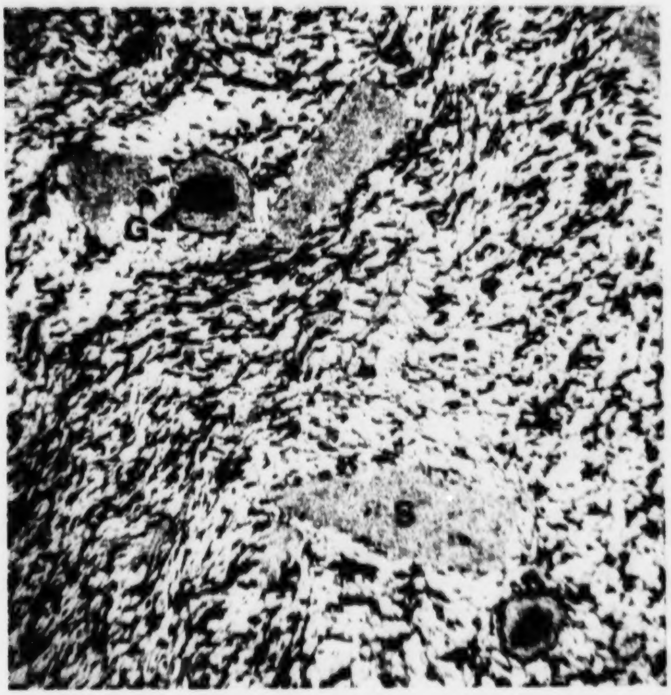

Photo 25. Photomicrograph of retrograde alteration of staurolite (S) and garnet (G) in biotite schist, Redgut Bay area. Staurolite is replaced by white mica and chlorite, and the garnets are rimmed by iron-chlorite. Scale as in Photo 22.

tail Lake pluton, as well as the increased size of porphyroblasts near pluton margins. On the other hand, amphibolite facies assemblages are found far beyond the pluton margins, and blocks of schist occur within the plutons. Furthermore, metamorphic textures that can be interpreted as evidence of synkinematic (Photo 26) to postkinematic (*see* Photos 22 and 23) mineral growth are common, suggesting that regional dynamothermal metamorphism was also important in this area.

Metamorphic temperatures, pressures and fluid compositions were estimated for amphibolite facies rocks from selected localities using 4 independent approaches:

1. graphical analysis of pelitic assemblages
2. mineral chemistry of pelitic assemblages, particularly garnet-biotite geothermometry
3. mineral analysis of metamorphosed sulphide minerals, in particular sphalerite geobarometry
4. analysis of stability conditions of skarn-like assemblages

General observations about metamorphic conditions come from considering the broad stability ranges dictated by the observed pelitic assemblages. The presence of both staurolite and chloritoid in the area, coupled with coexisting sillimanite and andalusite (Photo 27) suggest that a temperature range of 450 to 550°C at pressures less than that of the aluminosilicate triple point are quite probable (Figure 23a). An elegant first estimate of metamorphic pressure and temperature can be made for low-variance pelitic assemblages (*see* Table 6) in the Bear Passage–Redgut Bay area, as both biotite + garnet + andalusite and quartz + muscovite + staurolite + sillimanite assemblages are present, and these are diagnostic of the boundary between bathozones 2 and 3 of Carmichael (1978). The bathozone boundary corresponds to temperature and pressure estimates of 540°C and 3.4 kilobars, respectively.

Minerals from 2 fresh, low-variance specimens of a staurolite-garnet-biotite schist from the Redgut Bay locality were subjected to analysis by wavelength dispersive electron microprobe techniques (Appendix 3). Average results are listed in Table A3.1 along with structural formulae computed using programs designed by D.M. Carmichael (Department of Geological Sciences, Queen's University, personal communication, 1983). All minerals except garnet proved to be chemically uniform. Garnets show slight consistent zoning, with greater concentrations of magnesium, calcium and manganese in the core as compared to the rim. A particular problem in interpreting the mineralogical data is the presence of small but significant quantities of both muscovite and chlorite in these sillimanite-bearing specimens. Depending upon whether one, both or neither of the muscovite or chlorite are equilibrium phases, the computed variance of the assemblage is, respectively, 0, –1, or 1. Since both minerals appear to be in textural equilibrium with the other minerals (Figure 23b) and are nowhere in contact with one another, their presence may merely reflect local inhomogeneities in the bulk chemistry of the rocks, and the bathograd equilibrium, as

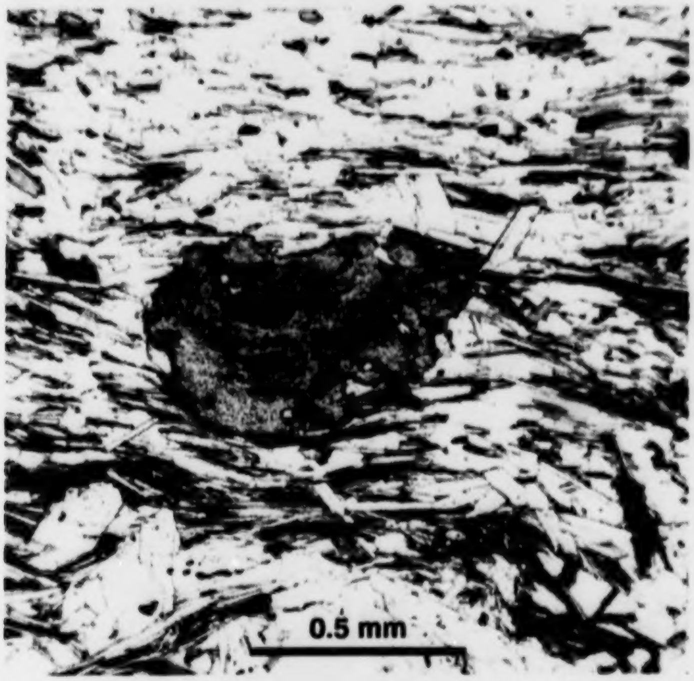

Photo 26. Photomicrograph of helicitic inclusion trails in garnet from biotite schist near Nickel Lake. The garnets are interpreted to be synkinematic.

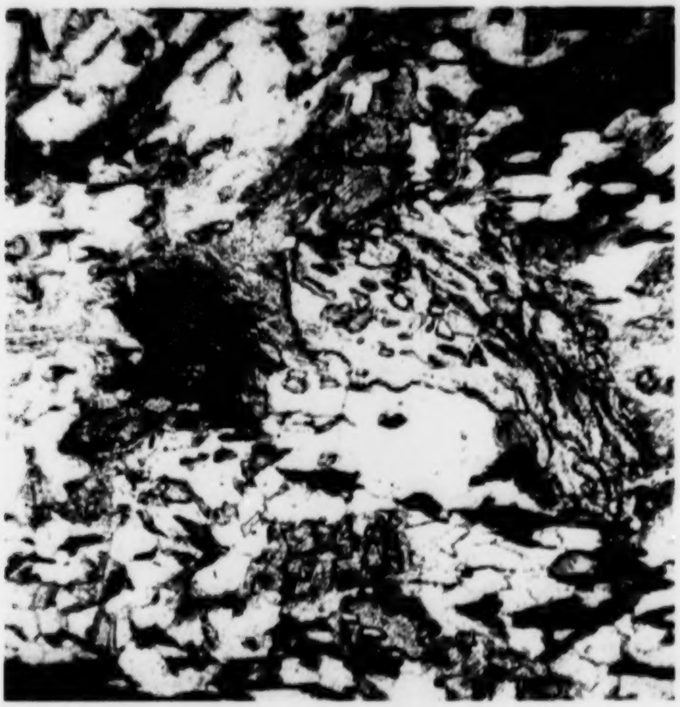

Photo 27. Photomicrograph of coexisting andalusite (A) and fibrous sillimanite (S), Redgut Bay area. The thin section also contains staurolite, biotite, garnet, and minor white mica and magnesium chlorite. Scale as in Photo 26.

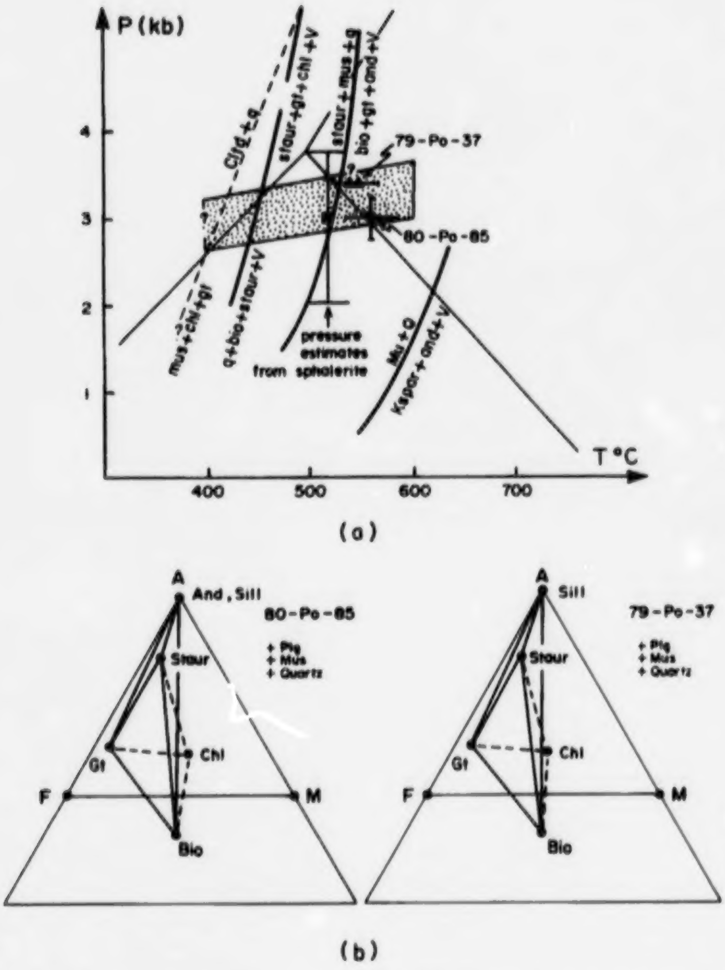

Figure 23. a) P-T diagram showing the estimated range of metamorphic conditions indicated for rocks in the study area. Petrogenetic grid *largely after* Carmichael (1978 and personal communication, 1980). The stippled area on the diagram shows the limits of the estimate, the solid square shows the pressure estimate by sphalerite geobarometry, and the solid circle and open triangles show estimates based on garnet-biotite geothermometry and the observed aluminosilicate phase. mus=muscovite, chl=chlorite, gt=garnet, q=quartz, bio=biotite, staur=staurolite, Kspar=potassium feldspar, and=andalusite, cltd=chloritoid, V=vapour. 79-Po-37 and 80-Po-85 are sample numbers. b) AFM diagrams for the ideal pelitic system showing the compositions of coexisting minerals for biotite schists, Redgut Bay area. And=andalusite, Sill=sillimanite, Staur=staurolite, Gt=garnet, Chl=chlorite, Bio=biotite, Plg=plagioclase feldspar, Mus=muscovite.

described previously, should provide reasonable estimates of metamorphic temperature and pressure. Furthermore, the staurolite breakdown curve (*see* Figure 23a), on which the bathograd estimates heavily depend, is only displaced to lower temperatures by less than 15°C when ideal activities for the Redgut Bay minerals, as estimated from Table A3.1, are substituted in the end member reaction for this curve.

Analyses of coexisting garnet-biotite pairs were used to obtain temperature estimates by the geothermometry method of Ferry and Spear (1978), who experimentally calibrated the temperature against the partition coefficients of Fe and Mg in these two minerals. Pigage and Greenwood (1982) showed that partitioning also depends on the Mn and Ca contents in garnets, and provided a correction factor for this effect. The results, using the methods of both pairs of authors, are shown in Table 7, along with estimates of pressure for the sample containing both andalusite and sillimanite (80-Po-85). Garnet cores provide higher estimates than rims, and the Pigage and Greenwood (1982) correction increases estimated temperatures for these specimens by approximately 70°C. The range of garnet rim temperatures (494 to 578°C) is in reasonable agreement with the bathograd estimate. The temperatures obtained using the Pigage and Greenwood (1982) correction are the most compatible with the known aluminosilicate mineralogy and their positions are shown in the P-T space in Figure 23a.

Independent pressure-temperature data were sought from metamorphosed sulphide ores from the eastern end of

Table 7. Pelite geothermometry and geobarometry at Redgut Bay[a].

Sample		Ferry and Spear (1978)			Pigage and Greenwood (1982)	
	core (T, C)	rim (T, C)	rim (P,kilobars)	core (T, C)	rim (T, C)	rim (P,kilobars)
80-Po-85a)	558	509	3.72	636	575	3.02
b)	547	514	3.63	607	580	2.98
c)	573	532	3.48	666	599	2.75
d)	558	491	n/a	644	557	3.20
mean	559	512	3.61	638	578	2.99
79-Po-37a)	555	476	n/a	627	539	n/a
b)	525	486	n/a	590	547	n/a
c)	540	521	n/a	607	579	n/a
mean	540	494		608	555	

(a) *Temperature estimates made from garnet–biotite microprobe analyses using an estimate of 3.5 kilobars pressure except for sample 80–Po–85, for which pressure estimates were obtained using the intersection of the temperature calibration with the andalusite–sillimanite univariant curve (Holdaway 1971).*

Nickel Lake, where nearby metapelites contain staurolite, garnet and biotite. Although the assemblage arsenopyrite + pyrite + pyrrhotite occurs in these rocks, a high cobalt content in the arsenopyrite precludes its use as a geothermometer (Kretschmar and Scott 1976). However, a sample containing pyrite, pyrrhotite and sphalerite shows good triple junction contacts between these minerals, which is characteristic of metamorphosed sulphide ores (*see* "Mineralization"). X-ray diffraction analysis showed the pyrrhotite to be hexagonal (Arnold 1966), and microprobe analyses of FeS (Appendix 4) were obtained from 5 points at each of 5 such grains of sphalerite: 1 analysis was made at each triple point, and 2 analyses each were made along nearby contacts with pyrrhotite and pyrite, respectively (Table A4.1).

These results are shown graphically in Figure 24a, along with those from an internal standard, S121, for comparison. The data show the same range of natural variation in comparable studies (Hutchison and Scott 1980) and are skewed to lower values. Note that the sphalerites are unusually manganiferous (6.40 to 8.60 weight % Mn, Table A4.1) but this is not thought to affect their usefulness as a geobarometer (Hutchison and Scott 1981). The median value of 16.8 mole % FeS in sphalerite ($Fe_{16.8}Mn_{12.9}Zn_{74.8}S$, median of 25 analyses) was chosen to represent the data, and the probable uncertainties associated with this value (+1.2%, -0.9%) were chosen subjectively by excluding only 4 extreme analyses and including all of the measurements made directly at the triple junction. A pressure of 3.0 +0.8/-1.0 kilobars was derived from the experimentally derived calibration curve of Hutchison and Scott (1981). The well-defined upper limit represents a reasonable maximum pressure and is compatible with the silicate interpretation.

A stratiform unit composed of marble and skarn-like rocks with associated iron formation occurs at Pocket Pond. Calcite is the dominant phase and clinopyroxene, garnet and epidote are abundant. Minor actinolite occurs as an alteration product of the primary minerals. Table A3.3 gives analyses of these minerals and Figure 24b shows the observed coexisting phases in the ACF projection. It is significant that coexisting calcite, grossularite and epidote form part of this assemblage. These represent a univariant equilibrium assemblage in the system CaO-Al_2O_3-SiO_2-H_2O-CO_2 if one of the variables of pressure, temperature or mole fraction CO_2 in the vapour phase is fixed. Such an equilibrium was computed at 3 kilobars along with relevant dehydration curves (Figure 24c) using the programs of D.M. Carmichael (Department of Geological Sciences, Queen's University, personal communication, 1983). The sensitivity of these curves to both pressure and the substitution of iron for aluminum and calcium in the minerals was tested, and neither factor appears to be particularly significant. The equilibrium curves show that, while the assemblage is stable over a wide permissible range of temperature and total pressure, the mole fraction of CO_2 in the vapour phase must be low. The CO_2 generated by decarbonation and mixed with water-rich, externally derived fluid is probably sufficient to account for its presence.

In summary, amphibolite facies metamorphism in the northwestern part of the study area was broadly synchronous with deformation and granite plutonism. Metamorphic temperatures of 500 to 600°C and a pressure of approximately 3 kilobars involved fluids with very low mole fractions of CO_2. The presence of chloritoid with chlorite, muscovite and quartz in the southeastern part of the area suggests temperatures of at most 400°C for the greenschist facies rocks. However, there is no evidence to suggest that metamorphic pressure was necessarily less than that for the amphibolite facies rocks. The contrasting metamorphic facies further distinguishes the western from eastern lithostratigraphic domains. Offset of the facies boundary in the Bear Passage area shows that some domain boundaries were formed after the peak of metamorphism.

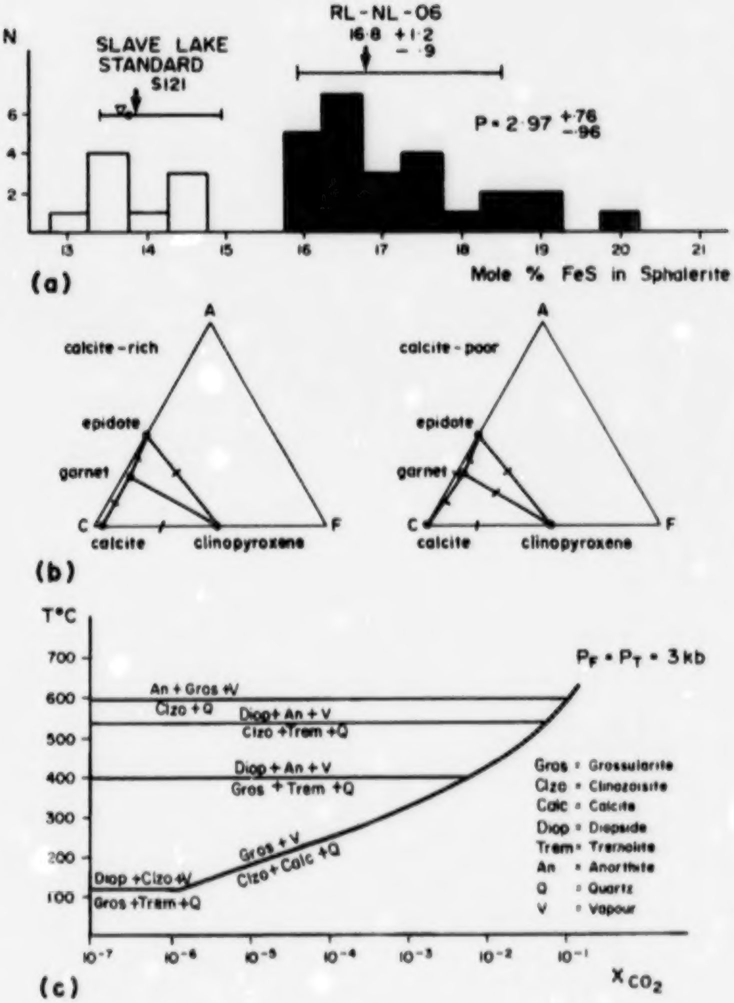

Figure 24. a) Histogram of analyses of FeS in sphalerite from Nickel Lake. The Slave Lake (Grenville Subprovince) sample was analyzed concurrently and the range of values for it above the histogram was that obtained by analysis with respect to a well-studied synthetic standard. The open triangle on this bar is the previously proposed "recommended" value for this standard, the closed circle is the median for the calibration versus the synthetic standard, and the arrow corresponds to the median for the analytical runs concurrent with the Nickel Lake data. Note that these discrepancies are small in comparison to the wide natural range of compositions. b) ACF diagram illustrating observed calc-silicate assemblages in skarn-like rocks, Pocket Pond. Mineral compositions were determined by microprobe analysis (*see* Table A3.1). c) T versus X_{CO_2} diagram illustrating the wide range of permissible metamorphic conditions for the assemblage calcite + clinozoisite + grossularite in the presence of quartz and diopside. kb = kilobars

Mineralization

CLASSIFICATION AND DISTRIBUTION

The Rainy Lake area has a long history of mineral exploration and exploitation since the discovery of gold at Mine Centre in 1893. At that time, 3 small deposits, the Olive, Golden Star and Foley were mined, and coupled with renewed activity during the 1930s, a total production of 485 kg gold and 20 kg silver was realized (Beard and Garratt 1976). The apparent similarity of iron formations at Nickel Lake with those at Wawa, 600 km to the east, led to exploration in the area for iron at the turn of the century and for sulphur at the end of World War I. Magnetite-ilmenite mineralization at Seine Bay was tested by diamond drilling in 1920 and in 1955 (Rose 1969). Since the 1950s, exploration in the region has focussed largely on the search for base metal mineralization. North Rock Mines Limited, in 1973, sank a 70 m two-compartment shaft on mineralization discovered in gabbro by Noranda Exploration Co. Ltd. prospectors at Grassy Portage Bay in 1959. Numerous base metal occurrences have recently been evaluated by diamond-drill and geophysical programs, but none of these have proven economically viable.

There were 89 staked properties, including mines, prospects and occurrences, in the Rainy Lake area in 1984: 87 of these lie between the Quetico and Rainy Lake–Seine River faults. A combination of field observations and data available in reports and assessment files (Assesment Files, Resident Geologist's Office, Kenora) was used to classify the mineral deposits into descriptive groups. The classification (Table 8) is based on the following features:

1. host rocks: volcanic, plutonic, sedimentary or fault rocks
2. morphology: stratabound, stratiform, lenticular, vein or disseminated mineralization
3. composition: mineral association, commodities

Each mineral deposit type is subdivided according to variations within the group. Figure 25 illustrates the distribution of the various types of mineralization in the study area. The location and extent of each property at the time it was worked, and a full description of each, are included in Poulsen (1984, 2000).

Type 1: Metavolcanic-Hosted Mineralization

Zinc-copper mineralization at Rainy Lake occurs in a number of specific volcanic environments. For example, the mineralization at Gagne Lake (Type 1A, Table 8) consists of lenses of massive sphalerite and galena as wide as 20 cm, which parallel similar overlying pyritic layers. Rocks of the footwall to the south of the mineralized zone consist dominantly of rhyolitic lapillistone that locally contains a distinctive spotted alteration ("dalmatianite") of chlorite and centimetre-sized porphyroblasts of pinitized cordierite. The hanging-wall rocks consist of fine-grained siltstone and chert that locally form a coarse breccia with clasts as large as 50 cm in diameter. Mineralization at the Pidgeon property occupies a similar setting, where a diamond-drill intersection of approximately 2 m true width yielded assays of 0.53% Zn and 1.76% Pb. Low silver values (as high as 0.3 ounce per ton) have been reported from sulphide-rich material. Pyritic blebs in felsic lapilli tuff typify the zones of footwall alteration, which are laterally more extensive than individual sulphide lenses.

Although the mineralogy of the Type 1B occurrences is similar to that of the massive sulphide (Type 1A) deposits—consisting of sphalerite, pyrite, pyrrhotite, chalcopyrite and minor galena—the Type 1B occurrences possess a number of distinctive characteristics. Firstly, the host rock is commonly an amygdaloidal, brecciated, intermediate to mafic metavolcanic rock. Secondly, the mineralization occurs as discrete seams 1 to 20 cm wide, which are separated by substantial widths (1 to 20 cm) of barren chloritic host rock.

At the Wind Bay property, a typical drill section through 50 m of tuffaceous chlorite schist indicated two mineralized zones, 7 m and 8.6 m in true width, which averaged 1.5% Zn and 0.2% Cu, and 1.1% Zn and 0.09% Cu, respectively (G. Armstrong, Prospector, personal communication, 1980). The mineralization at Wind Bay is underlain to the south by rhyolite lapillistone and tuff, which near the contact contains alteration consisting of abundant pyrite and pyrrhotite blebs with minor chalcopyrite. The chlorite schists are overlain by relatively unaltered quartz-eye rhyolite tuffs.

The stratigraphic setting of the mineralization at the Port Arthur Copper Co. Mine is virtually identical to that at the Wind Bay property. Diamond drilling by Stratmat Limited in 1916 revealed a zonal arrangement of copper and zinc within the host rock, with zinc-rich zones being underlain to the south by copper-rich mineralization. The Port Arthur Copper Co. deposit was mined in 1916, yielding a limited tonnage grading approximately 3% copper. The mineralized horizon is succeeded abruptly to the north by a cherty horizon approximately 1 m in thickness, which is in turn overlain by felsic quartz-eye tuffs, forming a thick hanging-wall sequence.

At least 9 occurrences of the Wind Bay–Port Arthur Copper type of mineralization (Type 1B) occupy a single stratigraphic horizon that is exposed over a strike length exceeding 25 km. Although these deposits collectively represent a substantial amount of base metal mineralization, no single prospect has been shown to have sufficient grade or tonnage to be economically viable at this time.

Mineralization of Type 1C likewise represents a substantial dispersion of metal with a resulting low grade. At Pocket Pond (*see* Figures 25 and 29), significant quantities of sphalerite and chalcopyrite are associated with iron formation, which is dominantly composed of chert-magnetite and sulphide-bearing carbonates. The base metal min-

Table 8. Mineral deposits classification, Mine Centre–Fort Frances area.

Type 1: Stratabound Mineralization Hosted by Felsic to Mafic Metavolcanic Rocks

A. Sphalerite-galena-chalcopyrite associated with siliceous volcanic rocks: (Golden Star Mine (1)); Gagne Lake prospect (37); Hanna prospect (50); Pidgeon prospect (51)

B. Sphalerite-chalcopyrite associated with intermediate to mafic amygdaloidal volcanic flows, tuffs and breccias: Port Arthur Copper Co. Mine (4); Stratmat–Copperlane prospect (16); Ronda–Satellite prospect (17); Wind Bay prospect (38); Lochart Lake prospect (39); Farrington Boundary prospect (40); (Blondeau–Merryth prospect (49)); Hickerson occurrence (59); Mathieu occurrence (67); Anomaly 44A occurrence (69); Barber Lake base metal occurrence (70)

C. Sphalerite-chalcopyrite associated with iron formation: Pocket Pond prospect (24); McTavish prospect (26); Paramaque prospect (27); Nickel Lake prospect (28); Daley–Galbraith prospect (29); Sims Station prospect (30); Rocky Islet Bay prospect (33); Ottertail Lake prospect (35); Moosehorn occurrence (82)

D. Lean iron formation (mainly chert-magnetite and massive pyrite-pyrrhotite, minor chalcopyrite common): (Pocket Pond prospect (24)); Noranda Pocket Pond prospect (25); (McTavish prospect (26)); (Nickel Lake prospect (28)); (Brunette prospect (31)); Stanol prospect (32); (Rocky Islet Bay prospect (33)); (Ottertail Lake prospect (35)); (Young–Corrigan prospect (36)); Shoal Lake iron occurrence (52); Moose Point occurrence (75); Rice Bay occurrences (79); Cooper–Weiss occurrence (80); Wallace occurrence (81); Kotnick occurrence (83); Reef Point occurrence (84); Croome occurrence (85); Miller's Bay occurrence (86); Parry Strait occurrence (89)

Type 2: Mineralization Hosted by Layered Gabbroic Intrusions

A. Chalcopyrite associated with gabbro and leucogabbro near the base of sills: North Rock Mine (5); (Stratmat–Copperlane prospect (16)); Hupchuk prospect (19); PCE prospect (21); (Belacoma prospect (22)); Redgut Bay prospect (23); (Daley–Galbraith prospect (29)); Stang prospect (42); Island Bay copper occurrences (63); Amalgamated Rare Earths occurrence (65); Drawbridge occurrences (77)

B. Disseminated chalcopyrite associated with siliceous phases of intrusions: Mironsky prospect (18); (Traverse Inlet prospect (20)); (Drawbridge occurrences (77))

C. Ilmenite-magnetite-apatite-rutile lenses in the upper portions of the intrusions: (Mironsky prospect (18)); Traverse Inlet prospect (20); Seine Bay iron prospects (41); Bear Pass iron occurrence (76)

Type 3: Vein Mineralization

A. Quartz-gold-sulphide veins in shear zones and cleavage-parallel dilatant zones: Golden Star Mine (1); Foley Mine (2); Olive Mine (3); Pacitto prospect (6); Isabella Mine (7); Ferguson Mine (8); Golden Crescent Mine (9); Russell C. Cone Mine (10); Cone prospect (11); Stagee prospect (12); Alice "A" Mine (13); Turtle Tank prospect (14); Saundary Mine (15); (Stratmat–Copperlane prospect (16)); Young–Corrigan prospect (36); (Gagne Lake prospect (37)); Stellar Mine (43); South Vermilion Mine (44); McKenzie–Gray prospect (45); Dinosaur prospect (46); Lucky Coon Mine (47); Manhattan–Decca mines (48); Blondeau–Merryth prospect (49); Emma Abbot occurrence (53); Gold Bug occurrence (54); East Turtle River occurrence (55); West Turtle River occurrence (56); Turtle Siding occurrence (57); McMillan occurrence (58); Emperor Mine (60); Gibson occurrence (61); Smylie occurrence (62); Stone occurrence (64); Corrigan occurrence (66); Thompson occurrence (68); Barber Lake gold occurrence (71); Scott Island occurrence (72); Swell Bay occurrence (73)

B. Quartz-molybdenite-pyrite veins and disseminations in unmetamorphosed granitoid rocks: Bear Pass prospect (34); (Ottertail Lake prospect (35)); Tunnel Bay occurrence (74); Highway 11 molybdenum occurrence (78); Hopkins Bay occurrence (87); Otter Bay occurrence (88)

Type 4: Disseminated chalcopyrite-pyrrhotite mineralization hosted by ultramafic metavolcanic rocks: (North Rock Mine (5)); Belacoma prospect (22)

Note: ( ) parentheses around a property name are used to indicate that this type of mineralization is secondary to another type that also occurs on the same property.

eralization is hosted by a unit of pyritic black shale and siltstone that is immediately beneath the iron formation. A single drill intersection through this mineralization yielded assays averaging 1.73% Zn and 0.09% Cu over a true width of 10 m (G. Armstrong, Prospector, personal communication, 1980). Chip sampling across a similar zone by Noranda Mines Limited at the McTavish prospect, Nickel Lake, yielded average assays of 0.3% Zn and 0.1% Cu (Assessment Files, Resident Geologist's Office, Kenora). A second type of mineralization more massive than this occurs at the main showing at Pocket Pond, where a small lens of massive pyrrhotite-sphalerite less than 0.5 m wide occurs in a laterally extensive lenticular zone of massive pyrrhotite-pyrite.

The host rocks for all of the Type 1C mineralization are mafic in composition and consist of basaltic flows and coarse-grained amphibolites which likely represent metadiabase sills.

Iron formation (Type 1D) is a common constituent of the predominantly mafic volcanic terrane in the western part of the study area at localities such as Nickel Lake and Reef Point. There is a common association of chert-magnetite beds immediately adjacent to a massive pyrite-pyrrhotite zone, which at some localities contains minor chalcopyrite. Total thicknesses of a few metres are rarely exceeded, and whereas the immediate host is commonly a biotitic metasedimentary rock, the iron formations are broadly associated with sections in which metabasalt is abundant.

Type 2: Gabbro-Hosted Mineralization

Two large, steeply dipping, layered gabbroic sills in mafic volcanic sequences are exposed in the study area (*see* Map 2525): the Grassy Portage and Seine Bay–Bad Vermilion intrusions.

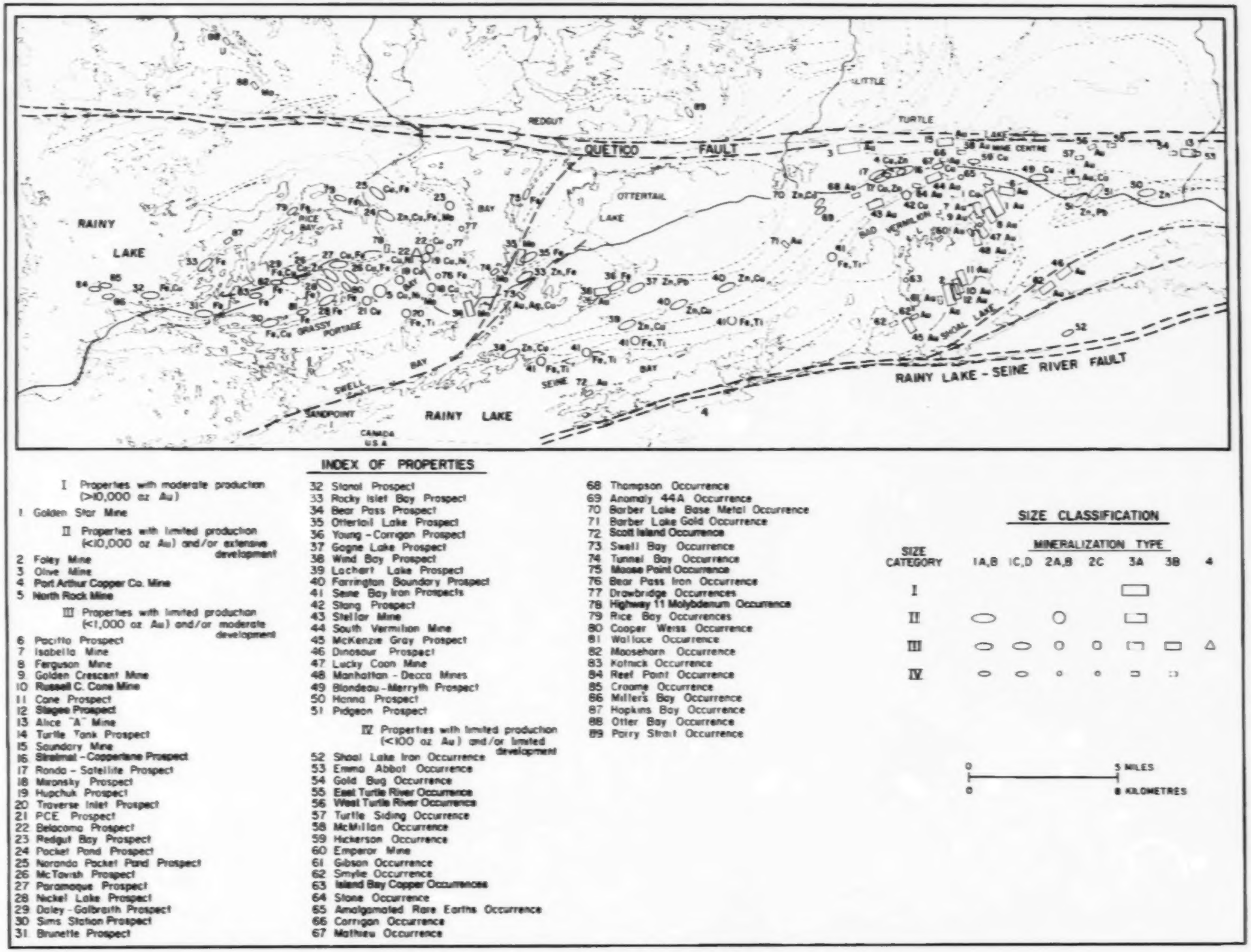
RAINY
LAKE
RAINY LAKE
REDGUT
LITTLE
TURTLE
LAKE
OTTERTAIL
LAKE
QUETICO FAULT
RAINY LAKE - SEINE RIVER FAULT
RICE BAY
BAY
GRASSY PORTAGE
SWELL BAY
SANDPOINT
CANADA
U.S.A.
SEINE
BAY
BAD VERMILION L.
SHOAL LAKE
MINE CENTRE
SIZE CLASSIFICATION
SIZE CATEGORY
MINERALIZATION TYPE
1A,B
1C,D
2A,B
2C
3A
3B
4
I
II
III
IV
0
5 MILES
0
8 KILOMETRES

INDEX OF PROPERTIES

I Properties with moderate production (>10,000 oz Au)

1 Golden Star Mine

II Properties with limited production (<10,000 oz Au) and/or extensive development

2 Foley Mine
3 Olive Mine
4 Port Arthur Copper Co. Mine
5 North Rock Mine

III Properties with limited production (<1,000 oz Au) and/or moderate development

6 Pacitto Prospect
7 Isabella Mine
8 Ferguson Mine
9 Golden Crescent Mine
10 Russell C. Cone Mine
11 Cone Prospect
12 Slagee Prospect
13 Alice "A" Mine
14 Turtle Tank Prospect
15 Saundary Mine
16 Stralmet - Coppertane Prospect
17 Rondo - Satellite Prospect
18 Maronsky Prospect
19 Hupchuk Prospect
20 Traverse Inlet Prospect
21 PCE Prospect
22 Belacoma Prospect
23 Redgut Bay Prospect
24 Pocket Pond Prospect
25 Noranda Pocket Pond Prospect
26 McTavish Prospect
27 Paramaque Prospect
28 Nickel Lake Prospect
29 Daley - Galbraith Prospect
30 Sims Station Prospect
31 Brunette Prospect
32 Stanol Prospect
33 Rocky Islet Bay Prospect
34 Bear Pass Prospect
35 Ottertail Lake Prospect
36 Young - Corrigan Prospect
37 Gagne Lake Prospect
38 Wind Bay Prospect
39 Lochart Lake Prospect
40 Farrington Boundary Prospect
41 Seine Bay Iron Prospects
42 Stang Prospect
43 Stellar Mine
44 South Vermilion Mine
45 McKenzie Gray Prospect
46 Dinosaur Prospect
47 Lucky Coon Mine
48 Manhattan - Decca Mines
49 Blondeau - Merryth Prospect
50 Hanna Prospect
51 Pidgeon Prospect

IV Properties with limited production (<100 oz Au) and/or limited development

52 Shoal Lake Iron Occurrence
53 Emma Abbot Occurrence
54 Gold Bug Occurrence
55 East Turtle River Occurrence
56 West Turtle River Occurrence
57 Turtle Siding Occurrence
58 McMillan Occurrence
59 Hickerson Occurrence
60 Emperor Mine
61 Gibson Occurrence
62 Smylie Occurrence
63 Island Bay Copper Occurrences
64 Stone Occurrence
65 Amalgamated Rare Earths Occurrence
66 Corrigan Occurrence
67 Mathieu Occurrence
68 Thompson Occurrence
69 Anomaly 44A Occurrence
70 Barber Lake Base Metal Occurrence
71 Barber Lake Gold Occurrence
72 Scott Island Occurrence
73 Swell Bay Occurrence
74 Tunnel Bay Occurrence
75 Moose Point Occurrence
76 Bear Pass Iron Occurrence
77 Drawbridge Occurrences
78 Highway 11 Molybdenum Occurrence
79 Rice Bay Occurrences
80 Cooper Weiss Occurrence
81 Wallace Occurrence
82 Moosehorn Occurrence
83 Kotnick Occurrence
84 Reef Point Occurrence
85 Croome Occurrence
86 Miller's Bay Occurrence
87 Hopkins Bay Occurrence
88 Otter Bay Occurrence
89 Parry Strait Occurrence

Figure 25. Summary map showing the distribution of mineral deposits in the study area.

Mineralization occurs at 3 specific horizons in the intrusions. Basal segregations of chalcopyrite, pyrrhotite and pentlandite (Type 2A) form important occurrences along the northern margin of the Grassy Portage intrusion. The best example of this type occurs at the North Rock deposit, where 300 000 t of material grading 1.89% copper have been outlined. The mineralization is hosted by gabbro, melagabbro and leucogabbro near the base of the Grassy Portage intrusion where it is in contact with pillow lava and pillow breccia of unit 1 (*see* Map 2525). Mineralization consists of abundant disseminations of chalcopyrite and pyrrhotite, with minor pentlandite and pyrite.

Near the top of the Grassy Portage intrusion, disseminated pyrrhotite-chalcopyrite mineralization is related to siliceous zones within the intrusion (Type 2B). Known as the Mironsky prospect, this showing was drilled by Phelps Dodge Corporation of Canada Limited in 1966 and again by Belacoma Mines Limited in 1978. Approximately 300 000 t of material grading 0.8% copper are present (Harris 1974).

In the central to upper levels of both intrusions, substantial accumulations of iron-titanium mineralization (Type 2C) occur as lenticular zones of disseminated to massive magnetite and ilmenite, with local rutile.

Type 3: Vein Mineralization

Quartz veins are common throughout the study area. Although most are unmineralized, 2 particular types host gold, and molybdenite mineralization, respectively. Gold-bearing veins (Type 3A) in the area have been developed and exploited intermittently since the 1890s. In most cases, the veins appear to be related to discrete shear zones.

The veins range from 10 cm to 2 m in width and are composed primarily of quartz with minor carbonate and local tourmaline. Visible gold and electrum were identified in a few veins, and sulphide minerals such as pyrite, sphalerite, galena, chalcopyrite, arsenopyrite and argentite are common.

The gold content of veins is variable, but a study of available assay data suggests that 15 ppm Au over widths of approximately 1 m represents an approximate average grade for the 2 most successful past producers, the Olive and Golden Star mines (Beard and Garratt 1976).

The molybdenite-bearing veins (Type 3B) in the Bear Passage–Rice Bay area show no evidence of being associated with shear zones. These veins generally show sharp contacts with undeformed granodiorite or quartz monzonite, and are spatially associated with contacts of these intrusions with biotite schist. The best occurrence is located on Highway 11 at Bear Passage, where molybdenite and pyrite are abundant in extensional quartz veins in the Bear Pass pluton. The veins strike in northerly and westerly directions, and the best mineralization is located in veins near the pluton margins. A number of other quartz-pyrite-molybdenite occurrences are related to dikes and sills of granodiorite well removed from the main plutons.

Type 4: Ultramafic-Hosted Mineralization

The magnetic clastic ultramafic unit in the Rice Bay–Redgut Bay area hosts a number of showings of low-grade copper-nickel mineralization, referred to as the Belacoma prospect. Disseminated pyrrhotite with some chalcopyrite occurs as blebs and stringers in narrow zones of foliated ultramafic metavolcanic rocks. Reported grades are variable, with best grab samples assaying as much as 0.29% Cu, 1.23% Ni and 0.17% Co, and best diamond-drill intersections assaying 0.45% Cu and 0.12% Ni over 0.55 m (Assessment Files, Resident Geologist's Office, Kenora). Away from the mineralized areas, the ultramafic metavolcanic rocks contain approximately 1150 ppm Ni (average of 4 samples), indicating that sulphidization of the nickeliferous host rocks may have produced the low-grade sulphide zones, perhaps during regional metamorphism.

Distribution Patterns of Mineralization, and Summary

The patterns of distribution of the various types of mineralization are shown on Figure 25. While base metal mineralization of felsic association (Types 1A and 1B), by definition, is restricted to the felsic volcanic-rich lithostratigraphic domains to the east, base metal mineralization associated with iron formation (Types 1C and 1D) is associated only with mafic volcanic rocks that occur in the mafic volcanic-rich western domains. Sulphide mineralization in gabbro is particularly well developed in the Grassy Portage domain, although similar mineralization occurs locally in gabbro in intrusions at Bad Vermilion Lake. The different types of quartz vein mineralization also show a clear geographic separation. Molybdenite-bearing veins are restricted to the western domains, while gold-bearing veins are restricted to the eastern domains. Thus, the domainal pattern of distribution of lithologic units is also reflected by the distribution of mineralization: a clear link between styles of mineralization and geological environment is indicated.

The classification scheme outlined in Table 8 was established early in the present study to deal with all deposits in a purely descriptive fashion. It became apparent with further study that some of the distinctions are somewhat artificial. For example, all of the iron formations were found, upon microscopic examination, to contain at least some base metal mineralization, and it was difficult to distinguish between Type 1C and Type 1D. In addition, the classification makes no allowances for economic merit or metallogenic significance of each type of mineralization. Thus, while the low-grade ultramafic-hosted nickel mineralization and the local molybdenite-bearing veins represent interesting occurrences, they do not have the same economic potential as the copper, zinc and gold mineralization. Therefore, considering the economic factor, 4 specific mineralized environments were considered to merit study in greater detail:

1. base metal mineralization associated with felsic volcanic rocks exemplified by Gagne Lake, Wind Bay and Port Arthur Copper Co. deposits
2. base metal mineralization associated with mafic volcanic rocks and iron formation, as exemplified by occurrences at Pocket Pond and Nickel Lake
3. gabbro-hosted mineralization, particularly that associated with the Grassy Portage intrusion
4. gold-bearing quartz veins in the Mine Centre area

Each of these types is described in terms of its morphology, host rocks, composition and origin by comparison with similar well-documented examples in other areas.

BASE METAL MINERALIZATION ASSOCIATED WITH FELSIC VOLCANIC SEQUENCES

Setting

Mineralization of this type is exemplified by the Gagne Lake, Wind Bay and Port Arthur Copper Co. deposits. At Gagne Lake (Figure 26a), lead-zinc mineralization occurs at the top of a sequence of rhyolite and felsic lapilli tuff where it is overlain by siltstone (Photo 28) with local chert beds that grade upward into silicate and oxide facies iron formation. The mineralization is closely associated with a spotted chloritic rock resembling the "dalmatianite" at Noranda, Quebec (Cooke 1930). The dalmatianite forms a paraconformable unit at the contact between the 2 major host rock types but, at the local scale, is clearly discordant (Photo 29). Coarse- to fine-grained lithic breccias are characteristic of the mineralized horizon and contain not only footwall and hanging-wall fragments, but locally include clasts of massive pyrite and pyrrhotite that are up to 10 cm in diameter (Photo 30). These rocks have the characteristic textures of rocks of probable hydrothermal explosive origin (Hodgson and Lydon 1977) which Sangster (1972) noted is the characteristic "mill rock" of the volcanogenic massive sulphide deposit environment.

The deposits at Wind Bay and the Port Arthur Copper Co. Mine are widely spaced examples of mineralization that occurs at a minimum of 9 localities along, or near, 1 stratigraphic horizon, which can be traced for at least 30 km in the Mine Centre domain. At these deposits the host rock is typically an intensely schistose chloritic unit that appears to have a variety of protoliths including amygdaloidal flows (Photo 31), coarse mafic breccia and lapilli tuff with a chloritic matrix. In many cases, primary structures are absent and a tectonic foliation penetrates the host rock, which is best termed a phyllonite. The mineralized unit is overlain on a regional scale by quartz-eye tuffs of rhyolite to dacite composition and is underlain by various types of felsic to intermediate tuffs, lapilli tuffs and agglomerates. A distinctive, 1 m thick chert unit containing pyrite laminae (Photo 32) caps the mineralized unit at the Port Arthur Copper Co. Mine, and a coarse felsic-clast breccia (Photo 33) and lapillistone containing centimetre-sized pyrite blebs locally comprises the footwall rocks at Wind Bay. Metadiabase sills transect both the volcanic sequence and the mineralization at both localities (e.g., Figure 26b).

The absolute size of each of these deposits is not known owing to limited exploration drilling. A shallow diamond-drill program at the Port Arthur Copper Co. Mine outlined a zone approximately 220 m long and up to 30 m wide. Mineralization was encountered continuously in 20 drill holes over a strike length of 1300 m at Wind Bay. Local occurrences of zinc have been noted over a strike length of 100 m at Gagne Lake.

Composition

The mineralization encountered at each of these deposits is rarely massive. At Gagne Lake, sulphide minerals occur in stratiform zones, 1 mm to 10 cm thick, within siltstone beds (Photo 34); this is suggestive of a possible detrital origin. Pyrite predominates (Table A6.1), along with sphalerite, pyrrhotite, galena and chalcopyrite (Photo 35). Disseminations and veinlets of chalcopyrite were also noted in the dalmatianite.

The sphalerite-pyrite-chalcopyrite mineralization at the Port Arthur Copper Co. Mine and at Wind Bay also occurs as discrete seams, 1 mm to 20 cm wide, that are separated by similar widths of barren chloritic host rock (Photo 36). The resulting lamination parallels a strong phyllitic foliation in the host rock, and its tectonic origin is evident from both silicate and sulphide mineral textures (Photo 37). In local, weakly foliated, competent units at Wind Bay (Photo 38), the sulphide minerals occur in discordant stringers, suggesting that the foliation-parallel mineralization may also have been of similar type but was tectonically transposed. Narrow lenticular massive sulphide units, composed mainly of pyrite with lesser sphalerite and chalcopyrite, are also present at the Port Arthur Copper Co. Mine. Pyrrhotite and galena were noted locally in the Wind Bay area. The compositions of typical mineralized specimens (Table A7.1) show that there are both copper- and zinc-rich types. Diamond drilling at the Port Arthur Copper Co. Mine has revealed a metal zoning on both a large and a small scale (Figure 26c), which is characterized by zinc enrichment at the top and copper enrichment at the bottom of individual mineralized zones. Mineralized specimens from all of the deposits, particularly from Gagne Lake and the Pidgeon prospect, the latter of which is also hosted by rhyolite, are moderately rich in lead (Figure 27a).

Alteration

Each of the 3 deposits studied is associated with altered rocks. The most striking example is the dalmatianite at Gagne Lake, which is composed of pinitized cordierite porphyroblasts (Photo 39) up to 1 cm in diameter, in a matrix composed of chlorite and, locally, biotite. Rare tourmaline and altered amphibole (anthophyllite?) were also noted. As is the case at Noranda (de Rosen-Spence 1969), the dalmatianite is developed as a result of the occurrence of a rock of unique chemical composition within

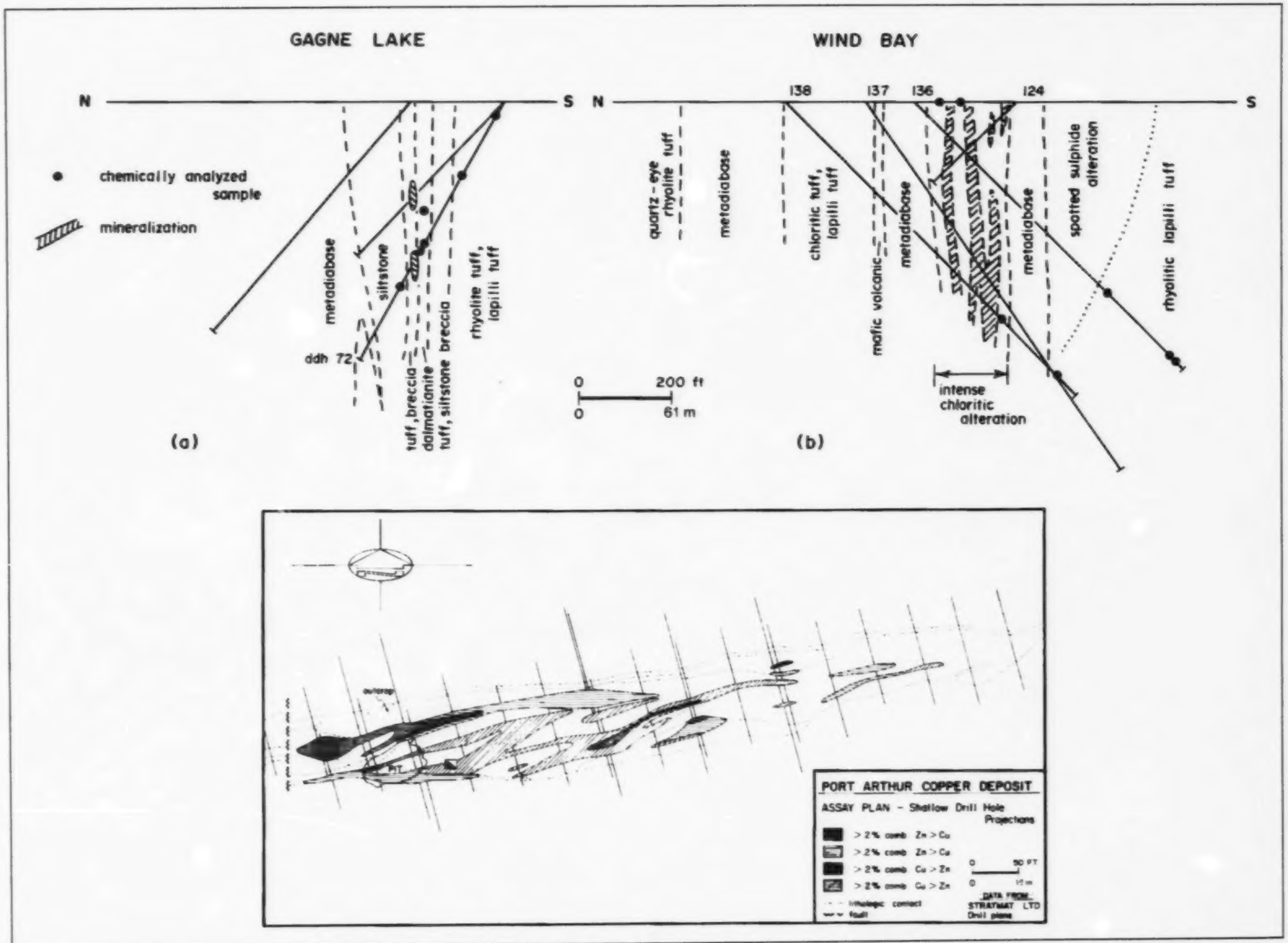
GAGNE LAKE
WIND BAY
N
S
N
S
● chemically analyzed sample
mineralization
metadiabase
siltstone
ddh 72
tuff, breccia
dalmatianite
tuff, siltstone breccia
rhyolite tuff, lapilli tuff
0 200 ft
0 61 m
(a)
(b)
138
137
136
124
quartz-eye rhyolite tuff
metadiabase
chloritic tuff, lapilli tuff
mafic volcanic
metadiabase
metadiabase
spotted sulphide alteration
rhyolitic lapilli tuff
intense chloritic alteration
outcrop
PORT ARTHUR COPPER DEPOSIT
ASSAY PLAN - Shallow Drill Hole Projections
> 2% comb Zn > Cu
> 2% comb Zn > Cu
> 2% comb Cu > Zn
> 2% comb Cu > Zn
lithologic contact
fault
0 50 FT
0 15 m
DATA FROM:
STRATMAT LTD
Drill plans

Figure 26. a) Cross section through the main showing, Gagne Lake prospect. b) Cross section through the main showing, Wind Bay prospect. c) Assay plan of the Port Arthur Copper Co. deposit. The plan represents a projection to the horizontal of assay data from shallow inclined diamond drill holes.

Photo 28. Siltstone that forms the hanging-wall unit, Gagne Lake prospect.

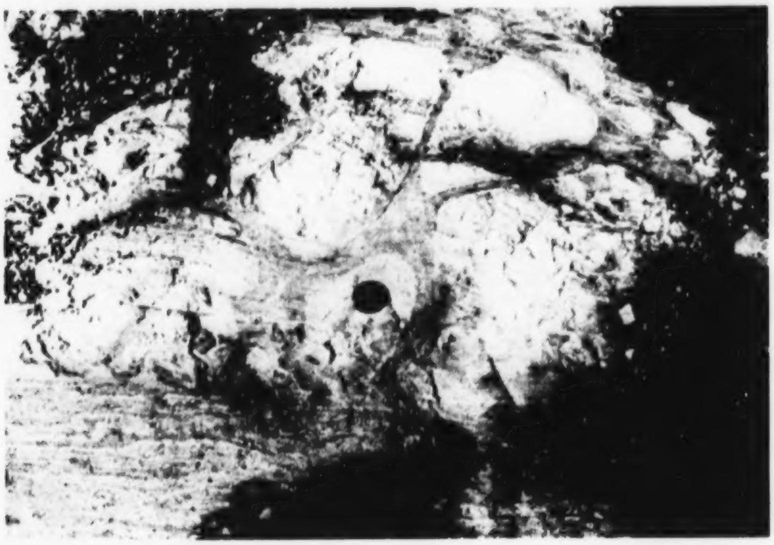

Photo 29. Breccia at Gagne Lake composed of siltstone clasts in an altered spotted matrix of "dalmatianite". Lens cap is 5 cm in diameter.

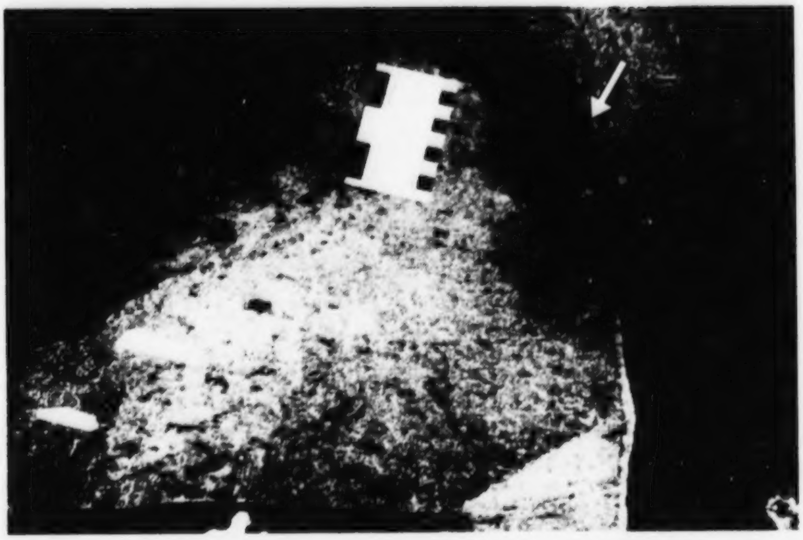

Photo 30. Massive sulphide clast (arrow) in polymictic breccia, Gagne Lake prospect. Note angular felsic clasts as well.

Photo 31. Amygdaloidal volcanic rocks, Port Arthur Copper Co. deposit. Note that some amygdules are very large (arrows) and are filled with quartz and ankerite.

Photo 32. Pyritic cherty "exhalite" that overlies the ore zone at Port Arthur Copper Co. deposit. Dark laminae are composed of pyrite.

Photo 33. Coarse felsic-clast breccia with chloritic and pyritic matrix in footwall mineralization at Wind Bay. Hammer is 27.5 cm long.

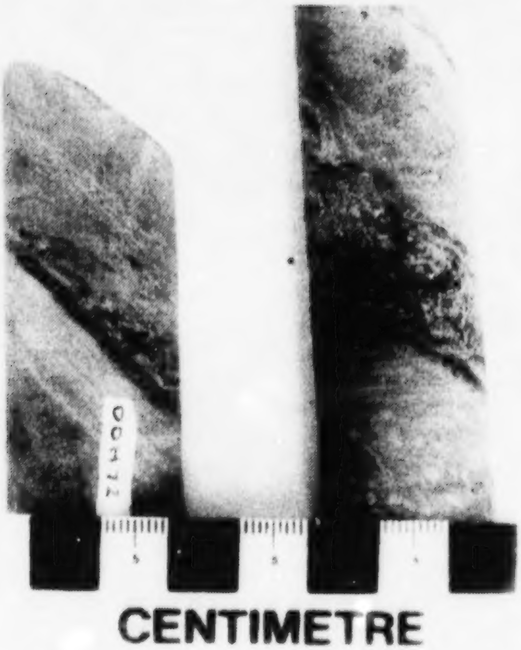

Photo 34. Sphalerite-galena laminae (dark grey) in siltstone beds, Gagne Lake.

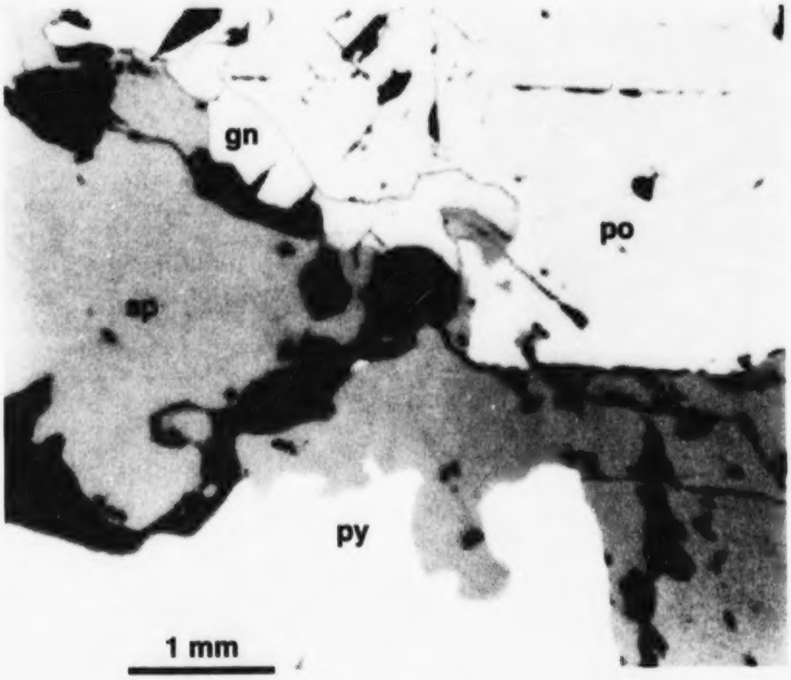

Photo 35. Photomicrograph of polymetallic sulphide ore, Gagne Lake prospect. Sphalerite (sp), galena (gn) and pyrite (py) predominate, with lesser pyrrhotite (po).

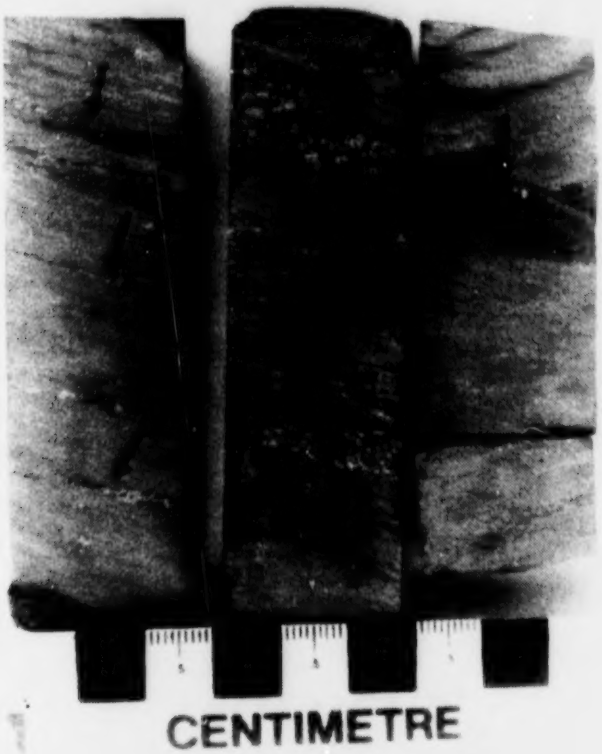

Photo 36. Sphalerite and chalcopyrite seams (arrows) in chloritic phyllite, Wind Bay prospect.

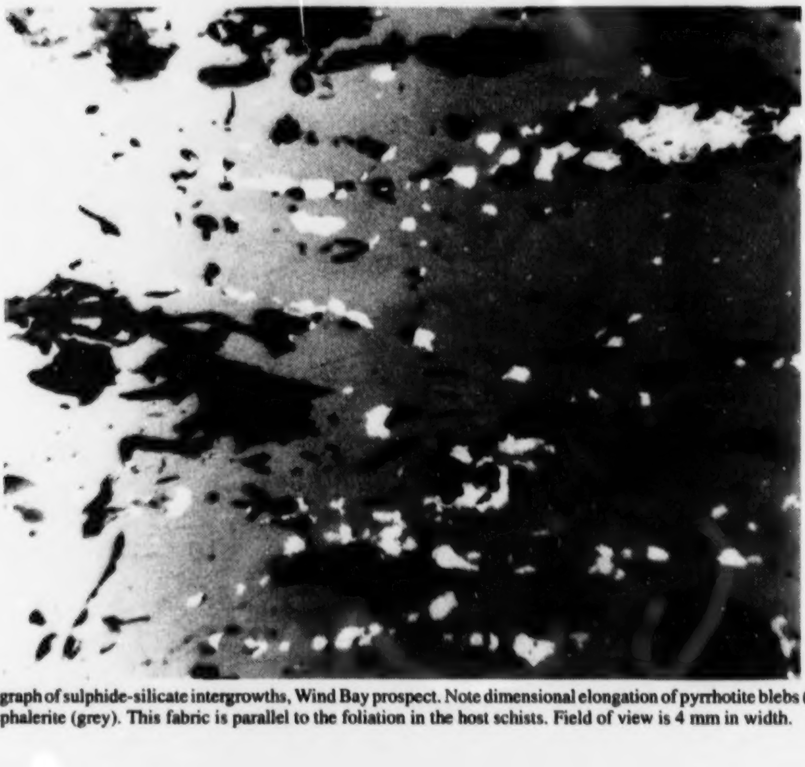

Photo 37. Photomicrograph of sulphide-silicate intergrowths, Wind Bay prospect. Note dimensional elongation of pyrrhotite blebs (white) and chlorite grains (dark grey) in sphalerite (grey). This fabric is parallel to the foliation in the host schists. Field of view is 4 mm in width.

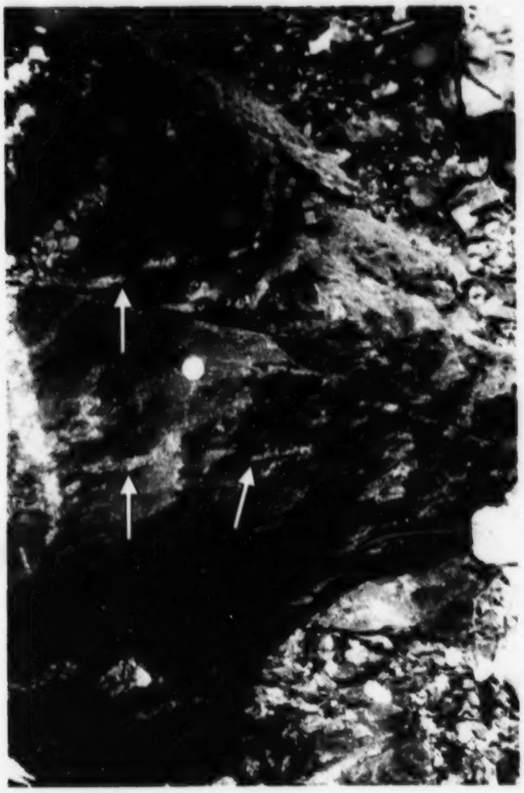

Photo 38. Sulphide "stringers" in relatively competent quartz-chlorite unit, main pit, Wind Bay. The veins contain both pyrrhotite and chalcopyrite, and are discordant to the weak schistosity in the host rock. Coin is 2.1 cm in diameter.

the contact aureole of a granodiorite pluton (here, the Ottertail Lake intrusion). This unique composition is the result of the alteration of originally felsic rocks. A similar discordant alteration at the Thompson occurrence near the Port Arthur Copper Co. deposit (*see* Figure 25) shows the pervasive replacement of the original mineralogy of the felsic rocks by chlorite without the destruction of primary textures. The chloritic and pyritic fragmental felsic rocks in the footwall at Wind Bay (*see* Photo 33) are only locally developed, and the intensity of alteration decreases in either direction along strike from the mineralization. This "pod" of alteration underlies the highest grade mineralization encountered in the deposit. Furthermore, the immediate host rocks for the mineralization are extremely chloritic and locally retain textures that suggest they were originally felsic; blue quartz eyes, typical of many of the unaltered felsic rocks nearby, were noted in the main pit at Wind Bay.

Whole rock analyses of selected specimens of "fresh" and "altered" rock from Gagne Lake and Wind Bay were obtained. The chemical changes that accompany increasing intensity of alteration, as judged subjectively from hand specimens, are shown clearly on the "tetrahedral" cation plot (Figure 27b) devised by Riverin and Hodgson (1980). These data show that, while the rhyolite associated with the Gagne Lake deposit is extremely rich in K_2O (5%) as compared to that at Wind Bay (1% K_2O), increasing intensity of alteration reduces the differences in their original chemistry. These patterns of alteration are virtually identical to those at the Millenbach deposit at Noranda (Riverin and Hodgson 1980), and reflect the dominance of chlorite as an alteration mineral. Furthermore, the chemical plots (*see* Figure 27b) show that the alteration processes produced bulk compositions that followed significantly different paths than the differentiation trends shown by "average" Wabigoon Subprovince volcanic rocks (Goodwin 1972). This provides further support for the idea that the laterally extensive units composed of chloritic rocks at Wind Bay are products of hydrothermal alteration.

The data of Table A5.1 and Table A7.1 also show that these rocks are enriched in manganese, which is characteristic of footwall alteration at the Mattabi massive sulphide deposit (Franklin, Kasarda and Poulsen 1975). Enrichment of TiO_2 and Al_2O_3 in dalmatianite specimens (*see* Table A5.1) contradicts the commonly cited notion that these elements are immobile.

Origin

While the deposits described would not properly be described as "massive", their setting, composition and alteration are characteristic of volcanogenic massive sulphide deposits (Sangster 1972). The localization of the deposits along particular volcanic horizons (Figure 28) is particularly diagnostic, and the presence of a probable subvolcanic sill complex provides a potential heat source for a mineralizing hydrothermal system (Hodgson and Lydon 1977). The regular spacing of the deposits on the lowermost mineralized horizon (*see* Figure 28) is typical of deposits in many massive sulphide camps, and may reflect the size of the convective hydrothermal systems (Elder 1977). While the metals are dispersed in these deposits, the simple massive sulphide mineralogy of sphalerite-pyrite-chalcopyrite is preserved. The dalmatianite alteration at Gagne Lake is identical to that developed in the footwall of Noranda area deposits (de Rosen-Spence 1969; Riverin and Hodgson 1980), and the coarse breccia in the footwall at Wind Bay is typical of Sangster's (1972) "mill rock". Chert in the hanging wall of the Port Arthur Copper Co. and Gagne Lake deposits is similar to tuffaceous exhalites occurring immediately above or along the lateral extensions of deposits in the Noranda and Mattagami Lake areas (Franklin, Sangster and Lydon 1981).

While there is little question that the deposits are products of volcanogenic hydrothermal processes, they do possess some characteristics that are somewhat anomalous with respect to typical deposits of this class. The most distinctive feature of the Rainy Lake deposits is the paucity of "massive" sulphide mineralization. The presence of pyrite clasts within lithic breccias suggests that the mineralization at Rainy Lake is resedimented, reflecting proximity to a massive sulphide deposit along strike or at a lower stratigraphic level in the volcanic sequence (MacGeehan,

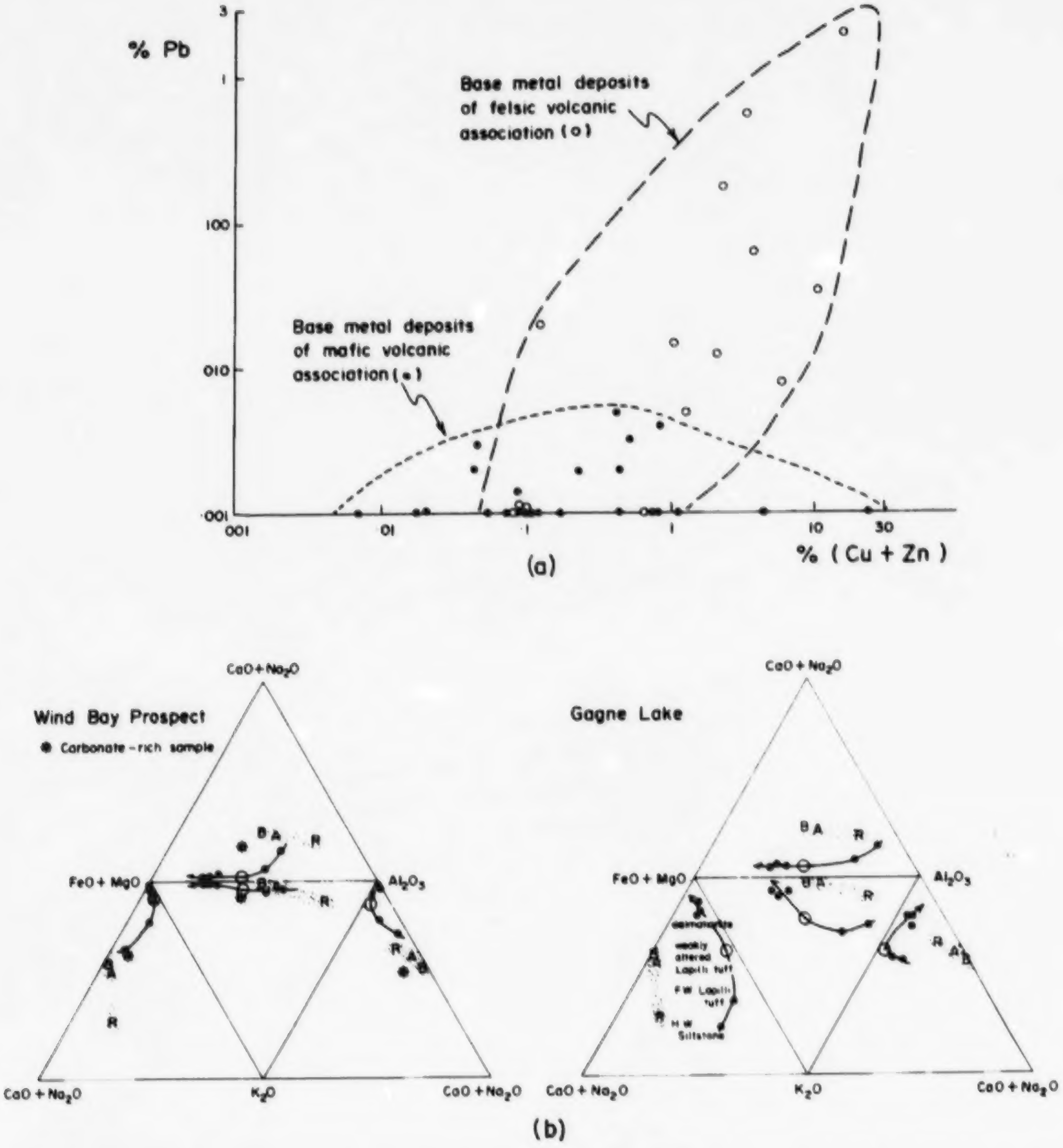

Figure 27. a) Pb versus Cu+Zn content of specimens of volcanic-associated base metal sulphide mineralization. The fields are drawn to illustrate the greater correlation of lead with deposits of felsic affiliation. b) Riverin and Hodgson (1980) plots of whole-rock chemical data of "fresh" and chemically "altered" wall-rock specimens from the Gagne Lake and Wind Bay prospects. The arrows indicate increasing degrees of chloritization as estimated by visual inspection. The stippled areas indicate the range of average chemical compositions of unaltered basalts (B), andesites (A) and rhyolites (R). F.W.=footwall, H.W.=hanging wall

MacLean and Bonenfant 1981; Clark 1983; Watkins and Stensrud 1983). In the case of the deposits on the Wind Bay–Port Arthur Copper Co. horizons (*see* Figure 28), the irregular morphology and stringer-like nature of the mineralization suggest that these deposits largely represent extensive subseafloor alteration zones with local seafloor deposition of sulphide minerals above them. The mineralization and the chloritic host rocks satisfy the criteria for "self-seal cap rocks" (Hodgson and Lydon 1977) in that they reflect an originally permeable horizon now charged with sealant (sulphide minerals and chlorite). These minerals are locally associated with coarse altered breccias in an environment that may have been subject to syndepositional boiling, evidenced by the presence of abundant amygdaloidal rocks. Considering that, in all cases, the rocks deposited immediately following the mineralization

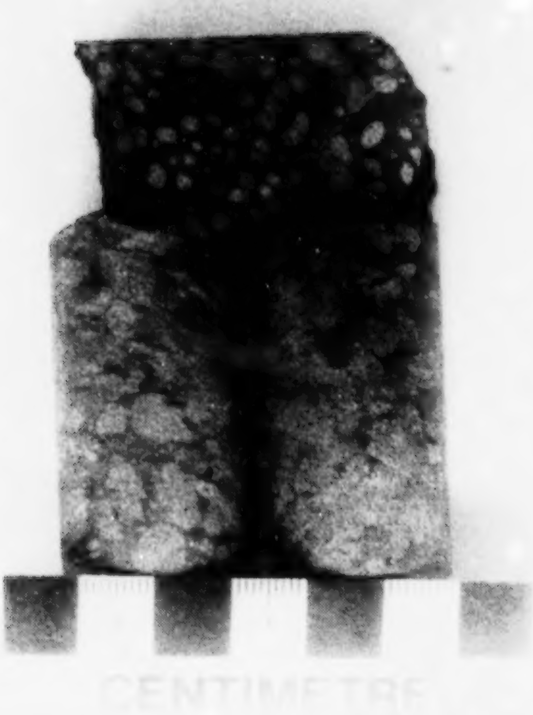
CENTIMETRE

Photo 39. Dalmatianite in diamond-drill core, Gagne Lake prospect. Porphyroblasts (grey) are composed of chlorite, but commonly show idioblastic boundaries suggestive of pre-existing cordierite.

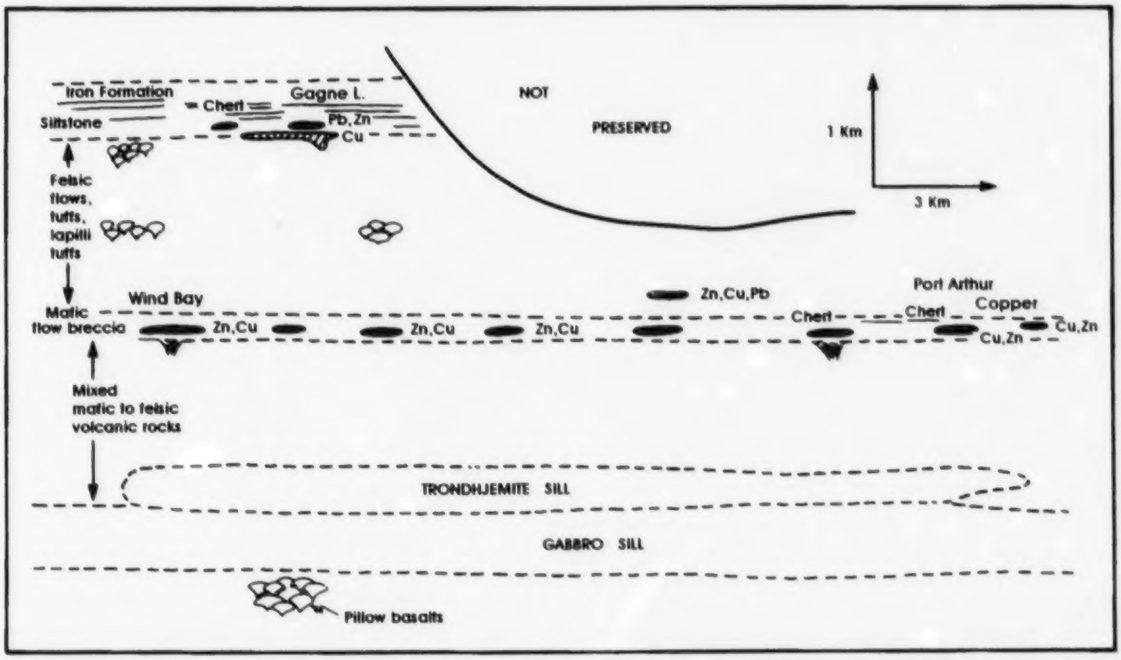
Iron Formation
Chert
Gagne L.
Siltstone
Pb, Zn
Cu
NOT
PRESERVED
1 Km
3 Km
Felsic flows, tuffs, lapilli tuffs
Wind Bay
Zn,Cu,Pb
Port Arthur
Copper
Mafic flow breccia
Zn,Cu
Zn,Cu
Zn,Cu
Chert
Chert
Cu,Zn
Cu,Zn
Mixed mafic to felsic volcanic rocks
TRONDHJEMITE SILL
GABBRO SILL
Pillow basalts

Figure 28. Schematic diagram illustrating the stratigraphic position and relative spacing of base metal deposits associated with felsic rocks in the study area. Scale is approximate.

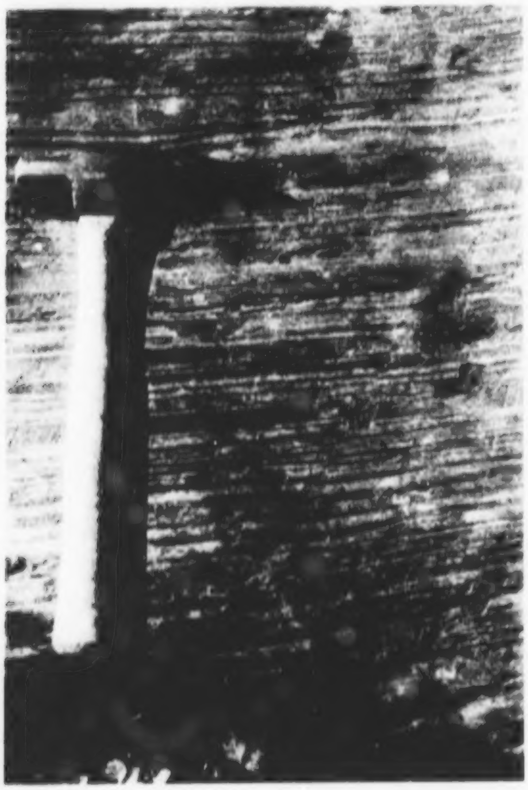

Photo 40. Metamorphosed chert-magnetite iron formation, No.9 zone, Pocket Pond prospect. Hammer is 35 cm long.

are felsic volcanic rocks or siltstones, the Rainy Lake deposits show a greater similarity to the Japanese Kuroko deposits (Sato 1974) than most Precambrian massive sulphide deposits (Sangster 1972).

BASE METAL MINERALIZATION ASSOCIATED WITH IRON FORMATION IN MAFIC VOLCANIC ROCKS

Setting

This type of mineralization is exemplified by prospects at Pocket Pond and Nickel Lake, and at other localities restricted to the western lithostratigraphic domains (*see* Figure 25). The host sequences contain abundant mafic (*see* Photo 1) and ultramafic (*see* Photo 3) volcanic rocks, pelitic sedimentary rocks, gabbros and iron formation. These rock sequences are metamorphosed to amphibolite facies assemblages (*see* "Metamorphic Petrology") and are strongly deformed, with the result that, at Pocket Pond (Figure 29a) and Nickel Lake, they face downward. Medium- to coarse-grained amphibolites, commonly lacking diagnostic igneous textures, are a dominant rock type. In some cases they are clearly gabbros, while in others they likely represent thick basaltic flows.

The iron formations (Photo 40) are extensive units that occupy specific stratigraphic horizons within the sequence (Figure 29b). A quartz-magnetite-grunerite facies is most common (Anglin 1982), and is commonly accompanied by fine-grained clastic sedimentary rocks that have been metamorphosed to siliceous biotite schists. Impure carbonate units occur with the iron formation at the Pocket Pond and McTavish prospects. Sulphide mineralization occurs within conformable, lenticular to stratiform units.

Composition

The sulphide mineralization that is associated with iron formation has various modes of occurrence: as disseminations in oxide iron formation, as disseminations in the impure carbonate units, as laminations and disseminations in black shale, as semimassive breccia matrix to a siliceous host, and as massive sulphide lenses.

The chert-magnetite-grunerite iron formation (Photo 41, top) contains little sulphide mineralization. Locally, however, chalcopyrite and pyrrhotite occur as interstitial grains with magnetite or as disseminations in pelitic interbeds.

The impure carbonate units are metamorphosed to marble and skarn-like assemblages (Photo 41, right). They are composed of calcite, quartz, clinopyroxene, garnet and epidote (*see* Table A3.3 for mineral analyses). The calc-silicate minerals are intergrown in coarse aggregates (Photo 42), and locally make up a massive calc-silicate rock. Pyrrhotite, chalcopyrite and local coarse sphalerite occur as disseminations in both the impure marbles and calc-silicate rocks.

Black, possibly graphitic shales are commonly associated with the iron formations, and contain up to 50% sulphide minerals. Laminae of pyrite or pyrrhotite, or both (Photo 41, bottom), are generally parallel to bedding in the shales, but local deformation and recrystallization have resulted in contorted to discordant sulphide layers. Textural evidence in many samples shows that coarse pyrite has crystallized at the expense of pyrrhotite. Sphalerite and chalcopyrite are ubiquitous in modest quantities in the sulphidic shales, resulting in consistent grades of approximately 0.5% Zn and 0.1% Cu.

Quartz-rich rocks containing up to 50% sulphide minerals are present at both Nickel Lake and Pocket Pond. These rocks are commonly brecciated (Photo 41, left), with silicate fragments showing internal contorted trails of sulphide inclusions in a manner characteristic of the *durchbewegung* texture of Vokes (1969). The principal sulphide minerals—pyrrhotite, pyrite, sphalerite and chalcopyrite—show good triple junction terminations of probable metamorphic origin (Photo 43). Arsenopyrite (Photo 44) is present locally, and analyses of several grains from a single specimen (Table A4.2) show that it contains significant amounts of cobalt ($Fe_{30.3}Co_{1.4}As_{31.1}S_{36.1}$, average of 10 microprobe analyses).

Massive sulphide mineralization, consisting mainly of pyrrhotite and/or pyrite, occurs as lenses, up to 10 m

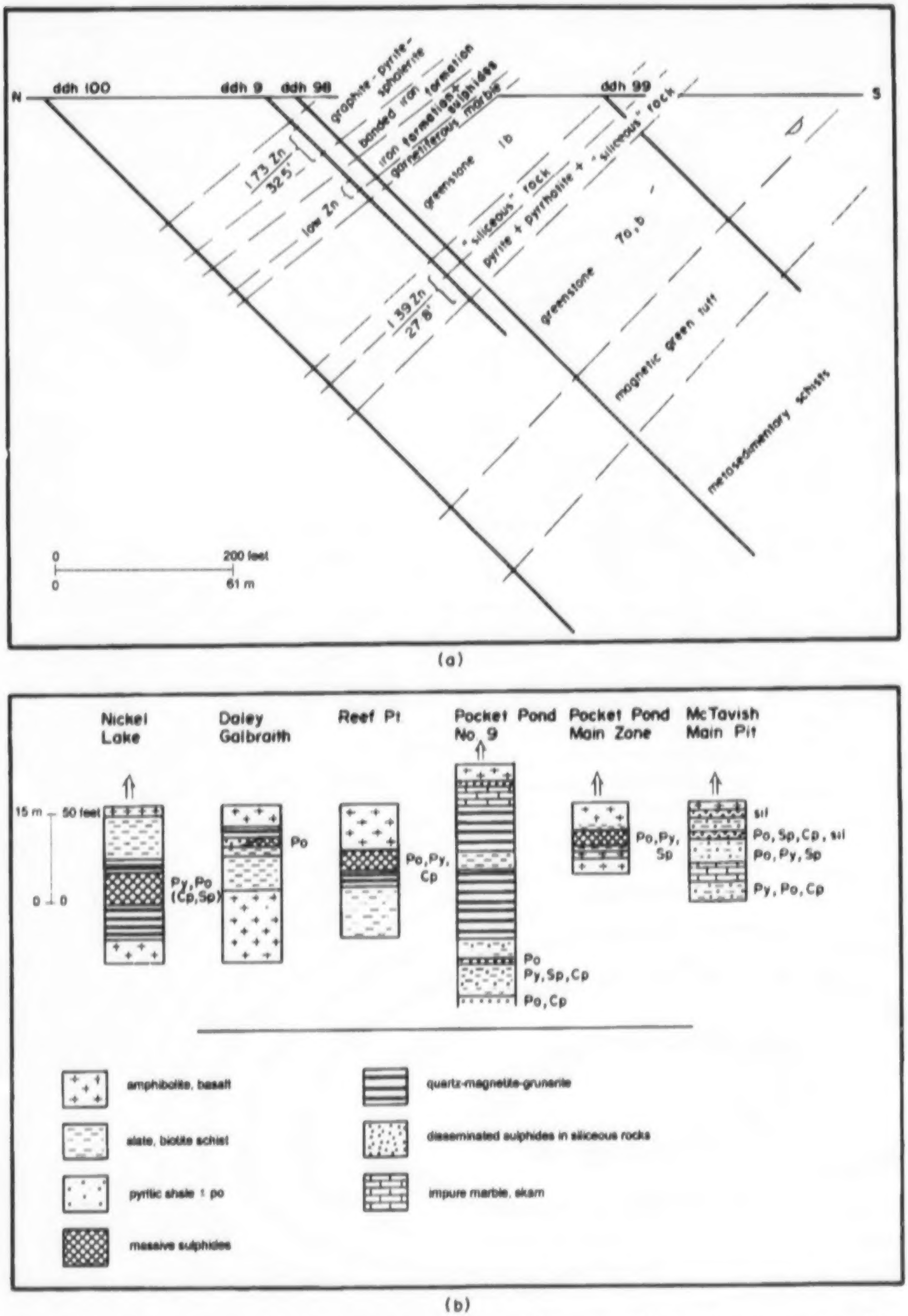
N
ddh 100
ddh 9
ddh 98
ddh 99
S
graphite - pyrite - sphalerite
banded iron formation
iron formation + sulphides
garnetiferous marble
1.73 Zn / 32.5'
low Zn
greenstone 1b
"siliceous" rock
pyrite + pyrrhotite + "siliceous" rock
greenstone 7a,b
1.39 Zn / 27.8'
greenstone
magnetic green tuff
metasedimentary schists
0 200 feet
0 61 m
(a)
Nickel Lake
Daley Galbraith
Reef Pt
Pocket Pond No 9
Pocket Pond Main Zone
McTavish Main Pit
15 m 50 feet
0 0
Py, Po (Cp, Sp)
Po
Po, Py, Cp
Po
Py, Sp, Cp
Po, Cp
Po, Py, Sp
sil
Po, Sp, Cp, sil
Po, Py, Sp
Py, Po, Cp
amphibolite, basalt
slate, biotite schist
pyritic shale ± po
massive sulphides
quartz-magnetite-grunerite
disseminated sulphides in siliceous rocks
impure marble, skarn
(b)

Figure 29. a) Cross section showing the position of mineralized zones at the Pocket Pond prospect. Note that the sequence is structurally inverted. b) Stratigraphic columns showing the immediate host rocks for sulphide mineralization associated with mafic volcanic rocks. Note that stratigraphic younging directions are only known for the Nickel Lake, Pocket Pond and McTavish examples. Py=pyrite, Po=pyrrhotite, Cp=chalcopyrite, Sp=sphalerite, sil=sillimanite.

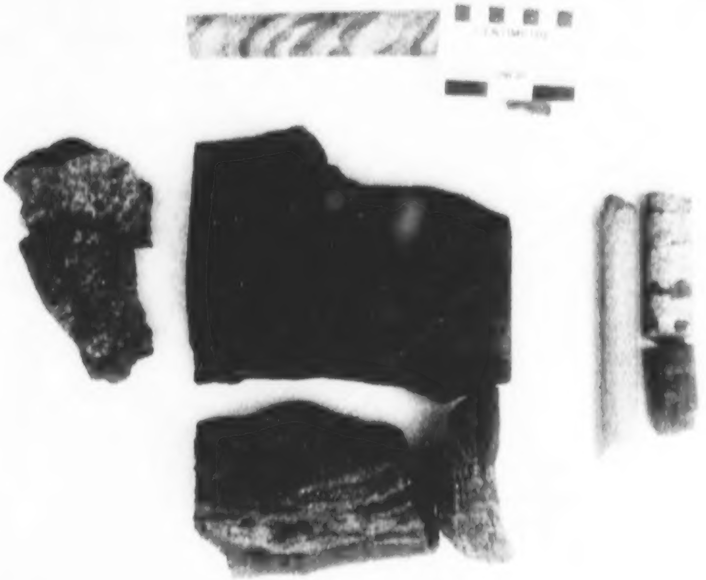

Photo 41. Types of mineralization associated with iron formation in mafic volcanic rocks. At centre is banded massive pyrrhotite (light)-sphalerite (dark) ore, Pocket Pond, main pit. In clockwise order from the top: chert-magnetite-grunerite iron formation, Nickel Lake; marble and marble plus skarn (dark) in drill core, McTavish prospect and Pocket Pond; sulphide-rich shale (black) with fine pyrrhotite laminae (grey) and local sphalerite, McTavish prospect; sulphide breccia composed of siliceous rock fragments in a matrix of pyrrhotite and pyrite, Nickel Lake.

wide, either adjacent to oxide iron formation, or at short distances above or below it in the stratigraphic sequence. The massive sulphide mineralization includes small quantities of sphalerite and chalcopyrite. At the main zone of the Pocket Pond prospect, part of the massive sulphide lens is particularly zinc-rich (Photo 41, centre) and also contains significant quantities of molybdenite. Again, metamorphic textures are present in all of the sulphide ores (Photo 45).

The various types of mineralization are intercalated at all deposits of this type, but the order of their superposition is difficult to assess in most cases due to a lack of nearby younging direction indicators. In the most well-documented example at the No. 9 zone at Pocket Pond, sulphidic shale, intercalated with siliceous sulphide rocks, is overlain by oxide iron formation, which in turn is overlain by marble and skarn (*see* Figure 29a, b). The massive sulphide lenses of the Pocket Pond main zone occur with some siliceous sulphide rocks, approximately 50 m higher in the mafic volcanic sequence.

A mineralogical summary of the various types of ore is given in Table A6.1 and the chemical compositions of selected mineralized specimens are shown in Table A7.2. With the notable exception of the high-grade mineralization at the Pocket Pond main zone, most sulphide-bearing specimens contain less than 1% total of all base metals. Zinc is more abundant than copper, and the low content of lead distinguishes these deposits from those of felsic volcanic association (*see* Figure 27a). Several specimens contain low but significant quantities of nickel and cobalt, the latter probably related to the presence of arsenopyrite.

Alteration

Unlike the base metal deposits of felsic association, the sulphide deposits associated with iron formation lack obvious alteration features. This may reflect either the higher grades of metamorphism for these deposits, the difficulty of distinguishing chloritic alteration in originally mafic host rocks, or the absence of alteration for this type of deposit. The siliceous rocks, which are intimately associated with the sulphide minerals in many of these deposits, may be partly a product of chemical alteration, but in most cases they are more likely recrystallized sedimentary units.

Origin

Deposits of this type, because of their apparent sedimentary nature and their iron content of greater than 15% (*see* Table A7.2), are commonly termed "sulphide facies of iron formation" (Gross 1965; Goodwin 1973; Boyle 1976). This term is seemingly appropriate, considering the close spatial association of the sulphide mineralization with iron formation of the oxide facies. However, it does not properly reflect either the elevated base metal content of these deposits compared to that found in iron deposits, or the presence of lenses of material which one would normally consider to be massive sulphide mineralization. For these reasons, it is suggested that the Rainy Lake deposits of this type compare more closely to Besshi-type massive sulphide deposits (Kanehira and Tatsumi 1970; Fox 1983) and similar European deposits (Klau and Large 1980), than to either Algoman iron formations (Gross 1965) or most Pre-

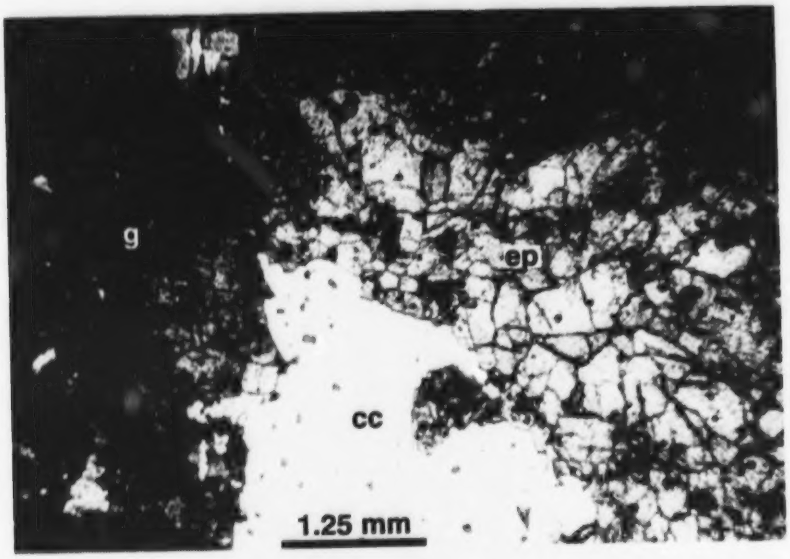

Photo 42. Photomicrograph of garnet (g)-epidote (ep) intergrowth, calc-silicate rock, Pocket Pond. Calcite (cc) appears as white grains.

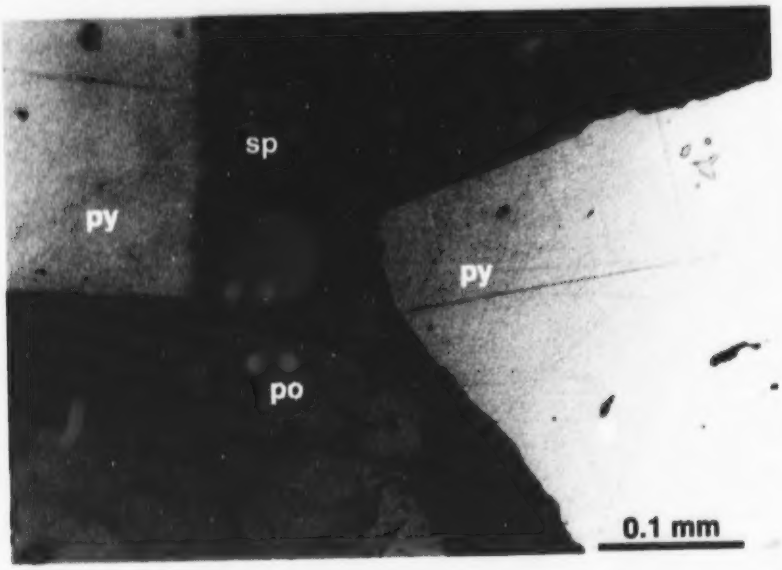

Photo 43. Photomicrograph of triple junction termination of sphalerite (sp), pyrite (py) and pyrrhotite (po), Nickel Lake.

cambrian massive sulphide deposits (Sangster 1972). Several observations support this analogy:

1. Both the Rainy Lake and Besshi-type deposits occur in environments dominated lithologically by pillowed basalts, gabbros, pelitic rocks and local ultramafic rocks (Kanehira and Tatsumi 1970; Vokes 1976; Klau and Large 1980).
2. The sulphide deposits in both cases are thin, laterally extensive, deformed and metamorphosed.
3. Iron-rich exhalites (magnetite-garnet-quartz schist) both overlie and underlie the sulphide mineralization at Besshi, and stratigraphic units composed of chert-magnetite-sulphide iron formation overlie and are laterally equivalent to similar deposits in Norway (Grenne, Grammeltvedt and Vokes 1980). Both of these relationships are also observed at Rainy Lake.
4. Sulphide minerals associated with Besshi-type deposits contain quantities of cobalt on the same order

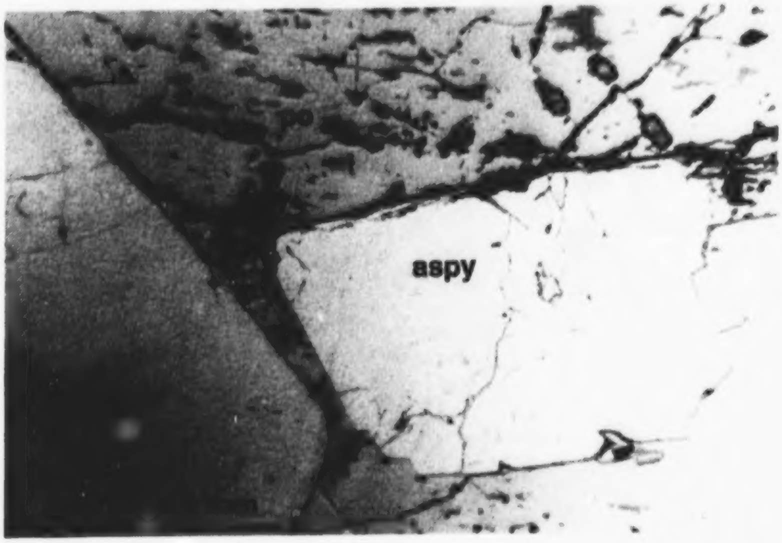

Photo 44. Photomicrograph of arsenopyrite (aspy) euhedra in pyrrhotite (po), Nickel Lake.

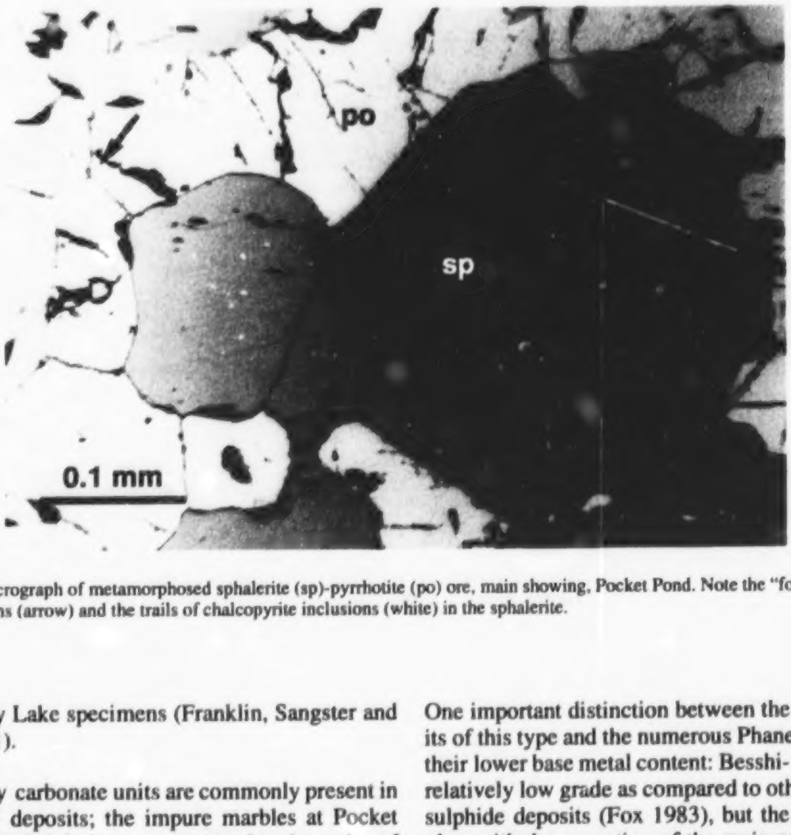

Photo 45. Photomicrograph of metamorphosed sphalerite (sp)-pyrrhotite (po) ore, main showing, Pocket Pond. Note the "foam" texture with triple junction terminations (arrow) and the trails of chalcopyrite inclusions (white) in the sphalerite.

as the Rainy Lake specimens (Franklin, Sangster and Lydon 1981).

5. Sedimentary carbonate units are commonly present in Besshi-type deposits; the impure marbles at Pocket Pond and Nickel Lake are presumed to be units of similar type.

6. Molybdenite, as observed at Pocket Pond, is a characteristic minor constituent of Besshi-type ores (Fox 1983).

One important distinction between the Rainy Lake deposits of this type and the numerous Phanerozoic examples, is their lower base metal content: Besshi- type deposits are of relatively low grade as compared to other types of massive sulphide deposits (Fox 1983), but the Rainy Lake examples, with the exception of the main zone at Pocket Pond, have grades that are factors of two to five times lower than economically viable Besshi-type deposits. Furthermore, the Besshi-type ores are commonly, though not always, rich in copper relative to zinc, in contrast to the Rainy Lake deposits.

GABBRO-ASSOCIATED MINERALIZATION

Setting

Sulphide and oxide mineralization occurs within gabbroic intrusions in both the Seine Bay–Bad Vermilion Lake area and the Grassy Portage domain, where the Grassy Portage intrusion (Figure 30) forms part of a sequence comprising ultramafic volcaniclastic rocks, pillowed basalts and biotite schists. Mineralization associated with this intrusion is quite extensive and typifies this class.

The Grassy Portage intrusion is a layered gabbroic sill that is exposed for a strike length of approximately 20 km. Exposure is limited in the southwest by fault truncation, and in the northwest by extreme tectonic attenuation. The mean dip of the body is northwestward (*see* Figure 30); diamond-drill data from the North Rock deposit and rare modal layering suggest a dip of 80° at the northwestern contact of the intrusion, while several observations of modal layering along the southeastern margin indicate a 60° dip. The dip variation prevents unequivocal determination of the true thickness of the intrusion, but 1800 m is a reasonable estimate (*see* Figure 30). While the intrusion dips moderately northwestward, the following observations suggest that it is overturned and faces southeastward:

1. The intrusion is paraconformable with volcanic and sedimentary rocks at its margins. Pillow lavas along the northwestern contact and graded beds at the southeastern contact face southeastward.
2. Modal trends are compatible with a southeastward facing. Quartz and apatite are preferentially enriched in the southeastern part of the intrusion.
3. Modal layering (Photo 46) near the southeastern margin locally shows melanocratic to leucocratic grading toward the southeast. Such grading is not conclusive (Irvine 1982) but is supportive of a southeastward facing.

Based on the above interpretation of structural inversion, the intrusion may be internally divided into a lower (northwestern) zone and an upper (southeastern) zone (*see* inset, Figure 30). The lower zone comprises the coarse-grained part of the intrusion, while the upper zone contains finer grained gabbros and diorite with abundant xenoliths, oxide-rich units and quartz-rich phases. Petrographic aspects of the individual units that constitute each zone are outlined in Table 9.

The lower zone consists of a variety of gabbroic and anorthositic rocks, which define roughly concordant members that parallel the gross outlines of the intrusion. This conformability may reflect either gravitational settling (or flotation), or may have resulted from autointrusion, as gabbroic xenoliths were observed in anorthosite 500 m south of the North Rock Mine, and roadcuts through leucogabbroic rocks along Highway 11 expose local lenticular xenoliths of fine-grained anorthosite. However, many of the rocks of the lower zone do show some evidence of cumulus growth: the leucogabbroic rocks are dominantly poikilitic cumulates consisting of hornblende megacrysts that may be of metamorphic origin, enclosing framework grains of plagioclase, while the anorthosite is an adcumulate composed of mutually interfering andesine grains. With the exception of andesine in the anorthosites, labradorite is the dominant plagioclase, as determined using microscopic, microprobe and normative analyses.

The upper zone is characterized by abundant modal quartz, apatite and, locally, garnet. Andesine is the dominant plagioclase, and many of the rocks encountered are properly classified as quartz diorites (Streckeisen 1976). The rocks are fine to medium grained and commonly thoroughly recrystallized, and xenoliths of black amphibolite and quartz-plagioclase schist are common. A distinctive rhythmic layering is displayed in the upper member of this zone, which is locally composed of successions of modally graded layers ranging from 2 to 20 m thick (*see* Photo 46).

In addition to the gabbroic members within the 2 zones, several minor rock types are also present. Distinctive magnetite-actinolite rocks occur at 2 horizons, a lower member at the transition from gabbro to anorthosite in the lower zone, and an upper member overlying the garnetiferous quartz diorite in the upper zone. Various coarse- to fine-grained dike rocks also are present, with gabbroic compositions being dominant (Hodgson 1959). Grey dikes (possibly anorthosite) are spatially associated with the magnetite-actinolite rocks. Patches of pegmatitic gabbro less than 1 m in diameter locally contain high percentages of hornblende. Rusty shear zones composed of biotite, garnet and sulphide minerals are common discordant structures.

Whole rock chemical analyses of typical rock specimens from both gabbroic zones have been reported by Harris (1974) and Poulsen (1980a). CIPW norms were computed from these, and the results reflect the general differences between the upper and lower zones: rocks from the lower zone show normative olivine, high normative anorthite content in plagioclase, and low normative apatite and ilmenite; upper zone rocks show normative quartz, a lower normative anorthite content in plagioclase, and high normative apatite and ilmenite. This chemical asymmetry further supports the interpretation that the intrusion is overturned and faces southeasterly.

Sulphide Mineralization

Copper sulphide mineralization occurs in 3 distinct settings associated with the Grassy Portage intrusion: as lenses of disseminated to massive pyrrhotite-chalcopyrite at the base of the intrusion, as disseminations and stringers in a siliceous member in the upper zone, and as disseminations and stringers in and near gabbroic dikes that cut the mafic and ultramafic volcanic rocks beneath the sill.

Basal sulphide mineral accumulations occur at 7 localities along the northwestern contact of the intrusion. The largest and economically most significant of these is the Beaver Pond zone of the North Rock Mine (Figure 31a), which is itself composed of several subsidiary lenses. A

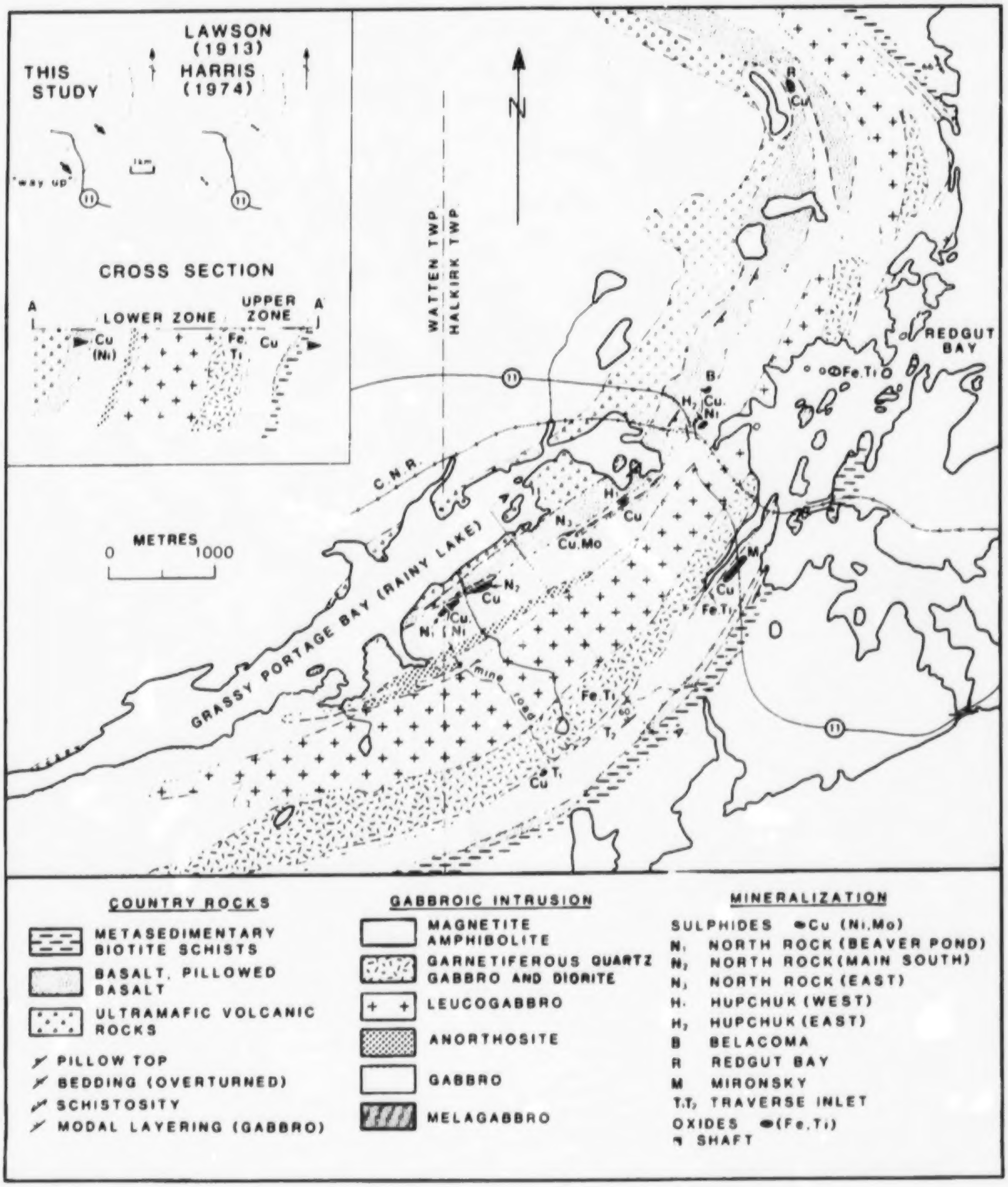
LAWSON (1913)
HARRIS (1974)
THIS STUDY
"way up"
11
CROSS SECTION
A
A'
LOWER ZONE
UPPER ZONE
Cu (Ni)
Fe, Ti
Cu
N
WATTEN TWP.
HALKIRK TWP.
C.N.R.
METRES
0
1000
GRASSY PORTAGE BAY (RAINY LAKE)
REDGUT BAY
R
B
H₂
Cu, Ni
H₁
N₁
N₂
N₃
Cu, Mo
M
Fe, Ti
T₁
T₂
mine road
COUNTRY ROCKS
METASEDIMENTARY BIOTITE SCHISTS
BASALT, PILLOWED BASALT
ULTRAMAFIC VOLCANIC ROCKS
PILLOW TOP
BEDDING (OVERTURNED)
SCHISTOSITY
MODAL LAYERING (GABBRO)
GABBROIC INTRUSION
MAGNETITE AMPHIBOLITE
GARNETIFEROUS QUARTZ GABBRO AND DIORITE
LEUCOGABBRO
ANORTHOSITE
GABBRO
MELAGABBRO
MINERALIZATION
SULPHIDES Cu (Ni, Mo)
N₁ NORTH ROCK (BEAVER POND)
N₂ NORTH ROCK (MAIN SOUTH)
N₃ NORTH ROCK (EAST)
H₁ HUPCHUK (WEST)
H₂ HUPCHUK (EAST)
B BELACOMA
R REDGUT BAY
M MIRONSKY
T₁T₂ TRAVERSE INLET
OXIDES (Fe, Ti)
SHAFT

Figure 30. Summary geological map and schematic cross section of the Grassy Portage intrusion, *based on* mapping by C.J. Hodgson in 1959 and K.H. Poulsen from 1980 to 1982, and private company maps.

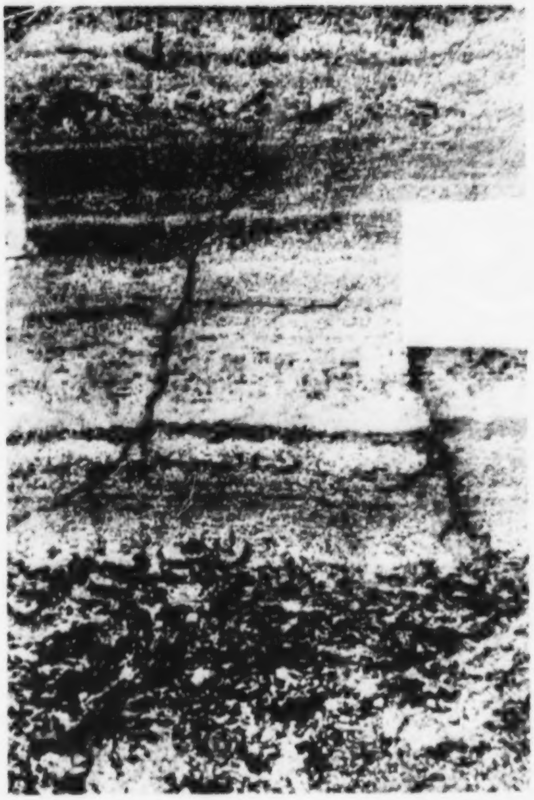

Photo 46. Modal layering of plagioclase and hornblende in metagabbro, Redgut Bay. Compass is 7.5 cm wide.

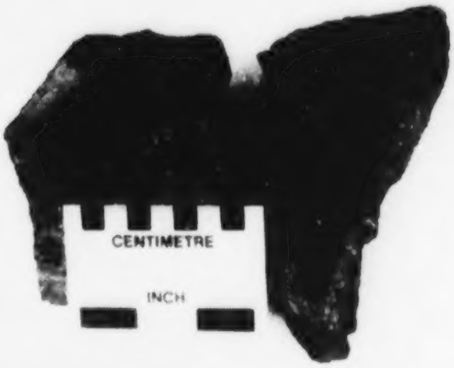

Photo 47. Net textures, disseminations and stringers in chalcopyrite ore, North Rock Mine. The sulphide minerals (grey) are interstitial to hornblende and plagioclase (light grey).

suite of specimens and polished sections from 2 of these lenses, A and C (*see* Figure 31a), as well as selected specimens from the Hupchuk prospect (*see* Figure 30) were examined to characterize the ore (Table A6.2). High-grade "grey" ores and lower grade "black" ores are present. The black ores consist of coarse hornblende gabbro with disseminations, blebs and stringers of chalcopyrite, pyrrhotite and pentlandite. Molybdenite occurs locally with the other sulphide minerals or within grey saussuritized patches in the gabbro. These grey patches are a characteristic feature of the low-grade mineralization and give a distinctive spotted appearance to the rock, in part resulting from the localization of glomerophenocrysts. The "grey" ores consist of copper sulphide and pyrrhotite in approximately a 2:1 ratio in a net-textured ore (Photo 47).

The dominant copper sulphide is chalcopyrite, but most specimens from the C lens contain up to 50% exsolved cubanite (Photo 48). Pyrrhotite occurs as poly-

Table 9. Mineralogical compositions of rocks in the Grassy Portage intrusion.

UPPER ZONE

Gabbro, Quartz Gabbro, Diorite – up to 250 m thick; medium-grained equigranular amphibolite, locally well-developed modal layering

Quartz-Plagioclase Schist – leucocratic rock with less than 20% actinolite and biotite; 30 to 40% quartz; rock occurs as lenses and blocks up to 20 m thick

Magnetite-Apatite Amphibolite – actinolite, anthophyllite, talc, magnesium chlorite and apatite with 5 to 50% magnetite; local siliceous rutile-bearing masses

Garnetiferous Quartz Diorite – medium-grained black amphibolites composed of hornblende, plagioclase (An_{30-38}) and quartz eyes; garnets up to 1 cm are common; also abundant apatite, epidote; average 250 m thick

LOWER ZONE

Leucogabbro – 60 to 90% plagioclase (An_{48-52}) as framework grains, commonly poikilitically enclosed by hornblende megacrysts; locally contains xenoliths of anorthosite; up to 750 m thick

Actinolitic Amphibolite – lenses of actinolite with 5 to 20% magnetite with local diopside, clinozoisite, phlogopite, sphene and plagioclase (Hodgson 1959)

Anorthosite – 95% medium-grained plagioclase (An_{40}); local epidote and minor biotite; xenoliths of gabbro observed

Gabbro – medium- to coarse-grained, equigranular to locally porphyritic and glomeroporphyritic; 50% interstitial hornblende, 50% plagioclase (An_{50-55}); local magnesium chlorite and biotite; averages 300 m thick

Melagabbro – 50-foot-wide (15 m) lenses at or near the base of the intrusion; 80% hornblende, 10% plagioclase (An_{50}), plus biotite and sulphides

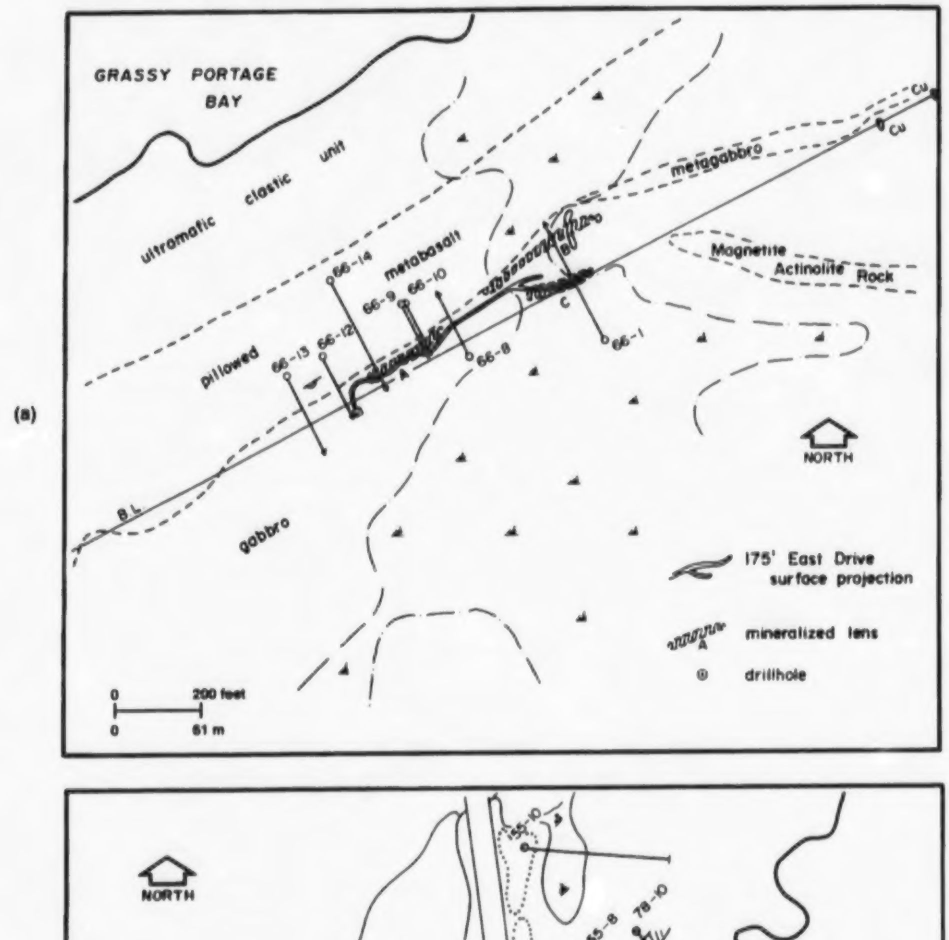
(a)
GRASSY PORTAGE BAY
ultramafic clastic unit
pillowed metabasalt
metagabbro
Magnetite Actinolite Rock
gabbro
66-13
66-12
66-14
66-9
66-10
66-8
66-1
A
B
C
Cu
B.L.
NORTH
175' East Drive surface projection
mineralized lens
drillhole
0 200 feet
0 61 m
(b)
NORTH
RAINY LAKE
gabbro
gabbro, quartz gabbro
many volcanic inclusions
actinolitic basalt
staurolite biotite schist
oxide layers
Hwy 11
55-10
55-9
55-8
78-10
78-11
78-8,9
55-7
55-1
78-1
78-5
78-3,4
78-2
78-6
55-2
55-4
78-7
Tr
321'
400'
198'
175', 170'
205'
402'
472'
271'
130'
305'
268'
209'
350'
45
Tr mineralized lens
drillhole
overturned bedding

Figure 31. a) Summary geological map of the Beaver Pond zone, North Rock Mine. *Adapted from* Hodgson (1959). b) Summary geological map of the Mironsky prospect.

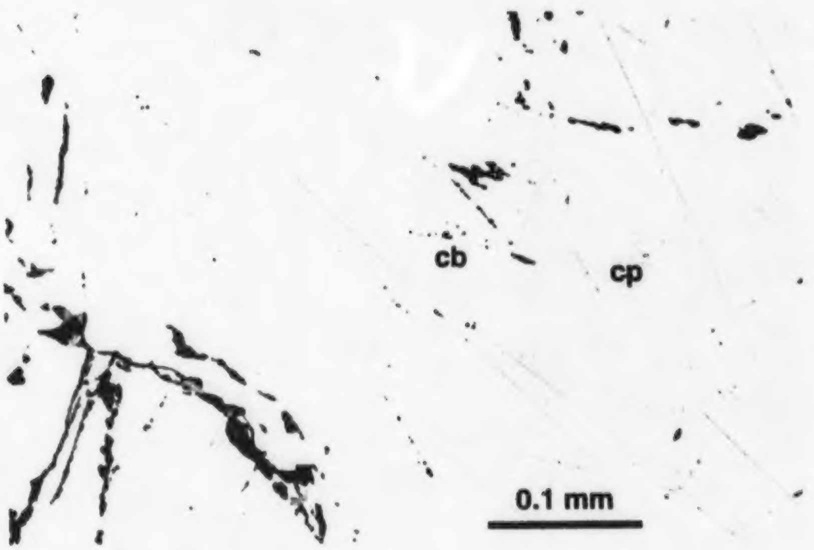

Photo 48. Photomicrograph of cubanite (cb) lamellae in chalcopyrite (cp), North Rock Mine.

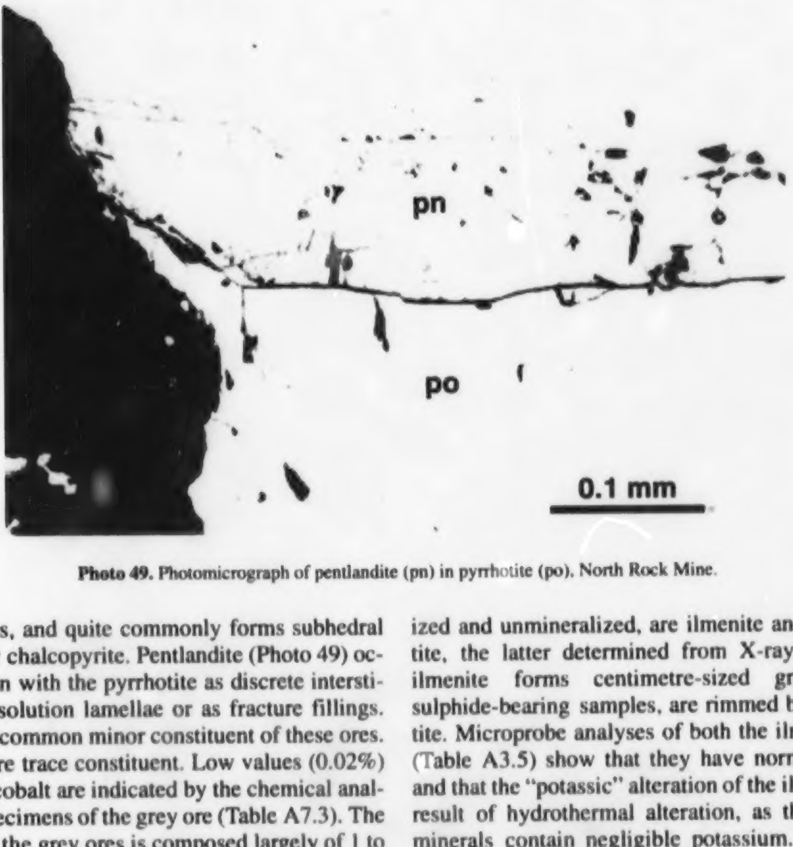

Photo 49. Photomicrograph of pentlandite (pn) in pyrrhotite (po), North Rock Mine.

crystalline masses, and quite commonly forms subhedral cores enclosed by chalcopyrite. Pentlandite (Photo 49) occurs in association with the pyrrhotite as discrete interstitial grains, as exsolution lamellae or as fracture fillings. Molybdenite is a common minor constituent of these ores. Sphalerite is a rare trace constituent. Low values (0.02%) of both zinc and cobalt are indicated by the chemical analyses of typical specimens of the grey ore (Table A7.3). The silicate matrix of the grey ores is composed largely of 1 to 10 mm long laths of saussuritized plagioclase. Clinozoisite (Hodgson 1959) in the feldspars imparts grey, pale green, brown and pink tones to silicate-rich specimens. Common constituents of these light-coloured rocks, both mineralized and unmineralized, are ilmenite and pale green apatite, the latter determined from X-ray diffraction. The ilmenite forms centimetre-sized grains which, in sulphide-bearing samples, are rimmed by coronas of biotite. Microprobe analyses of both the ilmenite and biotite (Table A3.5) show that they have normal compositions, and that the "potassic" alteration of the ilmenites is likely a result of hydrothermal alteration, as the typical gabbro minerals contain negligible potassium. Locally, the sulphide ores are slightly schistose and small massive sulphide mineral patches result from tectonic remobilization. Pentlandite concentration is greatest in the remobilized ores.

The sulphide minerals that occur in the upper zone of the intrusion, principally at the Mironsky prospect (*see* Figures 30 and 31b), are hosted by a fine- to medium-grained, weakly schistose quartzofeldspathic rock containing biotite, actinolite, magnesium chlorite and sphene. Chalcopyrite and pyrrhotite occur in roughly equal proportions as interstitial grains less than 1 mm in diameter. The result is a grey-green siliceous rock that grades up to 1% Cu. In form, the deposit is that of a tabular unit at least 600 by 25 m in section, which is mineralized throughout but contains narrower higher grade zones. Similar smaller lenses were noted by the author at the same horizon along strike in the Redgut Bay area. There, the bodies have the appearance of assimilated metasedimentary blocks within the sequence of modally layered gabbros. The siliceous blocks, if sedimentary, must have been entirely reconstituted: diagnostic sedimentary textures and structures, which are common in overlying biotite schists, are lacking in them.

Oxide Mineralization

An extensive magnetite-bearing member is closely associated with xenolithic gabbro in the upper zone. This member consists of disseminated magnetite and apatite (Photo 50) in a fine-grained silicate matrix composed of talc, magnesium chlorite and tremolite. The oxides constitute up to 50% by volume of this rock, and local modal grading of the minerals was noted. On the Traverse Inlet prospect (*see* Figure 30 for location), a unique pegmatoid mass, probably intrusive into the magnetite-apatite rock, contains rutile (Photo 51) as poikilitic grains up to 1 cm in diameter in a matrix of plagioclase, tremolite and magnesium chlorite. Plagioclase, with a distinctive green weathered surface, occurs with the rutile in patchy segregations.

Origin

The mineralization associated with the Grassy Portage intrusion is typical of many layered sills. The intrusion has many of the attributes of a synvolcanic layered anorthositic sill (Naldrett 1981), and shows an internal stratigraphy and mineral zonation similar to the Doré Lake Complex at Chibougamau, Quebec (Allard 1970, 1976). The basal sulphide minerals with their characteristic net textures (Naldrett 1973), associated ilmenite euhedra and exsolved sulphide phases, are probably magmatic segregations. The high (50:1) copper to nickel ratio reflects the mafic rather than ultramafic composition of the intrusion (Naldrett 1973). The common clinozoisite "bleaching" of the silicate host, the development of biotite rims on the ilmenite and the presence of molybdenite all suggest that hydrothermal alteration, possibly of deuteric origin, has occurred. Further, the sulphide minerals probably have been mechanically remobilized at a local scale into shear zones during regional deformation.

The close spatial association in the upper zone of the siliceous copper-bearing unit, the magnetite-apatite unit and the abundant xenoliths suggests a possible genetic relationship. The iron-titanium oxide rocks fall broadly into the category of nelsonites (Ross 1941), which are known associates of many anorthositic bodies (Kolker 1982). Three interpretations of the origin of such rocks have been proposed:

1. normal crystallization and settling from a melt (Emslie 1975)
2. eutectic crystallization of a magnetite-apatite liquid that is the product of immiscible separation from an iron-, phosphorous- and titanium-enriched silicate liquid (Philpotts 1967)
3. sialic contamination of a liquid (Irvine 1975; Klemm et al. 1982)

The third of these is supported, in the present example, by the abundant xenoliths. It is not known to what extent contamination has influenced sulphide mineral deposition, but a similar mechanism is possible (Irvine 1975).

Abundant sulphide facies iron formation and sedimentary rocks elsewhere within the sequence (*see* Map 2525) are a suitable source of sulphur (Naldrett and Gasparrini 1971; Mainwaring and Naldrett 1977). This may explain the abundance of sulphide mineralization associated with the Grassy Portage intrusion, while large volumes of similar rocks in the Seine Bay–Bad Vermilion Lake area contain relatively little sulphide mineralization.

GOLD-BEARING QUARTZ VEINS

Morphology

Laminated gold-bearing quartz veins occur in the Mine Centre area within ductile shear zones and as dilations of regionally developed cleavage. Veins are typically 0.5 to 1 m wide, are notably lenticular, and occur within a wide variety of rock types (Table 10). The statistical preference for granitoid rocks was once thought to reflect a cogenetic relationship (Tanton 1935), but probably simply reflects the types of rocks in which ductile shear zones readily form (Ramsay and Graham 1970). The shear zones are tabular, centimetres to metres wide, and contain an internal oblique foliation not present in the mechanically isotropic rocks that they transect.

The essential geometric features of the gold-bearing shear zones are illustrated in Figure 32a. Two common shear zone orientations are present in the area, each with a consistent orientation of internal foliation. Shear zones that strike east have a foliation asymmetry that is consistent with dextral shear displacements (Ramsay and Graham 1970), while north-northwest striking zones are sinistral. A gold-bearing principal vein most commonly occupies the geometric centre of a shear zone (Photo 52) and is steeply dipping. Locally, it cuts second-order veins, which are approximately perpendicular to foliation, forming sigmoidal arrays (*see* Figure 32a). Third-order veins locally branch from principal veins and occupy a position parallel to foliation (Photo 53). The third-order veins likely reflect mechanical delamination of the foliated host rock, while the second-order veins are interpreted to be extensional.

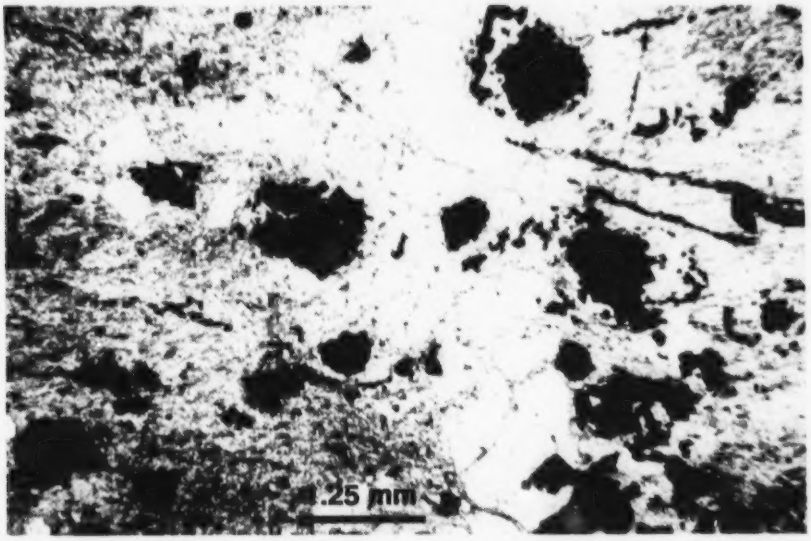

Photo 50. Photomicrograph of magnetite (black)-apatite (white) intergrowths, Traverse Inlet prospect. Matrix is composed dominantly of talc, tremolite and magnesium chlorite.

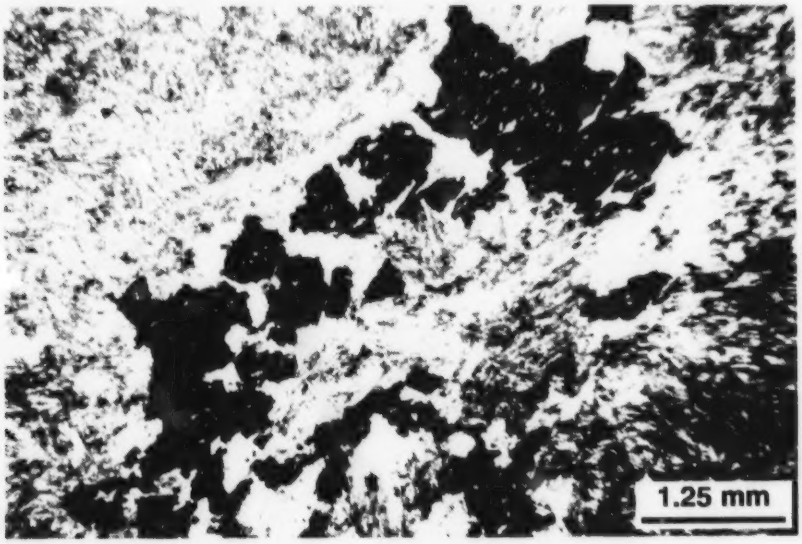

Photo 51. Photomicrograph of rutile (black) masses, Traverse Inlet prospect. Note the abundant quartz inclusions in the rutile and the plagioclase-tremolite-magnesium chlorite matrix.

Locally, misoriented angular inclusions of foliated wall rocks were noted within principal veins, and the resulting lamination appears to be due, in part, to the inclusion of narrow selvages of sericitic and chloritic host rock within the vein during vein growth. While the shear zones and principal veins are approximately plane-parallel features at the local scale, they can be seen to be decidedly curviplanar where sufficient exposure permits detailed mapping. This curved nature of several veins (Figures 32b and 32c) is accompanied by a branching of veins to yield a characteristic "bull's nose" or "cymoid" structure (McKinstry 1948). Both branches of the shear zones show the same sense of displacement. The creation of dilatancy for the principal veins is therefore attributable to repeated shear displacements along a curved shear fracture (Newhouse 1940) that was initiated in the highly deformed central portions of a shear zone.

The relationship of the veins to the host rock structure is quite different where the veins occur in initially mechanically anisotropic host rocks. This second structural association is exemplified by the Olive Mine and several occurrences of similar type. The host rocks, in this case, are tuffs and metasedimentary rocks with well-developed cleavage

Table 10. Lithologic controls on gold-bearing quartz veins, Rainy Lake.

Host Rock Type	Number of Veins
tonalite, trondhjemite	46
felsic and intermediate metavolcanics	16
metadiabase, amphibolite	9
metabasalt, chlorite schist	5
gabbro, anorthosite	4
conglomerate	2
quartz monzonite-granodiorite	0
Total Number of Veins	82

that is locally subparallel to bedding. Laminated veins commonly parallel this cleavage (Photo 54) and, where there is local folding or brecciation of the host rocks, highly irregular vein networks with a cleavage-parallel component are developed.

Composition

The primary constituent of the gold-bearing veins is quartz. While some coarse crystals, which probably formed during open-space filling, are discernible in some veins, virtually all of the quartz shows evidence of postdepositional deformation at moderate temperatures (Photo 55): undulatory extinction, serrated grain boundaries, deformation bands and lamellae, stylolites, subgrains, and polycrystalline aggregates characteristic of recrystallization are all common features. The result is a general reduction in grain size of vein material from coarse equant primary growth crystals to fine-grained, "cherty", locally laminated, polycrystalline aggregates. Visible gold is most commonly associated with this fine-grained, deformed quartz.

Carbonate minerals also show evidence of early open-space growth, followed by deformation. Coarse carbonate grains commonly occur interstitially to quartz, but locally, at the Stellar and South Vermilion mines, evidence of fibrous growth of ankerite was noted. Blades of ankerite (Photo 56) project comb-like into the vein with a curvature that is a result of either incremental syntectonic growth (Durney and Ramsay 1973) or postdepositional inhomogeneous strain. Carbonate minerals are most abundant in the veins at the northern end of Bad Vermilion Lake (Stellar, South Vermilion, Golden Star and Isabella mines), where both ankerite and siderite were noted. Ankerite alone forms but a minor component of most veins away from this general area.

Sulphide minerals are relatively abundant in the Mine Centre veins. Pyrite is most ubiquitous and occurs as well-developed euhedra, which are locally brecciated. Some veins are associated with mafic host rocks (Isabella No.1, Turtle Tank, Stellar No.6 vein, South Vermilion "Shoreline" vein) and contain abundant chalcopyrite, with malachite as a secondary alteration. Veins that are hosted by felsic rocks, commonly gold and silver bearing, locally contain abundant sphalerite and galena. Sphalerite contains oriented inclusions of pyrrhotite and chalcopyrite, while galena occurs as inclusions in pyrite, as anhedral interstitial grains, and as veinlets in other brecciated sulphide grains. Arsenopyrite has been reported from many of the veins (Poulsen 1984) but was rarely observed by the author. A large museum specimen from the Isabella No.2 vein contains abundant arsenopyrite intergrown with gold. It is reportedly cobalt-rich (Bruce 1925b), but microprobe analysis (Table A4.2) indicated less than 1% Co. The references to cobalt-rich sulphide mineralization (Bruce 1925b) probably reflect the presence of a local pink stain, most likely erythrite, which was noted by the author at several veins.

Pyrrhotite occurs locally at the Young–Corrigan prospect, molybdenite has been reported (Wood et al. 1980a, 1980b) in the Finger Lake area (1 km south of Bad Vermilion Lake), and Wood et al. (1980a, 1980b) reported 0.26% Bi in a single sample from a vein in the Dumbbell Lake area (1 km south of Bad Vermilion Lake). Native gold was observed by the author, associated with arsenopyrite as noted above, as discrete scales and grains in laminated "cherty" quartz (Olive, Foley, and Stellar mines), intergrown with galena (Photo 57), and as minute inclusions within pyrite (Cone prospect). Representative assays for chip channel samples from selected veins in the Shoal Lake area are given in Table A7.4. Silver is also present in many veins, particularly if sphalerite and galena are present. Tourmaline was noted in several veins (Young–Corrigan, Dinosaur and Cone prospects) but is generally not abundant. Harris (1974) reported a few grains of scheelite at the Young–Corrigan prospect, and sphene, rutile and ilmenite were noted locally by the author. Chlorite and sericite seams impart a ribbon structure (McKinstry and Ohle 1949) to some veins.

Alteration

The foliated wall rocks that make up the shear zones adjacent to the veins show evidence of mechanical and chemical alteration. For example, equigranular tonalite and trondhjemite away from a shear zone (Photo 58) grade laterally toward a vein into schist and protomylonite (Photo 59), in which plagioclase feldspar has been converted entirely into foliated sericitic matrix and quartz porphyroclasts show evidence of grain size reduction. Ankerite is a common component of this alteration, and the development of hydrous potassium-poor rocks suggests metasomatism within the shear zones. Pyrite euhedra form approximately 1% of the altered rocks adjacent to some veins. The width of altered rock associated with a given vein is variable (1 cm to a few metres) but does not correlate directly with vein width.

The chemical characteristics of the alteration adjacent to veins are illustrated by whole rock analyses (Table A5.2) of "fresh" versus "altered" specimens from 3 sites, the Cone prospect No.1 vein, and the Stellar No.1 and unnamed veins. The data are plotted (Figure 33a) in the alteration diagram of Riverin and Hodgson (1980). The transition to increasingly altered material, as determined visually, is shown by arrows, and the 4 specimens from the Cone prospect clearly show the path of alteration.

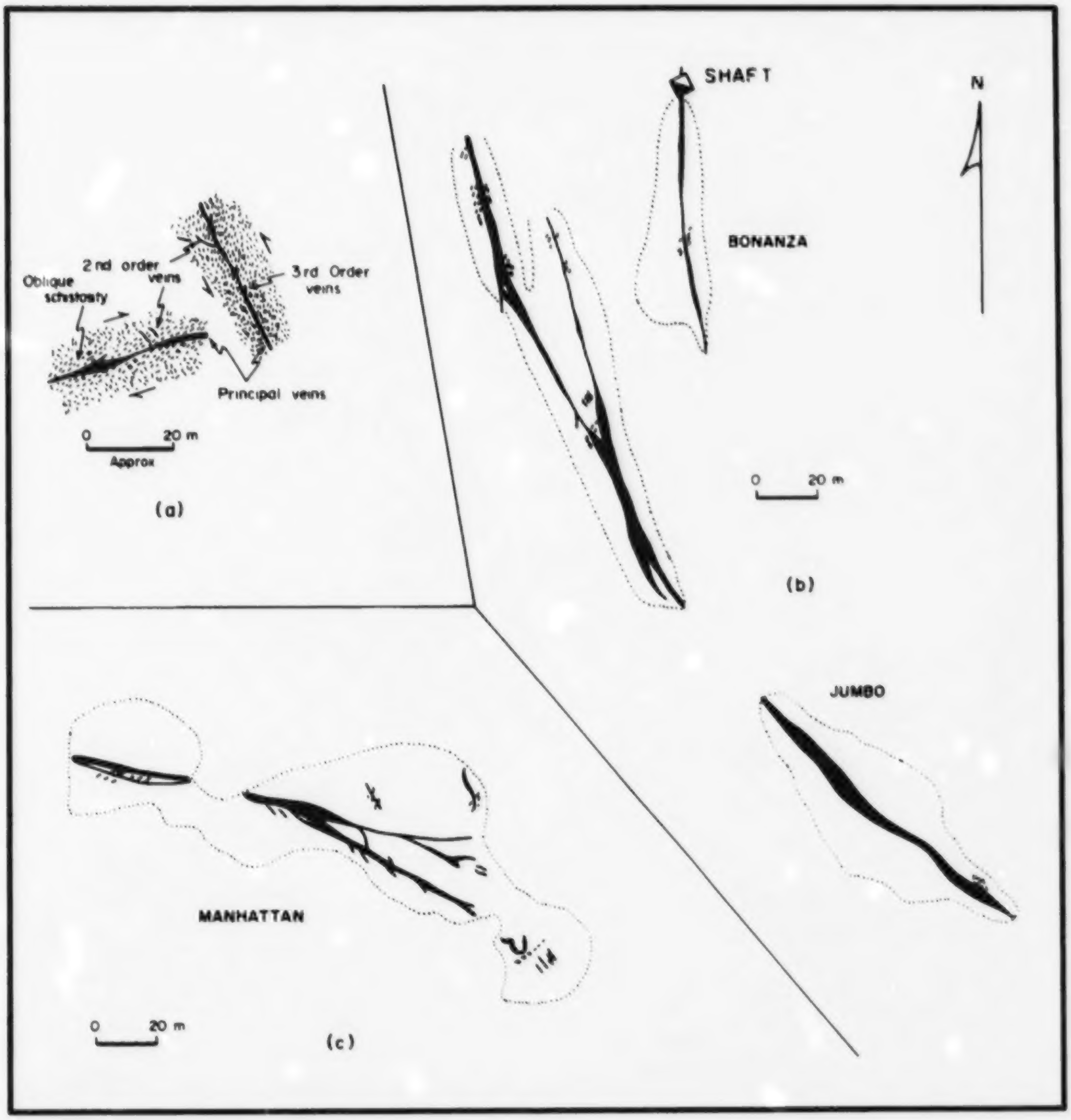

Figure 32. a) Schematic plan showing the geometry of veins associated with shear zones at Rainy Lake. b) Detailed geological map of vein system at the North shaft, Foley Mine. Jumbo and Bonanza veins are shown. c) Detailed geological map of the vein system at the Manhattan Mine.

Potassic alteration at the expense of the plagioclase components sodium and calcium is clearly indicated, and contrasts with the chlorite-dominated alteration associated with the volcanic-hosted base metal deposits (*see* Figure 27b). It is also significant that the conversion of the gabbro into chlorite schist involves less net chemical change than is indicated for the felsic rocks. This may reflect a greater chemical disequilibrium between the alteration fluids and the felsic rocks as compared to the rocks that have a mafic bulk composition.

Isotopic Composition of Lead in Galena

As noted previously, galena is a common constituent of the gold-bearing quartz veins, and in one case (*see* Photo 57) was observed to be in direct contact with native gold. The isotopic composition of lead was determined for 11 galena specimens from the veins, and for 3 specimens from base metal deposits associated with felsic volcanic rocks. Anal-

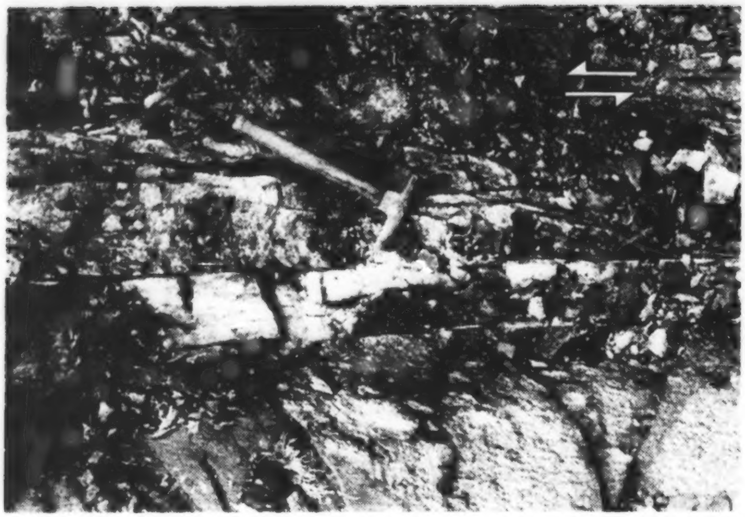

Photo 52. Principal laminated vein in shear zone, Cone prospect. Note the oblique foliation adjacent to the vein. Hammer is 30 cm long.

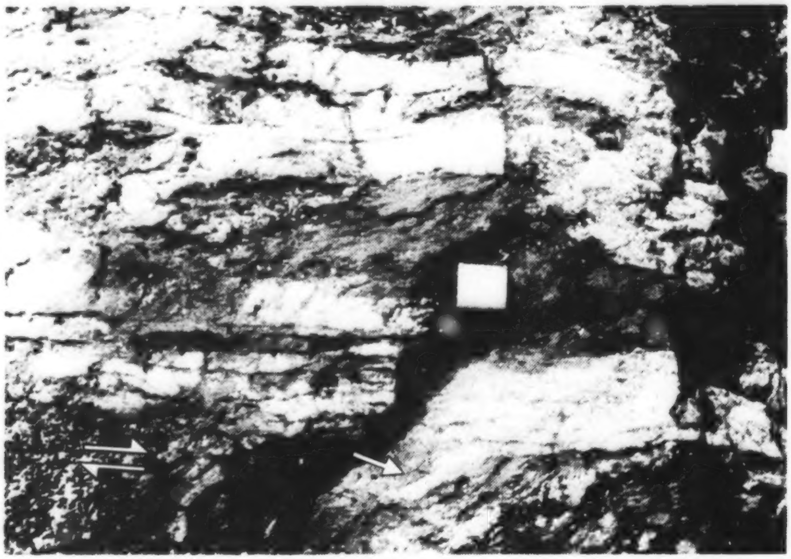

Photo 53. Principal laminated vein in shear zone with foliation-parallel third-order veins (arrow), Stellar Mine. Compass is 7.5 cm wide.

yses were performed, under contract to the Geological Survey of Canada, by laboratories at the University of Alberta and the University of Toronto (*see* Appendix 8).

The data define a clear trend in the thorium-free $^{207}Pb/^{204}Pb$ versus $^{206}Pb/^{204}Pb$ system (Figure 34), with quartz-vein galena clearly more radiogenic than galena from the base metal deposits. Three different approaches were taken to interpret these data.

The first approach is based on an analysis of the data in terms of primary isochrons, which are dependant on the choice of a suitable growth curve (Figure 35a). The two-stage growth curve (Stacey and Kramers 1975), the continuously changing growth curve (Cumming and Richards 1975), the episodic mixing "plumbo tectonic" model (Doe and Zartman 1979), and the empirical Precambrian sulphide mineralization model (Thorpe 1982) were all considered, but the trend of the Rainy Lake area data does not correspond to an isochron in any of these ideal systems. Thus, model ages must be calculated only for individual data points (Table A8.1). This approach seems reasonable for the massive sulphide mineralization for which the model ages are very close (average 2715 Ma using the Thorpe model), but is considered unreasonable for the veins, in

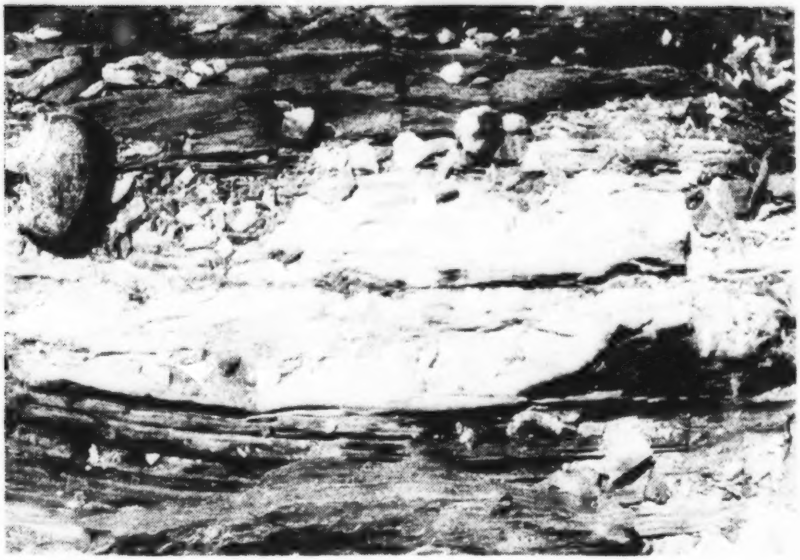

Photo 54. Cleavage-parallel quartz vein, Olive Mine. Hammer head is 10 cm long.

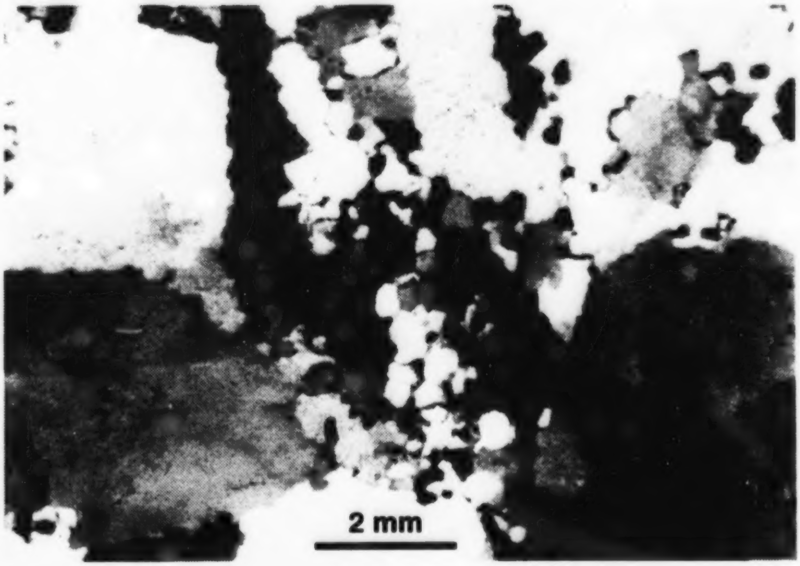

Photo 55. Photomicrograph illustrating deformational textures in vein quartz. Note the serrated grain boundaries, the subgrain development in large grains, and the total recrystallization of large grains into polycrystalline masses of smaller grain size.

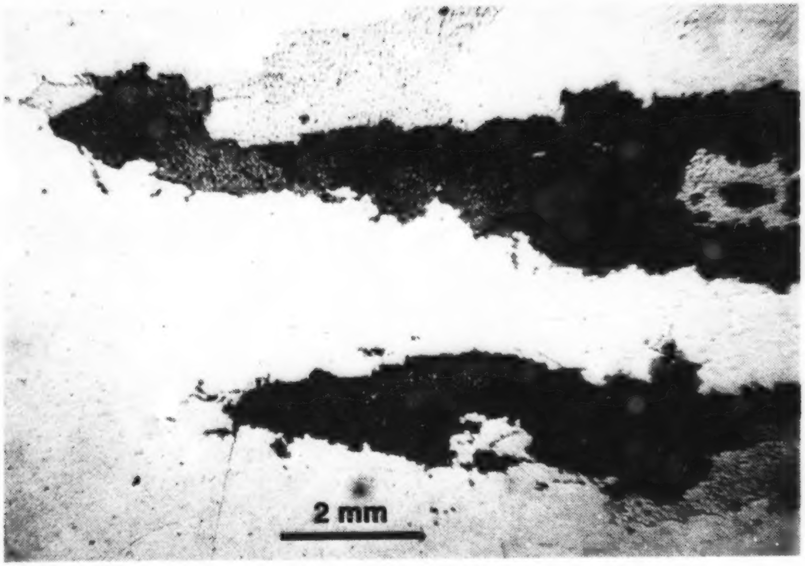

Photo 56. Photomicrograph of ankerite "fibres" (grey) in quartz, South Vermilion Mine.

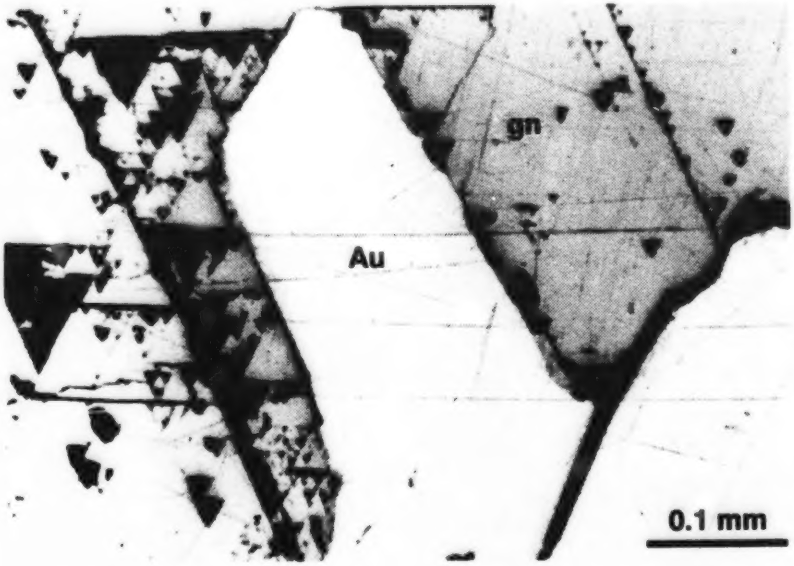

Photo 57. Photomicrograph of native gold (Au) intergrown with galena (gn), Cone prospect.

that the calculated model ages imply that the veins formed successively over a 200 Ma period rather than nearly synchronously. The model ages for the base metal deposits are in good agreement with those for other Superior Province massive sulphide deposits (Franklin and Thorpe 1982) and with the U-Pb zircon ages for the volcanic host rocks in the Rainy Lake area (*see* Table 1), and thus represent reasonable ages of mineralization for these deposits. On the other hand, the model ages for the vein galena only suggest that they are somewhat younger, and that other interpretative methods are required to estimate their ages.

The second interpretative approach attempts to put limits on the age of mineralization of the vein galena by considering their compositions to be collinear, defining an anomalous lead line. Four possible mechanisms to generate an anomalous lead line of slope 0.3326 (by two-way regression) were considered:

1. The data could represent the mixing of leads generated within a short time interval in a suite of rocks with variable uranium to lead ratio at 2376 Ma. This would represent "instantaneously" generated lead (Faure

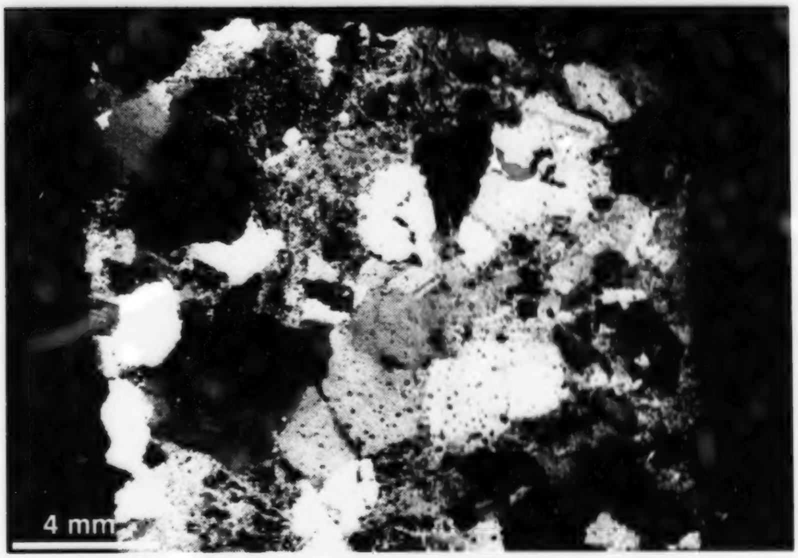

Photo 58. Photomicrograph of undeformed equigranular tonalite, Cone prospect.

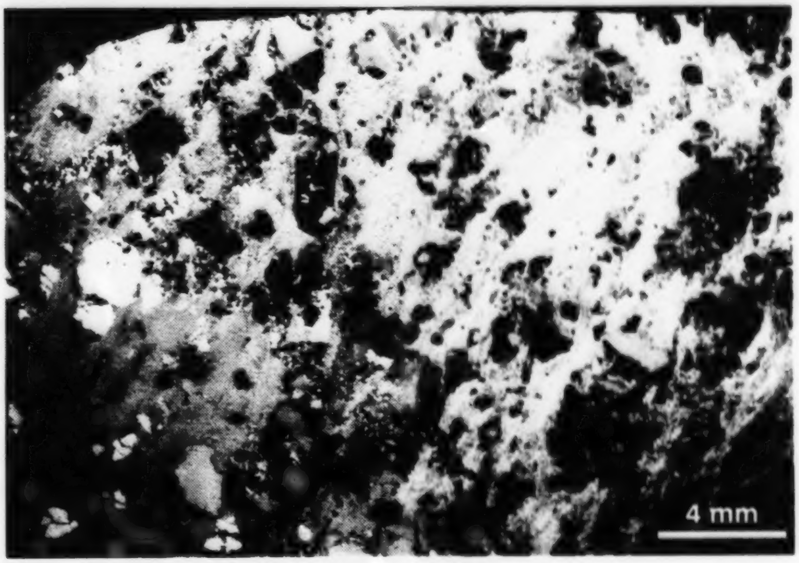

Photo 59. Photomicrograph of deformed equivalent of Photo 58 tonalite adjacent to a gold-bearing quartz vein. Note that the maximum grain size of quartz is similar in both samples, and that the rock in this photo is not an igneous "porphyry".

1977), but a convincing mechanism of separating it from existing lead in these rocks is required if this is to be a valid interpretation.

2. A "t-maximum" age (Faure 1977) of 3626 Ma was calculated for the Rainy Lake data. This means that, only if very young ages of mineralization are permitted, can old crust have contributed lead to these veins. As an older age of mineralization is required, so too is an increasingly younger source area required. The limiting case is the t-instantaneous age of 2376 Ma in which the age of the source rock and the age of the mineralization are permissibly the same.
3. A secondary isochron age of 2002 Ma was computed for the age of mineralization assuming that radiogenic lead was generated in rocks that are 2715 Ma in age (Figure 35b), corresponding to the estimate for the

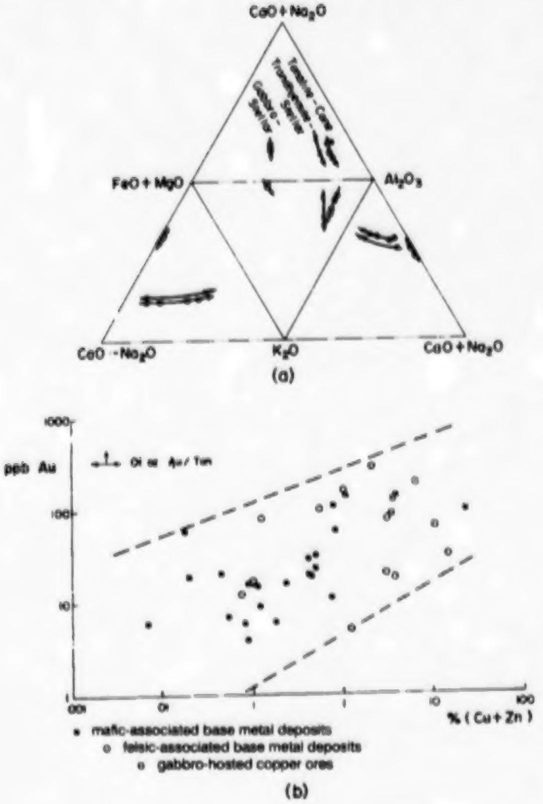

Figure 33. a) Riverin and Hodgson (1980) plot of whole-rock data for "fresh" and "altered" specimens associated with gold-bearing quartz veins at the Cone and Stellar prospects. Arrows show the tendency toward increased alteration as estimated visually from hand specimens. Contrast these "sericitic" alteration trends with the "chloritic" ones shown in Figure 27b. b) Graph of Au versus total Cu+Zn in specimens of sulphide mineralization at Rainy Lake.

base metal deposits. This type of model was applied to similar patterns of lead isotopic values from the Homestake Mine, South Dakota (Rye, Doe and Delevaux 1974) and from gold-bearing veins in Tanzania (Goomer and Robertson 1974). In the present example, the 2002 Ma age of mineralization in deformed quartz veins is in conflict with an older age of at least 2120 Ma (Beck and Murthy 1982) determined for undeformed diabase dikes that cut all other units in the Rainy Lake area. Thus, the secondary isochron interpretation does not appear to be appropriate for the Rainy Lake veins.

4. A linear array of points may result from the binary mixing of 2 end-member compositions in varying proportions (Figure 35c). The data of Figure 34 could be generated by mixing of the massive sulphide lead with a radiogenic component, at most 2500 Ma in age. Kanasewich (1968) has pointed out however, that binary mixing should also be evident by similar linear trends in plots of $^{207}Pb/^{204}Pb$ versus $^{206}Pb/^{204}Pb$. A suitable degree of linearity is not present in such plots of the Rainy Lake data.

The third approach to interpretation incorporates some features of the other methods, but does not rely on the assumption that the data are collinear. In its simplest form, this interpretation would allow that there are 3 likely sources for lead in the gold-quartz veins: lead trapped in sulphide minerals at approximately 2715 Ma, lead generated by the decay of uranium in silicate rocks that were also deposited at approximately 2715 Ma, and a third component, of unknown source, which is at least as radiogenic as the most radiogenic sample analyzed (Figure 35d). The first component would have a composition corresponding to that of the lead from the base metal deposits and the "lithic" component would be represented by a series of compositions corresponding to the secondary isochron for the age mineralization as shown by the dotted line in Figure 34. The slope of the resulting "line" would yield no absolute age information but does require, at least, components that are as young as 2500 Ma.

In summary, no single model of interpretation can be used to extract absolute age information from the lead isotope data. The data do require, however, that the veins be substantially younger than the base metal deposits, and that mixing of a volcanogenic component with younger radiogenic components is probable. The ages indicated (approximately 2500 Ma) are supported by independent geochronological data. A Rb-Sr whole rock isochron for the Bad Vermilion intrusion, host to many quartz veins, indicates an age of 2520±100 Ma (Hart and Davis 1969), although a zircon age of approximately 2700 Ma was determined for the same body. The authors attributed this discrepancy to the "highly altered and sheared character of the Bad Vermilion rocks; this suggests a pervasive hydrothermal event which could be very effective in bringing about open-system migration of strontium" (Hart and Davis 1969, p.609).

Origin

All of the above characteristics indicate that, in the Mine Centre area, gold-bearing quartz veins are epigenetic features of synkinematic origin. The shear zones that host most veins show evidence of transcurrent shear displacements, and the veins themselves show evidence of both open-space filling and subsequent deformation. Thus, vein formation is viewed by the author as a dynamic process involving development of probable hydraulic fractures to form second-order veins, propagation of curved principal shear fractures central to shear zones, dilation by continued shear displacements, filling to form principal veins, and continued deformation with repeated failure at quartz–wall rock interfaces to incorporate sericitic and chloritic "ribbons" and inclusions. Each failure episode may be considered a "seismic" event, and seismic pumping of fluids (Sibson, Moore and Rankin 1975) is an attractive mechanism, not only for moving fluids into and through dilatant openings, but also for transporting intragranular fluids that, along with the cataclastic deformation mechanism, effected the complete mechanical and chemical destruction of plagioclase in the altered zones.

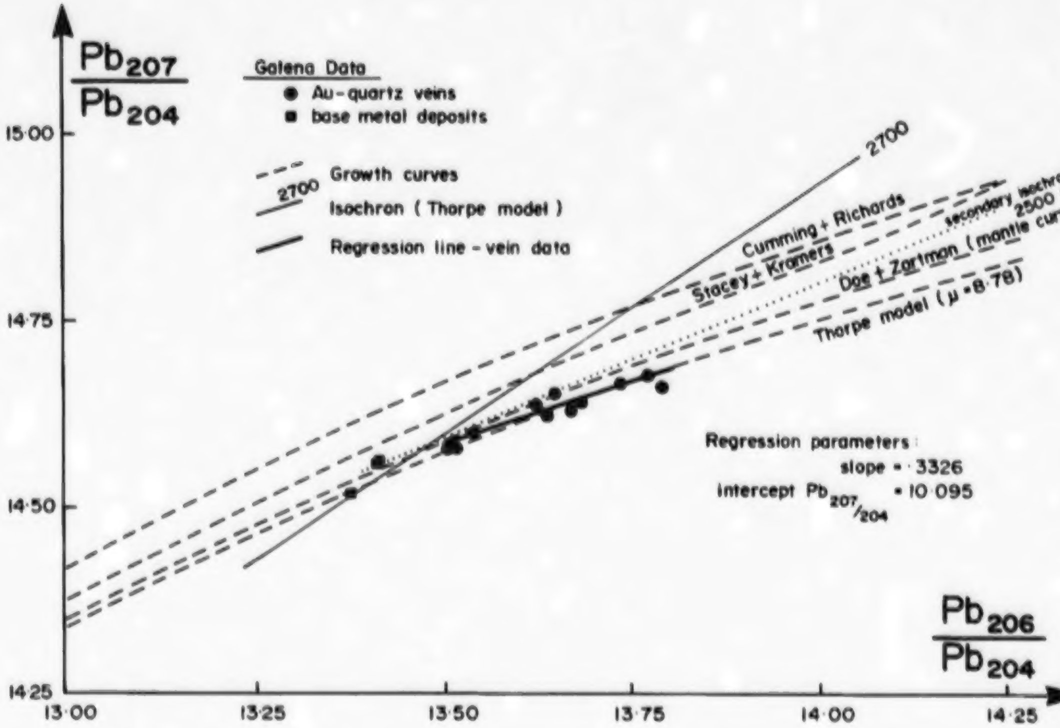

Figure 34. Graph of $^{207}Pb/^{204}Pb$ versus $^{206}Pb/^{204}Pb$ lead isotopic ratios in galena from Rainy Lake gold-bearing quartz veins and base metal deposits.

Current views on gold metallogeny hold that gold deposits are either synvolcanic or syntectonic in origin. Sources of metal for seemingly epigenetic gold-quartz veins may include "exhalite" that has been remobilized (Hutchinson, Ridler and Suffel 1971), magmatic fluids (Macdonald 1983) or metamorphic fluids (Fyfe and Henley 1973). The generation of the latter is usually ascribed to either subseafloor (Kerrich and Fryer 1981) or regional dynamothermal (Henley, Norris and Paterson 1976) metamorphism. The redistribution of gold that was preconcentrated in exhalites (Ridler, R.H.; *The Northern Miner*, November 29, 1973, p.59-61) is commonly cited as a possible way of forming epigenetic deposits. The gold content of Rainy Lake exhalites and mineralization associated with iron formation, as well as that of volcanic-associated base metal deposits and gabbro-hosted mineralization (*see* Tables A7.2 and A7.3) show that there is a good correlation between gold and copper-zinc contents of mineralization in all of these deposit types (*see* Figure 33b). On the other hand, there is no simple correlation between the amount of gold and either iron or sulphur content in these rocks. Thus, it appears that not only exhalites, but all copper- and zinc-bearing mineralization in the area is potentially a source of gold. However, it should be noted that: a) two orders of magnitude of enrichment are still required to establish a viable gold grade from this type of material (*see* Figure 33b); b) the gold is still present in these rocks; c) the volume of rocks with elevated (greater than 50 ppb) gold content is probably not large; and d) there is no spatial association between the gold-quartz veins and any of the above deposit types (*see* Figure 25). Nonetheless, the concentration of veins in the zone of greenschist facies metamorphism, the late tectonic timing of vein formation, and the possibility that the lead in the veins represents a mixture from different sources does favour a metamorphic origin. If this is the case, gold from exhalites may have contributed to the overall composition of the veins. However, the metamorphic origin of the ore-forming solution fails to account for the abundant barren quartz veins in the area and the paragenetically late time of deposition of gold in local deformed portions of previously deposited quartz veins.

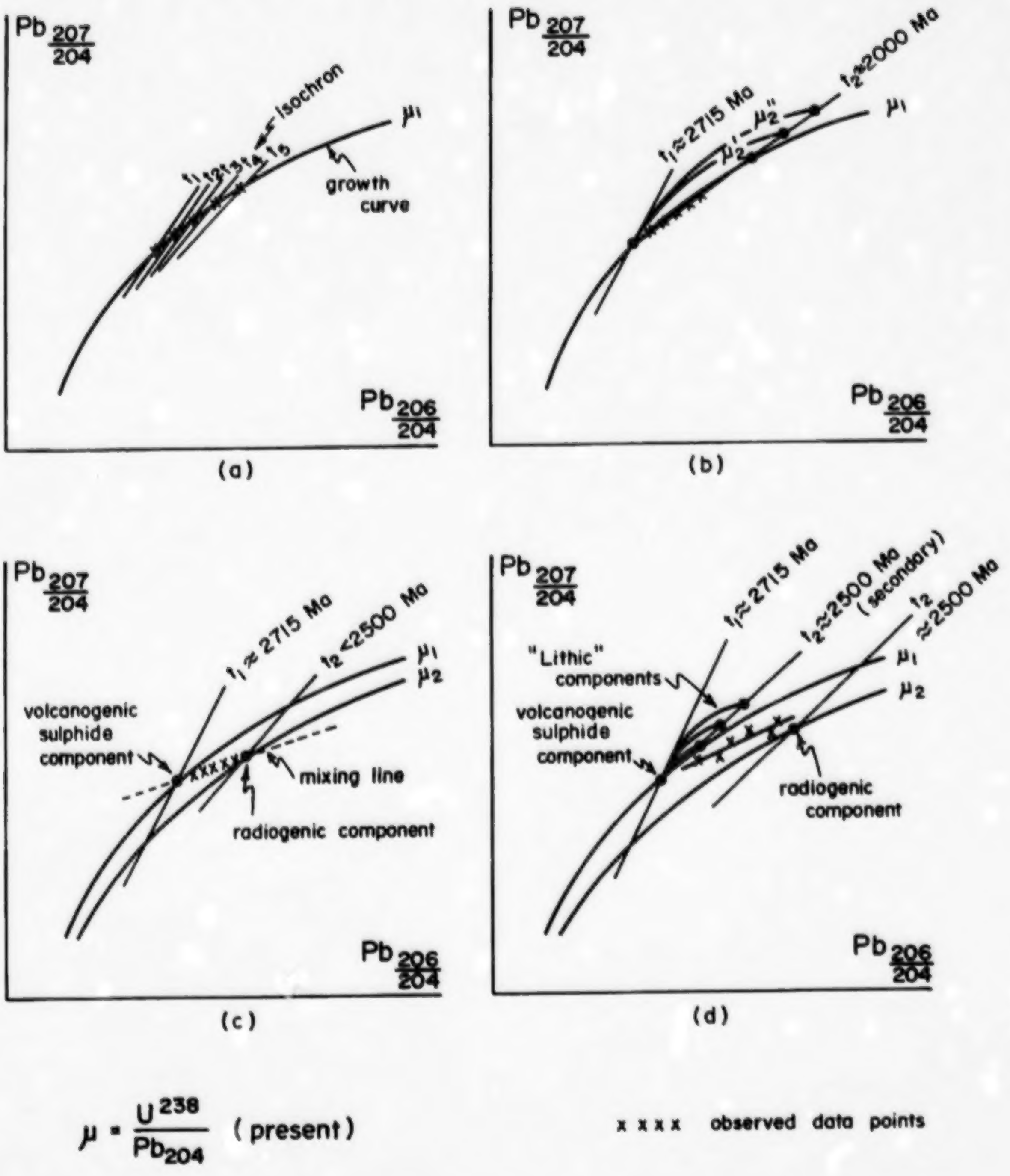
Pb 207/204
isochron
μ1
t1 t2 t3 t4 t5
growth curve
Pb 206/204
(a)
Pb 207/204
t2≈2000 Ma
t1≈2715 Ma
μ2′ – μ2″
μ1
Pb 206/204
(b)
Pb 207/204
t1≈2715 Ma
t2<2500 Ma
μ1
μ2
volcanogenic sulphide component
xxxxx
mixing line
radiogenic component
Pb 206/204
(c)
Pb 207/204
t1≈2715 Ma
t2≈2500 Ma (secondary)
t2 ≈2500 Ma
"Lithic" components
μ1
μ2
volcanogenic sulphide component
x x x x
radiogenic component
Pb 206/204
(d)
μ = U238/Pb204 (present)
x x x x observed data points

Figure 35. Schematic diagrams illustrating a) the growth curves and isochrons for the lead isotope system; b) secondary isochrons for the lead isotope data; c) binary mixing of the lead isotopes; and d) complex mixing of lead isotopes. The resulting compositions here are limited to a triangular area on the diagram formed with a secondary isochron base and the composition of a radiogenic additive as the opposite vertex. Since, in the present case, this triangle is very slender, a "pseudo-linear" array of data points may be generated.

Tectonics and Metallogeny

TECTONIC AND METALLOGENIC SUMMARY FOR THE RAINY LAKE AREA

The preceding chapters contain descriptions of the stratigraphy, structure, metamorphism and mineralization of that part of the Rainy Lake area that is bounded by the Quetico and Rainy Lake–Seine River faults. Within that area, diverse stratigraphic units are restricted to 2 groups of lithostratigraphic domains which contrast with each other in many respects (Table 11). The mafic, ultramafic and pelitic rocks of the western domains are similar to the lowermost sequences that are present in many volcanic piles within the Wabigoon Subprovince (Trowell, Blackburn and Edwards 1980), while the volcanic sequences in domains near Mine Centre, with abundant felsic volcaniclastics and felsic, probably subvolcanic intrusions, compare favourably with the upper mixed felsic to mafic sequences in the northern part of the Wabigoon Subprovince (Franklin et al. 1977; Trowell, Blackburn and Edwards 1980). Structural analysis shows that the rocks in these contrasting domains occur within a dextral wrench fault zone comprising not only the large boundary faults, but less obvious internal faults that define the domain boundaries. Thus, the original geographic relationship between the volcanic sequences in the 2 types of domains is not known, and the domains must be considered to contain remnants of dismembered volcanic piles. The domains are therefore allochthonous and have been transported relative to each other and to adjacent rocks in both of the bordering subprovinces (*see* Figure 3). The Seine-type sedimentary rocks, composed of alluvial to fluvial conglomerates and arenites, lie with angular unconformity on the volcanic sequences and are restricted spatially to the wrench zone. Greenschist to amphibolite facies metamorphism accompanied deformation and culminated in the emplacement of the Algoman granodiorite plutons. These, as well as isograds, have been offset by later faulting.

Mineral deposits were formed at intervals throughout the tectonic history of the area, and the metallogeny is dominated by 2 successive phases of that history.

During an early volcano-sedimentary phase (Figure 36a), base metal mineralization was deposited, probably at or near the seafloor, at particular stratigraphic horizons within both types of volcanic sequences. Zinc-copper mineralization in the mafic volcanic sequences occurs as disseminated to massive zones that are directly associated with oxide facies of iron formation. Zinc-lead-copper mineralization in felsic volcanic rocks is accompanied by intense chloritic host rock alteration and hanging-wall tuffaceous exhalites. It is possible that these 2 contrasting types of mineralization in the Rainy Lake area are analogous to Phanerozoic Besshi-type and Kuroko-type deposits, and may have formed in lower mafic and upper felsic sequences, respectively. Gabbroic to trondhjemitic intrusions of the type found at Rainy Lake are probably subvolcanic (Franklin et al. 1977; Davis and Trowell 1982; Ashwal et al. 1983). Copper, with minor nickel, is concentrated in basal sulphide mineral segregations within the gabbroic sills, and both titanium and iron oxides are concentrated in the upper portions of the sills. Contamination by assimilated sedimentary and volcanic roof rocks

Table 11. Lithologic, metamorphic and metallogenic characteristics of contrasting types of tectonostratigraphic domains at Rainy Lake.

Characteristic	Western Domains	Eastern Domains
Volcanic Rocks	basalt, ultramafic clastics; minor rhyolite	rhyolite, dacite; minor basalt
Mafic Plutonic Rocks	gabbro, diabase; minor anorthosite	anorthosite, gabbro, diabase
Felsic Plutonic Rocks	granodiorite, quartz-monzonite; some tonalite	tonalite, trondhjemite; some granodiorite
Sedimentary Rocks	wackes and mudstones of turbidite association; minor conglomerate	conglomerates and arenite of alluvial-fluvial association; minor wackes and mudstones
Metamorphic Facies	amphibolite; minor greenschist	greenschist; minor amphibolite
Iron Formation	in mafic volcanic rocks; chert-magnetite, pyritic shales	in siltstones and arenites; magnetite and minor chert-magnetite
Base Metal Sulphide Deposits	massive to disseminated stratiform in mafic volcanic rocks; disseminated to massive in gabbro; disseminated in ultramafic volcanic rocks	laminated to massive in felsic to intermediate volcanic rocks
Vein Deposits	quartz-pyrite-molybdenite	quartz-carbonate-gold±sulphides
Metal Association	Fe, Cu, Zn, Co, Ni, Mo	Zn, Cu, Pb, Au, Ag, Fe

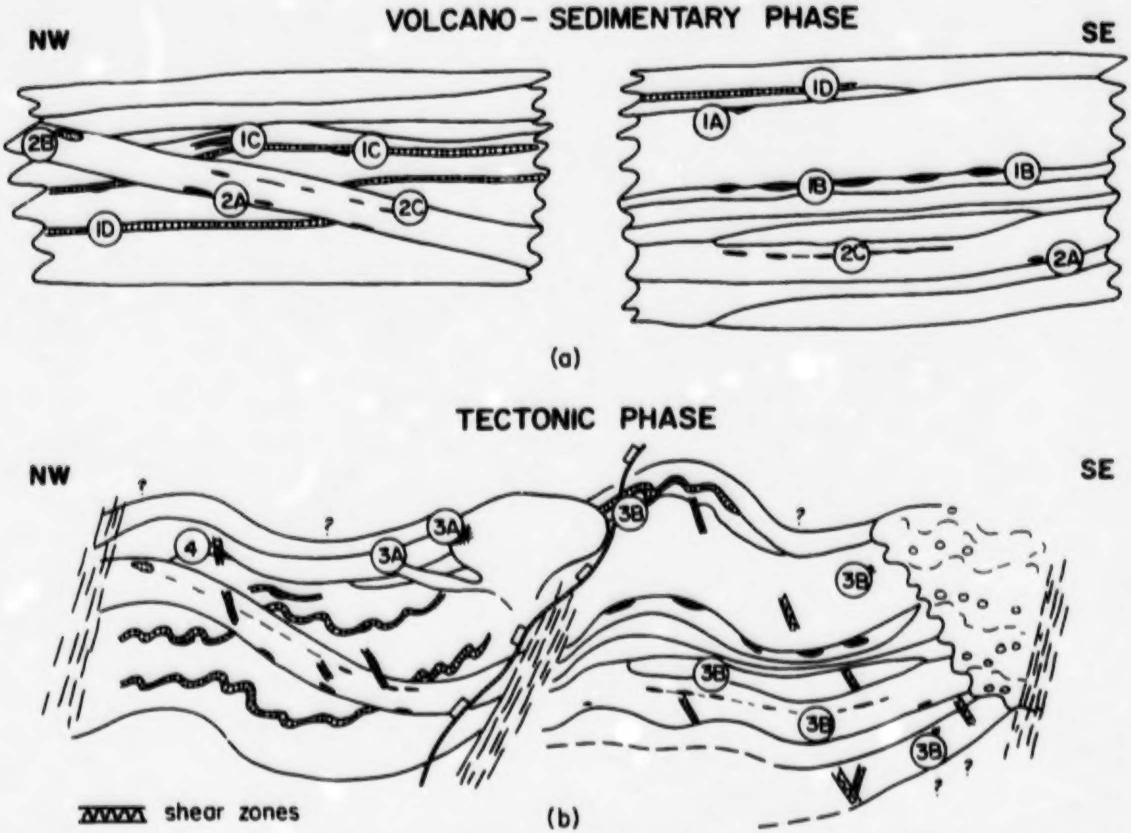

Figure 36. a) Schematic diagram illustrating the volcano-sedimentary phase of mineralization. The numbers refer to the types of mineralization listed in Table 8. b) Schematic diagram illustrating the tectonic phase of mineralization. The diagram is simplified in that the western and eastern groups of domains are shown as single blocks.

may have played a role in localizing mineralization by addition of silica, sulphur and/or metals, as well as altering the cooling history of the intrusions.

Folding, faulting, metamorphism and granodiorite plutonism constitute a tectonic phase in the history of the Rainy Lake rocks (Figure 36b). It was at this time that the rocks acquired their present geometric arrangement and pre-existing ores were deformed, metamorphosed and locally remobilized. Copper-nickel mineralization may have formed by sulphurization of ultramafic rocks at this time. More importantly, it was during this tectonic phase that quartz vein deposits were formed. Quartz-molybdenite veins in the western domains are clearly related to contacts between granodiorite and amphibolite facies pelites, while gold-bearing quartz veins near Mine Centre are hosted by syntectonic shear zones in greenschist facies rocks.

In summary, the presence of a dextral wrench zone at Rainy Lake has a profound influence on tectonic and metallogenic patterns. Not only is it responsible for the juxtaposition of diverse volcanic rock types and associated syngenetic mineralization, but it probably played an active role in the deposition of Seine-type sedimentary rocks, the emplacement of the Algoman intrusions, and the localization of late-stage vein mineralization.

IMPLICATIONS FOR TECTONICS AND METALLOGENY OF THE WABIGOON SUBPROVINCE AND ITS MARGINS

The Wabigoon Subprovince (Figure 38), as described in an earlier section, is a granite-greenstone terrane, the boundaries of which were defined, in broad terms, by Stockwell (1964), based on the contrasting structural style of this subprovince with neighbouring subprovinces, the latter of which are composed largely of metasedimentary and gneissic rocks. Several tectonic models have been proposed to explain the origin of the Wabigoon Subprovince and its relationship to neighbouring subprovinces. The earliest concepts, based on analogies with Phanerozoic mountain belts (Pettijohn 1943), have since evolved into 2 distinct types of models: those that are strictly uniformitarian in approach (Douglas and Price 1972; Langford and Morin 1976; Blackburn 1980), and those that ascribe unique features to Archean crustal development (Wilson,

Table 12. Summary of tectonic models for the origin of the Wabigoon Subprovince and its margins.

Items		Goodwin (1977)	Wilson, Morrice and Ziehlke (1974)	Young (1978)	Douglas and Price (1972)	Langford and Morin (1976)	Blackburn (1980)
1.	Pre-existing basement	sialic	simatic	sialic	sialic	sialic	sialic
2.	Basement to volcanic rocks	simatic	simatic	sialic	simatic	simatic	simatic
3.	Source of volcanic magmas	mantle plume–partial melt	fractional crystallization of molten mantle	mantle plume	subducted oceanic crust	subducted oceanic crust	mantle melts and subducted oceanic crust
4.	Volcanic types preserved	oceanic crust	layered volcanic complex	n/a	island arc	island arc, back arc	oceanic crust, island arc, back arc
5.	Nature of marginal belts such as the Quetico Subprovince	rift basin parallel to volcanic basin	younger aulacogen	"compressive" basin	pericratonic basin	forearc basin	n/a
6.	Sedimentary provenance	predominantly sialic	volcanic	volcanic	sialic	volcanic	volcanic
7.	Source of batholiths	partial melt of sagging mafic crust	fractional residual liquid from mantle	melt from sialic crust	subduction of oceanic crust	subduction of oceanic crust	subduction of oceanic crust
8.	Symmetry about the Wabigoon Subprovince central axis	bilateral	random	bilateral	asymmetrical	asymmetrical	bilateral

Morrice and Ziehlke 1974; Goodwin 1977; Young 1978). There are many differences among these models (Table 12), and one of these is the way in which the marginal subprovinces such as the Quetico Subprovince are viewed in relation to the Wabigoon Subprovince.

Although Stockwell's (1964) criteria for defining the subprovinces were structural, no precise location for the Wabigoon–Quetico boundary was given at that time, and since then lithologic and metamorphic criteria have also been applied to its definition. Mackasey, Blackburn and Trowell (1974) and Blackburn and Mackasey (1977) applied the model of Ayres (1969) to argue that the subprovince margin is a facies transition which marks the change from predominantly volcanic rocks in the north to sedimentary rocks in the south. Similar facies changes are known to occur at a much smaller scale within many volcano-sedimentary sequences in the interior of the Wabigoon Subprovince (Shegelski 1978). Conglomerates at the Wabigoon–Quetico interface are depicted (Mackasey, Blackburn and Trowell 1974, p.7) as lateral facies equivalents to the volcanic rocks of the Wabigoon Subprovince and to "distal" sedimentary rocks in the Quetico Subprovince —the Quetico metasediments. Kehlenbeck (1976) proposed that the subprovince boundary is defined by an amphibolite facies, polymetamorphic zone resulting from emplacement of basement-derived magmas into supracrustal sequences. Pirie and Mackasey (1978) verified that such a metamorphic transition occurs along the entire length of the subprovinces in pelites that were regarded by them to form part of the interior of the Quetico Subprovince.

The results of the present study, which provides new information about the nature of the subprovince margin at its western end, can be used to evaluate some of the concepts outlined above. The abrupt changes in structural trend (*see* Figure 12), which have been imparted by the dextral wrench zone, clearly illustrate the validity of the structural definition proposed by Stockwell (1964). The parallelism in trend of metamorphic isograds with the subprovince axes is further illustrated in the present study. It is significant, however, that the northward increase in metamorphic grade that is documented in the present study, contrasts with the southward increase in metamorphic grade in the Quetico metasediments (Kehlenbeck 1976; Pirie and Mackasey 1978). Thus, the use of metamorphic isograds alone to define the subprovince boundary would lead to considerable confusion in this area. Furthermore, the pressure of metamorphism (3 kilobars) that has been documented in the present study is comparable to that suggested for the centre of the Quetico Subprovince (Pirie and Mackasey 1978). Such pressures correspond to approximately 10 km of postmetamorphic unroofing at both localities, so that the high metamorphic temperatures that are indicated for the Quetico Subprovince need not also reflect a deeper level of erosion (Ayres 1978). The concept that Seine-type conglomerates represent a transitional facies between volcanic rocks and turbidites finds little support in the results of this study. Not only are the conglomerates restricted to different structural and lithostratigraphic domains than the turbidites, they lie with clear angular unconformity on the volcanic rocks. Nonetheless, the presence of conglomerate at their common margin is an important cornerstone of many interpretations of Wabigoon–Quetico tectonics (*see* Goodwin (1977) with subsequent discussion by Walker (1978)), and it is instructive to inquire whether satisfactory alternatives exist.

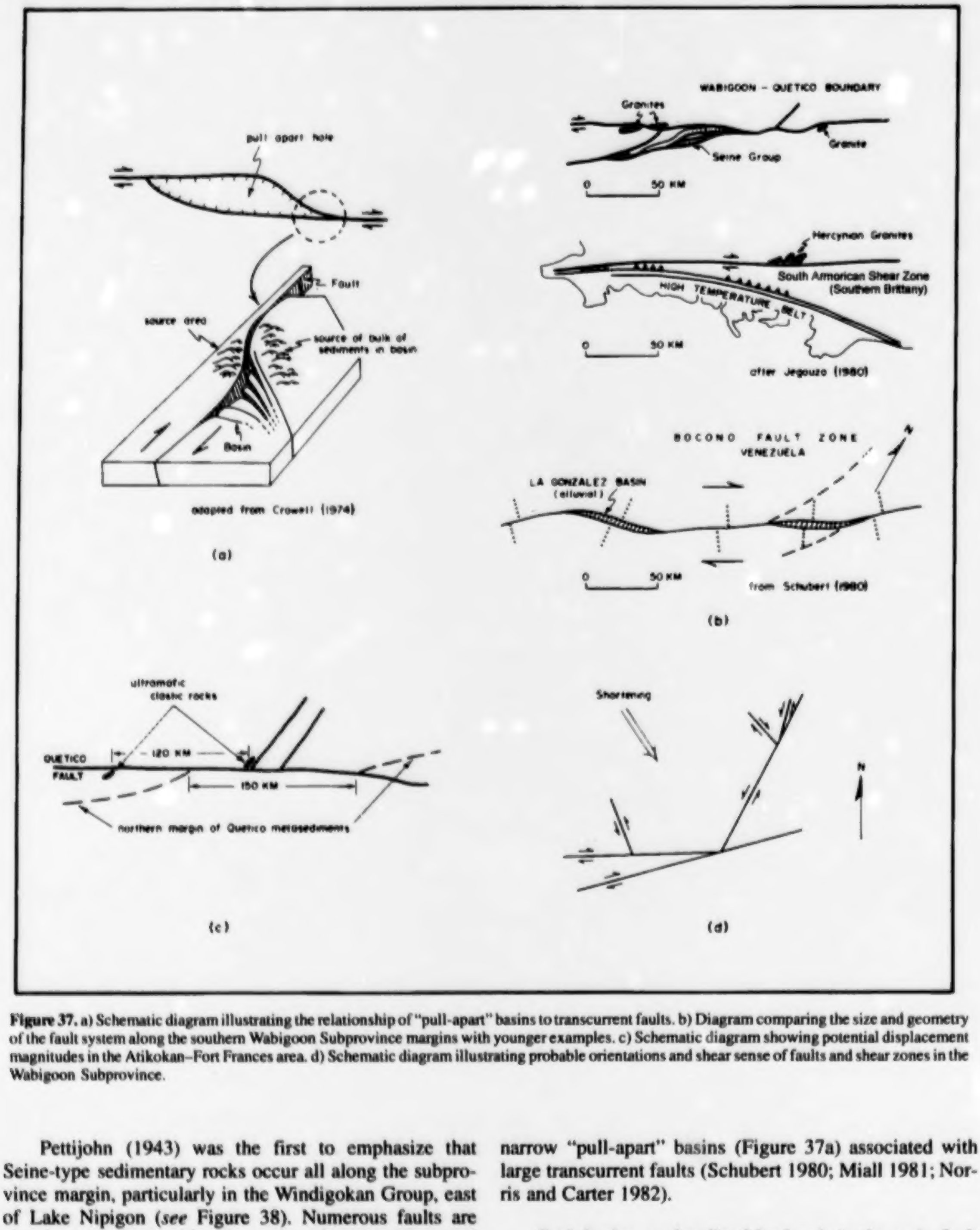
pull apart hole
Fault
source area
source of bulk of sediments in basin
Basin
adapted from Crowell (1974)
(a)
WABIGOON – QUETICO BOUNDARY
Granites
Granite
Seine Group
0
50 KM
Hercynian Granites
South Armorican Shear Zone
(Southern Brittany)
HIGH TEMPERATURE BELT
0
50 KM
after Jegouzo (1980)
BOCONO FAULT ZONE
VENEZUELA
N
LA GONZALEZ BASIN
(alluvial)
0
50 KM
from Schubert (1980)
(b)
ultramafic
clastic rocks
QUETICO
FAULT
120 KM
150 KM
northern margin of Quetico metasediments
(c)
Shortening
N
(d)

Figure 37. a) Schematic diagram illustrating the relationship of "pull-apart" basins to transcurrent faults. b) Diagram comparing the size and geometry of the fault system along the southern Wabigoon Subprovince margins with younger examples. c) Schematic diagram showing potential displacement magnitudes in the Atikokan–Fort Frances area. d) Schematic diagram illustrating probable orientations and shear sense of faults and shear zones in the Wabigoon Subprovince.

Pettijohn (1943) was the first to emphasize that Seine-type sedimentary rocks occur all along the subprovince margin, particularly in the Windigokan Group, east of Lake Nipigon (*see* Figure 38). Numerous faults are closely associated with this group of rocks (Horwood 1948), and a domainal pattern of rock distribution also exists in that area, further suggesting a link between wrench faulting and deposition of the conglomerates. Such a link is well known in Cenozoic environments, where thick alluvial, fluvial and lacustrine sequences are restricted to narrow "pull-apart" basins (Figure 37a) associated with large transcurrent faults (Schubert 1980; Miall 1981; Norris and Carter 1982).

Such basins are localized by bends in the main fault and intersections with splays. Lateral and vertical facies variations are present within such basins (Mann and Burke 1982), but these rocks are not contiguous with lateral facies equivalents external to the wrench fault environment. Furthermore, the size and geometry of the wrench fault system indicated for the southern part of the Wabigoon Subprovince is comparable to that of many younger faults (Figure 37b) that also juxtapose rock units of similar age but different lithology. In many of these examples, and possibly in the present one as well, the juxtaposed terranes have depositional histories that are quite independent, so that present geographic geometry has no paleogeographic significance.

The proposal that wrench faulting is significant at the subprovince boundary is not a new one. Hawley (1930a) first suggested a model of this type for rocks in the Atikokan area, but the emphasis of most discussions of faulting has been placed on late-stage displacements on the Quetico Fault (Mackasey, Blackburn and Trowell 1974; Schwerdtner et al. 1979) rather than the possibility, presented here, that this late faulting is merely a reflection of a larger, longer-lived system. Mackasey, Blackburn and Trowell (1974) considered that the discrete Quetico Fault displaced the subprovince margin—as defined by the transition from Seine-type to Quetico metasediments—approximately 120 km in a dextral sense (*see* Figure 37c). This suggestion is confirmed in the present investigation by the observation that the magnetic ultramafic unit from the study area, while unique among volcanic rocks in the Wabigoon Subprovince (Trowell, Blackburn and Edwards 1980), is chemically and texturally identical to the ashrock unit at Atikokan (*see* Figure 37c). If these 2 units are correlative, this suggests an offset almost identical to that estimated independently by Mackasey, Blackburn and Trowell (1974). A point of caution, however: the results of the present study imply a considerably more complex history of displacement than that for a single, independently acting, transcurrent fault.

In summary, the subprovince boundary should not be viewed as a sharp line, but as a zone of finite but variable width that is marked by sedimentological, metamorphic and structural changes. It is a mobile zone in which lithologic units are interleaved and stratigraphic correlations are quite uncertain. Wrench fault tectonics have played an important, if not dominant, role in shaping its geometry and in controlling the distribution of mineralization along it.

On a broader scale, production of gold, silver, zinc, copper, lead, iron, tungsten and chromium has been recorded from several localities in the Wabigoon Subprovince. Significant occurrences of other elements such as lithium, beryllium, uranium and molybdenum are also known. The mineralization within the Wabigoon Subprovince can be categorized into 6 types (*see* Figure 38):

1. Copper, zinc and lead have been produced from volcanic-hosted massive sulphide deposits. These deposits occur within the mixed tholeiitic to calc-alkalic edifices in which felsic volcanic products are abundant. Altered felsic fragmental footwall rocks and overlying mafic flows characterize the important Sturgeon Lake deposits.
2. Lode gold deposits occur throughout the subprovince. These are dominantly quartz-carbonate vein systems that are associated with structures of regional dimension. Most of the production has come from the Little Long Lac area where veins appear to be localized in fold hinges at contacts between quartz-feldspar porphyry and assorted clastic and chemical metasedimentary rocks (Horwood 1948; Macdonald 1983).
3. Nickel, copper and minor platinum and chromium occur in mafic to ultramafic intrusions. These range from discrete plutons to layered sills of gabbroic to ultramafic composition. Chalcopyrite, pyrrhotite, pentlandite and chromite are the dominant ore minerals.
4. Iron ore deposits of substantial size in the Wabigoon Subprovince are those associated with clastic metasedimentary rocks. The hematite deposits at Steep Rock (*see* Figure 38) occur in dolomite overlying conglomerate and are overlain by ultramafic fragmental rocks (Joliffe 1955). They account for most of the production of this element.
5. Molybdenite, with associated copper and gold, occurs within sills and plutons of granodiorite to trondhjemite composition, some of which may be subvolcanic (Franklin et al. 1977). Sulphide mineralization occurs in veins, stockworks and disseminations, within or at the margins of intrusions.
6. Lithophile mineralization, particularly lithium, cesium, niobium, tantalum and beryllium, occurs in granitoid pegmatites along the northern margin of the subprovince (Breaks 1980, 1981). Spodumene, beryl and tantalite are important minerals, and the composition and degree of albitization of pegmatites show a zonal pattern relative to metamorphic grade. Uranium is also associated with pegmatites in the Vermilion Bay area.

All but the last type are represented in the study area, therefore emphasizing that it is the density and overlap of deposits, not their type, that is unique at Rainy Lake. This study reveals the presence of a base metal-rich felsic volcanic environment in the southern part of the Wabigoon Subprovince, although the best prospects and all producing deposits to date representing this class of mineralization are found in the north of the subprovince. The present study also suggests that there may be a fundamental relationship between large faults and the deposition of gold. Figure 38 shows the distribution of gold deposits of the Wabigoon Subprovince relative to known faults, and it is evident that the two are commonly spatially related. The bulk of gold production from the subprovince has come from the Geraldton area where the loci of mineralization are the Tombill–Bankfield and Little Long Lac faults (Horwood 1948). Also, a fault network, which is internal to the subprovince and constitutes the Mimiss–Wabigoon–Manitou Lake structure, also shows a very prominent association with vein-type gold deposits. The fault and shear zone network of the Wabigoon Subprovince consists of 2 distinct elements: easterly striking dextral faults, and a sinistral set striking 030°. Subsidiary structures associated with these elements should have ranges of orientations and senses of

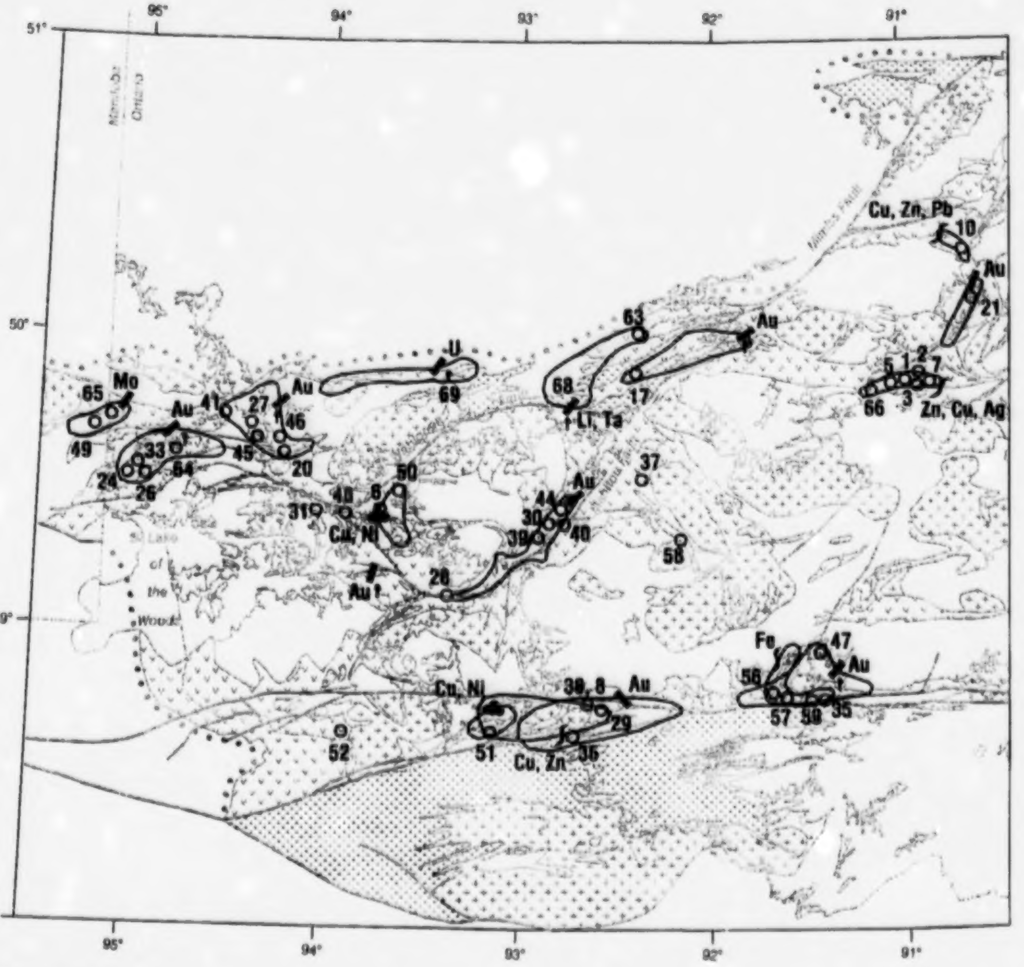
95°
94°
93°
92°
91°
51°
50°
49°
48°
Manitoba
Ontario
Cu, Zn, Pb
10
Au
21
63
Au
U
Mo
65
49
Au
41
27
Au
46
45
20
33
64
24
26
69
68
Li, Ta
17
5 1 2 7
66 3 Zn, Cu, Ag
37
50
48
6
31
Cu, Ni
44
Au
30
39
40
58
Au
28
Lake of the Woods
Fe
47
Au
56
57 59 35
Cu, Ni
38, 8
Au
29
51
Cu, Zn
36
52

Mineral Deposits

Cu, Zn ∫ **Zn-Cu-Pb deposits of mafic-felsic volcanic association**

1. Mattabi
2. Lyon Creek
3. Sturgeon Lake
4. NWT
5. F Zone
6. Maybrun
7. Lynx
8. Port Arthur Copper
9. Rickaby Mines
10. Evans Lake

Au **Lode gold (Au) deposits**

11. MacLeod-Cockshutt, Hardrock
12. Leitch
13. Little Long Lac
14. Consolidated Mosher
15. Northern Empire
16. Magnet Consolidated
17. Goldlund
18. Tombill-Bankfield
19. Sturgeon River
20. Wendigo
21. St. Anthony
22. Sand River
23. Tashota-Nipigon
24. Duport
25. Consolidated Louanna
26. Mikado
27. Sultana
28. Straw Lake Beach
29. Golden Star
30. Laurentian
31. Regina
32. Jellicoe
33. Cornucopia
34. Theresa
35. Atiko
36. Foley
37. Sakoose
38. Olive
39. Twentieth Century
40. Big Master
41. Kenricia
42. Orphan
43. Elmos (Talmora)
44. Elora
45. Ophir
46. Gold Hill
47. Sawbill
48. Dogpaw Lake
49. Sunbeam Kirkland

Cu, Ni **Cu-Ni (Pt, Cr) deposits of mafic-ultramafic plutonic association**

50. Kenbridge
51. North Rock
52. Dobie Township
53. Chrome Lake
54. Puddy Lake
55. Lac des Iles

Fe ∫ **Fe deposits**

56. Steep Rock
57. Caland
58. Jalore
59. Atikokan Iron
60. Skibi Lake
61. Barton Bay
62. Can Fer

Mo **Mo (Cu, Au) deposits of felsic-plutonic association**

63. Pidgeon (Lateral Lake)
64. Canoe Lake
65. Evenlode
66. Beidelman Bay

Li, Be **Li, Cs, Ta, U, Sn, Be deposits of pegmatitic association**

67. Zigzag Lake
68. Dryden area
69. Vermilion Bay area

Figure 38. Wabigoon Subprovince and its margins.

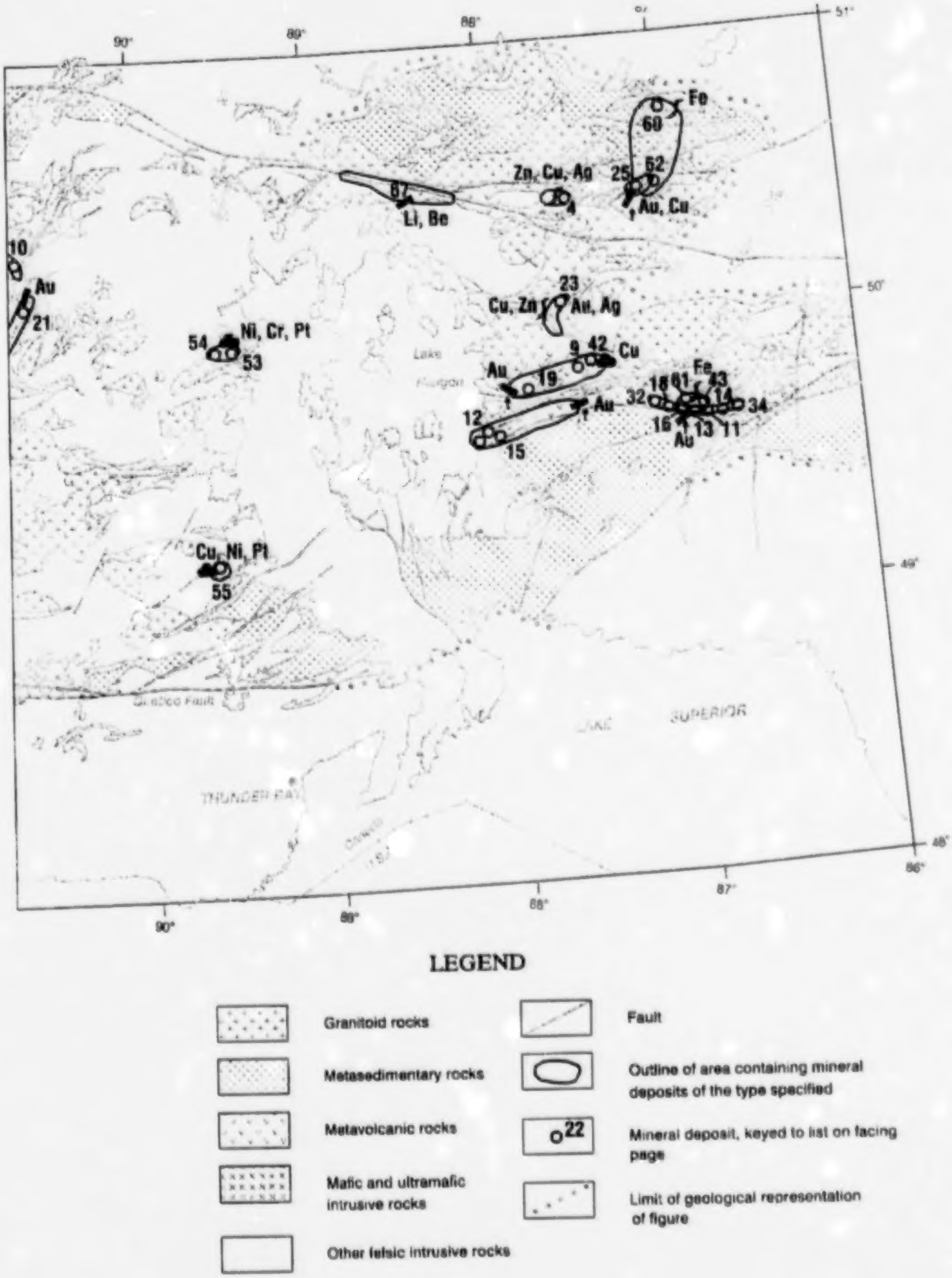
90°
89°
88°
87°
51°
50°
49°
48°
86°
Fe
60
Zn, Cu, Ag
25
52
Au, Cu
67
Li, Be
4
10
Au
21
23
Cu, Zn
Au, Ag
54
Ni, Cr, Pt
53
Lake Nipigon
9
42
Cu
Au
19
Au
18
61
Fe
43
32
14
34
12
16
13
11
Au
15
Cu, Ni, Pt
55
Quetico Fault
LAKE SUPERIOR
THUNDER BAY
Canada
U.S.A.
LEGEND
Granitoid rocks
Metasedimentary rocks
Metavolcanic rocks
Mafic and ultramafic intrusive rocks
Other felsic intrusive rocks
Fault
Outline of area containing mineral deposits of the type specified
o22 Mineral deposit, keyed to list on facing page
Limit of geological representation of figure

displacement (Figure 37d) compatible with those shown for the Rainy Lake area (*see* Figure 14).

CONCLUSIONS

This study illustrates the nature of an Archean subprovince boundary. Aspects of stratigraphy, structure, metamorphism and mineralization have been described and interpreted by a model of wrench fault tectonics. While the scale of the study is modest, it does illustrate several general problems in Archean metallogeny and tectonics.

The evolution of metallogenic history at Rainy Lake involves superposition of mineralization related to structural, metamorphic and plutonic processes, on mineralization that was coeval with volcanism and sedimentation. This is in accord with the results of other Archean studies (Hutchinson, Ridler and Suffel 1971; Boyle 1976; Groves and Gee 1980). At Rainy Lake, however, no genetic link can be established between the 2 types in the manner proposed for other areas, where late vein mineralization is considered to be a product of remobilization of early stratabound mineralization (Hutchinson, Ridler and Suffel 1971). Furthermore, spatial variations in facies of iron formation, which are interpreted to be lateral equivalents in the Abitibi and Michipicoten areas (Hutchinson, Ridler and Suffel 1971; Goodwin 1973), are also present at Rainy Lake. In the study area, oxide iron formation is associated with base metal sulphides in mafic volcanic rocks, with chert and siltstones overlying felsic volcanic rocks, and with arenaceous sedimentary rocks that are possibly part of the Seine metasediments. Each of these types is restricted to particular structural and stratigraphic domains which cannot be linked in a simple depositional way. At Rainy Lake, the changes in the types of iron formation probably reflect temporal evolution rather than lateral facies equivalence.

The demonstration of a mobile history for the subprovince margin has several tectonic implications. Firstly, lateral facies equivalence between dissimilar but adjacent stratigraphic units is commonly postulated to explain their mutual relationship. Such concepts as basin margins (Goodwin 1977) and precipitous Archean continental margins (Eriksson 1982) are dependent on this type of interpretation. Where, as at Rainy Lake, it can be demonstrated that these "facies boundaries" also coincide with recognizable tectonic structures such as fault zones, the applicability of facies concepts must be questioned. An equally viable speculation is that 2 stratigraphic sequences with independent depositional histories have been juxtaposed.

Secondly, the local structural inversion of stratigraphic panels at Rainy Lake is a significant consequence of tectonic mobility. By analogy with similar observations in other areas (Stowe 1974; Coward, James and Wright 1976; DeWit 1982), the inverted panels have previously been interpreted to be refolded limbs of a fold nappe (Poulsen 1980a). One of the criteria used in support of fold nappes is downward structural facing of beds with respect to a regionally developed cleavage (Coward, James and Wright 1976; Poulsen, Borradaile and Kehlenbeck 1980). The "transected" nature of cleavage in the Rainy Lake area, as shown in this study, prevents its unequivocal use to demonstrate fold nappes (Ramsay 1965; Borradaile 1978; Stringer and Treagus 1980). Nonetheless, some panels at Rainy Lake can be shown to be inverted without relying on this argument, and their presence may reflect either fold nappes or inhomogeneous wrench zone deformation.

Finally, complex stratigraphic relationships are a result of the mobile tectonic history along the boundary zone. Controversial stratigraphic interpretations have arisen, not so much by "incorrect" observations but by changes, through time, in the criteria that are considered appropriate for the definition of a stratigraphic sequence. The assessment of this situation by Lawson (1913, p.1) is relevant yet today:

> In a field so complicated and so extensive as that presented by the Archaean terranes of Canada it is not surprising that as investigation proceeds there should be conflict in opinion. The early records of the earth's history are obscure and difficult to decipher. They are susceptible in their imperfection of more than one interpretation. The acquisition of facts is so slow and laborious that no one geologist can hope to become familiar with the details of more than a very small portion of the entire field. The work to be done is appalling in its magnitude; yet none shrink from the task.

The "task" in the Rainy Lake area in the future will involve detailed remapping at 1:10 000 scale so that relationships at every outcrop may contribute to the overall interpretation. Precise geochronological data are essential to understanding both the depositional and deformational history of each tectonostratigraphic domain. Detailed gravity and seismic surveys may provide much needed three-dimensional data in an area of unquestionable structural complexity.

Appendix 1. Sources of Information and Nomenclature

SOURCES OF INFORMATION

Map 2525 (back pocket) is a compilation of all existing map information available for the area bounded by the Quetico and Rainy Lake–Seine River faults with reconnaissance mapping by the author.

Lithologic information has been taken principally from 3 sources (Ojakangas 1972; Harris 1974; Wood et al. 1980a, 1980b), with some reference to earlier maps (Lawson 1913; Tanton 1936). Figure A1.1 shows the area of coverage of previous mapping. Revisions at the local scale have been based, in part, on private company maps which are on file at the Resident Geologist's Office, Ontario Ministry of Northern Development and Mines, Kenora. Specifically, property maps for the Pocket Pond area (E. Grootenboer, North Rock Mines), eastern Nickel Lake area (J.C. Davies, consultant's report, Border City Cement Company), Belacoma prospect area (E. Debicki, Canico Limited), North Rock Mine area (C.J. Hodgson, Noranda Mines Limited), Gagne Lake area (J.C. Davies, consultant's report, Border City Cement Company), and Hanna prospect (N. Hogg, Hanna Mining Company) were used extensively in the compilation. Detailed mapping by Poulsen (1984, 2000) in each of these areas verified existing maps and brought them to a common format and nomenclature. In addition, Poulsen (1984, 2000) carried out new detailed mapping in the Nickel Lake, Bear Passage, Ottertail Lake, Wind Bay, Swell Bay, Port Arthur Copper Co. Mine, Golden Star Mine and Foley Mine areas, as well as local mapping around numerous prospects.

NOMENCLATURE

Throughout the report, the igneous rock nomenclature recommended by Streckeisen (1976) has been employed, and the terminology for layered intrusions is that proposed by Irvine (1982). Fault rock nomenclature is that of Sibson (1977), and the terminology for shear zones follows Ramsay (1980).

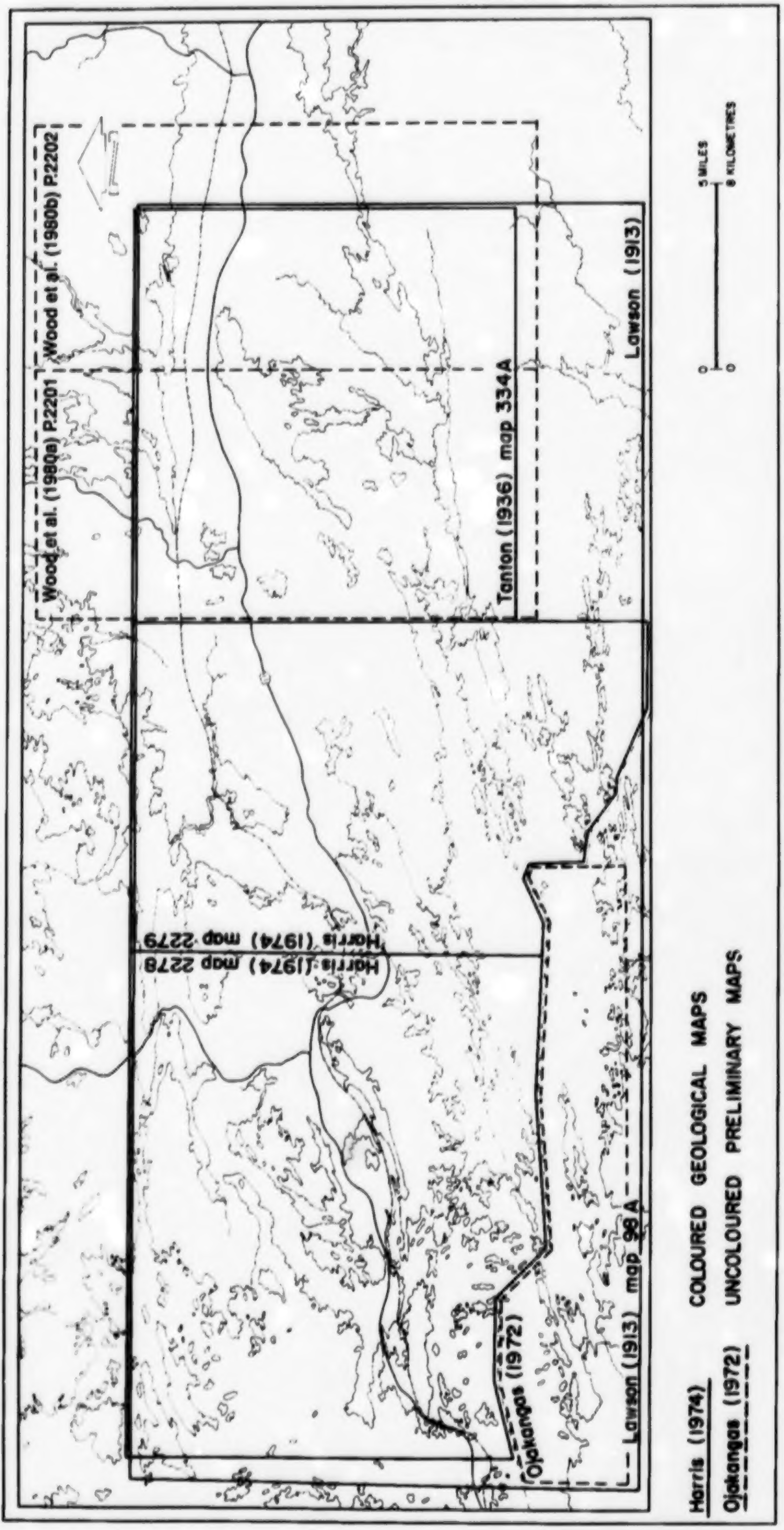
Wood et al. (1980a) P.2201
Wood et al. (1980b) P.2202
Tanton (1936) map 334A
Lawson (1913)
Harris (1974) map 2279
Harris (1974) map 2278
Ojakangas (1972)
Lawson (1913) map 98A
Harris (1974) COLOURED GEOLOGICAL MAPS
Ojakangas (1972) UNCOLOURED PRELIMINARY MAPS
0 5 MILES
0 8 KILOMETRES

Figure A1.1. Summary map of the study area showing the sources of information used for compilation of Map 2525 (back pocket).

Appendix 2. Petrographic Data for Metamorphic Rocks

Table A2.1 indicates the estimated modal mineralogies of the metamorphic rocks that were used to establish the distribution of metamorphic facies shown in Figure 22.

Table A2.1. Petrographic data, metamorphic rocks, Rainy Lake.

		Pelites[a]											
Sample	**Locality**	**mus**	**bio**	**Mg–chl**	**Fe–chl**	**cltd**	**hb**	**ep**	**gt**	**and**	**sill**	**staur**	**mrc**
76–Po–01	Rocky In.		P										
76–Po–02	"		P						p				
76–Po–04	Bear Pass.	P	P						P			(?)	
76–Po–07	Hwy 11		P					P					
76–Po–13	Ottertail L.	tr	P										
76–Po–15	Wind Bay	P			P								
76–Po–16	Morton Is.	p	P										
76–Po–17	Bear Pass.	r	P	p	r				P			(P)	
78–Po–01	"	p	P		r				p	(?)		(?)	
78–Po–02	Hwy 11	tr	P	p	r				(P)			(P)	
78–Po–06	Manitou Rd.	P	P	p	r								
78–Po–07	Pocket Pond	r	P						(P)	(?)		(?)	
78–Po–11	Hwy 11	tr	P	r			P						
78–Po–12	"	P	P	r					(p)				
78–Po–13	"	r	P		r				(p)			(P)	
78–Po–21	Bear Pass.	p	P						(p)				
78–Po–25	"	p	P						tr				
78–Po–30	Nickel L.		P				P						
78–Po–31	"	P	P	r					(?)	(?)			
78–Po–33	"	r	P		r				(P)				
78–Po–34	Rice Bay		P				P	P					P
78–Po–36	"		P				P						
78–Po–37	"		P		r		P						P
78–Po–40	"	P	p										
78–Po–50	Redgut Bay		P	p					P			P	
78–Po–54	Rice Bay	p	P	p	r				p		(?)		
78–Po–62	Rice Bay	p	P					p	P				P
78–Po–65	"	P	P		r				(P)			P	
78–Po–68	"	P	P	P	r								
78–Po–71	"	p	P		r				P		(?)		
79–Po–01	Pocket Pond	p	P		r				(P)				
79–Po–02	"	P	P		r				(P)		(?)		
79–Po–04	Manitou Rd.	r	P	p	r				(P)	(?)			
79–Po–05	"	r	P		r				P			(P)	
79–Po–07	Bear Pass.	P	P		r							(P)	
79–Po–08	"	tr	P						P			(P)	
79–Po–09	"	tr	P	p					P	p		P	
79–Po–10	"	p	P						P			(p)	
79–Po–11	"	p	P	P					P			(P)	
79–Po–12	"	tr	P	p					P			(P)	
79–Po–25	Sandpoint Is.	P	P		p								
79–Po–28	"	P	P		P					(?)			
79–Po–32	"	p	P		r					(?)			
79–Po–33	"	p	P		r				(p)			(P)	
79–Po–34	"	p	P		r				(p)			(P)	
79–Po–35	"	r	P					P					
79–Po–36	"		P	tr				p					
79–Po–37	Redgut Bay	p	P	p					p		tr	P	
79–Po–38	"	p	P	p					P		p	P	
79–Po–39	Bear Pass.	p	P		r				(p)				
79–Po–40	Bear Pass.	p			r				(p)	(?)			
79–Po–41	Knuckle Is.	p	P		r				(p)	(?)		(?)	
79–Po–42	"	r	P						(tr)	(?)		(?)	
79–Po–43	"	p	P		r				(p)	(?)		(?)	
79–Po–44	Nickel L.	P	p		r				p	(?)			
79–Po–45	"	p	P		r				p	(?)			
80–Po–14	Ottertail L.		P			p							
80–Po–20	Shoal L.	P			p	P							
80–Po–24	Ottertail L.	P	P										
80–Po–30	Swell Bay	p	P										
80–Po–52	Wind Bay	p			P								
80–Po–67	Wreck Pt.	p	P										
80–Po–68	Ottertail L.	p	P		r					(?)			
80–Po–72	Mine Centre	P	P		P								
80–Po–76	Rocky Inlet	P	P		r			p					
80–Po–77	"	P	P							(?)			

Table A2.1. Continued

						Pelites[a]							
Sample	**Locality**	**mus**	**bio**	**Mg–chl**	**Fe–chl**	**cltd**	**hb**	**ep**	**gt**	**and**	**sill**	**staur**	**mrc**
80–Po–78	Rocky Inlet	P	P	p	r				(p)	(?)			
80–Po–79	"	P	P	r	r					(?)			
80–Po–80	Redgut Bay	P	P		r								
80–Po–81	"	P	P		r								
80–Po–83	"	P					P						
80–Po–85	"	tr	P	p					p	P	p	P	
L1830	"	tr	P	tr					p	p	p	P	
L1828	"		P	tr					P			P	
L1829	Redgut Bay		P	p					P			P	
81–Po–52	Shoal L.	P		p			P						
81–Po–188	Traverse In.	P	P							(?)		(?)	
RL–FT–01	Rice Bay	p	P										
RL–FT–02	"	P	p										
RL–FT–04	"	P	P	r	r				P		(?)		
RL–FT–16	"	P	P										
RL–FT–08	"	P			P								

[a] *assemblages (other than those containing chloritoid) also include quartz and plagioclase as well as common apatite, tourmaline, and iron oxides.*

					Metabasites[b]					
Sample **diop**	**Locality**	**chl**	**bio**	**hb**	**plg**	**act**	**ep**	**spn**	**ap**	**calc**	
78–Po–03	Manitou Rd.			P	P		P	P			
78–Po–09	"		tr	P	P		P				
78–Po–19	Hwy 11			P	P						
78–Po–20	"		tr	P	P		tr				
78–Po–21	Bear Pass.	p	tr			P					
78–Po–32	Nickel L.			P	P						
78–Po–39	Rice Bay			P	P		p				
78–Po–49	Redgut Bay	r			p	P					
79–Po–06	Manitou Rd.		tr	P	tr				P		
79–Po–27	Sandpoint Is.	p	tr	P	P		P				
79–Po–30	"			P	P						
79–Po–31	"	p		P	p						
80–Po–01	Pocket Pond	p			P	p	P				
80–Po–08	Nickel L.			P	p		p	tr		tr	
80–Po–70	Mine Centre	P								p	
80–Po–71	"	P						tr		P	
80–Po–75	"	p			p			p		P	
RL–FT–05	Pocket Pond			P	P						
RL–FT–06	"			P	P	tr					p
RL–FT–07	"			P	P						
RL–FT–10	Mine Centre	P					P			P	
RL–GS–04	"	P			p		P				

[b] *all assemblages include quartz*

				Ultramafics			
Sample	**Locality**	**Mg–chl**	**hb**	**plag**	**trem**	**talc**	**oxide**
78–Po–04	Manitou Rd.	P		tr	P	tr	P
78–Po–08	Pocket Pond	P			P		p
79–Po–03	Manitou Rd.		P		P		P
78–Po–73	Hwy 11	p			P		P
81–Po–19	"	P			P		P

				Calc-silicate Rocks			
Sample	**Locality**	**quartz**	**calcite**	**epidote**	**garnet**	**diopside**	**amphibole**
DOH–98–137a	Pocket Pond	p	P	P	P		
DOH–98–137b	"		P	tr	p	P	r
81–Po–131	"	p		P	P	P	
81–Po–65	"		p	P	p	p	p

P – major component (>10%)
p – minor component (1–10%)
tr – trace (<1%)

r – retrograde product
() – pseudomorph only
(?) – Unknown pseudomorph, may be mineral indicated

mus – muscovite
bio – biotite
chl – chlorite
Mg–chl – magnesium chlorite
Fe–chl – iron chlorite

cltd – chloritoid
hb – hornblende
ep – epidote
gt – garnet
and – andalusite

sill – sillimanite
staur – staurolite
mrc – microcline
plg – plagioclase
act – actinolite

ap – apatite
trem – tremolite
spn – sphene
calc – calcite
diop – diopside

Appendix 3. Electron Microprobe Analyses of Silicate and Oxide Minerals

The analysis of silicate and oxide mineral grains in carbon-coated polished thin sections was performed using an ARL electron microprobe located at Queen's University, Kingston. Tables A3.1, A3.2, A3.3, A3.4 and A3.5 contain analytical data for minerals from a variety of rock types and geological settings in the study area. Structural formulae were computed using the MINERAL programs of D.M. Carmichael (Professor, Department of Geological Sciences, Queen's University, Kingston). These attempt to balance both mass and charge to arrive at a stoichiometric mineral formula.

Table A3.1. Average mineral analyses for pelites, Redgut Bay.

Analyses (wt %) : Sample 80-Po-85	**staurolite**	**muscovite**	**chlorite**	**andalusite**	**ilmenite**	**garnet core**	**garnet rim**	**biotite**
SiO_2	26.67	49.46	24.82	37.04	0.00	37.44	37.44	35.20
Al_2O_3	56.31	37.11	23.86	65.26	0.04	22.30	20.24	20.37
TiO_2	0.79	0.49	0.13	0.17	51.87	0.21	0.17	1.81
Fe_2O_3	0.00	1.13	0.00	0.39	3.33	0.00	0.00	0.00
FeO	14.57	0.00	24.59	0.00	43.85	34.02	34.88	19.86
MgO	1.54	0.46	14.81	0.04	0.26	2.97	2.59	10.21
MnO	0.22	0.06	0.20	0.00	2.05	4.46	3.93	0.12
CaO	0.02	0.02	0.05	0.05	0.03	1.74	1.50	0.06
Na_2O	0.01	0.25	0.00	0.00	0.00	0.03	0.01	0.19
K_2O	0.06	5.35	0.10	0.10	0.07	0.03	0.07	8.35
Cr_2O_3	0.00	0.00	0.00	0.00	0.00	0.00	0.00	0.00
H_2O	2.20	4.66	11.55	0.00	0.00	0.00	0.00	3.99
Total	102.39	98.99	100.11	103.05	101.50	103.20	102.83	100.16
N=	3	3	2	1	1	5	5	6
Structural Formulae:								
Si	3.634	3.182	2.575	0.973	0.000	2.869	2.895	2.641
Al^{4+}	0.366	0.818	1.425	0.073	0.000	0.000	0.000	1.359
Al^{6+}	8.676	1.997	1.493	1.994	0.001	2.014	1.027	0.441
Ti	0.081	0.024	0.010	0.003	0.969	0.012	0.010	0.102
Fe^{3+}	0.000	0.055	0.000	0.008	0.062	0.000	0.000	0.000
Fe^{2+}	1.660	0.000	2.134	0.000	0.911	2.180	2.256	1.246
Mg	0.313	0.044	2.290	0.002	0.010	0.339	0.299	1.142
Mn	0.025	0.003	0.018	0.000	0.043	0.289	0.257	0.008
Ca	0.003	0.001	0.006	0.001	0.001	0.143	0.124	0.005
Na	0.003	0.031	0.000	0.000	0.000	0.004	0.001	0.028
K	0.010	0.439	0.013	0.003	0.002	0.003	0.007	0.799
Cr	0.000	0.000	0.000	0.000	0.000	0.000	0.000	0.000
O	22.000	10.000	10.000	5.000	3.000	12.000	12.000	10.000
OH,F	2.000	2.000	8.000	0.000	0.000	0.000	0.000	2.000

Table A3.1. Continued.

Analyses (wt %) : Sample 79-Po-37	**plagioclase**	**staurolite**	**chlorite**	**biotite**	**garnet rim**	**garnet core**
SiO_2	60.52	28.05	24.69	35.00	37.30	37.62
Al_2O_3	25.12	57.21	23.98	20.2	22.15	22.29
TiO_2	0.22	0.59	0.21	1.70	0.15	0.14
Fe_2O_3	0.00	0.00	0.00	0.00	0.00	0.00
FeO	0.24	14.84	25.65	19.63	35.12	34.72
MgO	0.00	1.59	14.80	10.39	2.60	2.92
MnO	0.00	0.04	0.18	0.15	4.30	4.44
CaO	5.28	0.02	0.00	0.04	0.97	1.11
Na_2O	8.05	0.02	0.0	0.15	0.03	0.06
K_2O	0.20	0.04	0.05	8.01	0.01	0.07
Cr_2O_3	0.00	0.00	0.00	0.00	0.00	0.00
H_2O	0.00	2.25	11.63	3.97	0.00	0.00
Total	99.63	104.65	101.22	99.26	102.63	103.37
N=	1	1	2	4	4	5
Structural Formulae:						
Si	2.696	3.729	2.545	2.644	2.893	2.892
Al^{4+}	1.304	0.271	1.455	1.356	0.000	0.000
Al^{6+}	0.015	8.693	1.458	0.444	2.025	2.019
Ti	0.007	0.059	0.016	0.097	0.009	0.008
Fe^{3+}	0.000	0.000	0.000	0.000	0.000	0.000
Fe^{2+}	0.009	1.650	2.211	1.240	2.278	2.232
Mg	0.000	0.315	2.274	1.170	0.301	0.335
Mn	0.000	0.005	0.016	0.010	0.283	0.289
Ca	0.252	0.003	0.000	0.003	0.081	0.091
Na	0.695	0.005	0.006	0.022	0.005	0.009
K	0.011	0.007	0.007	0.772	0.001	0.007
Cr	0.000	0.000	0.000	0.000	0.000	0.000
O	8.000	22.000	10.000	10.000	12.000	12.000
OH,F	0.000	2.000	8.000	2.000	0.000	0.000

Table A3.2. Electron microprobe analysis of coexisting garnet-biotite pairs in pelites, Redgut Bay.

wt %	**garnet core**	**garnet rim**	**biotite**	**wt %**	**garnet core**	**garnet rim**	**biotite**
80-Po-85							
SiO_2	37.66	37.50	35.61	SiO_2	37.06	37.33	35.83
Al_2O_3	22.41	22.38	20.91	Al_2O_3	22.17	22.36	20.16
FeO	34.19	35.13	19.53	FeO	33.79	34.97	20.54
MgO	2.92	2.70	10.16	MgO	2.93	2.63	9.88
MnO	4.53	3.81	0.11	MnO	4.91	4.05	-
CaO	1.72	1.61	-	CaO	1.89	1.59	-
K_2O	-	-	8.22	K_2O	-	-	8.88
SiO_2	36.92	36.79	36.31	SiO_2	37.30	37.67	35.34
Al_2O_3	22.27	21.85	20.27	Al_2O_3	22.21	22.19	20.12
FeO	33.62	34.35	19.37	FeO	33.40	34.44	19.25
MgO	3.01	2.58	10.20	MgO	2.93	2.42	9.94
MnO	4.10	3.91	0.12	MnO	4.90	4.11	0.09
CaO	1.82	1.51	-	CaO	1.76	1.43	-
K_2O	-	-	8.00	K_2O	-	-	8.59
79-Po-37							
SiO_2	37.19	37.48	35.99	SiO_2	37.75	36.74	35.86
Al_2O_3	22.09	21.91	20.12	Al_2O_3	22.49	22.23	20.16
FeO	34.59	35.06	19.30	FeO	34.48	35.08	19.36
MgO	3.00	2.85	10.40	MgO	2.97	2.30	9.90
MnO	4.55	3.84	0.26	MnO	4.53	4.64	0.12
CaO	0.99	1.01	-	CaO	1.24	0.95	-
K_2O	-	-	8.22	K_2O	-	-	9.17
SiO_2	37.93	37.63	33.61				
Al_2O_3	22.28	22.09	20.41				
FeO	35.08	35.28	20.23				
MgO	2.80	2.46	10.58				
MnO	4.31	4.37	0.15				
CaO	1.10	0.95	-				
K_2O	-	-	7.44				

Table A3.3. Mineral analyses and structural formulae, calc-silicate rocks, Pocket Pond.

	Calcite-rich assemblage (includes quartz)					**Calcite-poor assemblage (includes quartz and calcite)**		
Analysis (wt %)	**garnet**	**epidote**	**calcite**	**clinopyroxene**	**actinolite**	**garnet**	**epidote**	**diopside**
SiO_2	35.19	36.67	-	50.02	49.76	36.45	37.18	51.56
Al_2O_3	3.67	21.98	-	1.18	4.45	8.13	22.47	0.25
TiO_2	0.36	0.22	-	0.08	0.47	0.35	0.33	0.22
Fe_2O_3[a]	25.54	17.28	-	-	1.93	19.18	15.01	-
FeO	2.86	0.26	0.45	14.68	23.47	2.82	1.71	13.12
MgO	0.06	0.05	0.23	8.63	8.17	0.11	0.03	10.19
MnO	1.22	0.08	0.64	1.90	0.87	0.55	0.10	0.50
CaO	29.70	21.85	54.16	22.40	11.30	31.48	21.64	22.10
Na_2O	-	-	-	0.47	0.57	-	-	0.48
K_2O	0.05	0.07	-	-	0.15	-	0.07	0.07
H_2O	-	1.86	-	-	2.03	-	1.87	-
CO_2	-	-	43.41	-	-	-	-	-
Total	98.65	100.32	98.89	99.36	103.16	99.07	100.42	98.49
N=	2	1	1	2	1	2	2	2
Structural Formulae								
Si^{4+}	2.982	2.96	-	1.862	7.357	2.992	2.973	2.006
Al^{6+}	0.018	0.04	-	0.027	0.643	0.008	0.027	-
Al^{3+}	0.349	2.051	-	-	0.132	0.779	1.091	0.011
Fe^{2+}	1.629	1.050	-	-	0.214	1.185	0.904	-
Fe^{3+}	0.202	0.017	0.006	0.481	2.902	0.193	0.114	0.427
Mg	0.008	0.006	0.006	0.504	1.800	0.013	0.004	0.591
Mn	0.088	0.005	0.009	0.063	0.109	0.038	0.007	0.017
Ca	2.697	1.890	0.979	0.941	1.790	1.769	1.854	0.922
O	12.000	12.000	1.000	6.000	22.000	12.000	12.000	6.000

[a] *Fe_2O_3 estimated from probe data by mass and charge balancing in structural formula.*

Table A3.4. Mineral analyses from ultramafic schist, Grassy Portage area.

Sample 79-Po-03 :	**hornblende, tremolite, chlorite, talc, magnetite**		
wt %	**hornblende**	**tremolite**	**chlorite**
SiO_2	41.49	52.73	26.15
Al_2O_3	13.47	1.34	19.90
TiO_2	0.39	0.20	0.08
Fe_2O_3	-	-	-
FeO	18.33	10.23	23.78
MgO	8.38	11.48	16.08
MnO	0.20	0.45	0.34
CaO	12.19	24.03	0.08
Na_2O	2.10	0.19	-
K_2O	0.67	0.08	0.06
N=	2	3	2

Table A3.5. Mineral analyses from hornblende gabbro, Grassy Portage intrusion.

	gabbro		**grey ore - North Rock Mine**		
wt %	**uralite**	**plagioclase**	**plagioclase**	**ilmenite**	**biotite**
SiO_2	43.14	52.80	58.45	-	34.83
Al_2O_3	11.81	28.87	27.64	-	17.73
TiO_2	0.30	-	-	54.40	2.27
Fe_2O_3	-	-	-	-	-
FeO	17.41	0.19	-	46.58	24.47
MgO	8.31	-	-	-	6.79
MnO	0.25	-	-	2.39	-
CaO	10.57	10.97	8.86	-	-
Na_2O	1.23	4.71	6.36	-	-
K_2O	0.53	-	-	-	9.49

Appendix 4. Sulphide Mineral Analyses

Precise analyses of sphalerite, pyrrhotite and arsenopyrite are required for sulphide geothermometry (Kretschmar and Scott 1976) and geobarometry (Hutchison and Scott 1980). For high-temperature (300°C) applications, hexagonal pyrrhotite is required. The presence of hexagonal pyrrhotite can be established by etching (Scott, Both and Kissin 1977; Craig and Vaughan 1981), magnetic colloid application (Hutchison and Scott 1980), or by X-ray diffraction (Arnold 1966). Minor element substitution in sphalerite (Mn, Cu, Cd), pyrrhotite (Co, Ni, Cu) and arsenopyrite (Co, Ni) may affect the interpretation of the results, and these elements were determined routinely as well. The choice of standards is critical, particularly for the determination of arsenic (S.D. Scott, Professor, Department of Geology, University of Toronto, personal communication, 1982). Therefore, ASP200, a well-analyzed standard that was used in experimental calibration of the geothermometer (Kretschmar and Scott 1976), was employed in this study.

Table A4.1 lists analyses of sphalerite coexisting with pyrrhotite and pyrite at Nickel Lake, and Table A4.2 gives arsenopyrite results.

Table A4.1. Analyses of Nickel Lake sphalerites, Sample RL–NL–06.

			Grain 1					Grain 2		
	sp–py	sp–py	sp–py–po	sp–po	sp–po	sp–po	sp–po	sp–py–po	sp–py	sp–py
Fe	9.36	9.36	9.69	9.38	9.52	9.41	9.57	9.56	10.43	9.77
Zn	51.00	50.04	51.55	49.42	51.61	52.85	52.70	53.16	50.40	51.43
Mn	7.19	7.37	7.41	7.02	7.02	6.62	6.91	6.81	7.02	7.43
S	33.42	33.36	33.71	33.50	33.20	33.86	33.73	33.89	33.74	33.79
Total	100.97	100.62	102.36	99.02	101.35	102.66	102.91	103.42	101.59	102.42
Mole%FeS	16.80	15.86	16.50	16.22	16.46	15.99	16.29	16.20	17.75	16.60

			Grain 3					Grain 4		
	sp–po	sp–po	sp–py–po	sp–py	sp–py	sp–py	sp–py	sp–py–po	sp–po	sp–po
Fe	11.17	11.92	9.30	10.37	10.45	11.07	10.84	10.74	10.28	9.83
Zn	50.67	48.59	53.49	51.73	49.84	50.71	50.17	51.37	50.28	51.96
Mn	8.11	8.60	6.40	7.79	7.93	8.11	8.28	7.49	7.85	8.16
S	33.89	33.85	33.57	34.01	33.60	33.54	33.65	33.58	33.78	33.47
Total	103.84	102.96	102.76	103.89	101.82	103.43	102.94	103.28	102.19	103.42
Mole%FeS	18.92	20.22	15.90	17.51	17.86	18.95	18.50	18.36	17.63	16.86

			Grain 5		
	sp–py	sp–py	sp–py–po	sp–po	sp–po
Fe	10.04	9.53	9.83	10.38	9.69
Zn	51.93	53.36	52.26	50.71	51.85
Mn	7.80	6.51	6.96	7.78	6.83
S	33.44	33.67	33.84	33.99	33.56
Total	103.21	103.06	102.89	102.89	101.93
Mole%FeS	17.24	16.25	16.68	17.53	16.58

Table A4.2. Arsenopyrite analyses.

RL–NL–4: massive sulphide, Nickel Lake

wt %	Range	Mean (N=10)
Fe	31.42–33.74	32.88
Co	1.54–4.48	2.62
As	43.39–46.03	44.37
S	20.69–22.41	21.75
Ni	0.01–0.29	0.08

mineral formula: $Fe_{30.3}\ Co_{1.4}\ As_{31.1}\ S_{36.1}$

83–Po–3: gold ore, Isabella Mine

wt %	Range	Mean (N=4)
Fe	31.44–33.98	33.18
Co	0.09–1.58	0.53
As	45.05–45.78	45.38
S	19.79–20.17	20.06

Appendix 5. Whole Rock Analyses

Analyses of rock powders were carried out by X-ray fluorescence techniques at Queen's University, Kingston, by F. Dunphy. Powders were fused in graphite crucibles with a measured quantity of lithium tetraborate flux, and the resulting glass bead was powdered and pressed, with an appropriate amount of binder, into a solid pellet. Count rates were obtained for standards and unknowns on a Siemen's X-ray spectrometer with counting times dictated by the concentration of a particular element in the specimen. Count rates were converted to concentrations by comparison to well-analyzed United States Geological Survey analytical standards.

Table A5.1 and Table A5.2 contain results of whole rock analyses for Rainy Lake rocks.

Table A5.1. Whole rock analyses of "fresh" and "altered" rocks associated with base metal mineralization.

A) Gagne Lake Prospect

wt %	hanging-wall cherty siltstone 72–441	footwall lapilli tuff 72–43	altered lapilli tuff 72–162	dalmatianite 72–360	dalmatianite 72–344	dalmatianite 63–389
SiO_2	80.17	79.13	78.36	47.45	64.87	59.00
Al_2O_3	8.53	11.11	10.60	19.04	12.71	15.02
TiO_2	0.15	0.12	0.13	1.31	1.04	1.08
FeO	2.70	1.02	1.91	8.50	7.96	6.88
MgO	0.76	0.91	2.33	12.30	4.68	7.36
CaO	0.46	0.26	0.19	0.73	1.15	1.19
Na_2O	0.84	2.13	0.15	0.18	0.20	0.10
K_2O	5.25	4.94	3.33	2.92	2.32	3.68
MnO	0.04	0.03	0.04	0.10	0.09	0.09
P_2O_5	0.01	0.01	0.01	0.32	0.25	0.26
L.O.I.	0.67	0.50	1.91	6.37	3.24	3.71
Total	100.58	100.16	98.96	99.22	98.51	98.37

B) Wind Bay Prospect

wt %	quartz-eye tuff 136–760	quartz-eye tuff 136–605	altered lapilli tuff 138–854	carbonate phyllite 136–830	chloritic quartz-eye tuff WB–6	magnetite-chlorite phyllite WB–7	magnetite-chlorite phyllite 138–622
SiO_2	73.25	72.94	70.92	47.10	46.12	32.68	27.80
Al_2O_3	11.78	11.27	9.35	11.70	12.56	13.01	14.30
TiO_2	0.32	0.32	0.27	1.67	0.71	0.80	0.87
FeO	6.82	7.15	13.16	13.84	27.73	33.70	37.19
MgO	1.25	2.04	1.20	3.56	5.15	6.35	7.40
CaO	0.27	0.15	0.08	7.32	0.16	0.28	0.16
Na_2O	3.32	1.15	0.10	0.21	0.10	0.10	0.13
K_2O	0.80	1.31	0.75	2.24	0.03	0.54	0.90
MnO	0.07	0.13	0.22	0.57	0.39	0.53	0.65
P_2O_5	0.02	0.01	0.01	0.27	0.06	0.06	0.06
L.O.I.	1.78	2.36	2.36	11.77	4.99	6.55	5.38
Total	99.68	98.83	98.42	100.25	98.00[a]	94.60[a]	94.84[a]

FeO : total iron expressed as FeO

L.O.I: loss on ignition

[a] *poor totals reflect abnormal compositions compared to typical silicate rocks*

Table A5.2. Whole rock analyses of "fresh" and "altered" rocks associated with gold mineralization.

A) Cone Prospect

wt %	**fresh tonalite 80–Po–39**	**weakly altered tonalite RL–Fo–13**	**moderately altered tonalite RL–Fo–15**	**altered tonalite RL–Fo–14**
SiO_2	70.48	71.50	73.38	72.85
Al_2O_3	14.68	13.52	14.19	13.63
TiO_2	0.25	0.28	0.29	0.26
FeO_t	1.83	2.02	2.38	2.13
MgO	0.65	0.68	0.48	0.48
CaO	2.14	1.90	0.92	1.81
Na_2O	4.32	4.12	3.02	1.41
K_2O	2.44	2.39	3.13	3.82
MnO	0.05	0.04	0.05	0.04
P_2O_5	0.05	0.04	0.08	0.07
L.O.I.	2.07	2.60	2.25	2.60
Total	98.96	99.09	100.17	99.10

B) Stellar Mine

wt %	**fresh trondhjemite 81–Po–16**	**altered trondhjemite 81–Po–15**	**fresh gabbro 81–Po–9**	**altered gabbro 81–Po–10**
SiO_2	75.70	76.50	42.32	42.86
Al_2O_3	11.45	11.58	15.24	14.61
TiO_2	0.19	0.20	2.61	1.71
FeO_t	2.57	2.31	17.23	14.88
MgO	0.29	0.32	5.26	5.35
CaO	1.55	2.03	11.32	8.14
Na_2O	4.87	0.39	1.62	2.32
K_2O	1.21	3.75	0.06	0.05
MnO	0.06	0.06	0.20	0.20
P_2O_5	0.01	0.02	0.03	0.04
L.O.I.	1.91	3.36	2.35	8.86
Total	100.01	100.52	98.21	99.02

Appendix 6. Petrographic Data for Rainy Lake Mineralization

The mineralogy of opaques was determined for suites of polished sections that represent each of the deposit types. Tables A6.1 and A6.2 summarize the sulphide and oxide mineralogy for volcanic-hosted and gabbro-hosted base metal mineralization, respectively.

Table A6.1. Modal estimates of sulphide and oxide minerals in ore specimens, volcanic-hosted mineralization.

Ores of Felsic Association

Locality	**Sample No.**	**pyrrhotite**	**pyrite**	**sphalerite**	**chalcopyrite**	**galena**	**magnetite**
Gagne Lake	81-Po-41	20	15	25	3	4	
	RL-LL-04		30				
	RL-LL-01	10	10		tr		
	81-Po-154		90				
Wind Bay	RL-WB-1	5	5	20	10		
	RL-WB-4		35				
	RL-WB-15	2	5	8	15		
Port Arthur Copper	RL-PA-01		65	5	5		
	RL-PA-03		10	1	35		
	RL-PA-08		25	3	25		

Ores of Mafic Association

Locality	**Sample No.**	**pyrrhotite**	**pyrite**	**sphalerite**	**chalcopyrite**	**arsenopyrite**	**magnetite**
Pocket Pond	76-Po-26	tr	30	35	tr		
	dd 98-40	30			1		
	dd 98-61	1	35	2			
	dd 98-86	1			1		50
	dd 98-112	30					
	dd 98-207	25	2		1		
	dd 98-292	30	30		1		
	RL-PP-151	40		35	5		
	RL-PP-15	10					5
	81-Po-114		30	1			
Nickel Lake	RL-NL-1A		90	tr			
	RL-NL-2	30		tr	tr		
	RL-NL-4	50	2	1	tr	1	
	RL-NL-5	tr	90	tr			
	RL-NL-6	30	25	3	1		
McTavish	RL-MT-2	40		tr	1		3
	RL-MT-4	10			1		
	RL-MT-10	6		tr	5		
	FRAMBOID		90				
Other	81-Po-95	80			2		10
	81-Po-98	30			tr		

tr = trace

Table A6.2. Modal estimates of sulphide and oxide minerals in ore specimens, Grassy Portage intrusion.

	Modal percent of sample						
Sample No.	**chalcopyrite**	**cubanite**	**pyrrhotite**	**pentlandite**	**molybdenite**	**sphalerite**	**ilmenite**
L902	5		10	tr			1
L910	15		25	tr			
L912	20	1	15	1			
L913	5		30				
L914	15	tr	10	2			10
L917	25	20		10			1
L918	25		5			tr	
L919	15	5	20	2			
L920	8		2				
L921a	40	15	10	1		tr	
L921b	25	10	10	tr			
L924	20	5	5	tr		tr	3
L925a	25	5	15	1		tr	
L925b	40	3	10	1		tr	
L926	12		10	1			1
L927	20		5				2
L936a	25		25	tr	2		
L936b	25	1	20		2		
L938	10		5	tr			
L940	50	5	10	1	tr		
L949a	8		2				25
L949b	3		1				
L950	4		3	1			
L952a	5		5				15
L952b							4
L954	tr		tr				4
L956	4		4	1			3
L969	25		10	1			5
L970	10		2				5
L972	30		10	3	2		4
L973	40		15				
L975a	20		10	tr	tr		20
L975b	25		10	1	1		25
L975c	30		5				20
L976a	10		15	3	tr		5
L976b	45		5				
L977	25		5	1			
L978	20		5	1			
L979							15
L981	10		2				15
L983	10		5	tr			
L988a	40		20		1		
L988b	30		20	1			3
L989	20		20	2	1		
76-Po-09	1		10	1			3
76-Po-10	20		10				15
76-Po-11	10		2				
76-Po-12	25	5	10		tr		
76-Po-23	30		5				
76-Po-05			tr				tr
76-Po-18	1			1			
76-Po-19	1		5	1			1

Note: All but the last three specimens, which are from the Hupchuk prospect, are from the North Rock deposit. L-series specimens were collected from the drift on the 175-foot level of the North Rock deposit and are arranged numerically with increasing distance eastward from the shaft.

tr = trace

Appendix 7. Assay Data for Typical Mineralized Rainy Lake Ore Specimens

Tables A7.1, A7.2, A7.3 and A7.4 contain assay data for selected mineralized specimens that typify the various deposit types. Analyses were performed at the Geoscience Laboratories, Ontario Geological Survey. All elements except for iron and lithium were determined by a volumetric method. Lithium was determined using an emission spectrophotometer and iron by atomic absorption. The trace element determinations of gold and silver were performed by atomic absorption following digestion of a fire assay bead (Riddle 1983). The gold and silver assays (Table A7.4) were performed by conventional fire assay techniques.

Table A7.1. Assay data for base metal mineralization of felsic volcanic association.

Sample No.	% Mn	% Fe	% Zn	% Cu	% Pb	ppb Au	ppm Ag	% Co	% Ni	% Cr	ppm Li	ppm Ba	Remarks
RL-PA-001 (8050) massive pyrite, Port Arthur Copper Co. Mine	0.3730	42.2	0.5250	0.1460	-	100	-	0.0117	-	-	6	10	
RL-Pa-003 (8043) Cu ore, Port Arthur Copper Co. Mine	0.1390	18.2	0.0945	6.88	0.0076	200	21	0.0097	-	-	10	10	
RL-WB-3 (8045) pyritic schist, Wind Bay	0.1900	18.7	0.0090	0.1160	0.0205	80	4	0.0044	0.0121	0.0188	10	30	
RL-WB-4 (8044) pyritic schist, Wind Bay	0.0181	9.1	0.0086	0.0760	-	12	-	0.0068	0.0235	0.0925	34	40	
WB-139-1 (8067) sphalerite-chlorite schist, Wind Bay	0.3670	7.7	1.01	0.0550	0.0148	160	3	0.0050	0.0170	0.0515	13	30	trace vanadium
WB-139-2 (8068) sphalerite-chalcopyrite -chlorite schist, Wind Bay	0.2980	15.1	0.9900	1.14	0.0125	280	17	0.0084	0.0200	0.0690	12	70	trace vanadium
WB-139-3 (8069) sphalerite-chlorite schist, Wind Bay	0.3370	10.7	1.25	0.0310	0.0052	5	-	0.0045	0.0191	0.0695	14	40	trace cadmium, trace vanadium
WB-139-4 (8070) sphalerite-chlorite schist, Wind Bay	0.3100	11.4	3.84	0.0500	0.0665	18	2	0.0049	0.0195	0.0650	16	10	trace cadmium, trace vanadium

Table A7.2. Assay data for base metal mineralization of mafic volcanic association.

Sample No.	% Mn	% Fe	% Zn	% Cu	% Pb	ppb Au	ppm Ag	% Co	% Ni	% Cr	ppm Li	ppm Ba	Remarks
RL-PP-1 (8041) massive sphalerite+ pyrrhotite, Pocket Pond	0.0380	26.9	23.2	0.2450	-	100	2	0.0215	0.0250	-	4	-	cadmium 0.05-0.5%
RL-PP-2(8040) massive pyrrhotite+ sphalerite, Pocket Pond	0.0106	40.1	3.96	0.0435	-	140	5	0.0245	0.0490	0.0029	8	30	trace cadmium
	0.0110	40.0	4.05	0.0425	-	150	5	0.0250	0.0495	0.0033	7	30	trace cadmium (duplicate)
PP-98-292 (8074) semimassive pyrrhotite+ pyrite, Pocket Pond	0.1490	39.6	0.032	0.0905	-	9	-	0.1210	0.0305	0.0053	5	20	
PP-98-112 (8075) pyrrhotite in siliceous sediments, Pocket Pond	0.1110	21.0	0.0585	0.1720	0.0020	16	3	0.0066	0.0054	0.0098	18	170	trace vanadium
	0.1130	21.1	0.0615	0.1740	0.0016	17	3	0.0070	0.0055	0.0092	17	150	trace vanadium (duplicate)
PP-98-86 (8076) magnetitic iron formation, Pocket Pond	0.0370	37.5	0.0020	0.0049	-	6	-	0.0008	-	-	4	10	
PP-98-61 (8078) laminated pyritic schist, Pocket Pond	0.0930	16.0	0.4200	0.0145	0.0019	20	-	0.0115	0.0052	0.0096	9	50	trace vanadium
PP-98-40 (8077) pyrrhotite in siliceous sediments, Pocket Pond	0.3830	17.4	0.0160	0.0740	-	16	-	0.0046	0.0132	-	4	20	
PP-98-307 (8079) pyrrhotite in siliceous sediments, Pocket Pond	0.1050	24.1	0.0950	0.0830	-	6	2	0.0048	0.0200	0.0005	6	90	
RL-NL-001 (8082) pyrrhotite-grunerite schist, Nickel Lake	0.2630	26.9	0.0425	0.0460	0.0014	4	-	0.0063	0.0058	0.0074	30	20	trace vanadium
RL-NL-001A (8046) massive pyrite, Nickel Lake	0.0052	38.9	0.0160	0.0037	0.0010	19	-	0.0047	0.0021	0.0026	4	10	
RL-NL-005 (8053) pyritic schist, Nickel Lake	0.0390	25.2	0.4000	0.0154	0.0049	30	-	0.0114	0.0041	0.0036	8	-	
RL-NL-006 (8047) sulphide breccia, Nickel Lake	0.0780	32.9	0.7150	0.1100	0.0042	60	-	0.1000	0.0405	0.0053	4	140	
RL-MT-2 (8048) carbonate sulphidic rock, Nickel Lake	0.0340	29.0	0.2950	0.1500	-	19	-	0.0186	0.0335	0.0068	4	120	
RL-MT-3 (8080) pyritic shale, Nickel Lake	0.0161	25.0	0.5280	0.2800	-	(90,150)	2	0.0560	0.0550	0.0041	5	110	

Table A7.2. Continued.

Sample No.	% Mn	% Fe	% Zn	% Cu	% Pb	ppb Au	ppm Ag	% Co	% Ni	% Cr	ppm Li	ppm Ba	Remarks
RL-MT-4 (8049) laminated sulphidic schist, Nickel Lake	0.0146	32.0	0.4600	0.0460	0.0031	23	-	0.0055	0.0420	0.0032	4	370	
RL-MT-5 (8081) siliceous sediments, pyrrhotite+carbonate, Nickel Lake	0.2180	13.4	0.0096	0.0660	-	6	-	0.0075	0.0200	0.1180	-	100	
RL-MT-10 (8051) chalcopyrite blebs, McTavish prospect	0.0545	7.7	0.0170	1.08	-	140	4	0.0106	0.0129	0.0036	4	80	
81-Po-114 (8052) pyritic schist, Nickel Lake	0.0840	18.5	0.4700	0.0335	0.0033	32	-	0.0210	0.0039	0.0102	12	160	
81-Po-95 (8054) massive pyrrhotite, Croome prospect	0.0130	54.2	0.0070	0.0975	-	15	2	0.0006	0.0235	0.0057	5	-	
81-Po-94 (8055) semimassive pyrite, pyrrhotite, Stanol prospect	0.0128	26.9	0.0092	0.7850	-	11	5	0.0240	0.0066	0.0016	20	60	
81-Po-97 (8057) semimassive pyrite, Windy Point	0.2770	29.9	0.0106	0.0067	-	(260,24)	-	0.0109	0.0108	0.0021	6	30	
81-Po-98 (8058) sulphidic schist, Kotnick prospect	0.0560	13.1	0.0250	0.0186	0.0020	20	-	0.0057	0.0111	0.0208	32	370	
81-Po-102 (8061) massive pyrrhotite, Daley–Galbraith prospect	0.0118	48.0	0.0320	0.0840	-	16	-	0.0019	0.0129	0.0011	4	120	
81-Po-156b (8059) sulphidic schist, Stang prospect	0.0915	20.2	0.0280	0.0260	-	7	-	0.0108	0.0035	0.0018	18	20	

Note: Numbers in brackets are replicated sample analyses.

Table A7.3. Assay data for copper mineralization in the Grassy Portage intrusion.

Sample No.	% Mn	% Fe	% Zn	% Cu	% Pb	ppb Au	ppm Ag	% Co	% Ni	% Cr	ppm Li	ppm Ba	Remarks
RL-SG-6 (8062) black ore, North Rock Mine	0.0820	17.4	0.0215	3.78	-	130	-	0.0191	0.0520	0.0005	16	80	
RL-SG-6 (8063) grey ore, North Rock Mine	0.0800	17.1	0.0200	3.70	-	90	4	0.0193	0.0500	0.0005	16	80	trace molybdenum

Table A7.4. Assay data for gold-bearing quartz veins, Shoal Lake area.

Vein[a]	Sample No.	Sample Width	oz/ton Au	oz/ton Ag
Foley Mine				
South Foley Sulphide	588001	51 in.	0.01	tr
Galena	588002	1 in. (3rd order)	tr	tr
Galena	588005	8 in.	0.02	tr
Lucky Joe	588008	12 in.	3.08	0.12
West	588009	14 in.	0.03	tr
"A"	588010	16 in.	0.02	tr
North Foley Sulphide	588011	39 in.	0.01	tr
Jumbo	588012	59 in.	0.01	tr
South Foley Sulphide	588013	39 in.	0.16	tr
South Foley Sulphide	588020	36 in.	tr	tr
Galena	588025	1 in. (2nd order)	0.01	tr
Cone Mine	588004	5 in.	0.25	tr
Cone Mine	588007	4 in. (2nd order)	tr	tr
Cone Mine	588016	20 in.	tr	tr
Cone Prospect				
No. 2	588003	26 in.	0.04	tr
Twin Vein	588014	10 in.	tr	tr
Twin Vein	588015	12 in.	0.01	tr
No. 1	588021	4.5 in.	0.16	0.80
No. 1	588022	10 in.	0.24	1.08
No. 1	588024	3 in. (2nd order)	tr	tr
No. 4	588060	6 in.	0.11	2.2
No. 4	588083	6 in.	tr	1.85
Stagee Prospect				
Middle Vein	588019	36 in.	0.27	0.89
Stagee South	588023	24 in.	tr	tr

---

[a] *See Poulsen (2000) for location of veins*

Appendix 8. Lead Isotopic Data

Analyses of the lead isotopic composition of galena from Rainy Lake mineralization were performed under contract to the Geological Survey of Canada by laboratories at the University of Toronto and University of Alberta, using the procedure of Cumming, Eckstrand and Peredery (1982). Table A8.1 lists the lead isotope analyses of galena for samples taken from a number of properties, the descriptions of which follow.

SAMPLE LOCATION DESCRIPTIONS

Gagne Lake Prospect

Galena sampled *in situ* from main trench. 15 cm (6-inch) wide lens of heavy to massive sphalerite-galena, concordant with host rhyolitic lapilli tuffs and overlying chert and siltstone. Footwall alteration zone consists of "dalmatianite" with disseminated chalcopyrite. Latitude 48°42′06″, Longitude 92°52′36″.

Wind Bay Prospect

Galena as a rare grain in drill core associated with sphalerite, pyrite, pyrrhotite and chalcopyrite, which are the common sulphide minerals. These occur in seams 1 mm to 10 cm wide in tuffaceous chlorite schist. A low-grade zinc body 1400 m long is outlined by diamond-drill holes spaced approximately 300 m apart. The host rock is likely metamorphosed andesitic breccia: some altered felsic volcaniclastics occur locally in the footwall. Latitude 48°40′05″, Longitude 92°58′33″.

Pidgeon Prospect

Galena from loose material beside trench. Samples contain roughly equal proportions of sphalerite, galena and iron sulphides; carbonate with blocks of schistose sericitic wall rock are common. Material of similar nature occurs at same stratigraphic horizon 1400 m to the southwest. Immediate host rocks are felsic lapilli tuffs with local patches of spotted pyritic alteration. Latitude 48°45′00″, Longitude 92°32′00″.

Ferguson Mine (Daisy Vein)

Galena sample from dump at westernmost shaft sunk on this vein. Southeast of the shaft, vein reportedly averages 0.33 ounce per ton gold over 30 cm (12 inches) for a length of 40 m. Visible gold noted in same quartz vein approximately 100 m to the northwest. Host rock is foliated tonalite. Latitude 48°44′13″, Longitude 92°36′57″.

Ferguson Mine (Government Vein)

Galena sample from dump beside shaft located 100 m south of the Daisy vein shaft. Samples of quartz, ankerite, pyrite, chalcopyrite, sphalerite and arsenopyrite, as well as galena, noted on dump. Average assay of 0.41 ounce per ton gold over 46 cm (18 inches) reported in drift along 50 m (165 feet). Moderate amounts of mineralization were reported in a drill program carried out on this vein in 1980 by Corporate Oil and Gas Limited. Latitude 48°44′12″, Longitude 92°36′59″.

Lucky Coon Mine (2A Vein)

Galena sample from loose vein material beside trench. Quartz vein 56 cm (22 inches) wide in foliated tonalite. Reported to have erratic gold values up to 1 ounce per ton gold over 36 cm (14 inches). Latitude 48°43′49″, Longitude 92°37′26″.

Stellar Mine (No.2 or Rainbow Vein)

Galena sample from dump adjacent to shaft on Rainbow vein. Vein material includes quartz, ankerite, siderite and sphalerite. Host rock is fine- to medium-grained trondhjemite that is intensely foliated and carbonate and sericite rich near the vein. Values averaging approximately 1 ounce per ton gold reported from 25 samples taken from the vein in the shaft. Latitude 48°44′41″, Longitude 92°42′16″.

Cone Prospect (No.1 Vein)

Galena sample taken *in situ* from well-exposed gold-bearing quartz vein. Assays of 0.21 ounce per ton gold and 0.99 ounce per ton silver over 20 cm (8 inches). Vein contains quartz, iron carbonate, sphalerite, galena and pyrite. Latitude 48°42′22″, Longitude 92°38′33″.

Cone Prospect (Nugget Vein)

Galena sample collected *in situ* from 15 cm (6-inch) wide quartz vein. Single crystal of galena extracted from an intergrowth of galena with native metal (electrum and gold). Latitude 48°42′46″, Longitude 92°38′09″.

Russell C. Cone Mine (Maclean Pit)

Galena with pyrite in dump material reportedly obtained from 30 cm (12-inch) wide sulphide-rich quartz vein that is parallel to, and separated by a 61 cm (24-inch) wide horse of schistose tonalite from, a 46 cm (18-inch) wide vein of gold-bearing blue quartz. The latter vein produced approximately 1000 ounces of gold from 1949 to 1956 from a small-scale mining operation. Latitude 48°42′09″, Longitude 92°38′33″.

Table A8.1. Lead isotope analyses of galena for Rainy Lake mineralization.

Deposit	$^{206}Pb/^{204}Pb$	$^{207}Pb/^{204}Pb$	$^{208}Pb/^{204}Pb$	Model Ages (Ma)				
				a	b	c*	d	Lab
Gold–Quartz Veins								
Stagee No.1	13.502	14.580	33.369	2686	2664	2740	2652	U.T.
Manhattan No.4	13.512	14.580	33.360	2679	2653	2735	2642	U.A.
Alice "A"	13.536	14.602	33.394	2677	2664	2710	2662	U.A.
Stellar Rainbow	13.618	14.641	33.555	2642	2633	2645	2613	U.T.
Stellar Rainbow	13.664	14.655	33.603	2631	2627	2655	2605	U.A.
Ferguson Daisy	13.633	14.625	33.430	2616	2585	2640	2577	U.A.
R.C. Cone	13.671	14.628	33.585	2589	2546	2595	2544	U.T.
Cone Nugget	13.682	14.641	33.509	2591	2557	2625	2551	U.A.
Lucky Coon 2A	13.734	14.661	33.537	2564	2530	2595	2524	U.A.
Ferguson Government	13.769	14.676	33.526	2550	2516	2595	2509	U.A.
Cone No.1	13.785	14.659	33.603	2522	2467	2560	2474	U.T.
Base Metal Deposits								
Pidgeon	13.376	14.516	33.236	2740	2705	2740	2700	U.A.
Gagne Lake	13.410	14.564	33.291	2750	2752	2790	2725	U.T.
Wind Bay	13.410	14.559	33.274	2746	2743	2785	2717	U.T.

**Note: Asterisk indicates values are estimated graphically from $^{207}Pb/^{206}Pb$ and $^{208}Pb/^{206}Pb$ systems.*

[a] *Cumming and Richards 1975*

[b] *Stacey and Kramers 1975*

[c] *Doe and Zartman 1979*

[d] *Thorpe 1982*

U.T. = University of Toronto

U.A. = University of Alberta

Stagee (Hopkins) Prospect

Galena in sample of quartz with pyrite and sphalerite from dump beside 30 m (100-foot) deep shaft (1934). Main vein is 30 to 102 cm (12 to 40 inches) wide and chip channel sample gave 0.27 ounce per ton gold and 2.06 ounces of silver per ton over 91 cm (36 inches). An assay of 1.26 ounces of gold per ton and 2.06 ounces of silver per ton was obtained from sulphide-rich grab samples. Latitude 48°41′59″, Longitude 92°38′38″.

Alice "A" Mine

Samples of dump material from westerly of 2 shafts. Galena seen *in situ* in irregular quartz veins with pyrite and chalcopyrite. Veins are dominantly of foliation-parallel type in sericitic rhyolites. These veins are similar to other occurrences near the Quetico Fault, including the Olive and Headlight (Saundary) mines. Latitude 48°45′51″, Longitude 92°28′25″.

Manhattan Mine (No.4 Vein)

Samples come from laminated quartz vein up to 91 cm (36 inches) wide. Host rock is foliated tonalite of the Bad Vermilion intrusion. Latitude 48°43′15″, Longitude 92°37′50″.

References

Adams, F.D., Bell, R., Lane, A.C., Leith, C.K, Miller, W.G. and Van Hise, C.R. 1905. Report of the special committee for the Lake Superior region; Journal of Geology, v.13, p.89-104.

Allard, G.O. 1970. The Doré Lake Complex, Chibougamau, Quebec—a metamorphosed Bushveld-type layered intrusion; *in* Symposium on the Bushveld igneous complex and other layered intrusions, Geological Society of Africa, Special Publication, Number 1, p.477-491.

——1976. Doré Lake Complex and its importance to Chibougamau geology and metallogeny; Quebec Department of Natural Resources, Geological Report DP 368, 446p.

Anglin, C.D. 1982. Stratigraphy, petrology and metamorphism of Archean Algoma type iron formation in the Fort Frances area, northwestern Ontario; unpublished BSc thesis, Queen's University, Kingston, Ontario, 87p.

Arnold, R.G. 1966. Mixtures of hexagonal and monoclinic pyrrhotite and the measurement of the metal content of pyrrhotite by X-ray diffraction; American Mineralogist, v.51, p.1221-1227.

Ashwal, L.D., Morrison, D.A., Phinney, W.C. and Wood, J. 1983. Origin of Archean anorthosites: evidence from the Bad Vermilion Lake anorthosite complex, Ontario; Contributions to Mineralogy and Petrology, v.82, p.259-273.

Ashwal, L.D., Wooden, J.L., Phinney, W.C., Morrison, D.A., Shih, C.-Y. and Wiesmann, H. 1981. The Bad Vermilion Lake anorthosite complex, Ontario: Sr and Nd isotopic evidence for depleted Archean mantle; *in* Abstracts with Programs, Geological Society of America 94th Annual Meeting, v.13, no.7, p.399.

Ayres, L.D. 1969. Early Precambrian stratigraphy of part of Lake Superior Provincial Park, Ontario, Canada and its implications for the origin of the Superior Province; unpublished PhD thesis, Princeton University, Princeton, New Jersey, 399p.

——1978. Metamorphism in the Superior Province of northwestern Ontario and its relationship to crustal development; *in* Metamorphism in the Canadian Shield, Geological Survey of Canada, Paper 78-10, p.25-36.

Baragar, W.R.A. and McGlynn, J.C. 1978. On the basement of Canadian greenstone belts: discussion; Geoscience Canada, v.5, p.13-15.

Beard, R.C. and Garratt, G.L. 1976. Gold deposits of the Kenora–Fort Frances area, districts of Kenora and Rainy River; Ontario Division of Mines, Mineral Deposits Circular 16, 46p.

Beck, W. and Murthy, R.V. 1982. Rb-Sr and Sm-Nd isotopic studies of Proterozoic mafic dikes in northeastern Minnesota; *in* Abstracts, 28th Annual Meeting, Institute on Lake Superior Geology, p.5.

Bell, T.H. 1981. Foliation development—the contribution, geometry and significance of progressive, bulk, inhomogeneous shortening; Tectonophysics, v.75, p.273-296.

Berthé, D. and Brun, J.P. 1980. Evolution of folds during progressive shear in the South Armorican shear zone, France; Journal of Structural Geology, v.2, no.1/2, p.127-133.

Birk, D. and McNutt, R.H. 1981. Geochronology of Wabigoon Belt granitoids, northwestern Ontario: Rb-Sr isochrons for seven late-tectonic plutons; Canadian Journal of Earth Sciences, v.18, p.157-175.

Birk, W.D. 1978. The nature and timing of granitoid plutonism in the Wabigoon volcanic-plutonic belt, northwestern Ontario; unpublished PhD thesis, McMaster University, Hamilton, Ontario, 521p.

Blackburn, C.E. 1973. Geology of the Otukamamoan Lake area, districts of Rainy River and Kenora; Ontario Division of Mines, Geological Report 109, 42p.

——1980. Towards a mobilist tectonic model for part of the Archean of northwestern Ontario; Geoscience Canada, v.7, p.64-72.

Blackburn, C.E. and Mackasey, W.O. 1977. Nature of the Quetico–Wabigoon boundary in the deCourcey–Smiley lakes area, northwestern Ontario: discussion; Canadian Journal of Earth Sciences, v.14, p.1959-1961.

Borradaile, G.J. 1978. Transected folds: a study illustrated with examples from Canada and Scotland; Geological Society of America, Bulletin, v.89, p.481-493.

——1982. Comparison of Archean structural styles in two belts of the Canadian Superior Province; Precambrian Research, v.19, p.179-189.

Borradaile, G.J. and Kennedy, M. 1982. Pseudotachylite; *in* Atlas of Deformational and Metamorphic Rock Fabrics, Springer-Verlag, Berlin, p.366.

Boyle, R.W. 1976. Mineralization processes in Archean greenstone and sedimentary belts; Geological Survey of Canada, Paper 75-15, 45p.

Breaks, F.W. 1980. Lithophile mineralization in northwestern Ontario: rare-element granitoid pegmatites; *in* Summary of Field Work and other Activities 1980, Ontario Geological Survey, Miscellaneous Paper 96, p.5-9.

——1981. Lithophile mineralization in northwestern Ontario: rare metal granitoid pegmatites; *in* Summary of Field Work and other Activities 1981, Ontario Geological Survey, Miscellaneous Paper 100, p.19-21.

Bruce, E.L. 1925a. The Coutchiching rocks of the Bear's Pass section, Rainy Lake; Royal Society of Canada, Proceedings and Transactions, 3rd series, v.19, section 4, p.43-46.

——1925b. Gold deposits of Kenora and Rainy River districts; Ontario Department of Mines, Annual Report, 1925, v.34, pt.6, p.1-42.

——1927. Coutchiching delta; Geological Society of America, Bulletin, v.38, p.771-782.

Carmichael, D.M. 1978. Metamorphic bathozones and bathograds: a measure of the depth of post-metamorphic uplift and erosion on the regional scale; American Journal of Science, v.278, p.769-797.

Clark, L.A. 1983. Genetic implications of fragmental ore texture in Japanese Kuroko deposits; Canadian Institute of Mining and Metallurgy, Bulletin, v.76, no.849, p.105-114.

Cobbold, P.R. and Quinquis, H. 1980. Development of sheath folds in shear regimes; Journal of Structural Geology, v.2, no.1/2, p.119-126.

Coleman, A.P. 1898. Fourth report on the west Ontario gold region; Ontario Bureau of Mines, Annual Report, 1897, v.7, pt.2, p.109-145.

Cooke, H.C. 1930. The Amulet Mine, Quebec; Canadian Institute of Mining and Metallurgy, Transactions, v.33, p.398-408.

Coward, M.P., James, P.R. and Wright, L. 1976. Northern margin of the Limpopo mobile belt, Southern Africa; Geological Society of America, Bulletin, v.87, p.601-611.

Craig, J.R. and Vaughan, D.J. 1981. Ore microscopy and ore petrography; John Wiley and Sons, New York, 406p.

Crowell, J.C. 1974. Sedimentation along the San Andreas Fault, California; *in* Modern and Ancient Geosynclinal Sedimentation, Society of Economic Paleontologists and Mineralogists, v.12, p.292-303.

Cumming, G.L., Eckstrand, O.R. and Peredery, W.V. 1982. Geochronologic interpretations of Pb isotope ratios in nickel sulfides of the Thompson Belt, Manitoba; Canadian Journal of Earth Sciences, v.19, p.2306-2324.

Cumming, G.L. and Richards, J.R. 1975. Ore lead isotope ratios in a continuously changing Earth; Earth and Planetary Science Letters, v.28, p.155-171.

Davies, J.C. 1973. Geology of the Fort Frances area, District of Rainy River; Ontario Division of Mines, Geological Report 107, 35p.

Davis, D.W., Blackburn, C.E. and Krogh, T.E. 1982. Zircon U-Pb ages from the Wabigoon–Manitou lakes region, Wabigoon Subprovince, northwest Ontario; Canadian Journal of Earth Sciences, v.19, p.254-266.

Davis, D.W., Blackburn, C.E., Trowell, N.F. and Edwards, G.R. 1980. Geochronology of the Savant–Crow lakes area, western Wabigoon Subprovince, districts of Kenora, Rainy River and Thunder Bay; *in* Summary of Geochronology Studies 1977-1979, Ontario Geological Survey, Miscellaneous Paper 92, 45p.

Davis, D.W. and Edwards, G.R. 1982. Zircon U-Pb ages from the Kakagi Lake area, Wabigoon Subprovince, northwest Ontario; Canadian Journal of Earth Sciences, v.19, p.1235-1245.

Davis, D.W. and Trowell, N.F. 1982. U-Pb zircon ages from the eastern Savant Lake–Crow Lake metavolcanic-metasedimentary belt, northwest Ontario; Canadian Journal of Earth Sciences, v.19, p.868-877.

de Rosen-Spence, A. 1969. Genèse des roches à cordiérite-anthophyllite des gisements cupro-zincifères de la région de Rouyn–Noranda, Québec, Canada; Canadian Journal of Earth Sciences, v.6, p.1339-1345.

DeWit, M.J. 1982. Gliding and overthrust nappe tectonics in the Barberton greenstone belt; Journal of Structural Geology, v.4, no.2, p.117-136.

Doe, B.R. and Zartman, R.E. 1979. Plumbotectonics, the Phanerozoic; *in* Geochemistry of Hydrothermal Ore Deposits, John Wiley and Sons, New York, p.22-70.

Douglas, R.J.W. and Price, R.A. 1972. Nature and significance of variations in tectonic styles in Canada; *in* Variations in Tectonic Styles in Canada, Geological Association of Canada, Special Paper 11, p.626-688.

Durney, D.W. and Ramsay, J.G. 1973. Incremental strains measured by syntectonic crystal growths; *in* Gravity and Tectonics, John Wiley and Sons, New York, p.67-96.

Dusanowskyi, T.H. and West, G.F. 1976. Gravity study of the Sturgeon Lake area; *in* Proceedings of the 1976 Geotraverse Conference, University of Toronto, p.56-60.

Elder, J.W. 1977. Thermal convection; Journal of the Geological Society of London, v.133, pt. 4, p.293-309.

Emslie, R.F. 1975. Major rock units of the Morin Complex, southwestern Quebec; Geological Survey of Canada, Paper 74-48, 37p.

Eriksson, K.A. 1982. Sedimentation patterns in the Barberton Mountain Land, South Africa, and the Pilbara Block, Australia: evidence for Archean rifted continental margins; Tectonophysics, v.81, p.179-193.

Faure, G. 1977. Principles of isotope geology; John Wiley and Sons, New York, 464p.

Ferry, J.M. and Spear, F.S. 1978. Experimental calibration of the partitioning of Fe and Mg between biotite and garnet; Contributions to Mineralogy and Petrology, v.66, no.2, p.113-117.

Fox, J.S. 1983. Besshi-type volcanogenic sulphide deposits: a review; lecture, Canadian Institute of Mining and Metallurgy, 85th Annual General Meeting, Winnipeg, Manitoba, April 17-20.

Franklin, J.M., Gibb, W., Poulsen, K.H. and Severin, P. 1977. Archean metallogeny and stratigraphy of the south Sturgeon Lake area; Mattabi Trip, 23rd Annual Meeting, Institute on Lake Superior Geology, Thunder Bay, 73p.

Franklin, J.M., Kasarda, J. and Poulsen, K.H. 1975. Petrology and chemistry of the alteration zone of the Mattabi massive sulphide deposit; Economic Geology, v.70, p.63-79.

Franklin, J.M., Sangster, D.F. and Lydon, J.W. 1981. Volcanic-associated massive sulfide deposits; *in* Economic Geology, 75th Anniversary Volume, p.485-627.

Franklin, J.M. and Thorpe, R.I. 1982. Comparative metallogeny of the Superior, Slave and Churchill provinces; *in* Precambrian Sulphide Deposits, Geological Association of Canada, Special Paper 25, p.3-90.

Freund, R. 1970. Rotation of strike slip faults in Sistan, southeast Iran; Journal of Geology, v.78, p.188-200.

Frye, J.K. 1959. Petrography of the ancient granites of the Minnesota–Ontario boundary region; unpublished MSc thesis, University of Minnesota, St. Paul, Minnesota, 55p.

Fumerton, S.L. 1982. Redefinition of the Quetico Fault near Atikokan, Ontario; Canadian Journal of Earth Sciences, v.19, p.222-224.

Fyfe, W.S. and Henley, R.W. 1973. Some thoughts on chemical transport processes, with particular reference to gold; Minerals Science and Engineering, v.5, p.295-303.

Geological Survey of Canada 1978. Metamorphic map of the Canadian Shield; Geological Survey of Canada, Map 1475A, scale 1:3 500 000.

Glikson, A.Y. 1978. On the basement of Canadian greenstone belts; Geoscience Canada, v.5, p.3-12.

Goldich, S.S. and Peterman, Z.E. 1980. Geology and geochemistry of the Rainy Lake area; Precambrian Research, v.11, p.307-327.

Goodwin, A.M. 1972. The Superior Province; *in* Variations in Tectonic Styles in Canada, Geological Association of Canada, Special Paper 11, p.527-623.

——1973. Archean iron-formations and tectonic basins of the Canadian Shield; Economic Geology, v.68, p.915-933.

——1977. Archean basin-craton complexes and the growth of Precambrian shields; Canadian Journal of Earth Sciences, v.14, p.2737-2759.

Goomer, P.G. and Robertson, D.K. 1974. A lead isotope study of Archean mineralized areas in Tanzania; Journal of the Geological Society of London, v.130, pt. 5, p.449-460.

Grenne, T., Grammeltvedt, G. and Vokes, F.M. 1980. Cyprus-type sulphide deposits in the western Trondheim district, central Norwegian Caledonides; *in* Ophiolites: Proceedings of the International Ophiolite Symposium, Cyprus, 1979, Republic of Cyprus, Geological Survey Department, p.727-743.

Gross, G.A. 1965. Geology of iron deposits in Canada—volume 1, general geology and evaluation of iron deposits; Geological Survey of Canada, Economic Geology Report, no.22.

Grout, F.F. 1925. Coutchiching problem; Geological Society of America, Bulletin, v.36, p.351-364.

Grout, F.F., Gruner, J.W., Schwartz, G.M. and Thiel, G.A. 1951. Precambrian stratigraphy of Minnesota; Geological Society of America, Bulletin, v.62, p.1017-1078.

Groves, D.I. and Gee, R.D. 1980. Regional geology and mineral deposits of the Kalgoorlie–Norseman region; *in* Excursion Guide, Second International Archean Symposium, Perth, West Australia, Geological Society of Australia, Western Australia Division, p.28-45.

Harris, F.R. 1974. Geology of the Rainy Lake area, District of Rainy River; Ontario Division of Mines, Geological Report 115, 94p.

Hart, S.R. and Davis, G.L. 1969. Zircon U-Pb and whole-rock Rb-Sr ages and early crustal development near Rainy Lake, Ontario; Geological Society of America, Bulletin, v.80, no.4, p.595-616.

Hawley, J.E. 1930a. "Seine" or "Coutchiching"; Journal of Geology, v. 38, p.521-547.

——1930b. Geology of the Sapawe Lake area, with notes on some iron and gold deposits of Rainy River District; Ontario Department of Mines, Annual Report, 1929, v.38, pt.6, p.1-58.

Henley, R.W., Norris, R.J. and Paterson, C.J. 1976. Multistage ore genesis in the New Zealand Geosyncline: a history of post metamorphic lode emplacement; Mineralium Deposita, v.11, p.180-196.

Hodgson, C.J. 1959. The Watten–Halkirk copper prospect, Rainy Lake Area, western Ontario; unpublished MSc thesis, McGill University, Montreal, Quebec, 94p.

Hodgson, C.J. and Lydon, J.W. 1977. Geological setting of volcanogenic massive sulphide deposits and active hydrothermal systems; some implications for exploration; Canadian Institute of Mining and Metallurgy, Bulletin, v.70, no.786, p.95-106.

Holdaway, M.J. 1971. Stability of andalusite and the aluminum silicate phase diagram; American Journal of Science, v.271, p.97-131.

Horwood, H.C. 1948. General structural relationships of ore deposits in the Little Long Lac–Sturgeon River area; *in* Structural Geology of Canadian Ore Deposits, Volume 1, Canadian Institute of Mining and Metallurgy, p.377-384.

Hsu, M.Y. 1971. Analysis of strain, shape, and orientation of the deformed pebbles in the Seine River area, Ontario; unpublished PhD thesis, McMaster University, Hamilton, Ontario, 167p.

Hutchinson, R.W., Ridler, R.H. and Suffel, G.G. 1971. Metallogenic relationships in the Abitibi Belt, Canada: a model for Archean metallogeny; Canadian Institute of Mining and Metallurgy, Transactions, v.74, p.106-115.

Hutchison, M.N. and Scott, S.D. 1980. Sphalerite geobarometry applied to metamorphosed sulfide ores of the Swedish Caledonides and United States Appalachians; Norges Geologiske Undersokelse, v.360, p.59-71.

———1981. Sphalerite geobarometry in the Cu-Fe-Zn-S system; Economic Geology, v.76, p.143-153.

Hutton, D.H.W. 1979. Tectonic slides: a review and reappraisal; Earth Science Reviews, v.15, p.151-172.

Irvine, T.N. 1975. Crystallization sequences in the Muskox Intrusion and other layered intrusions—II. origin of chromitite layers and similar deposits of other magmatic ores; Geochimica et Cosmochimica Acta, v.39, p.991-1020.

———1982. Terminology for layered intrusions; Journal of Petrology, v.23, p.127-162.

Jackson, P.A. 1982. The structure, stratigraphy and strain history of the Seine Group and related rocks near Mine Centre, northwestern Ontario; unpublished MSc thesis, Lakehead University, Thunder Bay, Ontario, 258p.

Jégouzo, P. 1980. The South Armorican shear zone; Journal of Structural Geology, v.2, no.1/2, p.39-47.

Joliffe, A.W. 1955. Geology and iron ores of Steep Rock Lake; Economic Geology, v.50, p.373-398.

Kanasewich, E.R. 1968. The interpretation of lead isotopes and their geological significance; *in* Radiometric Dating for Geologists, Interscience, New York, p.147-224.

Kanehira, K. and Tatsumi, T. 1970. Bedded cupriferous iron sulphide deposits in Japan, a review; *in* Volcanism and Ore Genesis, University of Tokyo Press, Tokyo, p.51-76.

Kehlenbeck, M.M. 1976. Nature of the Quetico–Wabigoon boundary in the de Courcey–Smiley lakes area, northwestern Ontario; Canadian Journal of Earth Sciences, v.13, p.737-748.

Kennedy, M.C. 1984. The Quetico Fault in the Superior Province of the southern Canadian Shield; unpublished MSc thesis, Lakehead University, Thunder Bay, Ontario, 287p.

Kerrich, R. and Fryer, B.J. 1981. The separation of rare elements from abundant base metals in Archean lode gold deposits: implications of low water/rock source regions; Economic Geology, v.76, p.160-166.

Klau, W. and Large, D.E. 1980. Submarine exhalative Cu-Pb-Zn deposits, a discussion of their classification and metallogenesis; Geologisches Jahrbuch, Section D, no.40, p.13-58.

Klemm, D.D., Snethlage, R., Dehm, R.M., Henckel, J. and Schmidt–Thome, R. 1982. The formation of chromite and titanomagnetite deposits within the Bushveld Igneous Complex; *in* Ore Genesis, Society of Geological Applications to Mineral Deposits, Special Paper 2, Springer–Verlag, Berlin, p.351-370.

Kolker, A. 1982. Mineralogy and geochemistry of Fe-Ti oxide and apatite (nelsonite) deposits and evaluation of the liquid immiscibility hypothesis; Economic Geology, v.77, p.1146-1158.

Kretschmar, U. and Scott, S.D. 1976. Phase relations involving arsenopyrite in the system Fe-As-S and their application; Canadian Mineralogist, v.14, p.364-386.

Langford, F.F. and Morin, J.A. 1976. The development of the Superior Province of northwestern Ontario by merging island arcs; American Journal of Science, v.276, p.1023-1034.

Lawson, A.C. 1887. Geology of Rainy Lake region, with remarks on the classification of the crystalline rocks west of Lake Superior; American Journal of Science, v.33, p.473-480.

———1889. Report on the geology of the Rainy Lake region; Geological and Natural History Survey of Canada, Annual Report, v.II, pt.1, report F, 182p.

———1913. The Archean geology of Rainy Lake re-studied; Geological Survey of Canada, Memoir 40, 111p.

———1916. The correlation of the Precambrian rocks of the region of the Great Lakes; Bulletin of the Department of Geology, California University, unpublished, Geological Sciences, v.10, p.1-19.

Leith, C.K., Lund, R.J. and Leith, A. 1935. Precambrian rocks of the Lake Superior region; United States Geological Survey, Professional Paper 184, 31p.

Lillie, A.R. and Gunn, B.M. 1964. Steeply plunging folds in the Sealy Range, Southern Alps; New Zealand Journal of Geology and Geophysics, v.7, p.403-423.

Longstaffe, F.J. and Birk, D. 1981. Oxygen isotope evidence for the origin of discrete granitoid plutons from the Archean western Wabigoon Belt, northwestern Ontario; Precambrian Research, v.14, p.21-30.

Lowell, J.D. 1972. Spitsbergen Tertiary orogenic belt and the Spitsbergen fracture zone; Geological Society of America, Bulletin, v.83, p.3091-3102.

Macdonald, A.J. 1983. The iron formation–gold association: evidence from Geraldton area; *in* The Geology of Gold in Ontario, Ontario Geological Survey, Miscellaneous Paper 110, p.75-83.

MacGeehan, P.J., MacLean, W.H. and Bonenfant, A.J. 1981. Exploration significance of the emplacement and genesis of massive sulphides in the main zone at the Norita Mine, Matagami, Quebec; Canadian Institute of Mining and Metallurgy, Bulletin, v.74, no.828, p.59-75.

Mackasey, W.O., Blackburn, C.E. and Trowell, N.F. 1974. A regional approach to the Wabigoon–Quetico belts and its bearing on exploration in northwestern Ontario; Ontario Division of Mines, Miscellaneous Paper 58, 29p.

Mainwaring, P.R. and Naldrett, A.J. 1977. Country-rock assimilation and the genesis of Cu-Ni sulfides in the Waterhen Intrusion, Duluth Complex, Minnesota; Economic Geology, v.72, p.1269-1284.

Mann, P. and Burke, K. 1982. Basin formation at intersections of conjugate strike-slip faults; examples from southern Haiti; *in* Abstracts of the Geological Society of America, 95th Annual Meeting, New Orleans, vol. 14, no. 7, p.555.

McKinstry, H.E. 1948. Mining geology; Prentice–Hall Incorporated, New York, 680p.

———1953. Shears of the second order; American Journal of Science, v.251, p.401-414.

McKinstry, H.E. and Ohle, E.L. 1949. Ribbon structure in gold quartz veins; Economic Geology, v.44, p.87-109.

Merritt, P.L. 1934. Seine–Coutchiching problem; Geological Society of America, Bulletin, v.45, p.333-374.

Miall, A.D. 1981. Sedimentation and tectonics in alluvial basins; Geological Association of Canada, Special Paper 23, 272p.

Moore, J.M. 1979. Tectonics of the Najd transcurrent fault system, Saudi Arabia; Journal of the Geological Society of London, v.136, pt.4, p.441-454.

Naldrett, A.J. 1973. Nickel sulphide deposits—their classification and genesis, with special emphasis on deposits of volcanic association; Canadian Institute of Mining and Metallurgy, Transactions, v.76, p.183-201.

———1981. Nickel sulfide deposits: classification, composition and genesis; *in* Economic Geology, 75th Anniversary Volume, p.628-685.

Naldrett, A.J. and Gasparrini, E.L. 1971. Archean nickel sulfide deposits in Canada, their classification, geological setting and genesis with some suggestions as to exploration; *in* Symposium on Archean Rocks, Geological Society of Australia, Special Publication 3, p.201-226.

Newhouse, W.H. 1940. Openings due to movement along a curved or irregular fault plane; Economic Geology, v.35, p.445-464.

Norris, R.J. and Carter R.M. 1982. Fault-bound blocks and their role in localizing sedimentation and deformation adjacent to the Alpine Fault, southern New Zealand; Tectonophysics, v.87, p.11-24.

Ojakangas, R.W. 1972. Rainy Lake area; *in* Geology of Minnesota: A Centennial Volume; Minnesota Geological Survey, p.163-171.

Ontario Geological Survey 1980. Airborne electromagnetic and total intensity magnetic survey, Atikokan–Mine Centre area, western part, District of Rainy River; Ontario Geological Survey; Maps 80 495 to 80 505, scale 1:20 000.

Parkinson, R.N. 1962. Operation overthrust; *in* Tectonics of the Canadian Shield, Royal Society of Canada, Special Publication 4, p.90-101.

Parsons, A.L. 1918. Mineral developments in northwestern Ontario; Ontario Bureau of Mines, Annual Report, 1918, v.27, pt.1, p.168-186.

Peterman, Z.E. 1959. Petrology of the metasediments of the Rainy Lake region; unpublished MSc thesis, University of Minnesota, St. Paul, Minnesota, 62p.

Peterman, Z.E., Goldich, S.S., Hedge, C.E. and Yardley, D.H. 1972. Geochronology of the Rainy Lake region, Minnesota–Ontario; *in* Studies in Mineralogy and Precambrian Geology, Geological Society of America, Memoir 135, p.193-215.

Pettijohn, F.J. 1937. Early Precambrian geology and correlational problems of the northern subprovince of the Lake Superior region; Geological Society of America, Bulletin, v.48, p.153-202.

——— 1943. Archean sedimentation; Geological Society of America, Bulletin, v.54, p.925-972.

Philpotts, A.R. 1967. Origin of certain iron-titanium oxide and apatite rocks; Economic Geology, v.62, p.303-315.

Pigage, L.C. and Greenwood, H.J. 1982. Internally consistent estimates of pressure and temperature: the staurolite problem; American Journal of Science, v.282, p.943-969.

Pirie, J. and Mackasey, W.O. 1978. Preliminary examination of regional metamorphism in parts of Quetico metasedimentary belt, Superior Province, Ontario; *in* Metamorphism in the Canadian Shield, Geological Survey of Canada, Paper 78-10, p.37-48

Poulsen, K.H. 1980a. The stratigraphy, structure and metamorphism of Archean rocks at Rainy Lake, Ontario; unpublished MSc thesis, Lakehead University, Thunder Bay, Ontario, 99p.

——— 1980b. The geological setting of mineralization in the Mine Centre–Fort Frances area, District of Rainy River; *in* Summary of Field Work and Other Activities 1980, Ontario Geological Survey, Miscellaneous Paper 96, p.162-168 .

——— 1981. The geological setting of mineralization in the Mine Centre–Fort Frances area, District of Rainy River; *in* Summary of Field Work and Other Activities 1981, Ontario Geological Survey, Miscellaneous Paper 100, p.190-195.

——— 1984. The geological setting of mineralization in the Mine Centre–Fort Frances area, District of Rainy River; Ontario Geological Survey, Open File Report 5512, 126p.

——— 2000. Geological setting of mineralization in the Mine Centre–Fort Frances Area; Ontario Geological Survey, Mineral Deposits Circular 29, 78p.

Poulsen, K.H., Borradaile, G.J. and Kehlenbeck, M.M. 1980. An inverted Archean succession at Rainy Lake, Ontario; Canadian Journal of Earth Sciences, v.17, p.1358-1369.

Ramsay, J.G. 1965. Structural investigations in the Barberton Mountain Land, Eastern Transvaal; Transactions and Proceedings of the Geological Society of South Africa, v.66, p.353-401.

——— 1980. Shear zone geometry: a review; Journal of Structural Geology, v.2, no.1/2, p.83-99.

Ramsay, J.G. and Graham, R.H. 1970. Strain variation in shear belts; Canadian Journal of Earth Sciences, v.7, p.786-813.

Riddle, C. 1983. Analytical methods for gold; *in* The Geology of Gold in Ontario, Ontario Geological Survey, Miscellaneous Paper 110, p.272-278.

Riverin, G. and Hodgson, C.J. 1980. Wall-rock alteration of the Millenbach Cu-Zn mine, Noranda, Quebec; Economic Geology, v.75, p.424-444.

Rose, E.R. 1969. Geology of titanium and titaniferous deposits of Canada; Geological Survey of Canada, Economic Geology Report, no.25, 177p.

Ross, C.S. 1941. Occurrence and origin of titanium deposits of Nelson and Amherst counties, Virginia; United States Geological Survey, Professional Paper 198, 59p.

Rye, D.M., Doe, B.R. and Delevaux, M.H. 1974. Homestake Mine, South Dakota: II. Lead isotopes, mineralization ages and source of lead in ores of the northern Black Hills; Economic Geology, v.69, p.814-822.

Sangster, D.F. 1972. Precambrian volcanogenic massive sulphide deposits in Canada: a review; Geological Survey of Canada, Paper 72-22, 44p.

Sato, T. 1974. Distribution and geological setting of the Kuroko deposits; *in* Geology of Kuroko deposits, Mining Geology, Special Issue, no.6, p.1-9.

Schubert, C. 1980. Late-Cenozoic pull-apart basins, Bocono fault zone, Venezuelan Andes; Journal of Structural Geology, v.2, no.4, p.463-468.

Schwerdtner, W.M. and Lumbers, S.B. 1980. Major diapiric structures in the Superior and Grenville provinces of the Canadian Shield; *in* The Continental Crust and Its Mineral Deposits, Geological Association of Canada, Special Paper 20, p.149-180.

Schwerdtner, W.M., Stone, D., Osadetz, K., Morgan, J. and Stott, G.M. 1979. Granitoid complexes and the Archean tectonic record in the southern part of northwestern Ontario; Canadian Journal of Earth Sciences, v.16, p.1965-1977.

Scott, S.D., Both, R.A. and Kissin, S.A. 1977. Sulfide petrology of the Broken Hill region, New South Wales; Economic Geology, v.72, p.1410-1425.

Shegelski, R.J. 1978. Stratigraphy and geochemistry of Archean iron formations in the Sturgeon Lake–Savant Lake greenstone terrane, northwestern Ontario; unpublished PhD thesis, University of Toronto, Toronto, Ontario, 251p.

Shirey, S.B. and Hanson, G.N. 1982. The Ottertail Pluton, Rainy Lake, Ontario: trace element evidence for a zoned-composite, Algoman intrusion; *in* Program with Abstracts, Geological Association of Canada—Mineralogical Association of Canada, v.7, p.81.

——— 1983. Granitic rocks in Archean crust, Rainy Lake, Ontario: Nd isotope evidence for chondritic Sm/Nd sources; EOS, v.64, p.330.

Sibson, R.H. 1977. Fault rocks and fault mechanisms; Journal of the Geological Society of London, v.133, pt. 3, p.191-213.

Sibson, R.H., Moore, J.McM. and Rankin, A.H. 1975. Seismic pumping—a hydrothermal fluid transport mechanism; Journal of the Geological Society of London, v.131, pt. 6, p.653-659.

Southwick, D.L. 1972. Vermilion granite-migmatite massif; *in* Geology of Minnesota: A Centennial Volume, Minnesota Geological Survey, p.108-119.

——— 1976. High-grade metamorphism associated with the Vermilion Batholith, Minnesota–Ontario; abstract, *in* Program, Institute on Lake Superior Geology, 22nd Annual Meeting, St. Paul, Minnesota, p.61.

Southwick, D.L. and Sims, P.K. 1980. The Vermilion Granitic Complex—a new name for old rocks in northern Minnesota; *in* Shorter Contributions to Mineralogy and Petrology, United States Geological Survey, Professional Paper 1124 A-F, p.A1-A11.

Stacey, J.S. and Kramers, J.D. 1975. Approximation of terrestrial lead isotope evolution by a two-stage model; Earth and Planetary Science Letters, v.26, p.207-221.

Stockwell, C.H. 1950. The use of plunge in the construction of cross-sections of folds; *in* Proceedings of the Geological Association of Canada, v.3, p.96-121.

——— 1964. Fourth report on structural provinces, orogenies, and time classification of rocks of the Canadian Precambrian Shield; *in* Age Determinations and Geological Studies, Part II, Geological Survey of Canada, Paper 64-17, p.1-21.

Stowe, C.W. 1974. Alpine-type structures in the Rhodesian basement complex at Selukwe; Journal of the Geological Society of London, v.130, pt. 5, p.411-425.

Streckeisen, A. 1976. To each plutonic rock its proper name; Earth Science Reviews, v.12, p.1-33.

Stringer, P. and Treagus, J.E. 1980. Non-axial planar S_1 cleavage in the Hawick Rocks of the Galloway area, Southern Uplands, Scotland; Journal of Structural Geology, v.2, no.3, p.317-331.

Sutcliffe, R.H. 1978. Geology of the Rainy Lake granitoid complex; *in* Proceedings of the 1978 Archean Geochemistry Conference, University of Toronto, p.235-244.

Tanton, T.L. 1927. Stratigraphy of the northern sub-province of the Lake Superior region; Geological Society of America, Bulletin, v.38, p.731-748.

——1935. Preliminary report on Mine Centre area, Ontario; unpublished report, Bureau of Economic Geology, Department of Mines, Ottawa.

——1936. Mine Centre area, Rainy River District, Ontario; Geological Survey of Canada, Coloured Map 334A, scale 1:31680.

Tchalenko, J.S. 1970. Similarities between shear zones of different magnitudes; Geological Society of America, Bulletin, v.81, p.1625-1640.

Teal, P.R. and Walker, R.G. 1977. Stratigraphy and sedimentology of the Archean Manitou Group, northwestern Ontario; *in* Report of Activities, Part A, Geological Survey of Canada, Paper 77-1A, p.181-184.

Thorpe, R.I. 1982. Lead isotope evidence regarding Archean and Proterozoic metallogeny in Canada; Revista Brasileria de Geolciencias, v.12, p.510-512.

Trowell, N.F., Blackburn, C.E. and Edwards, G.R. 1980. Preliminary geological synthesis of the Savant Lake–Crow Lake metavolcanic-metasedimentary belt, northwestern Ontario, and its bearing upon mineral exploration; Ontario Geological Survey, Miscellaneous Paper 89, 30p.

Turner, C.C. and Walker, R.G. 1973. Sedimentology, stratigraphy and crustal evolution of the Archean greenstone belt near Sioux Lookout, Ontario; Canadian Journal of Earth Sciences, v.10, p.817-845.

Turner, F.J. 1981. Metamorphic petrology: mineralogical, field and tectonic aspects; McGraw–Hill, New York, 524p.

Vokes, F.M. 1969. A review of the metamorphism of sulphide deposits; Earth Science Reviews, v.5, p.99-143.

——1976. Caledonian massive sulphide deposits in Scandinavia: a comparative review; *in* K. H. Wolf, ed., Handbook of Stratabound and Stratiform Ore Deposits, Elsevier, Amsterdam, v.6, p.79–127.

Walker, R.G. 1978. A critical appraisal of Archean basin-craton complexes; Canadian Journal of Earth Sciences, v.15, p.1213-1218.

Walker, R.G. and Pettijohn, F.J. 1971. Archean sedimentation: analysis of the Minnitaki Basin, northwestern Ontario, Canada; Geological Society of America, Bulletin, v.82, p.2099-2130.

Watkins, R. and Stensrud, H.L. 1983. Age of sulfide ores in the West Shasta and East Shasta districts, Klamath Mountains, California; Economic Geology, v.78, p.340-343.

Wilcox, R.E., Harding, T.P. and Seely, D.R. 1973. Basic wrench tectonics; American Association of Petroleum Geologists, Bulletin, v.57, p.74-96.

Wilson, H.D.B., Morrice, M.G. and Ziehlke, D.V. 1974. Archean continents; Geoscience Canada, v.1, p.12-20.

Wood, J. 1980. Epiclastic sedimentation and stratigraphy in the North Spirit Lake and Rainy Lake areas: a comparison; Precambrian Research, v.12, p.227-255.

Wood, J., Dekker, J., Jansen, J.G., Keay, J.P. and Panagapko, D. 1980a. Mine Centre area, District of Rainy River; Ontario Geological Survey, Map P.2201, scale 1:15840.

——1980b. Mine Centre area, District of Rainy River; Ontario Geological Survey, Map P.2202, scale 1:15840.

Young, G.M. 1978. Some aspects of the evolution of the Archean crust; Geoscience Canada, v.5, p.140-149.

Ziehlke, D.V. 1974. Aulneau Batholith project, geology and petrology; *in* 1974 Annual Report, Centre for Precambrian Studies, Part 2, University of Manitoba, Winnipeg, p.150-184.

Zoltai, S.C. 1961. Glacial history of part of northwestern Ontario; *in* Proceedings of the Geological Association of Canada, v.13, p.61-83.

——1965. Surficial geology, Kenora–Rainy River; Ontario Department of Lands and Forests, Map S165, scale 1:506 880.

Metric Conversion Table

Conversion from SI to Imperial			Conversion from Imperial to SI		
SI Unit	*Multiplied by*	*Gives*	*Imperial Unit*	*Multiplied by*	*Gives*
LENGTH					
1 mm	0.039 37	inches	1 inch	**25.4**	mm
1 cm	0.393 70	inches	1 inch	**2.54**	cm
1 m	3.280 84	feet	1 foot	**0.304 8**	m
1 m	0.049 709	chains	1 chain	20.116 8	m
1 km	0.621 371	miles (statute)	1 mile (statute)	**1.609 344**	km
AREA					
1 cm^2	0.155 0	square inches	1 square inch	**6.451 6**	cm^2
1 m^2	10.763 9	square feet	1 square foot	**0.092 903 04**	m^2
1 km^2	0.386 10	square miles	1 square mile	2.589 988	km^2
1 ha	2.471 054	acres	1 acre	0.404 685 6	ha
VOLUME					
1 cm^3	0.061 023	cubic inches	1 cubic inch	**16.387 064**	cm^3
1 m^3	35.314 7	cubic feet	1 cubic foot	0.028 316 85	m^3
1 m^3	1.307 951	cubic yards	1 cubic yard	0.764 554 86	m^3
CAPACITY					
1 L	1.759 755	pints	1 pint	0.568 261	L
1 L	0.879 877	quarts	1 quart	1.136 522	L
1 L	0.219 969	gallons	1 gallon	**4.546 090**	L
MASS					
1 g	0.035 273 962	ounces (avdp)	1 ounce (avdp)	28.349 523	g
1 g	0.032 150 747	ounces (troy)	1 ounce (troy)	**31.103 476 8**	g
1 kg	2.204 622 6	pounds (avdp)	1 pound (avdp)	**0.453 592 37**	kg
1 kg	0.001 102 3	tons (short)	1 ton (short)	**907.184 74**	kg
1 t	1.102 311 3	tons (short)	1 ton (short)	**0.907 184 74**	t
1 kg	0.000 984 21	tons (long)	1 ton (long)	**1016.046 908 8**	kg
1 t	0.984 206 5	tons (long)	1 ton (long)	**1.016 046 90**	t
CONCENTRATION					
1 g/t	0.029 166 6	ounce (troy)/ ton (short)	1 ounce (troy)/ ton (short)	34.285 714 2	g/t
1 g/t	0.583 333 33	pennyweights/ ton (short)	1 pennyweight/ ton (short)	1.714 285 7	g/t

OTHER USEFUL CONVERSION FACTORS

	Multiplied by	
1 ounce (troy) per ton (short)	31.103 477	grams per ton (short)
1 gram per ton (short)	0.032 151	ounces (troy) per ton (short)
1 ounce (troy) per ton (short)	20.0	pennyweights per ton (short)
1 pennyweight per ton (short)	0.05	ounces (troy) per ton (short)

Note: Conversion factors which are in bold type are exact. The conversion factors have been taken from or have been derived from factors given in the Metric Practice Guide for the Canadian Mining and Metallurgical Industries, published by the Mining Association of Canada in co-operation with the Coal Association of Canada.

M46

MAPS NOT FILMED

CARTES NON
REPRODUITES

micromedia
a division of IHS Canada

20 Victoria Street
Toronto, Ontario M5C 2N8
Tel.: (416) 362-5211
Toll Free: 1-800-387-2689
Fax: (416) 362-6161
Email: info@micromedia.on.ca